# CONFORMATIONAL ANALYSIS OF OLIGOMERIC PROFISETINIDINS

*Thesis submitted in fulfilment of the requirements for the degree*

## Philosophiae Doctor

*in the*

*Department of Chemistry*
*Faculty of Natural and Agricultural Sciences*

*at the*

*University of the Free State*
*Bloemfontein*
*South Africa*

*By*

## Eleonora Deborah Potgieter

**Promotor:      Dr D Ferreira**
**Co-promotor:  Prof E V Brandt**

## February 2007

# ACKNOWLEDGEMENTS

I hereby wish to express my sincere gratitude to the following people:

# TABLE OF CONTENTS

# LITERATURE SURVEY

<div align="right">

# DISCUSSION
</div>

## CHAPTER 6

**The conformational behaviour of free phenolic profisetinidin   dimers   from   *Acacia*
      *mearnsii.***

## CHAPTER 7

**The conformational behaviour of free phenolic profisetinidin dimers from *Schinopsis
balansae.***

## CHAPTER 8

**Circular Dichroism and the conformational behaviour of free phenolic**

# EXPERIMENTAL

# APPENDICES

# LITERATURE SURVEY

## INTRODUCTION

More than 4000 structurally unique flavanoids from plant sources have been identified.[1] They are natural phenolic compounds that usually occur as glycosylated and sulfated derivatives; all with a skeleton based on a $C_6$-$C_3$-$C_6$ carbon framework with a 2-phenyl-3,4-dihydro-2*H*-chromene moiety forming the basic unit, (Figure 1.1).[2]
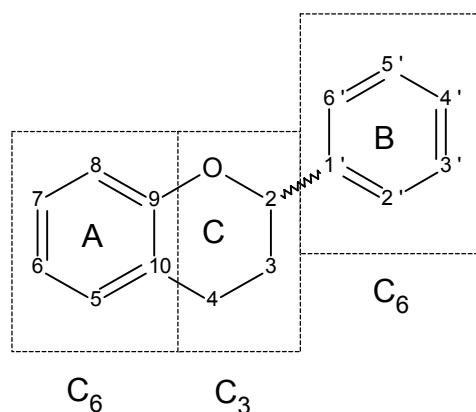


**FIGURE 1.1**

The different monomeric flavanoids may differ with respect to:

a)      The nature of the heterocyclic C-ring.

b)      The hydroxylation patterns of the aromatic rings A and B.

c)      The oxidation state of the heterocyclic C-ring and / or

d)      The configuration of the possible stereogenic centres of the heterocyclic C-ring.

The possible nucleophilic attack of C6 or C8 of the A-ring of e.g. a flavan-3-ol on the electrophilic centre at C4 of the heterocyclic C-ring of another unit leads to the condensation of monomeric units to form oligomers and finally polymers, also known as tannins or proanthocyanidins.[3]

---

[1]     J B Harborne, *Plant Flavonoids in Biology and Medicine: Biochemical, Pharmacological and Structure-Activity Relationships*, V Cody, E Middleton, J B Harborne and A Beretz, Editors, Alan R Liss Inc, New York, 1986, p 15 – 24.

[2]     R Thomas, *Comprehensive Organic Chemistry*, E Haslam, Editor, Pergamon Press, Oxford, 1979, 888.

[3]     L J Porter, R Y Wong and B G Chan, *J. Chem. Soc., Perkin Trans. II*, 1983, 1413.

Proanthocyanidins make up approximately half the dry weight (or more) of nut shells and most commercial tree barks as well as plant leaves.[4]

This study centres on the use of ^{1}H, ^{13}C, gradient COSY, COSY 45, COSY 90W, NOESY PH and HMQC NMR experiments as well as CD spectra to

a)    assign the hydrogen and carbon resonances
b)    define the absolute configuration
c)    study the conformations

of the free phenolic profisetinidins that are found in commercially important southern hemisphere trees, in particular dimers (Figure 1.2) and trimers (Figure 1.3) from Black Wattle (*Acacia mearnsii)* and dimers (Figure 1.4) from Quebracho *(Schinopsis balansae*).

---

[4]    R W Hemingway, P J Steynberg, J P Steynberg and T Hatano, *"Advances in Lignocellulosics Characterization"* D S Argyropoulos,, Ed., Atlanta, GA, TAPPI Press, 1999, 157-178.
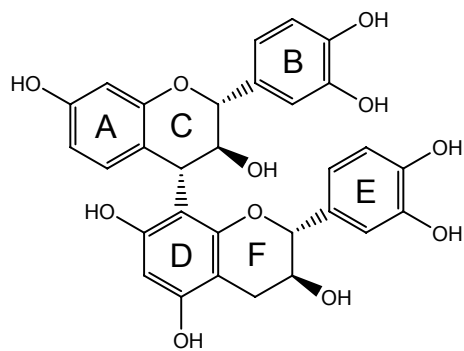
Fisetinidol-(4α→8)-catechin
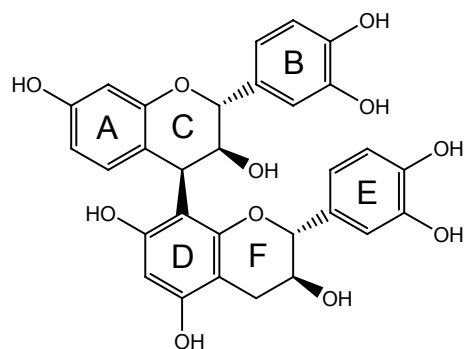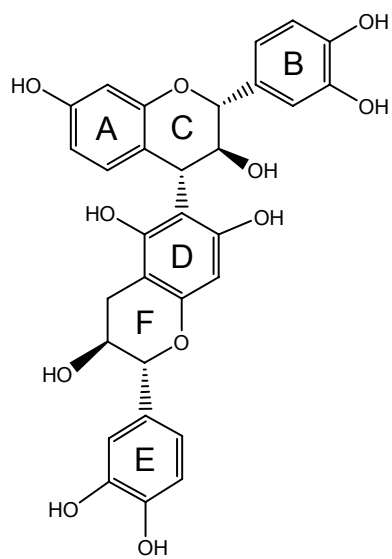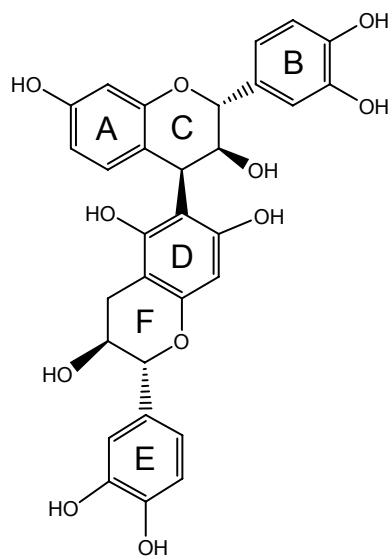
Fisetinidol-(4β→8)-catechin

Fisetinidol-(4α→6)-catechin

Fisetinidol-(4β→6)-catechin

**FIGURE 1.2**
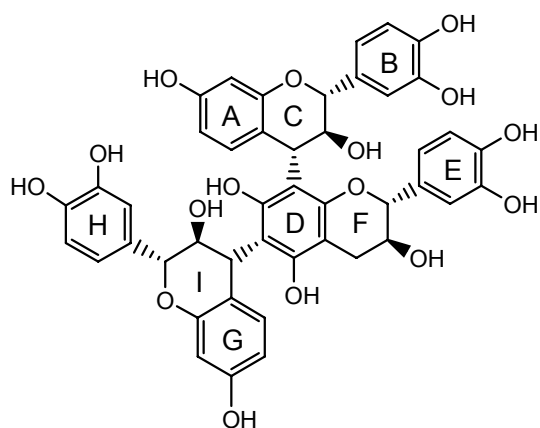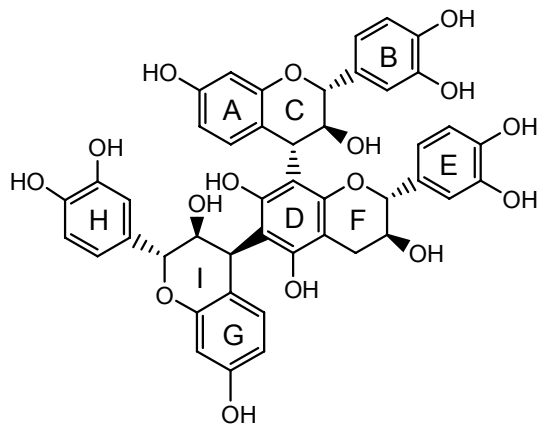
3

Fisetinidol-(4α→8)-catechin-(6→4α)-fisetinidol

Fisetinidol-(4α→8)-catechin-(6→4β)-fisetinidol

Fisetinidol-(4β→8)-catechin-(6→4α)-fisetinidol

Fisetinidol-(4β→8)-catechin-(6→4β)-fisetinidol

**FIGURE 1.3**

4

*Ent*-fisetinidol-(4α → 8)-catechin
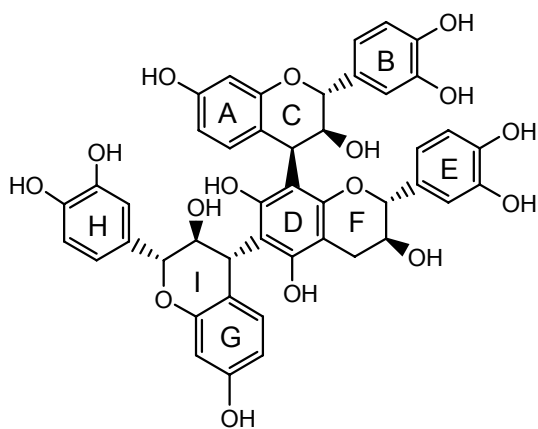
*Ent*-fisetinidol-(4β → 8)-catechin
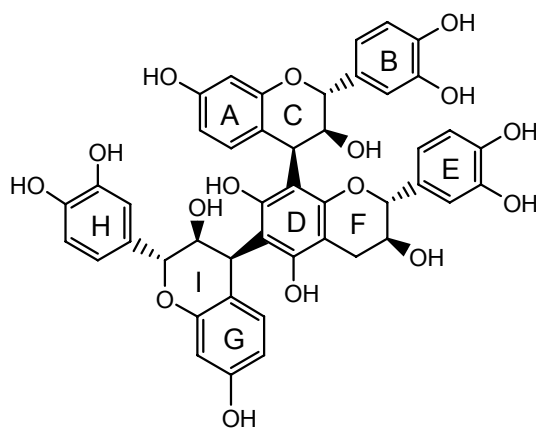
*Ent*-fisetinidol-(4α → 6)-catechin

*Ent*-fisetinidol-(4β → 6)-catechin
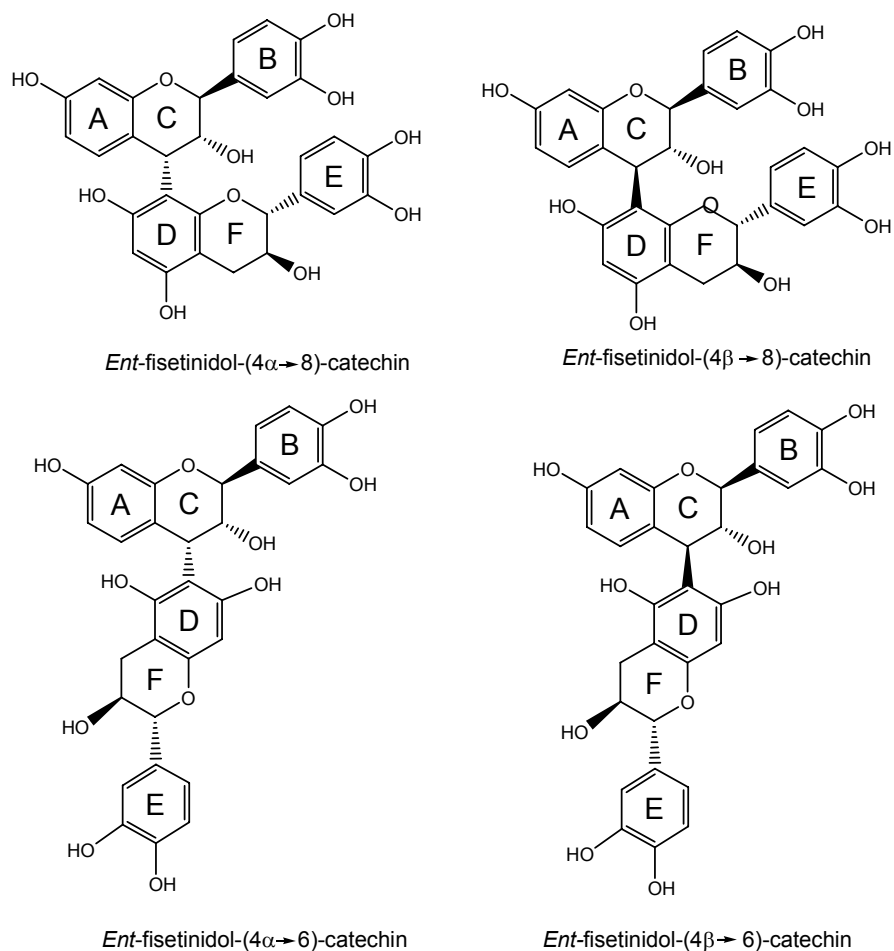
**FIGURE 1.4**

Both *Acacia mearnsii* and *Schinopsis balansae* contain mainly "5-deoxy" A-ring type flavan-3-ols and their polymers, compared to the procyanidins found in northern hemisphere trees such as loblolly pine, containing 5,7-dihydroxy type A-rings, e.g. catechin-(4α→8)-catechin (Figure 1.5).



Catechin-(4α → 8)-epicatechin
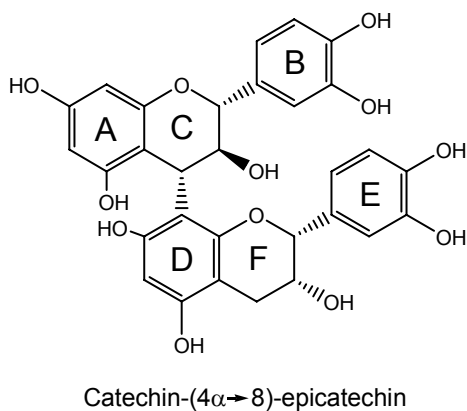
**FIGURE 1.5**

It is interesting to note that the lower or central units of the oligomeric profisetinidins are usually catechin, which also has a 5,7-dihydroxy type A-ring (Figure 1.6).
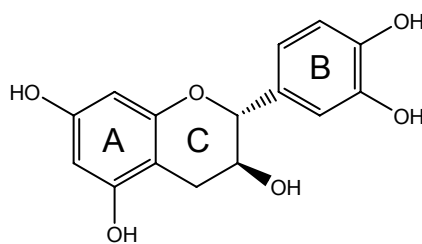


(+)-catechin

**FIGURE 1.6**

An understanding of the conformation of catechin is therefore paramount to the conformational analysis of both the *2R,3S* (fisetinidol) and *2S,3R* (*ent*-fisetinidol) type profisetinidins.

Oligomeric profisetinidins are found in their free phenolic forms in nature, and the study of their conformations at ambient temperatures in the free phenolic state should lead to a better understanding of their biological activity. It is, however, extremely difficult to obtain samples of the free phenolic forms of these compounds that are pure enough for NMR spectroscopic analysis.

As a result, only a few studies have been done on the free phenolic forms of these compounds. In contrast, a large number of studies have been done on the methyl ether acetates and the acetate derivatives of monomeric and oligomeric profisetinidins and procyanidins. A variety of NMR experiments[5,6,7,8,9,10,11,12] as well as X-ray crystallographic

5   J P Steynberg, E V Brandt, D Ferreira, C A Helfer, W L Mattice, D Gornik and R W Hemingway, *Magn. Res. Chem.*, 1995, 33, 611.
6   P M Viviers, Ph.D. Thesis, UOVS, 1983.
7   A L Botes, M.Sc Thesis, UOVS, 1983
8   L Y Foo and L J Porter, *J. Chem. Soc., Perkin Trans. I,* 1983, 1535.
9   F Baert, R Fouret, M Sliwa and H Sliwa, *Tetrahedron,* 1980, **36**, 2765.
10  F R Fronczek, G Gannuch, W L Mattice, R W Hemingway, G Chiari, F L Tobiason, K Houglam and A Shanafelt, *J. Chem.Soc. Perkin Trans. II,* 1985, 1383.
11  F Baert, R Fouret, M Sliwa and H Sliwa, *Acta Cryst.,* 1983, **B39**, 444.
12  C-C Shen, Y-S Chang and L-K Ho, *Phytochemistry*, 1993, **34**, 843.

data,[9,10,11,13,14,15] infrared spectroscopy,[9,10,11] time-resolved fluorescence,[16,17] Circular Dichroism[18,19,20] and a number of different computational methods (AM1,[21] MNDO,[21] MM2,[22] GMMX,[23,12] ab initio methods[24] and the MMH approach[25]) were used.

The results obtained from the study of free phenolic proanthocyanidin oligomers should provide a basis for the understanding of the behaviour of the higher polymers.

The conformational behaviour and structural features that relate to the shape and flexibility of flavanoids depend on the following four factors.[4,26]

a)      Rotation around the $2\text{-}C_C \rightarrow 1C_B$ bond.

b)      Rotation around interflavanyl bonds giving rise to rotational isomers where rotation is restricted.

c)      Conformational isomerism of the heterocyclic ring system due to flexing of the ring.

d)      Heterocyclic ring chemistry

13      F R Fronczek, G Gannuch, W L Mattice, F L Tobiason, J L Broeker, R W Hemingway and G Chiari, *J. Chem.Soc., Perkin Trans. II,* 1984, 1611.

14      D W Engel, M Hattingh, H K L Hundt and D G Roux, *J. Chem. Soc., Chem. Commun.,*1978, 695.

15      A L Spek,B Kojic-Prodic and P R Labadie, *Acta.Cryst.,* 1984,C40, 2068.

16      D. Cho, R Tian, L J Porter, R W Hemingway and W L Mattice, *J. Am. Chem., Soc.,* 1990, **112**, 4273.

17      C A Helfer and W L Mattice, "*Plant Polyphenols"* Ed R W Hemingway, and P E Laks, Plenum Press, New York, 1992, 479.

18      H van Rensburg, P J Steynberg, J F W Burger, P S van Heerden and D Ferreira, *J. Chem. Res. (S),* 1999, 450.

19      D Slade, D Ferreira and J P J Marais, *Phytochemistry,* 2005, **66**, 2177 – 2215.

20      D Ferreira, J P J Marais and D Slade, *J. Nat. Prod.,* 2004, **67**, 174.

21      F L Tobiason in *"Plant Polyphenols", Synthesis, Properties, Significance.* Ed. R W Hemingway and P E Laks, Plenum Press, New York, 1992, 459.

22      L J Porter, R Y Wong, M Benson, B G Chan, V N Viswanadhan, R D Gandour and W L Mattice, *J. Chem. Res.,* 1986, 830.

23      F L Tobiason and R W Hemingway, *Tetrahedron Lett.* 1994, **35**, 2137

24      C Cappelli, S Bronco and S Monti, *Chirality,* 2005, **17(9)**, 577 – 589.

25      E Codorniu-Hernández, A Mesa-Ibirico, L Montero-Cabrera, F Martinez-Luzardo and W-D Stohrer, *J. Mol. Struct.: THEOCHEM,* 2005, **715**, 227 – 239.

26      T Hatano and R W Hemingway, *J. Chem. Soc., Perkin Trans. II*, 1997, 1035 – 1043.

# CHAPTER 1

## The Industrial and Biological Importance of Proanthocyanidins

### 1.1    THE INDUSTRIAL IMPORTANCE OF PROANTHOCYANIDINS.

Because of their industrial importance, there has been a large emphasis on the study of the structure and conformation of oligomeric proanthocyanidins (tannins). Evidence of the use of vegetable tannins, derived from the bark, leaves, fruit, roots and growths of numerous types of plants to tan raw animal hides into leather, has been found in ancient Babylonian and Egyptian texts dating back to circa 5000 B.C.[27]

The Australian Black Wattle tree (*Acacia mearnsii)* has been used commercially in South Africa since 1864, when John van der Plank started the development of the first plantations in Kwa-Zulu Natal, mainly for the production of tannins. 31-51% of the dry weight of the bark consists of water soluble tannins that are mainly used for leather tanning and the manufacture of water resistant resins of adhesives for reconstituted wood products in South Africa.[28] Quebracho *(Schinopsis balansae* tannins are obtained from the heart-wood of the Quebracho tree that grows chiefly in Argentina and Paraguay. Powdered extracts, containing 70-75% of the tannins from both these sources are available commercially.[29]

The industrial use of polyflavanoids has now been expanded to the manufacturing of waterproof wood adhesives,[30] anti-corrosive additives,[30,31] rust converters, rust

---

[27]    http://www.jarnaginco.com/Vegetable%20tanned%20leather.htm

[28]    R Adair, "*Black Wattle: South Africa Manages Conflict of Interest"*
http://pest.cabweb.org/Journals/BNI/Bni23-1/Gennews.htm, March 2004

[29]    http://www.coba-chemicals.com/

[30]    G M Rivas and P Zaya in *"Tannin Produced from Pine Bark in Chile"*, http://web.idrc.ca/en/ev-3180-201-1-DO_TOPIC.html, 1998.

[31]    L Barbour in "*Tannin and Fuel Wood from Plantation Grown Bipinnate Acacias*", RIRDC Publication No 00/47, Project no AFT-3A, RIRDC, 2000

inhibitors[30,32] and super-plasticizers and strengtheners of cement and concrete mixtures.[33,34,35] Numerous patents have also been taken out with regards to the use of tannins, of which a selection of US Patents, referring mainly to industrial, non-biological applications of Quebracho, is listed below (Table 1.1.1).[36]

| US04637883 | 01/20/1987 | Fluid loss additives for oil base muds and low fluid loss compositions thereof |
| US04055502 | 10/25/1977 | Method and composition for acidizing subterranean formations |
| US04110226 | 08/29/1978 | Stabilized aqueous gels and uses thereof |
| US04618433 | 10/21/1986 | Drilling fluids and thinners therefore |
| US04952329 | 08/28/1990 | Separation of polymetallic sulphides by froth flotation |
| US04389320 | 06/21/1983 | Foamable compositions and formations treatment |

**TABLE 1.1.1**

## 1.2.    THE BIOLOGICAL IMPORTANCE OF FLAVANOIDS

Traditional Eastern Medicine has been using plants and spices containing flavanoids for thousands of years. A resurgence in pharmacognosy, as well as a renewed interest in Eastern Medicine in the West, has provided an impetus for an increase in the number of research efforts geared towards a better understanding of the interaction of flavanoids with mammalian cells and tissues.[37] Flavanoids are known to have, for example, extremely potent anti-oxidant properties,[38] antitrypanosomal and antileishmanial activities,[39] inhibitory

---

[32]   R W Hemingway in *"Opportunities to Use Bark Polyphenols in Specialty Chemical Markets"*, Proceedings, 2nd biennial residual wood conference, 1997 November4-5, Richmond, BC: MCTI Communications, Inc.: 80-85

[33]   H R E Kaspar and A Pizzi, *J. App. Pol. Sci.*, 1996, 59, 1181 – 1190.

[34]   K E Semple and P D Evans, *"Wood-Cement Composites in the Asia-Pacific Region"* P D Evans, Ed., ACIAR, 2002, 40

[35]   K E Semple, R B Cunningham and P D Evans, *"Wood-Cement Composites in the Asia-Pacific Region"* P D Evans, Ed., ACIAR, 2002, 29

[36]   http://www.patents.ibm.com

[37]   E Middleton Jr., C Kandaswami and T C Theoharides, *Pharm. Rev., 2000, 52, 673 – 751.*

[38]   G Luck, H Liao, N J Murray, H R Grimmer, E E Marminski, M P Williamson, T H Lilley and E Haslam, *Phytochemistry*, 1994, **37**, 357.

[39]   D Tasdemir, M Kaiser, R Brun, V Yardley, T J Schmidt, F Tosun and P Rüedi, *Antimicrobial Agents and Chemotherapy*, 2006, 1352 – 1364.

activities against DNA polymerase inhibitors,[40] chemical signalling activities in plant symbiosis with microrrhizal fungi,[41] and cyanobacteria.[42]

It is also believed that the biological significance and activity of polyflavanoids will be better understood if we know more about their conformational preferences and flexibility. This knowledge, in turn, could serve as a foundation towards our understanding of the complexation of flavanoids with other biopolymers, such as proteins and carbohydrates, inorganic compounds and metal ions and as a result, their biological activity and industrial applications.

[40] Y Mizushina, A Saito, A Tanaka, N Nakajima, I Kuriyama, M Takemura, T Takeuchi, F Sugawara and H Yoshida, *Biochem Biophys Res Commun.,* 2005, **333(1)**, 101 – 109.

[41] Z-P Xie, C Stachelin, A Vierheilig, A Wiemken, S Jabbouri, W J Broughton, R Vögeli-Lange and T Boller, *Plant Physiol.,* 1995, **108**, 1519 – 1525.

[42] M F Cohen and H Yamasaki, *J. Bact.*, 2000, 4644 – 4646.

# CHAPTER 2

## The Conformational Behaviour of Chromans

The chroman ring system consists of a benzene ring with an attached heterocyclic ring containing an oxygen atom in position 1 (Figure 2.1). The understanding of the conformational flexibility of this system and the effects that different substituents on both the aromatic and the heterocyclic rings have on its conformations, form the basis on which the configurational and conformational analysis of flavan-3-ols are built.
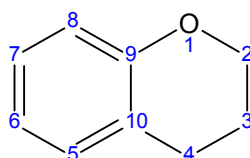
**FIGURE 2.1**

The heterocyclic ring of chroman is analogous to cyclohexene and the following conformations have been considered:

a)      A half-chair conformation[43,44,45,46] that can undergo a ring inversion to an energetically equivalent conformer was supported by molecular models.[47] Axial substituents become equatorial and vice versa during ring inversion[48] although it would be more accurate to describe the substituents as being quasi-equatorial and quasi-axial (Figure 2.2).

b)      An energetically unfavourable skewed or twisted boat conformation.[47]

43    E A H Robberts, *Chem & Ind*., London, 1955, 631.
44    V B Mahesh and T R Seshadri, *Proc. Indian Acad. Sci*., 1955, 41A, 210.
45    C G Joshi and Kulkarni, *Chem & Ind*., London, 1954, 1421.
46    F E King, J W Clark-Lewis and W F Forbes, *J.Chem. Soc*., 1955, 2498.
47    W B Whalley, *Symposium on Vegetable Tannins*, Cambridge, April 1956, Society of Leather Trades' Chemists, Croydon, 1956, 151.
48    W B Whalley, *The Chemistry of Flavonoid Compounds,* T A Geissmann, Editor, Pergamon Press, London, 1962, 441 – 467.

c)       A C-2 sofa, with atoms 1, 3 and 4 being co-planar with the aromatic ring.[49]



-OH in quasi-axial          -OH in quasi-equatorial
orientation                  orientation
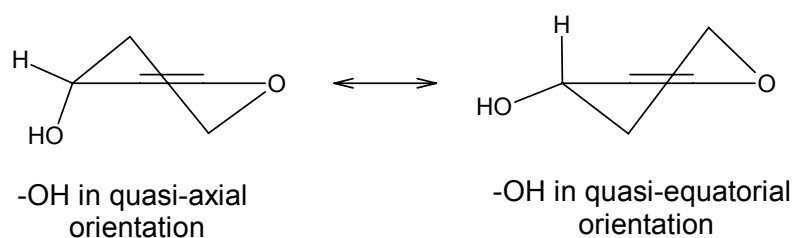
**FIGURE 2.2**

Since the middle sixties, Circular Dichroism has developed into a routinely used and powerful method to determine the absolute configuration and conformation of flavanoids and numerous flavanoid analogues.[19] This method can also be applied to determine the conformational behaviour of chromans.

Circularly polarised light rays travel through an optically active medium with different velocities due to the different indices of refraction for right- and left-circularly polarised light. This phenomenon is called optical rotation or circular birefringence. The variation of optical rotation as a function of wavelength is called Optical Rotatory Dispersion (ORD). Circular Dichroism (CD), however, concerns the different extents to which right- and left-circularly polarised light will also be absorbed due to differences in extinction coefficients for the two polarised rays. ORD spectra are dispersive whereas CD spectra are absorptive. They are interrelated in good approximation by the König-Kramers transform.[19]

There are two main chirality sector rules that have been formulated for various chromophores. They are also the most successful rules used to date. They both focus on chromophores and relate the chirality of the extra chromophoric environment to the Cotton effect associated with these chromophores. They are the Octant Rule[50] applicable to alkyl ketones and aldehydes and the Exciton Chirality Rule.[51]

---

[49]    E M Philbin and T S Wheeler, *Proc. Chem. Soc.,* 1958, 167.
[50]    W Moffitt, R B Woodward, A Moscowitz, W Klyne and C Djerassi, *J. Am.Chem.Soc.,* 1961, **83**, 4013.
[51]    N Harada and K Nakanishi, *"Circular Dichroic Spectroscopy. Exciton Coupling in Organic Stereochemistry",* University Science Books, Mill Valley, CA, 1983.

Aromatic systems show three main UV absorption bands (Table 2.1).[19,24]

| TYPE OF TRANSITION | WAVELENGTH[19] (nm) | WAVELENGTH[24] (nm) |
|---|---|---|
| $^1B$ | 180 – 190 | 190 – 215 |
| $^1L_a$ | 200 – 240 | 220 – 240 |
| $^1L_b$ | 260 – 280 | 250 – 270 |

**TABLE 2.1**

The $^1L_a$ and the $^1L_b$ bands have been predominantly used in the interpretation of CD spectra of flavanoids. The $^1L_b$ transition is formally forbidden, but becomes optically active in a dissymmetric aromatic system,[52] as is the case with flavanoids.

The study of different types of benzene chromophores with attached heterocyclic rings (the second chiral spheres) e.g. tetralin, tetrahydroisoquinoline, isochroman and 1,4-benzodioxan,[19] led to the establishment of a helicity rule that can be used to predict the sign of the CE of the $^1L_b$ band of these compounds. The benzene chromophore is said to be chirally perturbed by the second chiral sphere. This rule states that if the helicity of the half-chair conformation of the heterocyclic ring is considered, a *P*-helicity will lead to a negative CE in the $^1L_b$ band and an *M*-helicity will lead to a positive CE in the $^1L_b$ band (Figure 2.3).



*M*-helicity leading
to a positive CE
in the $^1L_b$ band

direction of view
of the chroman

*P*-helicity leading
to a negative CE
in the $^1L_b$ band
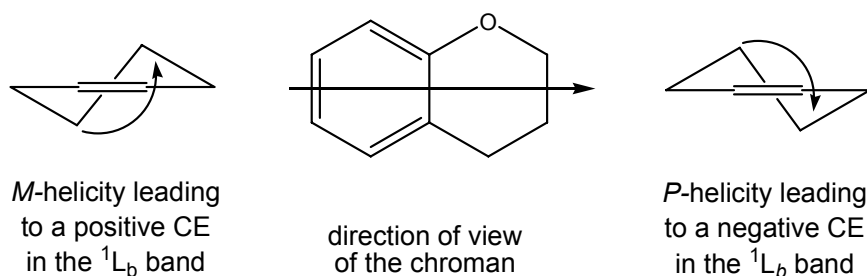
**FIGURE 2.3**

---

[52]   P Crabbé in *Topics in Stereochemistry*, Ed. N L Allinger, and E L Eliel, Wiley, New York, London and Sydney, 1967,, **1**, 93.

This could, however, not be applied if there was a pseudo axial substituent at the benzylic C-4 position or substituents on the benzene ring itself. Sector rules for the contribution of substituents on the heterocyclic ring (the third chiral sphere) to the chiral perturbation of the benzene chromophore were developed by several scientists. This is further discussed in Chapter 3.

# CHAPTER 3

# The Conformational Behaviour of Substituted Chromans

## 3.1    THE CONFORMATIONAL BEHAVIOUR OF 4-MONO-SUBSTITUTED AND 3,4-DISUBSTITUTED CHROMANS.

The mono-substituted chroman-4α-ol and its acetate derivative[53,54,55] both have unexpected quasi-axial orientations contributing 80% to the conformation of both molecules. The sterically more bulky 4-OH substituent would be expected to assume a less hindered equatorial position. (Figure 3.1.1) This can be explained by the pseudo-allylic effect or $A^{1,3}$-strain which is caused by the steric crowdedness between the quasi-equatorial α-hydroxy group and the C-5 hydrogen of the aromatic ring. This strain is increased as the bulkiness of the substituent on C-5 increases, e.g. in the case of methoxy or hydroxy groups of the 5,7-dihydroxy flavanols and their derivatives.



quasi-axial orientation

80%

quasi-equatorial orientation

20%
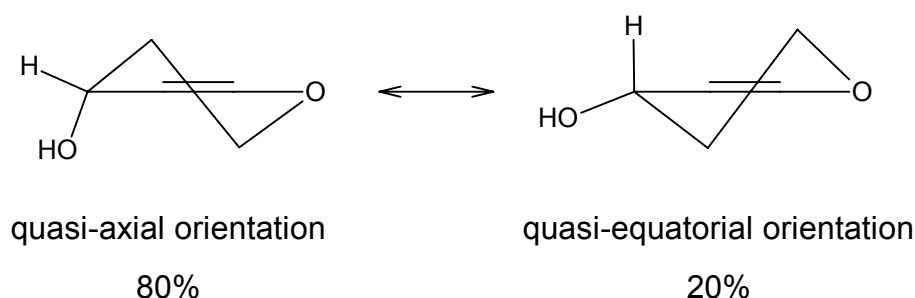
**FIGURE 3.1.1**

This same phenomenon is observed for 3α-chlorochroman-4α-ol,[56] where the 4α-OH assumes a quasi-axial position and the bulky 3α-chloro-group an equatorial position, both being energetically more favourable than a quasi equatorial position of the OH group with increased $A^{1,3}$-strain and an axial position of the 3-chloro-group with high energy 1,3-diaxial interactions (Figure 3.1.2).

53    G F Katekar and A G Moritz, *Aust. J. Chem*., 1967, **20**, 2235.
54    G F Katekar and A G Moritz, *Aust. J. Chem*., 1969, **22**, 2337.
55    S Yamaguchi, K Kabuto, Y Ninomiya and N Inoue, *Bull. Chem. Soc. Japan*, 1970, **43**, 3952.
56    W D Cotterill, J Cotram and R Livingstone, *J. Chem. Soc. (C),*1970, 1006.
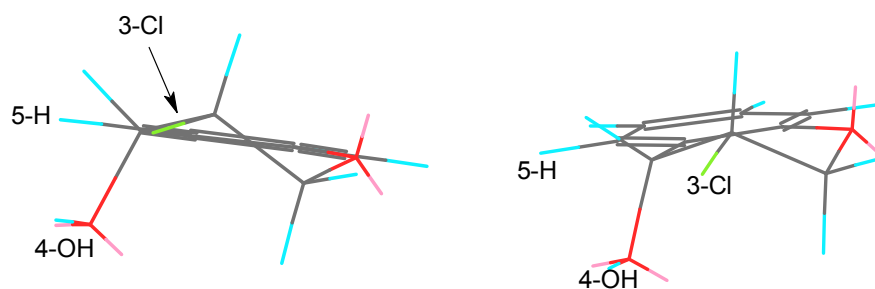
**FIGURE 3.1.2**

In the case of 3α-chlorochroman-4β-ol,[56] both the 4β-OH and 3α-chloro groups assume equatorial positions (Figure 3.1.3), as the $A^{1,3}$-strain seems to be energetically more favourable than:

a)   The 1,3-diaxial interaction between the 4-OH and 2-H groups

b)   The torsional strain between the 3-C substituent, $10\text{-}C_A$ and $1\text{-}O_C$.

c)   The torsional strain between the 4-C substituent, $2\text{-}C_C$ and $9\text{-}C_A$.
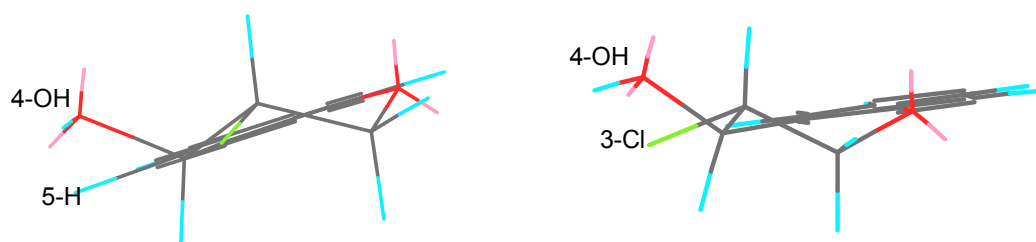


**FIGURE 3.1.3**

The Circular Dichroism of these compounds is characterised by the contributions made by the second and third spheres to the chiral perturbation of the homochiral chromophore. They have an effect on the signs of the $^1L_b$ band depending on the substitution pattern on the benzene ring itself,[57] and sector rules have been developed for third sphere contributions of non-aromatic ring substituents of the heterocyclic ring.[58,59]

These sector rules were, however, not applicable to the structures of monomeric flavan-3-ols due to aromatic substituents on one or two of the heterocyclic ring carbons. Therefore, theories had to be developed in order to apply CD to the configurational isomerism of

[57]   G Snatzke, M Kajtár and F Werner-Zamojska, *Tetrahedron,* 1972, **28**, 281.
[58]   M J Luche, A Marquet and G Snatzke, *Tetrahedron,* 1972, **28**, 1677.
[59]   S Hagishita and K Kuriyama, *Bull. Chem. Soc. Japan*, 1982, **55**, 3216.

monomeric and oligomeric flavans-3-ols, as is discussed in Chapter 4.

## 3.2    THE CONFORMATIONAL BEHAVIOUR OF MONOMERIC FLAVAN-3-OLS

There are two extreme half-chair/sofa conformations that the heterocyclic C-ring of the monomeric flavan-3-ols can assume. When the B-ring assumes an equatorial position, it is described as the E-conformer. The A-conformer has the B-ring is in an axial position. In general, the A-conformer has also been considered to be the energetically less favourable conformer due to 1,3-diaxial interactions of the B-ring with axial C-ring hydrogen atoms and/or substituents.

Several studies, however, has shown that a combination of several other factors also had to be considered in the determination of the stability, and therefore the preferred conformation, of the C-ring:

### 3.2.1.1    The effect of the formation of an intramolecular hydrogen bond between a 3-OH$_C$ group and the heterocyclic oxygen atom.

Early studies of (+)-catechin and (-)-epicatechin and some of their derivatives were done to determine the absolute configuration at C-2 and C-3. The results of these studies, combined with infrared studies, supported the existence of A-conformers in certain instances.[60,61,62,63,64,65] When the B-ring of the tetra-*O*-methylated derivative of (+)-catechin has an axial orientation, the 3-OH$_C$ group will also be axial. This enables the formation of a hydrogen bond between 3-OH$_C$ and the heterocyclic oxygen atom on the β-face of the C-ring (Figure 3.2.1), stabilizing the A-conformer.

[60]    K Freudenberg, H Fikentscher and W Wenner, *Annalen,* 1925, **443**, 309.
[61]    K Freudenberg and M Harder, *Annalen,* 1926, **451**, 309.
[62]    W Hűckel, O Neunhőffer, A Gerke and E Frank, *Annalen,* 1929, **477**, 159.
[63]    K Freudenberg, R F B Cox and E Braun, *J. Am. Chem. Soc.,* 1932, **54**, 1913.
[64]    T A Geissman and H Lischner, *J. Am. Chem. Soc.,* 1952, **74**, 3001.
[65]    H L Hergert and E F Kurth, *J. Org. Chem.,* 1953, **18**, 521.
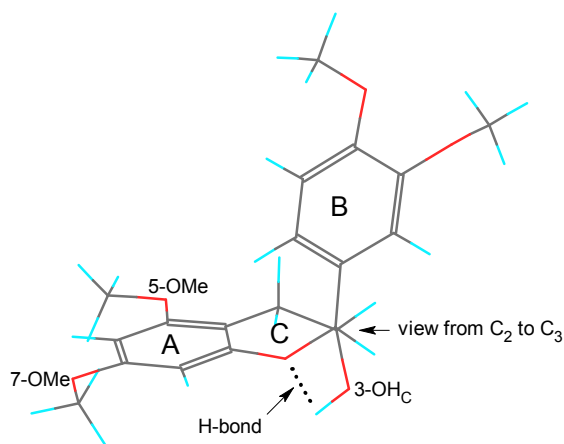
**FIGURE 3.2.1**

This A-conformer (Figure 3.2.1), however, is less stable than the corresponding E-conformer of the tetra-*O*-methylated derivative of (-) epicatechin (Figure 3.2.2) because of the possible inversion of the C-ring to an E conformer with the B-ring in a more stable equatorial position.

When the B-ring of the tetra-*O*-methylated derivative of (-)-epicatechin has an equatorial orientation, the axial 3-OH$_C$ group can form a hydrogen bond with the heterocyclic oxygen atom on the α-face of the C-ring (Figure 3.2.2), stabilizing the E-conformer.
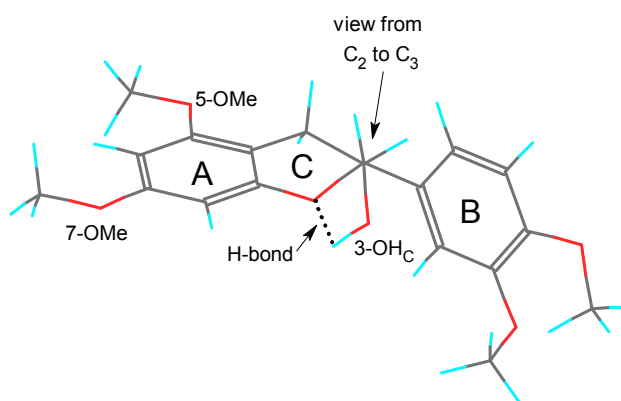


**FIGURE 3.2.2**

### 3.2.1.2 The effects of the relative sizes of the substituents on the C-ring on the torsional strain or *gauche* interaction between them.

Until the mid 1980's, a number of research groups[22,66,67,68,69,70,71,72,73] still assumed that the C-rings of both (+)-catechin and (-)-epicatechin as well as many of their derivatives, existed as preferred half-chair/sofa E-conformers.

It was shown that penta-*O*-acetyl-(+)-catechin existed mainly as an A-conformer in the solid state.[10] IR spectroscopy, $^1$H NMR coupling constants of the heterocyclic ring protons as well as X-ray crystallography were used to prove that both 2,3-*trans*- and 2,3–*cis*-diphenyl-(flavan-3-yl)-methanol exist mainly as A-conformers.[9,11] This was due to the preferred equatorial position of the sterically more bulky diphenyl methanol substituent on 3-$C_C$ and hence the B-ring on 2-$C_C$ assumed an axial position.

### 3.2.1.3 The combined effect of $A^{1,3}$-strain between the substituents on 4-$C_C$ and 5-$C_A$. and torsional strain as a result of the substituents on the C-ring.

$A^{1,3}$-strain was alleviated when the B-ring of 2,3-*trans*-3,4-*cis*-5-oxyflavanoids was in an equatorial position. The $A^{1,3}$-strain was smaller in the case of 2,3-*trans*-3,4-*cis*-5-deoxyflavanoids due to the less bulky substituent at 5-$C_A$.[22]

The observations discussed in Paragraphs 3.2.1.1 – 3.2.1.3, led to further systematic studies of the conformations of (-)-epicatechin and (+)-catechin and their derivatives in solution.[22] The results obtained from temperature dependent $^1$H NMR experiments, MM2 calculations as well as X-ray crystallographic data[3,13,14,15] were combined with those of earlier studies

[66]  J W Clark-Lewis, L M Jackman and T M Spotswood, *Aust. J. Chem.,* 1964, **17**, 632.
[67]  J W Clark-Lewis, *Aust. J. Chem.,* 1968, **21**, 2059
[68]  B R Brown and M R Shaw, *J. Chem. Soc., Perkin Trans. I,* 1974, 2036.
[69]  J P Steynberg, J F W Burger, D A Young, E V Brandt, J A Steenkamp and D Ferreira, *J. Chem. Soc. Chem. Commun.*, 1988, 1055.
[70]  J P Steynberg, J F W Burger, D A Young, E V Brandt, J A Steenkamp and D Ferreira, *J. Chem. Soc. Perkin Trans. I,* 1988, 1055.
[71]  J P Steynberg, J F W Burger, D A Young, E V Brandt, J A Steenkamp and D Ferreira, *J. Chem Soc. Perkin Trans. I,* 1988, 3323.
[72]  J P Steynberg, J F W Burger, D A Young, E V Brandt and D Ferreira, *Heterocycles,* 1989, **28**, 923.
[73]  J A Steenkamp, J C S Malan and D Ferreira, *J. Chem. Soc., Perkin Trans. I,* 1988, 2179.

that used the enthalpy values of the cyclohexene ring to predict the conformations of the flavanoid C-ring.[9,11] It was shown that all heterocyclic C-ring conformations similar to sofa or half-chair conformations could be considered as ground state conformations in an idealised energy profile. The boat conformation was shown to have the highest transition energy.[74]

This theory was then further developed by performing low temperature ^{1}H NMR experiments of some procyanidins and their derivatives. The data thus obtained were compared with MM2 energy calculations to prove that a dynamic interconversion between A and E conformers did take place.[22]

Conformations with A-E conformer interchange characteristically displayed relatively small $J_{2,3}$ coupling constants (in the order of 7Hz in acetone-d$_6$) as well as selective broadening of heterocyclic ring proton resonances at lower temperatures. This broadening was also much more pronounced where the contribution of both conformers of a molecule was of a similar magnitude.[22]

Because the relative conformer populations of monomers at a certain temperature are sometimes difficult to determine from ^{1}H NMR experiments, two methods were developed that made use of the coupling constants of the heterocyclic ring protons to calculate the dihedral angles between the vicinal protons.[22] Both methods utilised the Altona modification[75] of the Karplus equation.[76] The 3-substituent rendering of this equation[75] afforded coupling constants that concurred with observed values of the flavanoid skeleton (Equation 1).[22]

$$^3J_{HH} = 13.22\cos^2\phi - 0.99\cos\phi + \sum \Delta X_i \left\{0.87 - 2.46\cos^2\left(\xi_i\phi + 19.9|\Delta X_i|\right)\right\}$$   Equation 1

[74]  R Bucourt in *Topics in Stereochemistry*, E L Eliel and N L Allinger, Editors, Interscience, New York, 1974, **8**, 159 – 224.
[75]  C A G Haasnoot, F A A M de Leeuw and C Altona, *Tetrahedron,* 1980, **36**, 2783.
[76]  L M Jackman and S Sternhell in *Applications of Nuclear Magnetic Resonance Spectroscopy in Organic Chemistry,* Second Edition, Pergamon Press, Oxford, 1969, 283.

$^{3}J_{HH}$ = the relevant 3-substituent rendering coupling constant

$\Phi$ = the dihedral angle

$\xi_i$ = the sign of the non-hydrogen substituent as defined by Altona[75]

$\Delta X_i = X_i - X_H$ with $X$ being the Huggins electronegativity of hydrogen (H) and the substituent $i$ [77].

In the first method, the $^{3}J_{2,3}$-, $^{3}J_{3,4\alpha}$- and $^{3}J_{3,4\beta}$-values were utilised to directly calculate the dihedral angles between the C-ring protons of molecules where the C-ring had a single conformation only (Paragraph 3.2.1 2). A strong correlation between all the observed and calculated $J$-values of the C-ring proved the validity of the application of this method to the flavanoid skeleton. It did, however, predict an energetically unfavourable skewed boat conformation as the lowest energy conformer of (+)-catechin.[22]

The second method was applied to molecules where both the A and E conformers of the C-ring were in equilibrium with each other. An MM2 calculation was done to determine the optimum structures of the A- and E-ground state conformers. The dihedral angles of the vicinal C-ring hydrogen atoms of these optimised structures were observed and the theoretical $^{3}J_{2,3}$-, $^{3}J_{3,4\alpha}$-, $^{3}J_{3,4\beta}$-values for both the E- and A-conformers were calculated using Equation 1. The theoretical $^{3}J_{2,3}$ values for both the E conformer ($^{E}J_{2,3}$) and the A conformer ($^{A}J_{2,3}$), together with the observed $J_{2,3}$ value were then used to calculate the mole fraction ($X_E$) of the E-conformer (Equation 2).[22]

$$X_E = \frac{J_{2,3} - {}^{A}J_{2,3}}{{}^{E}J_{2,3} - {}^{A}J_{2,3}}$$

Equation 2

The relative total steric energies for the A and E conformers predicted by MM2 computations were, however, not always consistent with the distribution of these conformers as predicted from the $J_{2,3}$ coupling constants.[78]

An MNDO and AM1 analysis of the free phenolic forms and peracetate derivatives of (-)-epicatechin and (+)-catechin showed that the MNDO method best represented the energies

[77]   M L Huggins, *J. Am. Chem. Soc.,* 1953, **75**, 4123.
[78]   J P Steynberg, E V Brandt, M J H Hoffmann, R W Hemingway and D Ferreira, in *Plant Polyphenols: Synthesis, Properties, Significance.* Ed. R W Hemingway and P E Laks, Plenum Press, New York, 1992, 501.

of both compounds that will allow estimation of the equilibrium ratio of A and E conformers as determined by NMR experiments.

The AM1 method, however, afforded the following results:

a)      It showed that the energy of the heterocyclic ring depended on the rotational angle of the 3-$OH_C$ group.

b)      It generated the most reasonable structures especially in terms of optimising the torsional angles of the heterocyclic ring.

c)      It predicted a favoured A-conformer for (+)-catechin with the 3-C-O-H group rotated into the pyran ring, similar to the results obtained earlier (Figure 3.2.1 and related discussion).

d)      It predicted the relative energies for the A and E-conformers of the peracetate derivative of (+)-catechin to be nearly the same.

Coupling constants of the heterocyclic protons of tetra-*O*-methyl-(+)-catechin were obtained by computing Boltzmann-averaged torsional angles for an ensemble of conformers found in GMMX global search methods. They matched observed values better than those previously obtained.[78]

In vacuo DFT calculations and MM searches of (*2R,3S,4R)*-flavan-3,4-diol[24] showed that two stable and iso-energetic conformations with half-chair structures exist. In each of these conformations the B-ring was in an equatorial position and the highest number of intramolecular hydrogen bonds between the 3 and 4 hydroxy substituents was preferred. Optimisation in solution showed that the conformational flexibility is also larger in methanol solution than in vacuo.

Comparative NMR studies in a variety of solvents combined with molecular search modelling of free phenolic (+)-catechin and its tetra-*O*-methyl, tetra-*O*-methyl ether acetate and penta-*O*-acetyl derivatives, made significant contributions to the assignment of the A-, B- and C-ring proton and carbon NMR resonances as well as the coupling constants of the heterocyclic ring. This was accomplished by COSY, long range COSY, COLOC, HETCORR, NOESY and NOE difference NMR spectroscopy in DMSO, dioxane, methanol, acetone and

D$_2$O, as well as GMMX molecular search methods.[12,79]

The NMR experiments unambiguously showed that both 6-H$_A$ and 6-C$_A$ resonances have higher chemical shifts than the 8-H$_A$ and 8-C$_A$ resonances of the free phenolic form of (+)-catechin. In contrast, the 6-H$_A$ and 6-C$_A$ resonances of its tetra-*O*-methyl and tetra-*O*-methyl ether acetate derivatives, displayed lower chemical shifts than the 8-H$_A$ and 8-C$_A$ resonances in CDCl$_3$. The peracetate derivatives also displayed higher 8-H$_A$ values than 6-H$_A$ values, but the 8-C$_A$ values were lower than the 6-C$_A$ values in CDCl$_3$ as well as in benzene-d$_6$.

The coupling constants of the C-ring protons of (+)-catechin in different solvents showed that the solvents had a limited influence: $J_{2,3}$ = 7.0 – 7.8 Hz, $J_{3,4\alpha}$ = 4.6 -5.4 Hz and $J_{3,4\beta}$ = 7.5 - 8.4 Hz. Assuming that the different proportions of A and E conformers were reflected by these differences, MMX force field calculations were then used to predict the coupling constants of the E and A conformers, indicating A:E ratios of about 41:59 (DMSO), 30:70 (dioxane) and 33:67 (water).

Molecular modelling studies of the tetra-*O*-methylated derivative of (+)-catechin and (-) epicatechin (Figures 3.2.1/2) suggested that the relative orientation of the B-ring with respect to the C-ring was primarily influenced by the conformation of the C-ring,[80] with the steric repulsion between the 2-H$_B$ and 6-H$_B$ atoms and the pyran oxygen atom and/or the 3-OH$_C$ group being the major contributing factor.

The plane of the B-ring of both the E- and A-conformers formed a preferred angle of between 136º and 157º with respect to 1-O$_C$→2-C$_C$ bond in an MM2 study,[81] confirming the results of earlier studies.[22]

The hydrogen and carbon assignments of the B-ring of free phenolic (+)-catechin and two of its derivatives were also determined by 300MHz NMR experiments.[79] A small NOE

---

[79]   R W Hemingway, F L Tobiason, G W McGraw and J P Steynberg, *Magn. Reson. Chem*., 1996, **34**, 424

[80]   W L Mattice, F L Tobiason, K Houglam and A Shanafelt, *J. Am. Chem.Soc*., 1982, **104**, 3359.

[81]   V N Viswanadan and W L Mattice, *Int. J. Biol. Macromol*., 1988, **10**, 209.

association between 6-H$_B$ and 4-H$_C$ was also reported,[78] which indicated the presence of the A-conformer, lending further credibility to the fact that coupling constants must be considered as time-averaged values of a rapidly flexing heterocyclic ring.

## 3.3    CIRCULAR DICHROISM AND THE CONFORMATIONS OF MONOMERIC FLAVAN-3-OLS

It is clear from the discussion on the CD behaviour of simple chroman ring systems in Chapter 2, that the rules that were developed for those systems cannot be applied, "as is", to flavan-3-ols because of the following reasons:

a)      The presence of substituents on the benzene A-ring.

b)      The presence of aromatic substituents at C-2 in monomers as well as at C-4 of the heterocyclic rings in dimers and higher polymers.

c)      The possibility of pseudo axial substituents at C-4 in dimers and higher polymers.

It was reported that hydroxy and/or methoxy substituents on C-5 and C-7 of the aromatic ring as well as C-2 and C-44 of the heterocyclic ring have no effect on the chroman helicity rule. [82] Because flavans-3-ols have two benzene rings, an absorption band for each one of these chromophores is to be expected,[83] the B-ring and the substituent on 3-C of the heterocyclic ring forming the third chiral sphere.[84]

The preference of the B-ring to be in an equatorial position[66] determines the chirality of the C-ring. This, in turn, determines the sign of the Cotton effect of the $^1L_b$ transition. The $^1L_b$ transition is also influenced to a much smaller extent by the configuration of C-3 of the heterocyclic ring. The following Cotton effects were observed for the two types of flavans-3-ols that form part of the profisetinidins from *Acacia mearnsii (2R,3S)* and *Schinopsis balansae (2S,3R)*'[18,20] (Table 3.3.1).

| Stereochemistry | Conformer | Helicity | Sign of $^1L_a$ band (ca. 240 nm) | Sign of $^1L_b$ band (ca. 280 nm) |
|---|---|---|---|---|
| *(2R,3S) 2,3,-trans* | E | P | Positive | Negative |

[82]   S Antus, T Kurtán, L Juhász, L Kiss, M Hollósi and Z S Májer, *Chirality*, 2001, **13**, 493

[83]   O Korver and C K Wilkins, *Tetrahedron,* 1971, **27**, 5459.

[84]   G Snatzke, M Katjár and F Snatzke, *"Fundamental Aspects and Developments in Optical Rotatory Dispersion and Circular Dichroism."* Ed. F Ciardelli and P Salvadori, Heyden & Son Ltd., London, 1973, 148.

| (2R,3S) 2,3,-trans | A | M |  | Positive |
|---|---|---|---|---|
| (2S,3R) 2,3,-trans | E | M | Negative | Positive |
| (2S,3R) 2,3,-trans | A | P |  | Negative |

**TABLE 3.3.1**

These results are the opposite to what is expected according to the helicity rules for tetralins, and are presumed to be due to the fact that the $C_{2v}$ symmetry of the tetralin chromophore is absent in the chroman chromophore. In addition, it is thought that an n→π* transition from the $p_z$ orbital of the oxygen in position 1 of the heterocyclic ring to the π* orbital of the A-ring might also be involved.[83]

The absolute configuration at C-3 of the heterocyclic ring seems to determine the sign of the CE of the $^1L_a$ transition. Flavan-3-ols with 2,3-*trans* configuration are therefore expected to have opposing signs for the CE's of their $^1L_a$ and $^1L_b$ bands, which is indeed, the case. The only exception so far, being the compounds where the A-ring is devoid of any hydroxyl substituents.[18]

DFT methods, using a 6-31+G* basis set were found to be acceptable for the calculation of simulated CD spectra of (2R,3S,4R)-flavan-3,4-diol.[24] The data thus obtained were consistent with experimental data.[20] The negative signs of both the $^1L_a$ and $^1L_b$ bands in the calculated and experimental spectra, were consistent with a mixture of conformations. The calculated values were negative irrespective of the orientation of the hydroxy groups of the catechol moiety.

# CHAPTER 4

# The Conformational Behaviour of 4-Arylflavan-3-ols

## 4.1    NMR STUDIES OF SELECTED FREE PHENOLIC 4-ARYLFLAVAN-3-OLS

A series of unique free phenolic, diastereomeric 4-arylflavan-3-ols, with stereochemistry analogous to the most common procyanidins and profisetinidins found in nature, were synthesised. Their spectroscopic properties were determined with a view to use the data in order to model the structure and conformations of naturally occurring polyflavanoids.[85,86]

Two of the 12 compounds synthesised have similar heterocyclic ring stereochemistry and 4-$C_C$ substituents to the profisetinidins found in *Acacia mearnsii,* namely the (*2R,3S,4R) or 2,3-trans-3,4-cis* (Figure 4.1.1, Compound B) and *(2R,3S,4S) or 2,3-trans-3,4-trans* (Figure 4.1.1, Compound A) diastereomers*. They also have phloroglucinolic substituents on 4-$C_C$, with D-ring oxygenation patterns analogous to those of the profisetinidin dimers.

300MHz NMR experiments displayed, as expected, ABX spin systems for rings A and B of both compounds, with the D-rings having AA' systems with coupling constants of 2.5 – 3.0 Hz at – 40$^o$C, which were broadened at room temperature in each case due to slow rotation on an NMR time scale around the 4-C→2 bonds. The B-ring protons were more deshielded than the A-ring protons, with the D-ring protons being the most shielded in each case.

---

[85]   P W van Zyl, M.Sc Dissertation, University of the Orange Free State, 1993.

[86]   P W van Zyl, J P Steynberg, E V Brandt and D Ferreira, *Magn. Reson. Chem.* 1993, **31**, 1057.

Fisetinidol-(4α→2)-phloroglucinol          Fisetinidol-(4β→2)-phloroglucinol
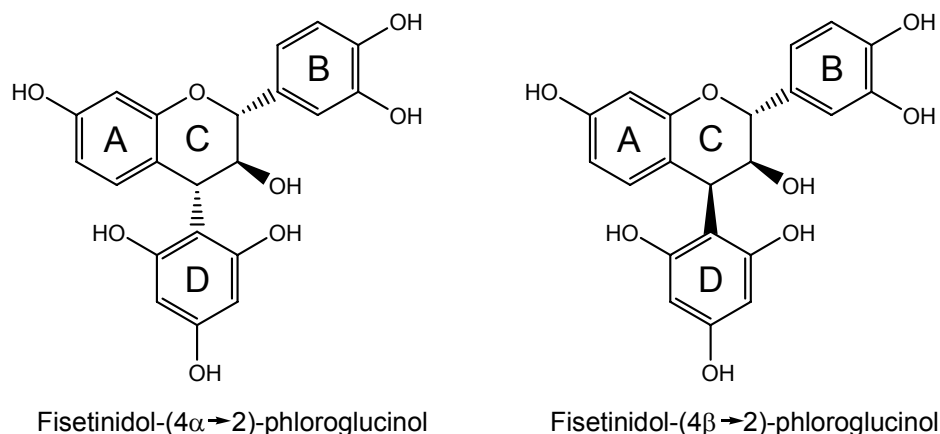
**FIGURE 4.1.1**

The C-ring protons of the *2,3-trans-3,4-trans* isomer, fisetinidol-(4α→2)-phloroglucinol (Figure 4.1.1), gave a second order spectrum at room temperature as a result of coincidental equivalence, which simplified to a typical ABC system at –40$^\circ$C. All C-ring protons displayed coupling constants equal to 9.5 Hz, indicating a notable presence of the E-conformer at this temperature, which is consistent with/indicative of a 2,4-cis aromatic substitution pattern.

This is in contrast to the small coupling constants observed for the C-ring protons of the *2,3-trans-3,4-cis* isomer, fisetinidol-(4β→2)-phloroglucinol (Figure 4.1.1) indicating a major contribution by the A-conformer, as has been observed in many analogous "5-deoxy" proanthocyanidins.[85] The *2,3-trans-3,4-cis* isomer also displayed NOE effects between 4-H$_C$ and 2/6-H$_B$, further supporting the contribution of an A conformer with the B-ring in an axial position.

The existence of the A-conformer of fisetinidol-(4α→2)-phloroglucinol is energetically unfavourable according the classical stereochemical theory of the instability of 1,3-diaxial interactions in a six-membered ring. It can, however, be explained by the existence of π-π stacking.[87] When two aryl groups are within proximity of each other with an offset face-to-face arrangement, the net force between their respective π-systems becomes attractive. These interactions also have implications for the conformational analysis of oligomeric and polymeric tannins, as well as their complexation with proteins and other bio-molecules having similar π-systems.

---

[87]   C A Hunter and J K M Sanders, *J. Am. Chem, Soc.,* 1990, **112**, 5525.

## 4.2 CIRCULAR DICHROISM AND THE CONFORMATIONS OF 4-ARYL-FLAVAN-3-OLS

Two Cotton effects are observed for these compounds: a $^1L_a$ band at around 200-240 nm and a $^1L_b$ band at around 260-280 nm. If the relationship between the helicity of the pyran ring and the sign of the $^1L_b$ band is known, the conformation of the heterocyclic ring can be deduced from the CD spectrum.[19] Complimentary information, derived from NMR experiments, is then used to assign the relative configuration between the constituents of the third chiral sphere.

If there are minor changes in the chiral centres close to the chromophore, it will cause large changes to the sign and amplitude of their Cotton effects. Hence, small changes in the spatial orientation and the conformation of the heterocyclic ring of methyl ether acetate and peracetate derivatives of 4-arylflavan-3-ols have been shown to cause large changes to both the amplitude and the sign of the observed CE's.[88,19]

### 4.2.1 METHYL ETHER 3-ACETATE DERIVATIVES OF 4-ARYL-FLAVAN-3-OLS.

The CD curves of the methyl ether acetate derivatives of 2,3-*trans* and 2,3-*cis*-4-arylflavan-3-ols have multiple, high amplitudes CE's in the region of the $^1L_a$ band at 220 – 240 nm due to the presence of the C4-aryl chromophores when compared to the CE's of flavan-3-ols.[89] These CE's completely overshadow the CE's caused by the chiral perturbation of the C2 and C3 substituents which are normally observed at higher wavelengths. As a rule, a positive CE indicates a β-orientated quasi-axial C4-aryl group and a negative CE an α-orientated quasi-equatorial C4-aryl group.

Deviations in the dihedral angles of the heterocyclic ring substituents have a significant effect on the sign of the CE. The aromatic quadrant rule[90] can been applied to rationalise this phenomenon: With the plane of the A-ring in a horizontal position, looking down the C4-C5a bond, a line perpendicular to the plane of the A ring divides the space around the C4-C5a bond into four quadrants. The sign of the low wavelength CE caused by the C4-aryl

---

[88]    J H van der Westhuizen, D Ferreira and D G Roux, *J. Chem. Soc., Perkin Trans. I*, 1981, 1220 – 1226.

[89]    J J Botha, D Ferreira and D G Roux, *J. Chem. Soc., Chem. Commun*., 1978, **16**, 698 – 700.

[90]    G G DeAngelis and W C Wildman, *Tetrahedron*, 1969, **25**, 5099 – 5112.

chromophore will depend on the quadrant in which the D-ring chromophore is (Figure 4.2.1).

Plane of the A-ring $\longrightarrow$
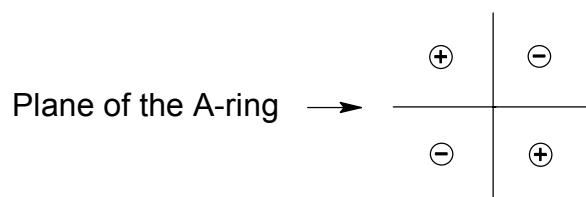
FIGURE 4.2.1

Conformational studies of 4-(2,4-dihydroxyphenyl)-5-oxyflavan-3-ol derivatives[91] indicate that the E-conformers of the 2,4-*cis* isomers experience 1,3-allylic strain between the D-ring and the 5-OMe group. This is relieved by inversion of the heterocyclic ring to a half-chair A-conformer with the C4-α aryl group in a quasi-axial orientation relative to the plane of the A-ring.

Although A-conformers with 1,3-diaxial interactions are considered to be energetically less favourable, the following factors are considered to contribute to their stability:

a)      The aromaticity of the C2 and C4 aryl substituents and their associated geometry with an offset face to face arrangement, lends itself to π-stacking which is a stabilising π-π attraction.[87]

b)      A π-σ stabilising interaction between the π-system of the A-ring and a CH-bond of the C3-OMe group of the B-ring could further contribute to the stability of the A-conformer.[92]

In contrast, the E-conformer of the 2,4-*trans* isomers will experience less 1,3-allylic strain between the D-ring and the 5-OMe group with the C4-β-aryl group being in a quasi-axial position. This is consistent with the ^{1}H NMR coupling constants observed as well as the CD spectra of these compounds.[91]

## 4.2.2    FREE PHENOLIC 4-ARYLFLAVAN-3-OLS

[91]   J P Steynberg, E V Brandt and D Ferreira, *J. Chem. Soc., Perkin Trans. II*, 1991, 1569 – 1573.
[92]   M Nishio and M Hirota, *Tetrahedron*, 1989, **45**, 7201 – 7245.

A series of 3',4',5,7-tetrahydroxy- and 3',4',7-trihydroxyflavan-3-ols coupled to resorcinol or phloroglucinol afforded CD spectra with negative CE's at 230-240 nm for those structures with C-4α substituents and positive CE's for those structures with C-4β substituents. Two of these compounds, as well as their permethyl ether acetates had reverse results. The sign of the CE in each case was rationalised by using the aromatic quadrant rule.

Catechin-(4α→2)-phloroglucinol and catechin-(4α→2)-resorcinol also displayed abnormal CE's.[85,86] The latter two compounds both displayed positive CE's at around 237 nm, even though they have C-4α substituents. Predicted and experimental CE's observed could be explained only if the C-ring were in boat conformations. This would, however, result in a considerable amount of steric strain.

2R and 2S configurations were also confirmed by negative CE's and positive CE's at 290 nm, respectively.

# CHAPTER 5

# The Conformational Behaviour of Dimeric Profisetinidins and Procyanidins

## 5.1    DECAY OF FLUORESCENCE AND POLYMERIC DISORDER.

The polymeric disorder of free-phenolic procyanidins[16,17] as well as profisetinidins[16] was determined by steady state fluorescence and time–resolved fluorescence decay. The absorption spectra as well as the quantum yields of both sets of compounds are similar, implicating that they also have the same radiative decay processes.

The decay of fluorescence intensities of the profisetinidin dimers fisetinidol-(4α→8)-catechin and fisetinidol-(4β→8)-catechin, were best described by the sum of two exponentials, which indicates that they both exhibit slow rotation about the interflavan bond on a fluorescence time scale (ns).

The fraction of fluorescence intensity ($f_i$) contributed by each rotamer was calculated. The relative amounts of the two rotational isomers of fisetinidol-(4α→8)-catechin are near 50:50. A higher fraction of one of the two rotamers of fisetinidol-(4β→8)-catechin was observed ($f_i$ = 0.3–0.5). It was concluded, therefore, that profisetinidins with (4α→8)-interflavan bonds should have more disordered, compact conformations than the profisetinidins with (4β→8) interflavan bonds in aqueous solutions.

Procyanidins with (4α→8)-interflavan bonds display fluorescence intensity ($f_i$ = 0.6–0.8) similar to that of the profisetinidin with a (4α→8)-interflavan bond. The procyanidins with (4β→8)-interflavan bonds display fluorescence intensity ($f_i$ = 0.9-0.95), which is very different to their profisetinidin counterparts.

## 5.2 NMR STUDIES AND CONFORMATIONAL BEHAVIOUR OF FREE PHENOLIC DIMERIC PROCYANIDINS

The first unambiguous proton and carbon assignments of a free phenolic proanthocyanidin dimer, catechin-(4α→8)-catechin (Figure 1.5), from 2D NMR, were reported in 1996.[93] Duplication of all resonances indicated the presence of two rotamers. Trace amounts of cadmium nitrate monohydrate [94] was added to the acetone-$d_6$ solution of the dimer in order to afford sharp resonances for the aromatic C-5 and C-7 hydroxy groups of both the A and D rings, thereby facilitating the identification of the resonances of the two different rotamers.

Further studies of this free phenolic dimer[95,96,97] as well as catechin-(4α→8)-epicatechin (Figure 5.2.1) utilising different NMR techniques, as well as line shape analysis,[98] afforded more detailed data with respect to the conformations of procyanidins in different solvents. They were both shown to have a more extended as well as a compact rotational conformer at room temperature. The extended rotamer has the E- and F- rings in front of the upper unit and the compact rotamer has the E- and F-rings of the terminal unit behind the upper unit.

In organic solvents (e.g. acetone-$d_6$ or dioxane), the more compact rotamer of catechin-(4α→8)-catechin (Figure 5.2.1) is slightly preferred, and in water only trace amounts of the more extended rotamer are detected.

---

[93]  T de Bruyne, L A C Pieters, A Dommisse, H Kolodziej, V Wray, T Domke and A J Vlietinck, *Phytochemistry,* 1996, **43(1)**, 265.
[94]  E. Kiehlmann and A.S. Tracey, *Can.J. Chem.,* 1986, 64, 1998.
[95]  T Hatano and R W Hemingway, *J. Chem. Soc., Perkin Trans. II,* 1997, 1035.
[96]  R W Hemingway in [*Proceedings] Polyphenols 96, Bodeaux, France*. Paris INRA: 1996, 81.
[97]  T Hatano, T Yoshida and R W Hemingway, *Plant Polyphenols 2: Chemistry, Biology, Pharmacology, Ecology,* Ed. Gross et.al. Kluwer Academic / Plenum Publishers, New York, 1999.
[98]  PCPMR Spectrum Simulation Program, Version 1. Serena Software, Bloomington, Indiana.
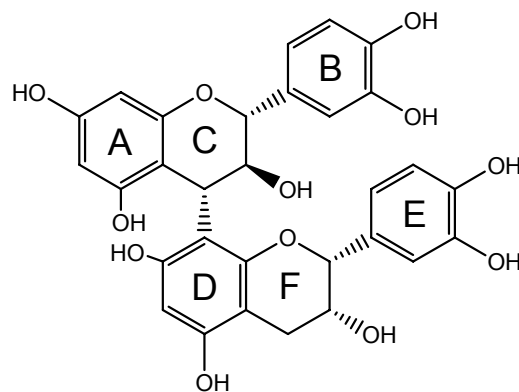
Catechin-(4α→8)-epicatechin

**FIGURE 5.2.1**

The C-rings of both compounds were shown to have an approximate half-chair conformation. In contrast, coupling constants of the F-ring protons indicated a substantial contribution of the A-conformer with the E-ring in an axial position. Line shape analysis of the 3-$H_F$ resonances however, indicated that no E-A conformational interchange is taking place. Adding results obtained from NOE experiments, the F-ring of the catechin-(4α→8)-epicatechin dimer was shown to have a skewed boat conformation. The measured coupling constants of the F-ring of the catechin-(4α→8)-catechin dimer indicated a conformation between a half-chair and a skewed boat (Figure 5.2.2).
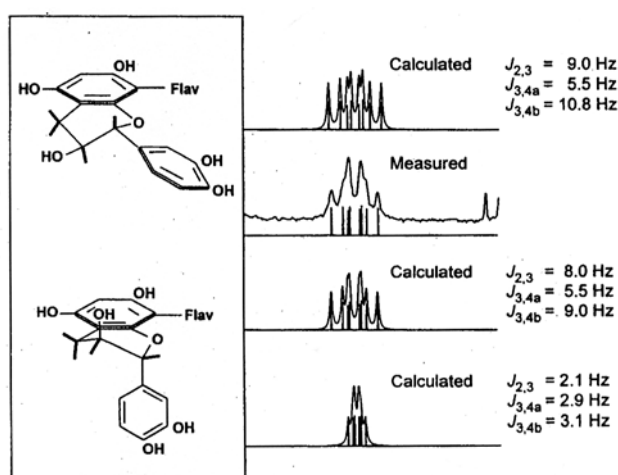


**FIGURE 5.2.2**

Some important features with regards to the use of NMR to assign resonances and distinguish between different rotamers and heterocyclic ring conformations were observed:

a)  Despite the fact that two sets of sharp resonances were observed for each rotamer, correlations between protons of different rotamers in NOE experiments indicated that there is still conformational exchange in the time scale of these experiments.

b)  Long-range COSY experiments show strong cross peaks between 4-$H_C$ and the A-ring protons: 6-$H_A$ and 8-$H_A$. This is analogous to allylic coupling when the dihedral angle between the C-H σ-bond and the π-orbitals is $0^o$. Because the A-ring forms an approximate $90^o$ orientation relative to the 4-$H_C$→4-$C_C$ bond, both rotamers will show these cross peaks.

c)  The cross peaks between 4-$H_C$ and 6-$H_D$ in long-range COSY experiments give an indication of the angle between the upper and lower units of the rotamer. The absence of cross peaks between 4-$H_C$ and 6-$H_D$ is indicative of an angle of closer to $180^o$ or $0^o$ between the 4-$H_C$→4-$C_C$ and 6-$H_D$→6-$C_D$ bonds. A major cross peak indicates an angle of $90^o$ between the 4-$H_C$→4-$C_C$ and 6-$H_D$→6-$C_D$ bonds.

d)  One can distinguish between the protons of the B- and E- rings by cross peaks between 2-$H_C$ and 2-$H_B$/6-$H_B$, as well as between 2-$H_F$ and 2-$H_E$/6-$H_E$.

e)  NOE between 4-$H_C$ and 2-$H_E$ is indicative of the extended rotamer.

f)  The difficulties to distinguish between 6-$H_A$ and 8-$H_A$ in procyanidin dimers are eliminated in the profisetinidin dimers because the "5-deoxy" A-ring has an AMX type proton NMR system.

g)  Hydroxy coupling to 3-$H_C$ can result in broad complex multiplets, which can be resolved by a series of HODEC experiments.

h)  The broad multiplets caused by hydroxy coupling to 3-$H_C$ can be eliminated by addition of small amounts of $D_2O$ to a sample in dry acetone-$d_6$. This can cause overlap of the 3-$H_C$ and 4-$H_C$ resonances resulting in the "virtual coupling" of 2-$H_C$. The 2-$H_C$ doublet can be converted to the expected doublet by adding more or less $D_2O$ to the sample.

i)  One can distinguish between the 2-$H_C$ and 2-$H_F$ resonances by working from the 4-$H_C$ and the 4-$H_F$ resonances in a long range COSY experiment.

j)    The B- and E-ring resonances can be resolved by cross peaks between their 2-H/6-H resonances and the 2-$H_C$ and 2-$H_F$ resonances, respectively.

k)    The B– and E-ring resonances are shifted upfield in the more compact rotamer of both catechin-(4α→8)-epicatechin and catechin-(4α→8)-catechin. This is due to the anisotropic effects between the B- and E-rings when they are in close proximity.

l)    The coupling constants of the heterocyclic F-ring of the more compact rotamer of the catechin-(4α→8)-epicatechin dimer show a skewed boat conformation. If this is combined with the distorted C-ring, appropriate orientation is provided for π-π interaction[87] of the B- and E-rings, accounting for the strong upfield shifts of these resonances.

m)    The coupling constants of the heterocyclic F-ring of the more compact rotamer of the catechin-(4α→8)-catechin dimer show apparently more half-chair character than skewed boat conformation as indicated by line shape analysis and NOESY and NOE correlations between 2-$H_E$ and 4-$H_C$. Calculations with PC Model indicate hydrogen bonding between the 3-$OH_C$ group and the pyran oxygen of the F-ring, placing the B- and E- rings in close proximity.

n)    The more extended rotamer seems to be stabilised by hydrogen bonding between the 3-$OH_C$ and the 7-$OH_D$ groups, according to MMX force field calculations in PC Model.

o)    The compact rotamer is also stabilised by π-π interaction[87] of the B- and E-rings, and hydrogen bonding between the 3-$OH_C$ group and the pyran oxygen of the F-ring. This is also the most abundant rotamer in $D_2O$.

p)    Although the coupling constants of the F ring of the catechin-(4α→8)-catechin dimer in $D_2O$ indicate a time-average of multiple conformations, the line shape analysis does not support this.


## 5.3    NMR STUDIES AND THE CONFORMATIONAL BEHAVIOUR OF FREE PHENOLIC DIMERIC PROFISETINIDINS

The first reported study of a free phenolic profisetinidin dimer, fisetinidol-(4α→8)-catechin (Figure 1.4) also indicated that it has two rotamers in more or less equal quantities when dissolved in organic solvents at ambient temperatures.[78]

NMR spectra were obtained in rigorously dried acetone-$d_6$ in order to obtain a moisture free

environment, slowing down exchange between protons to the extent that they could be observed under NOE conditions. NOE between 4-$H_C$ and 7-$OH_D$ indicated the presence of a compact (crowded), slightly more preferred conformer and NOE between 3-$H_C$ and 7-$OH_D$ indicated the presence of the extended rotamer.

As for the catechin-(4α→8)-catechin and catechin-(4α→8)-epicatechin dimers, the chemical shifts of 2/6-$H_E$ of the compact conformer (6.54 and 6.07 ppm) are significantly lower than those (6.97 and 6.84 ppm, respectively) for the extended conformer and indicate π interaction with the B-ring. This effect could serve as a "fingerprint" for identifying the crowded conformers of procyanidins and profisetinidins.

The exclusive presence of the compact conformer in water was supported by the 6-$H_D$ resonance at 6.05 ppm in the preferred rotamer. Although full assignment of NMR resonances was mentioned, none of them have been published to date, other than those mentioned above.

## 5.4    CIRCULAR DICHROISM AND THE CONFORMATIONS OF DIMERIC PROCYANIDINS.

The CD curves of the deca-acetate derivatives of catechin-(4α→8)-catechin, catechin-(4α→8)-*ent*-catechin, epicatechin-(4ß→8)-catechin and epicatechin-(4ß→8)-*ent*-epicatechin displayed an exciton split Cotton effect appearing as a CD-couplet at λ ≈ 205 nm,[99,51] which is in the region of the [1]B UV absorption band.[19,24] All these compounds also displayed rotamers that were confirmed by a set of duplicate resonances in ^{1}H NMR experiments at ambient temperatures.[100] The conformational ratios between the compact and extended rotamers were related to the sign of their respective couplets, as well as to the chirality of the transition moment vectors of the A and D-rings (Table 5.4.1).

The electronic transition moment vectors are directed along the 10-$C_A$→7-$C_A$ axis and the 8-$C_D$→4-$C_D$ axis of the A- and D-rings, respectively. If the D-ring has an α-orientation with respect to the C-ring, the transition moment vectors display positive chirality which is in

[99]   W Gaffield, L Yeap Foo and L J Porter, *J.Chem. Res. (S)*, 1989, 144 – 145.
[100]   A C Fletcher, L J Porter, E Haslam and R K Gupta, *J. Chem. Soc., Perkin Trans. I*, 1977, 1628 – 1637.

accordance with a positively signed couplet. In a similar manner, a β-orientation of the D-ring with respect to the C-ring will result in negative chirality of the transition moment vectors in accordance with a negatively signed couplet (Figure 5.4.1).
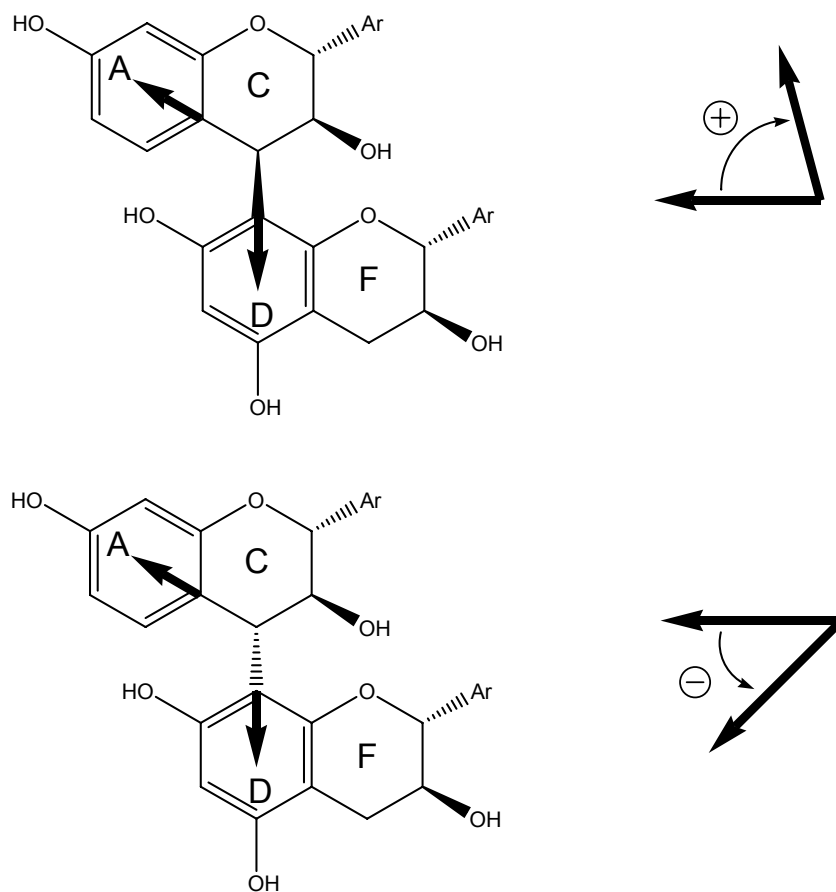


**FIGURE 5.4.1**

The sign of a couplet is the mathematical sign of its amplitude (*A*), which is calculated as follows:[101,102]

$$A = \Delta\varepsilon_1 - \Delta\varepsilon_2$$

$$\Delta\varepsilon = \frac{[\theta]}{3300}$$

*Δε₁* = the differential dichroic absorption at the long wavelength maximum of the couplet

*Δε₂* = the differential dichroic absorption at the short wavelength maximum of the couplet.

| Compound | Δε | λ (nm) | Couplet sign | Conformational ratio compact : extended |
|---|---|---|---|---|
| catechin-(4α→8)-catechin | -66.7 +22.2 | 206 190 | - | 20 : 1 |
| catechin-(4α→8)-*ent*-catechin | -67.5 0 | 205 190 | - | 10 : 1 |
| epicatechin-(4ß→8)-catechin | +73.2 0 | 206 195 | + | 1.5 : 1 |
| epicatechin-(4ß→8)-*ent*-epicatechin | +70.0 0 | 213 198 | + | 1.3 : 1 |

**TABLE 5.4.1**

---

[101]  A I Meyers, T Nguyen, D Soianova, N Sreerama, R W Woody, A Koslowksi and J Fleischhauer, *Chirality,* 1997, **9**, 431 - 434

[102]  P Crabbé, *ORD and CD in Chemistry and Biochemistry*, Academic Press Inc., 1972, 7.

# DISCUSSION

## CHAPTER 6

## THE CONFORMATIONAL BEHAVIOUR OF FREE PHENOLIC PROFISETINIDIN DIMERS FROM *Acacia mearnsii*

**6.1 THE CONFORMATIONAL BEHAVIOUR OF FISETINIDOL-(4α→8)-CATECHIN IN ACETONE-d$_6$.**

The structure of this compound was studied by $^1$H, $^{13}$C, COSY 45, HMQC and NOESY PH NMR experiments in deuterated acetone[103] and CD in methanol (Chapter 8). Several $^1$H NMR experiments were performed on this compound, each differing with respect to the amount of water present (Figure 6.1.1/3), as well as the concentration of cadmium nitrate in the drier samples (Figure 6.1.2/4) The amount of water or cadmium nitrate in the solvent had minor, but not significant effects on the chemical shifts of the aromatic protons (Table 6.1.1), as well as greater or lesser differentiation of especially the heterocyclic ring proton resonances.

---

[103]   Paragraph 9.3, Appendix D
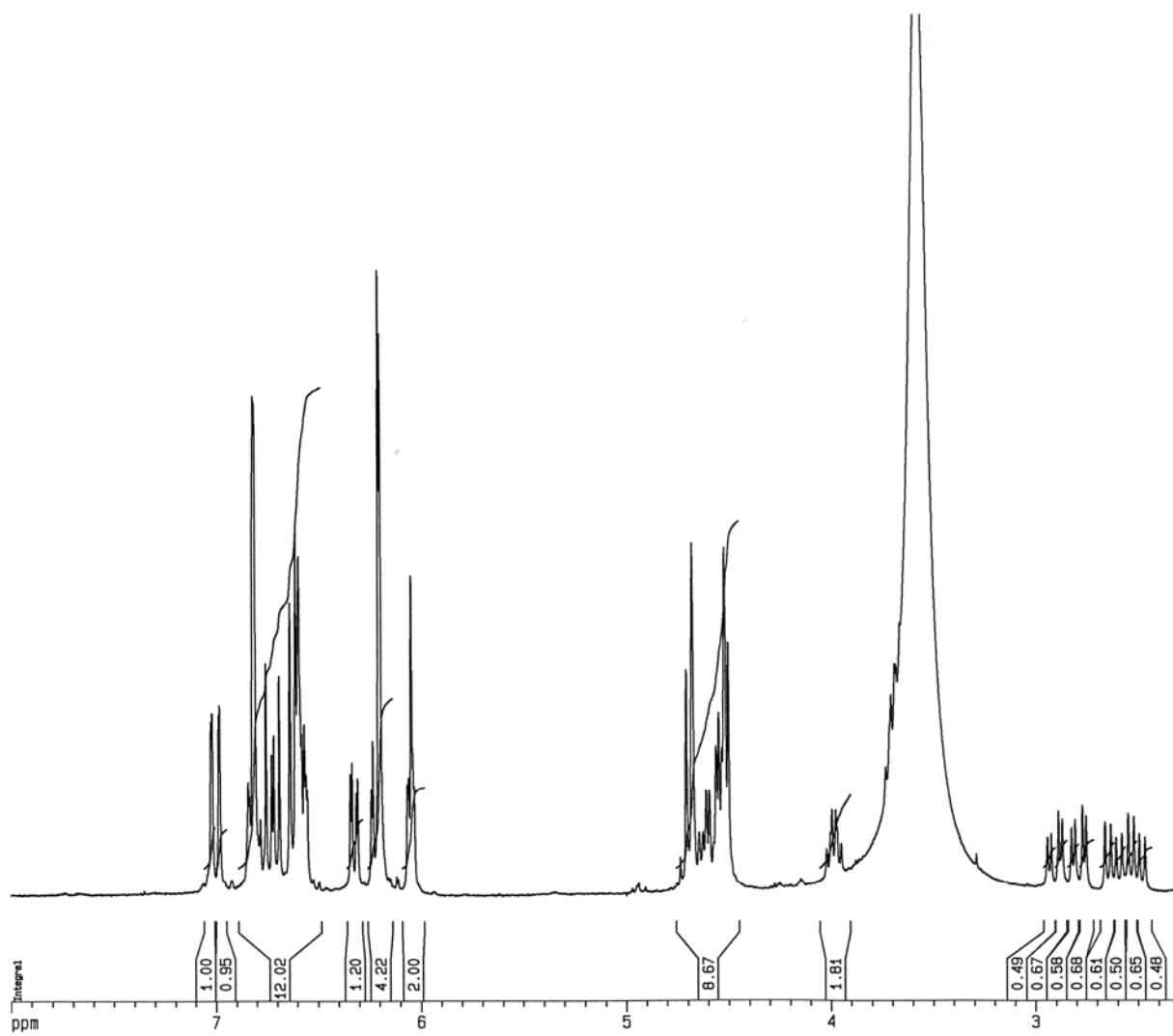
**FIGURE 6.1.1**
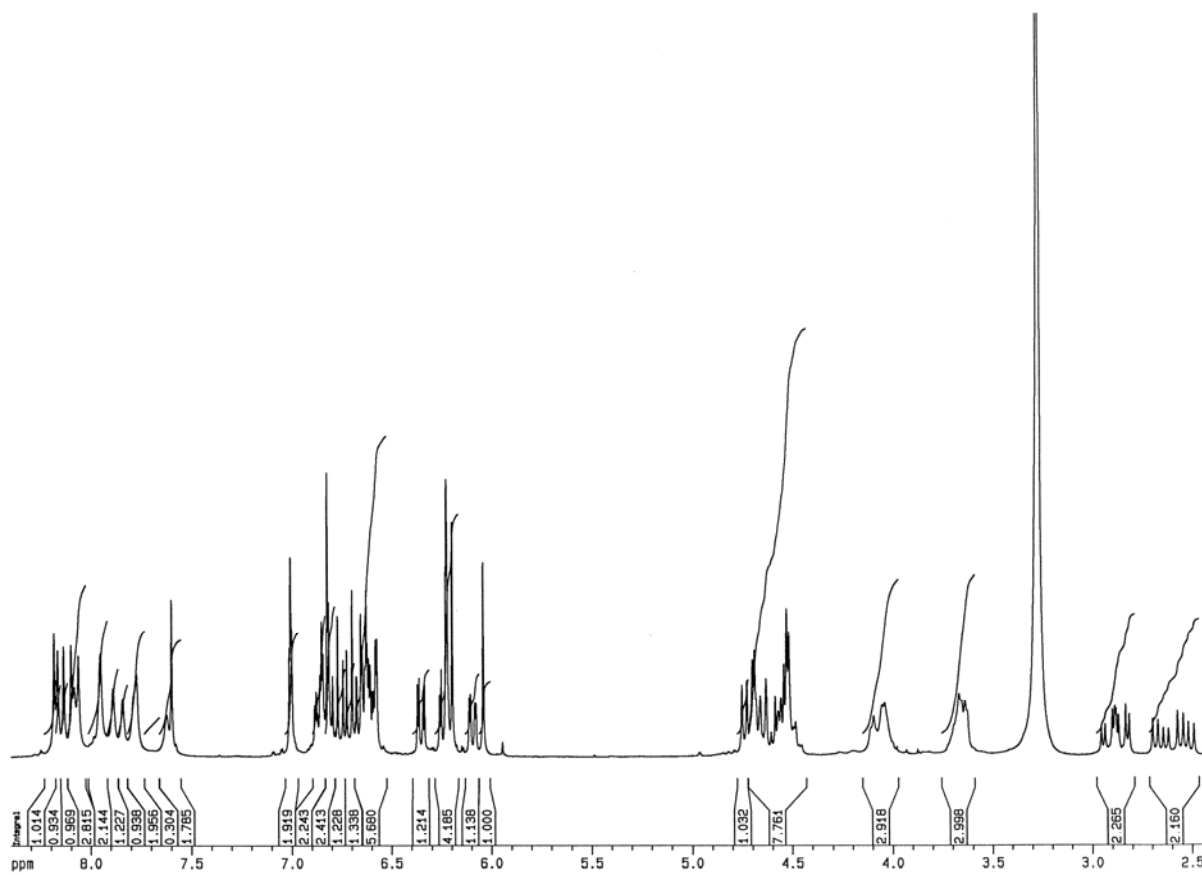
**FIGURE 6.1.2**
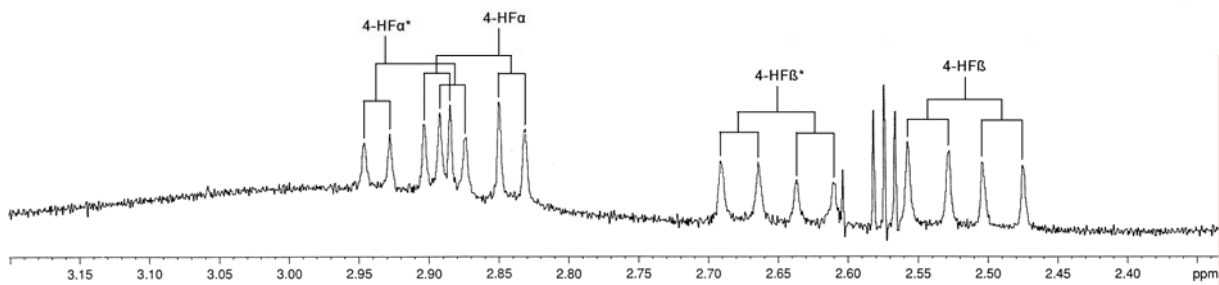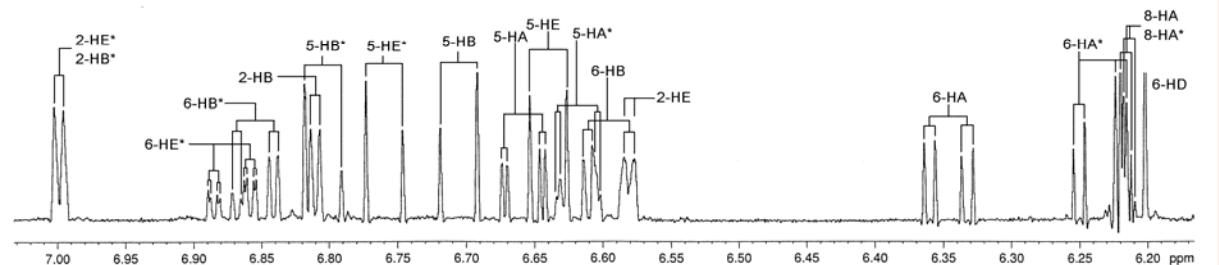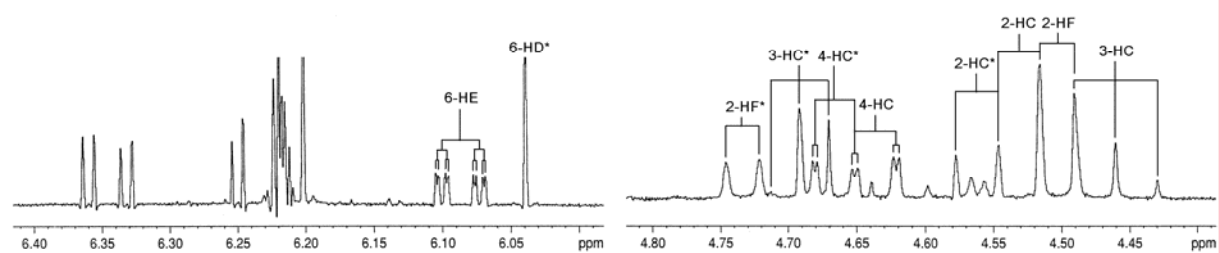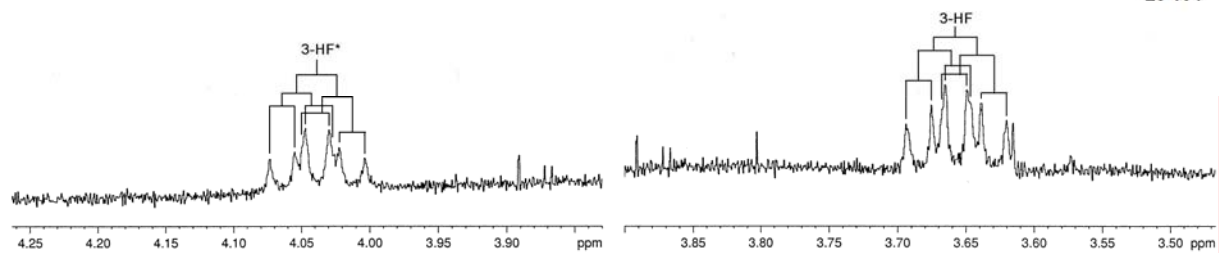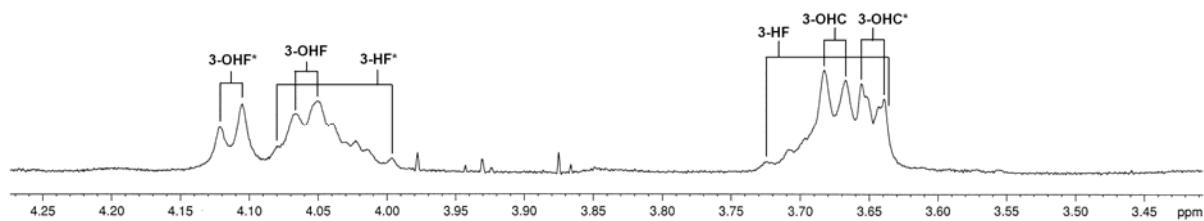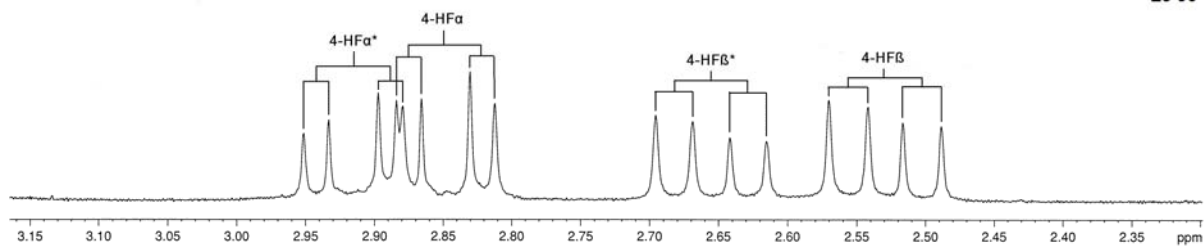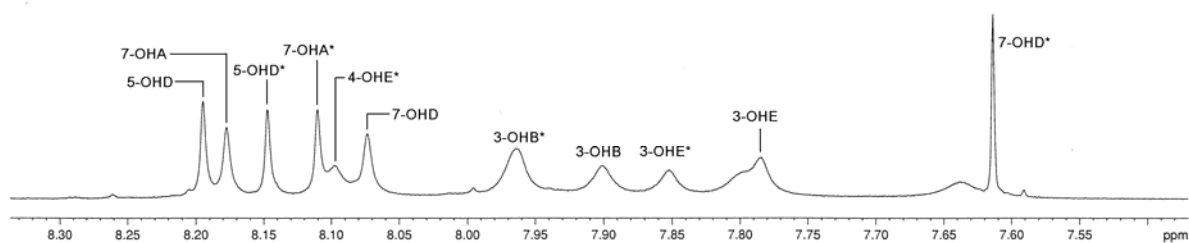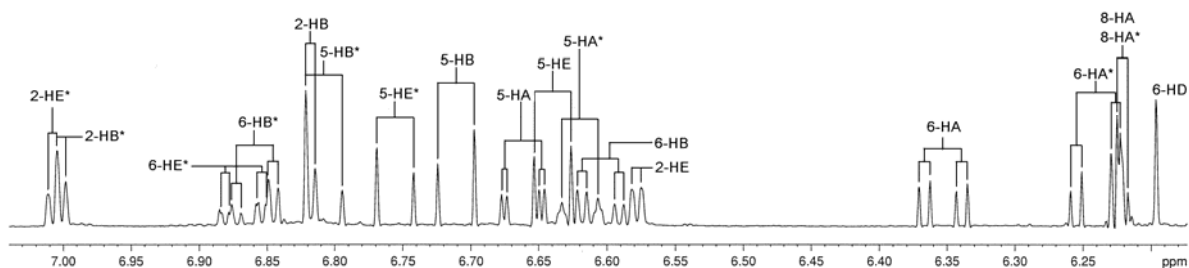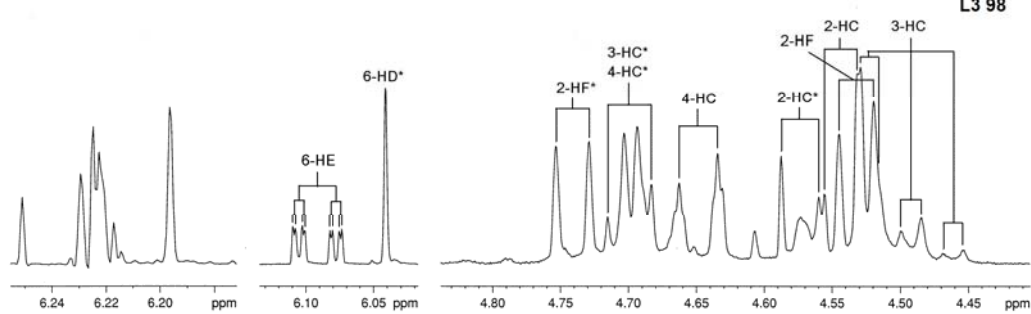
**FIGURE 6.1.3**

**FIGURE 6.1.4**

The chemical shifts of the aromatic A-, B-, D- and E-ring proton resonances of both spectra in acetone were the same if rounded to three significant figures (Table 6.1.1). This indicated that a very small presence of water or cadmium nitrate in the acetone does not have any significant effect on the chemical shifts.

| | (Chemical shift, δ) | | | | | | | |
|---|---|---|---|---|---|---|---|---|
| | B-ring | | E-ring | | A-ring | | D-ring | |
| | $^1H$ | $^{13}C$ | $^1H$ | $^{13}C$ | $^1H$ | $^{13}C$ | $^1H$ | $^{13}C$ |
| 2/8*extended | 7.00 | 114.76 to 115.76 | 7.00 | 114.76 to 115.76 | 6.23 | 102.62 | | |
| 2/8 compact | 6.81 | | 6.78 | | 6.23 | 102.99 | | |
| 5* extended | 6.81 | | 6.76 | | 6.62 | 129.40 | | |
| 5 compact | 6.72 | | 6.54 | | 6.66 | 129.07 | | |
| 6*extended | 6.86 | 120.12 | 6.87 | 119.50 | 6.24 | 108.35 | 6.04 | 96.60 |
| 6 compact | 6.61 | 120.40 | 6.09 | 118.35 | 6.35 | 108.52 | 6.20 | 95.55 |

**TABLE 6.1.1**

The addition of cadmium nitrate mono hydrate slows down hydroxylic hydrogen exchange, hence affording sharper resonances as well as observable coupling of aliphatic hydroxy groups with hydrogen nuclei attached to the same carbon (Figure 6.1.5/6). This results in more complex resonances of the heterocyclic ring protons.
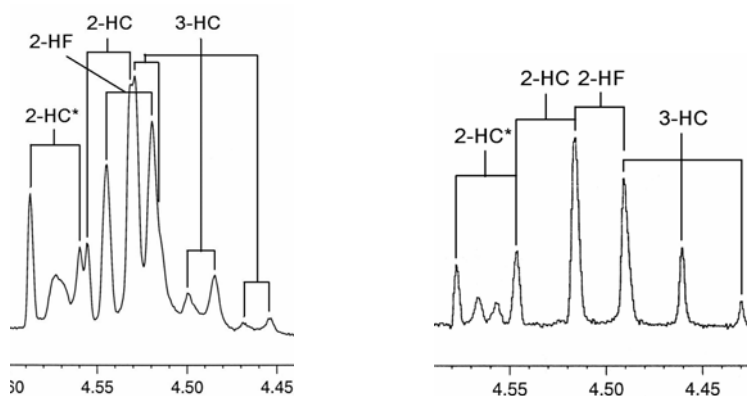


Spectrum with cadmium nitrate     Spectrum without cadmium nitrate

**FIGURE 6.1.5**

The 3-OH$_F$ and 3-OH$_C$ resonances also overlap with the 3-H$_F$ resonances, making any identification of the complex line shapes of the 3-H$_F$ resonances impossible. The assignment of the 3-OH$_F$ and 3-OH$_C$ resonances however greatly contributes to the overall understanding of the conformation of these molecules because of their usefulness in NOE and NOESY experiments. Changes in the concentration of cadmium nitrate (traces of or saturated solutions), and of water in the solution, have different effects on the hydrogen exchange rate.
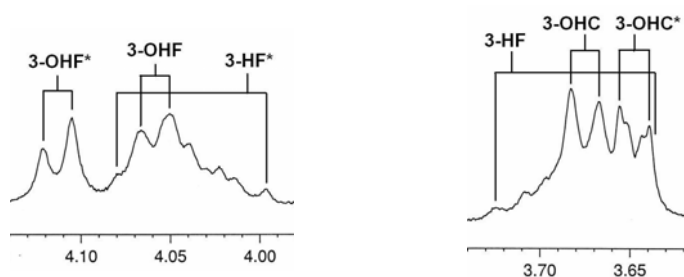


**Spectrum with cadmium nitrate**
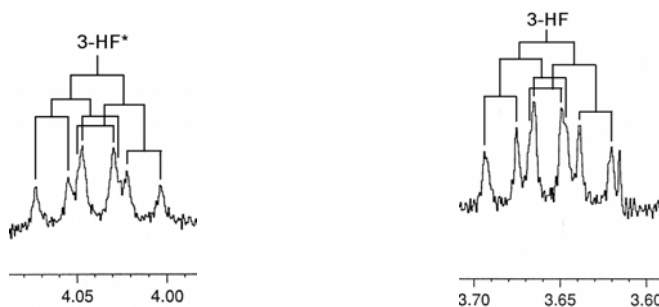


**Spectrum without cadmium nitrate**

**FIGURE 6.1.6**

NMR experiments with and without cadmium nitrate therefore yield complimentary information with regards to the conformational analysis of free phenolic proanthocyanidins.

### 6.1.1  NMR ASSIGNMENTS IN ACETONE D-$_6$ SOLUTION WITH TRACES OF WATER:

A COSY 45 experiment was performed on a sample containing traces of water. The 4-H$_{F\alpha}$ and 4-H$_{F\beta}$ resonances were first assigned (Figure 6.1.7, L3 124). Since half the responses are missing, the lean of the cross peaks confirms the magnitude and the negative sign of the $^2J_{4HF\alpha,4HF\beta}$ vicinal coupling constant.[104,105]
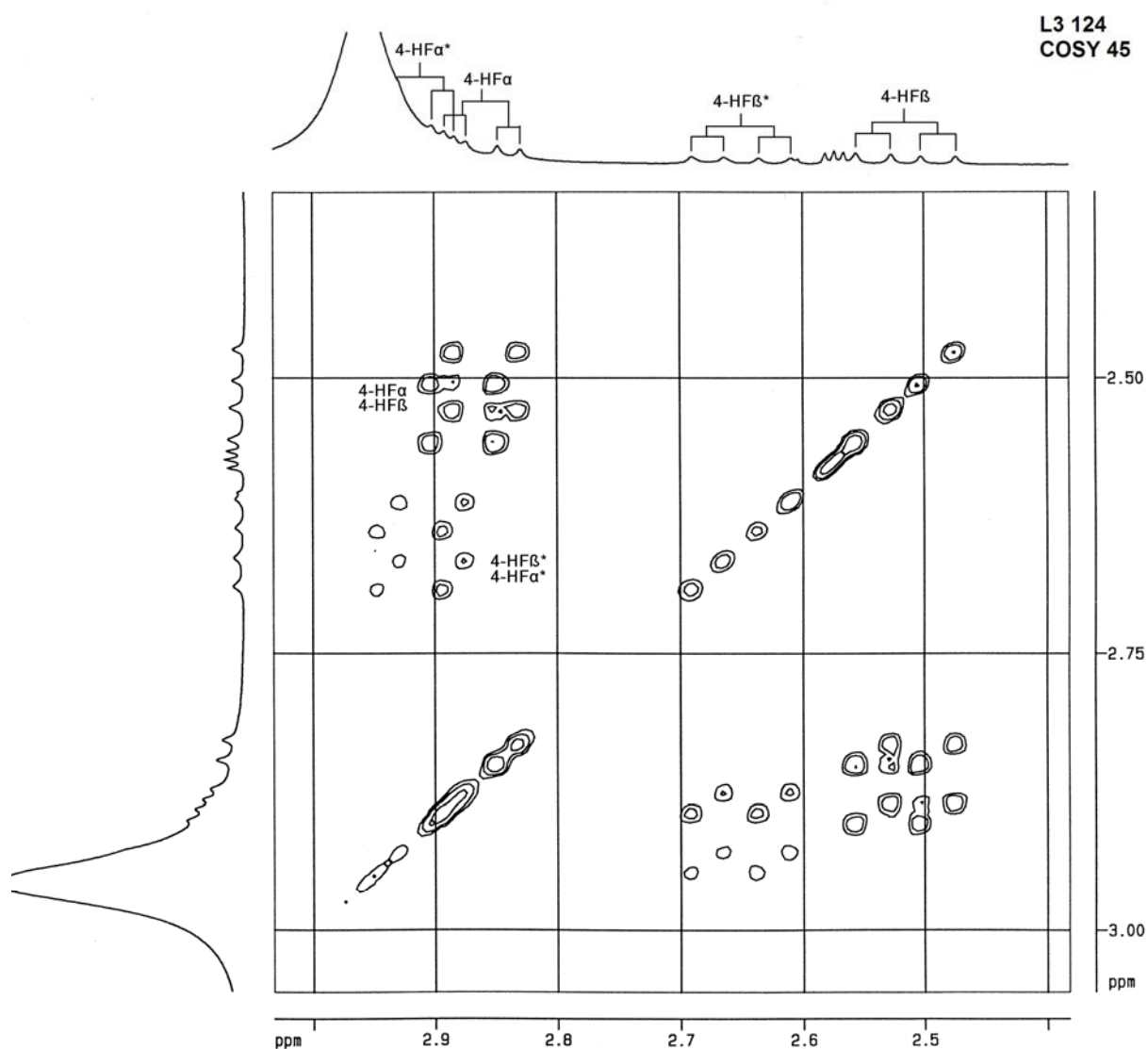


**FIGURE 6.1 7**

104    J W Akitt and B E Mann, *NMR and Chemistry*, 4$^{th}$ Edition, Stanley Thomas, 2000, 285 – 289.
105    S Berger and S Braun, *200 and More NMR Experiments*, Wiley-VCH, 1998, 383 – 385.

These assignments were then used to assign the 3-H$_F$ (Figure 6.1.8, L3 140) and 2-H$_F$ (Figure 6.1.9, L3 142) resonances. The cross peaks between the 4-H$_{F\beta}$ and 3-H$_F$ resonances are stronger and more clearly defined than the cross peaks between the 4-H$_{F\alpha}$ and 3-H$_F$ resonances.
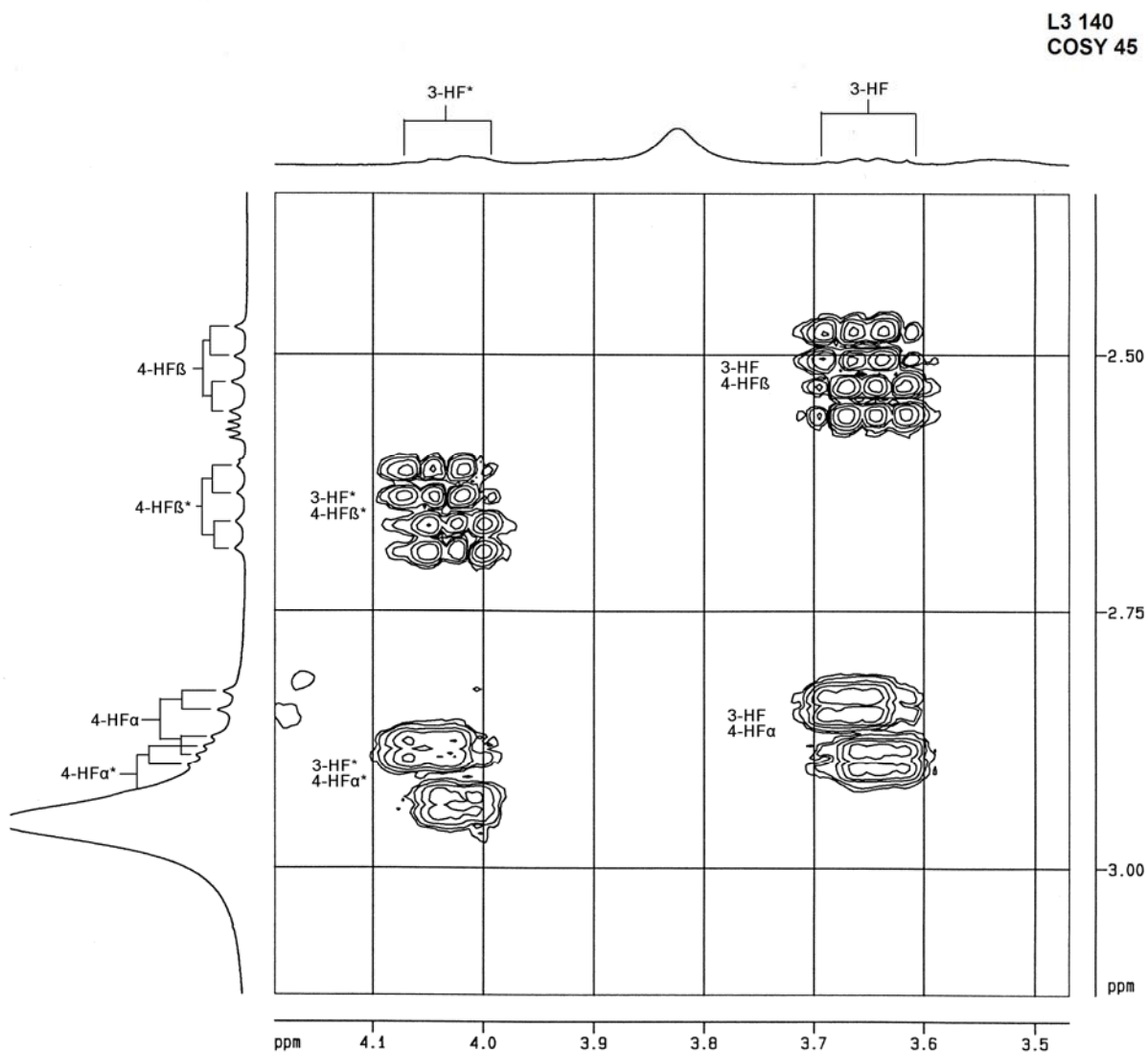


**FIGURE 6.1.8**
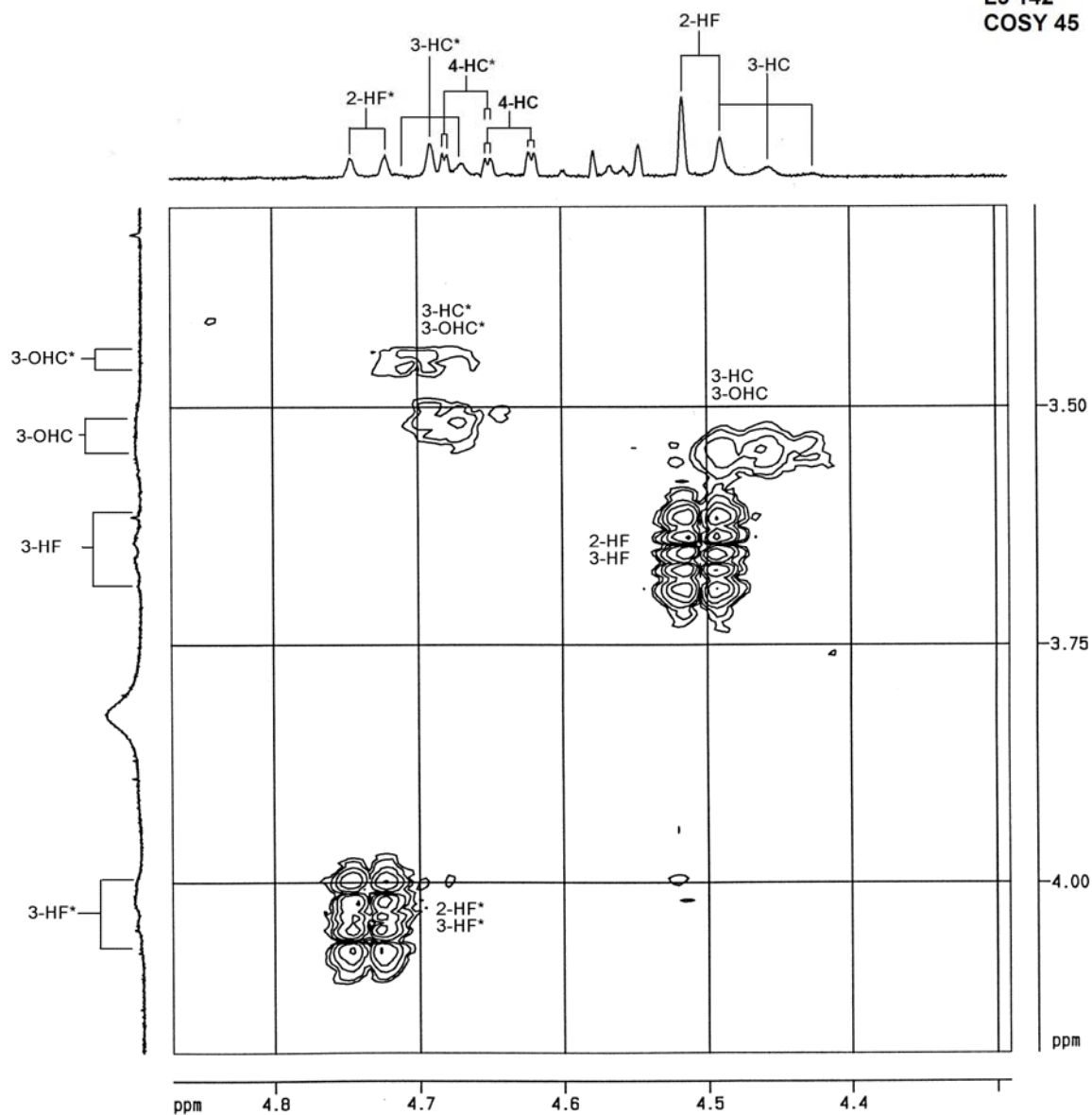
**FIGURE 6.1.9**

Cross peaks are also observed between the 4-H$_{F\beta}$ and 2-H$_F$ resonances (Figure 6.1.10, L3 144). Half of the responses are missing and the lean of the cross peaks confirms the magnitude and positive sign of the coupling constant $^4J_{3HF,2HF}$.
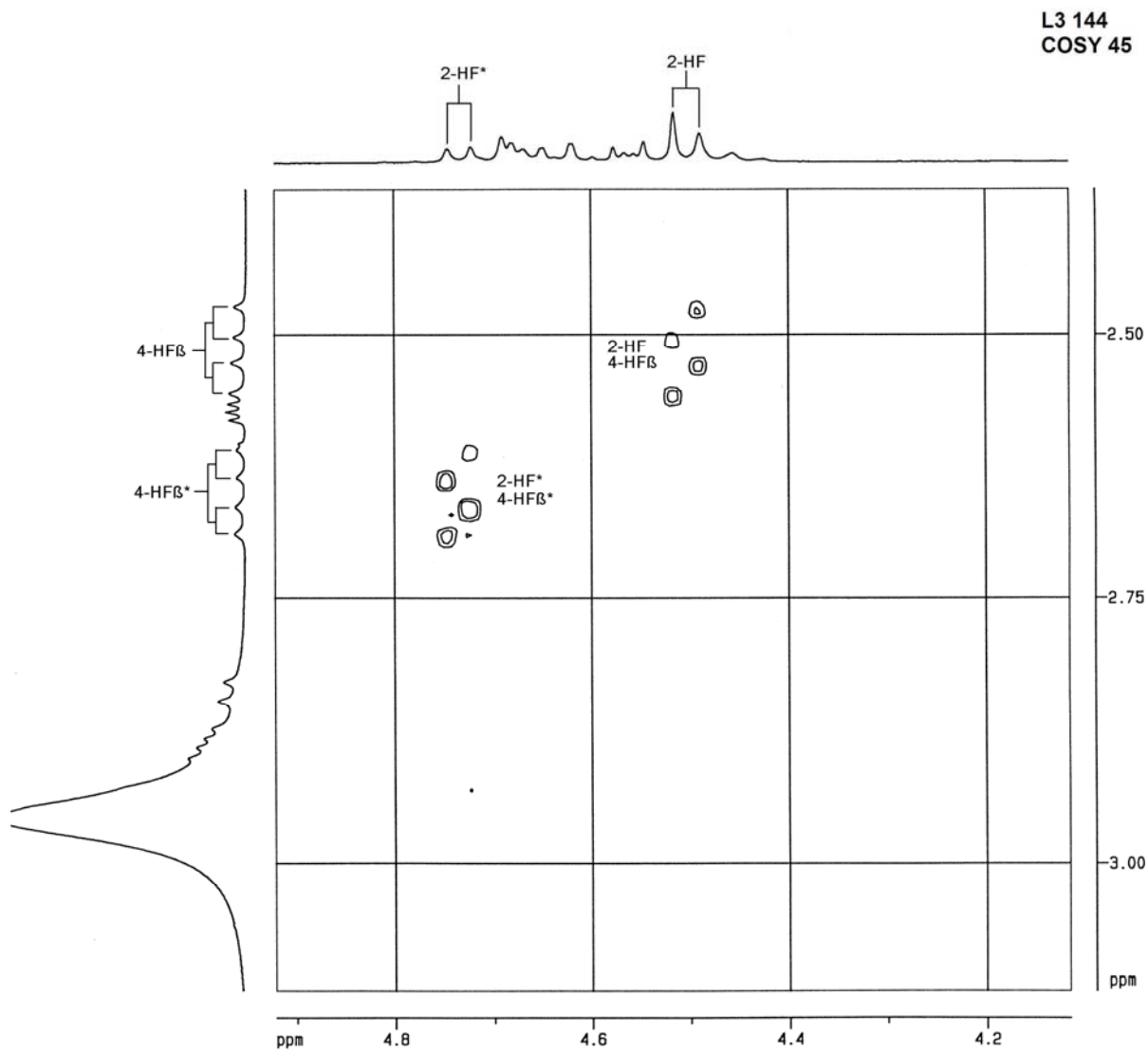


**FIGURE 6.1.10**

Cross peaks are also observed between both sets of 4-H$_F$ and 6-H$_D$ resonances (Figure 6.1.11, L3 125). Strong coupling between a 4-H$_F$ and 6-H$_D$ resonance implies that the 4-H$_F$→4C$_F$ bond is at a 90$^{\circ}$ angle with the 6-H$_D$→6C$_D$ bond and therefore also with respect to the plane of the D-ring. Because of the apparent similarity in cross peak intensity between both sets of 4-H$_{F\alpha}$ and 4-H$_{F\beta}$ resonances with the respective 6-H$_D$ resonances, it can be interpreted that the F-rings of both conformers undergo conformational exchange, with both the 4-H$_{F\alpha}$→4C$_F$ and 4-H$_{F\beta}$→4C$_F$ bonds forming 90$^{\circ}$ angles with the 6-H$_D$→8C$_D$ bond and therefore also with respect to the plane of the D-ring in each case.[97]
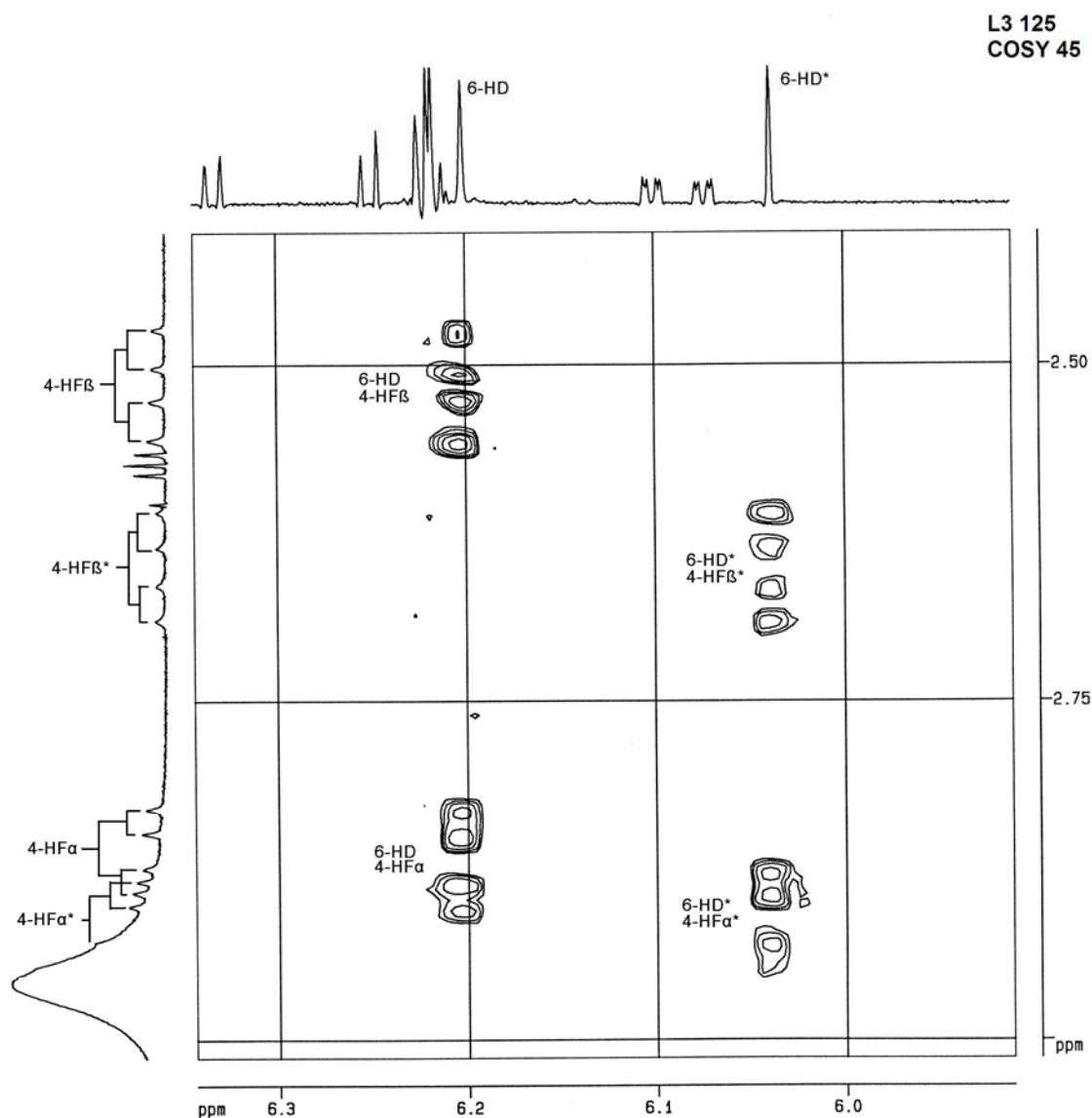


**FIGURE 6.1.11**

The C-ring proton resonances are all in the 4.4 - 4.8 ppm region (Figure 6.1.12, L3 129) with the hydroxy proton resonances being observed in the COSY 45 experiment, but not as clearly on the $^1$H spectrum (Figure 6.1.9, L3 142). Unambiguous assignments were difficult due to the proximity of the C*-ring resonances to the diagonal.
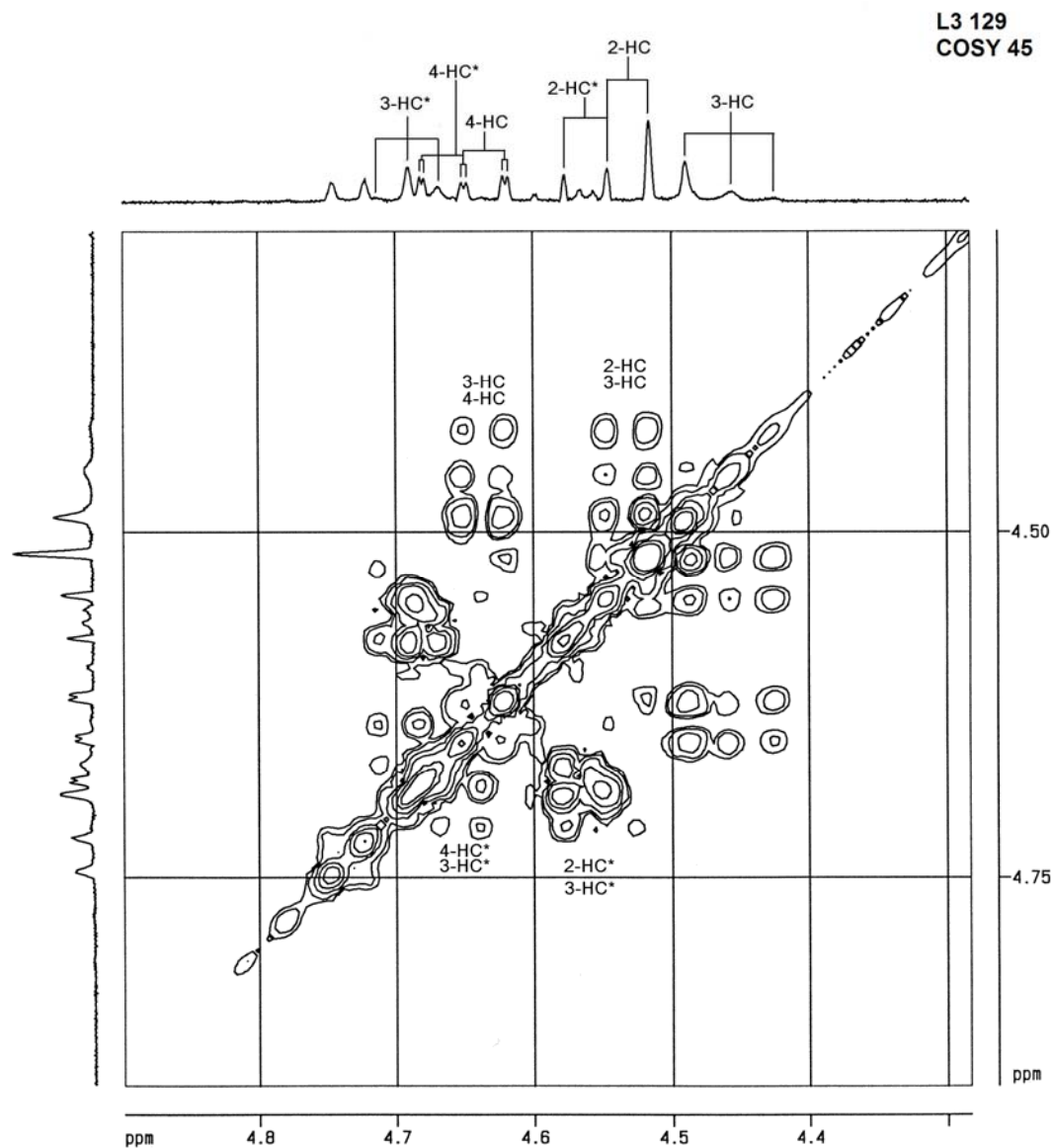


**FIGURE 6.1.12**

An initial set of some of aromatic proton resonances of both rotamers was assigned from their cross peaks with heterocyclic resonances (Figure 6.1.13, L3 146). The COSY plot used to assign the signals showed only strong cross peaks, allowing for unambiguous assignments.
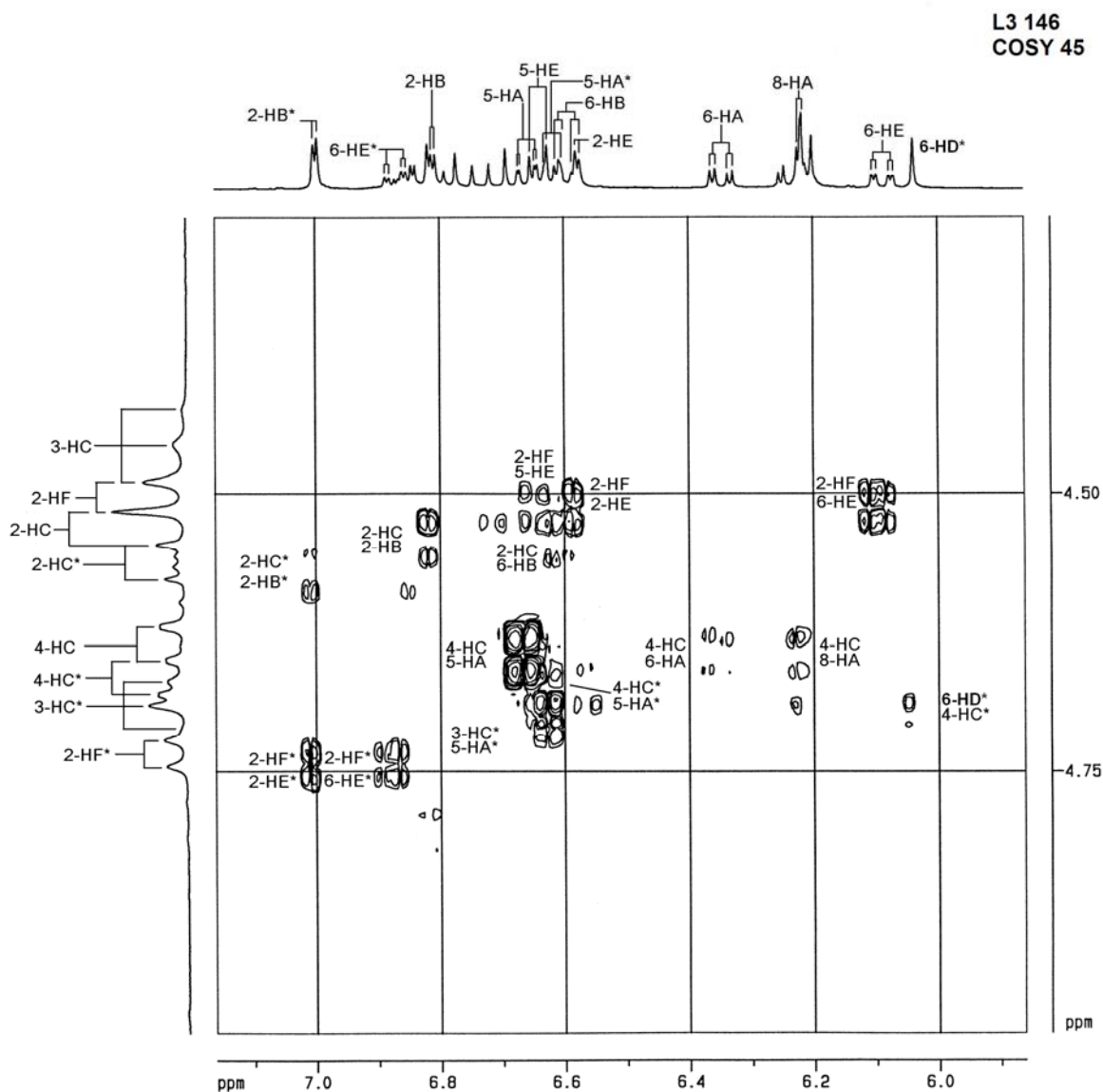


**FIGURE 6.1.13**

The aromatic resonances assigned in Figure 6.1.13 were then used (shown on the horizontal axis in Figure 6.1.14, L3 136) to complete assignment of all aromatic resonances (shown on the vertical axis in Figure 6.1.14, L3 136): The 8H$_A$*/5-H$_A$* cross peaks are partially on the diagonal.
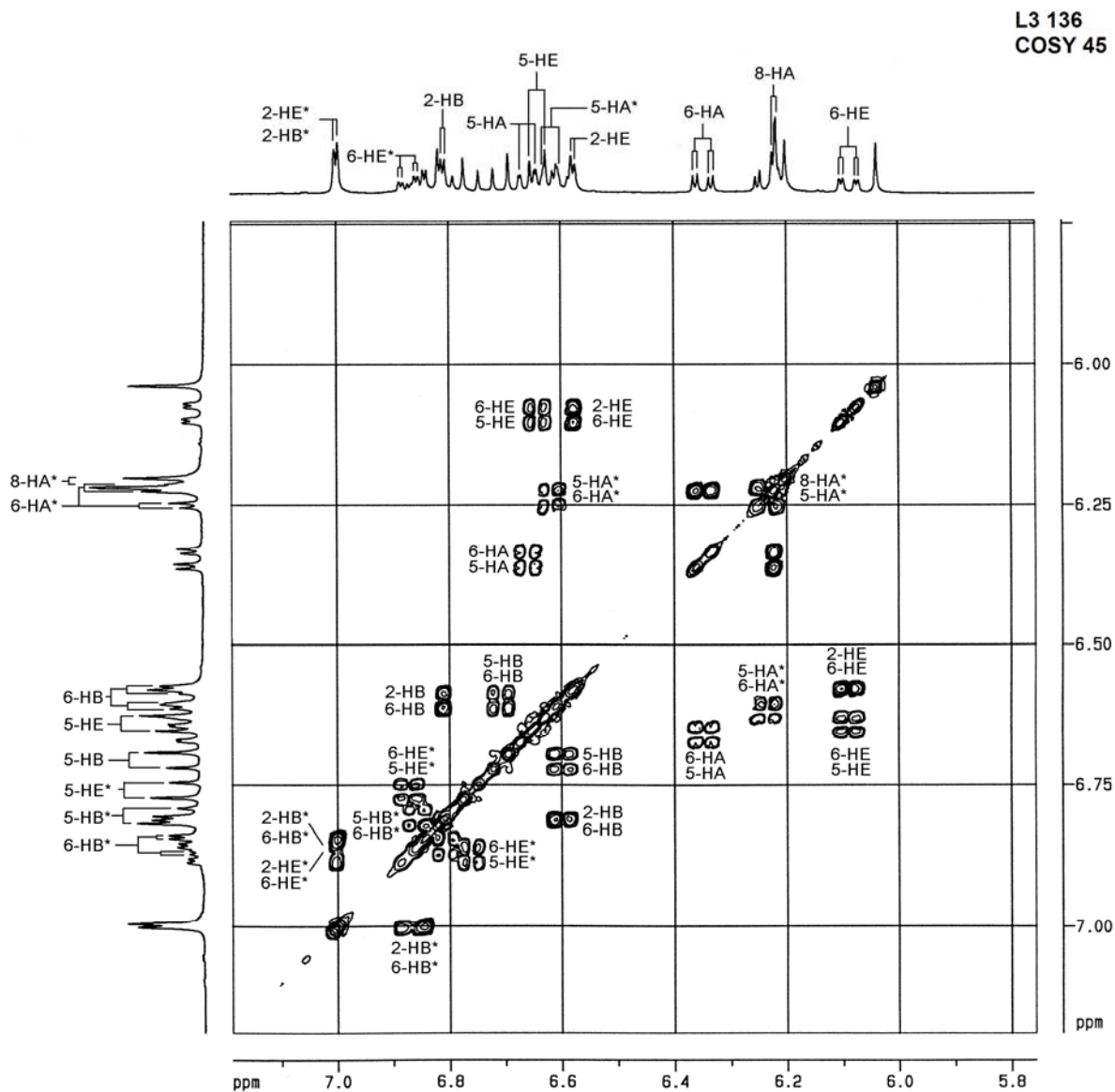


**FIGURE 6.1.14**

## 6.1.2   NMR ASSIGNMENTS IN ACETONE-D$_6$ SOLUTION WITH CADMIUM NITRATE:

The $^1$H NMR, COSY 45 and NOESY PH experiments of the fisetinidol-(4α→8)-catechin dimer in extensively dried acetone-d$_6$ with traces of cadmium nitrate monohydrate were performed in order to assign resonances for the hydroxy groups and then use them to gain more insight in the conformations of the two rotamers. The wet sample also did not have pronounced cross peaks between the 4-H$_C$ and 6-H$_D$ resonances (Figure 6.1.13, L3 146). They are clearly observed in the COSY 45 experiment performed on the sample in extensively dried acetone-d$_6$ with traces of cadmium nitrate monohydrate (Figure 6.1.14, L3 34). These assignments also confirmed the presence of a bond between the D- and A-rings and are therefore vital to the further assignment of aromatic proton resonances.
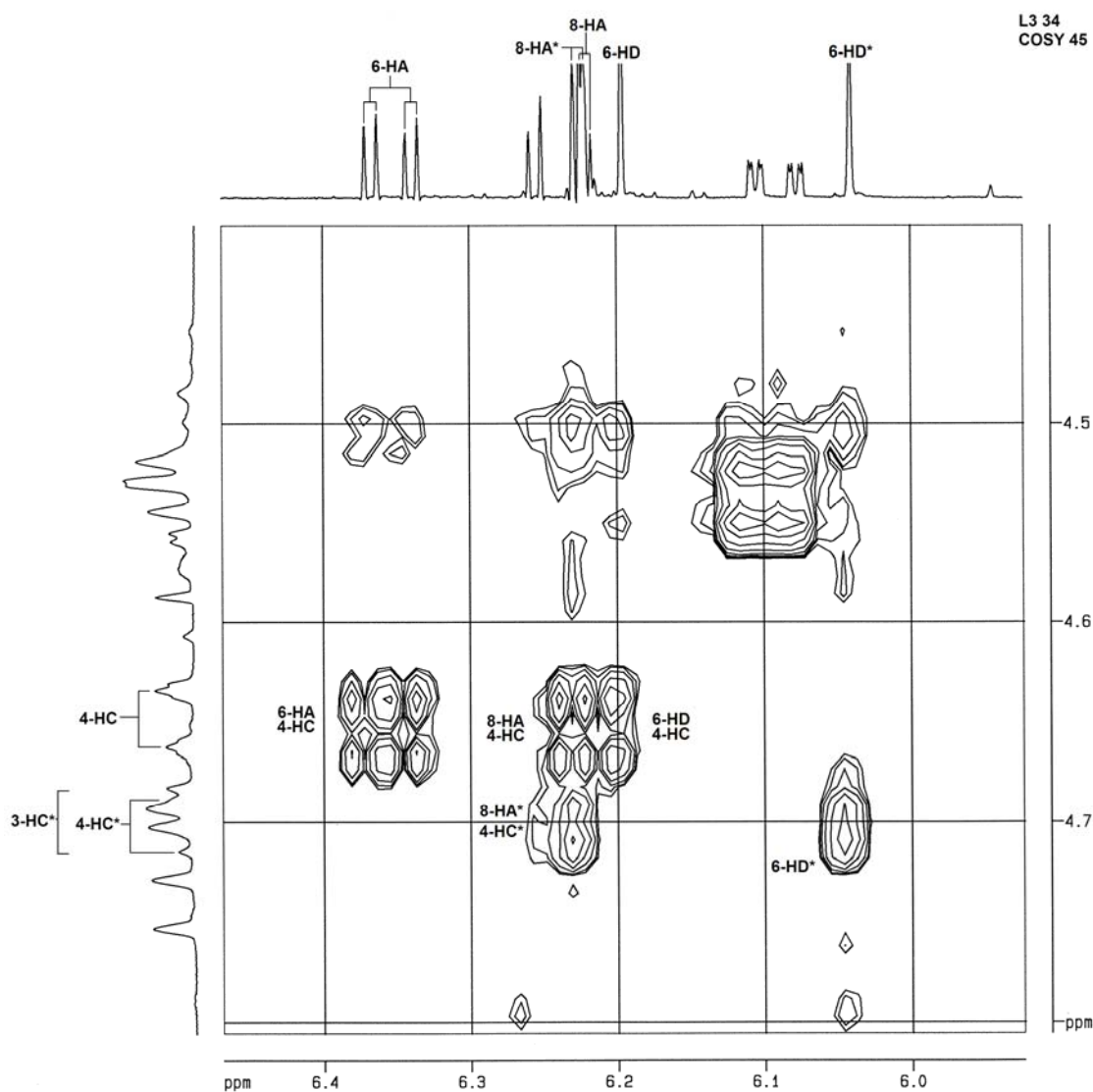


**FIGURE 6.1.15**

The COSY 45 experiment did not afford unambiguous assignment of the 5/7-OHD resonances vital to the recognition of the two different rotamers (Figure 6.1.16, L3 29).
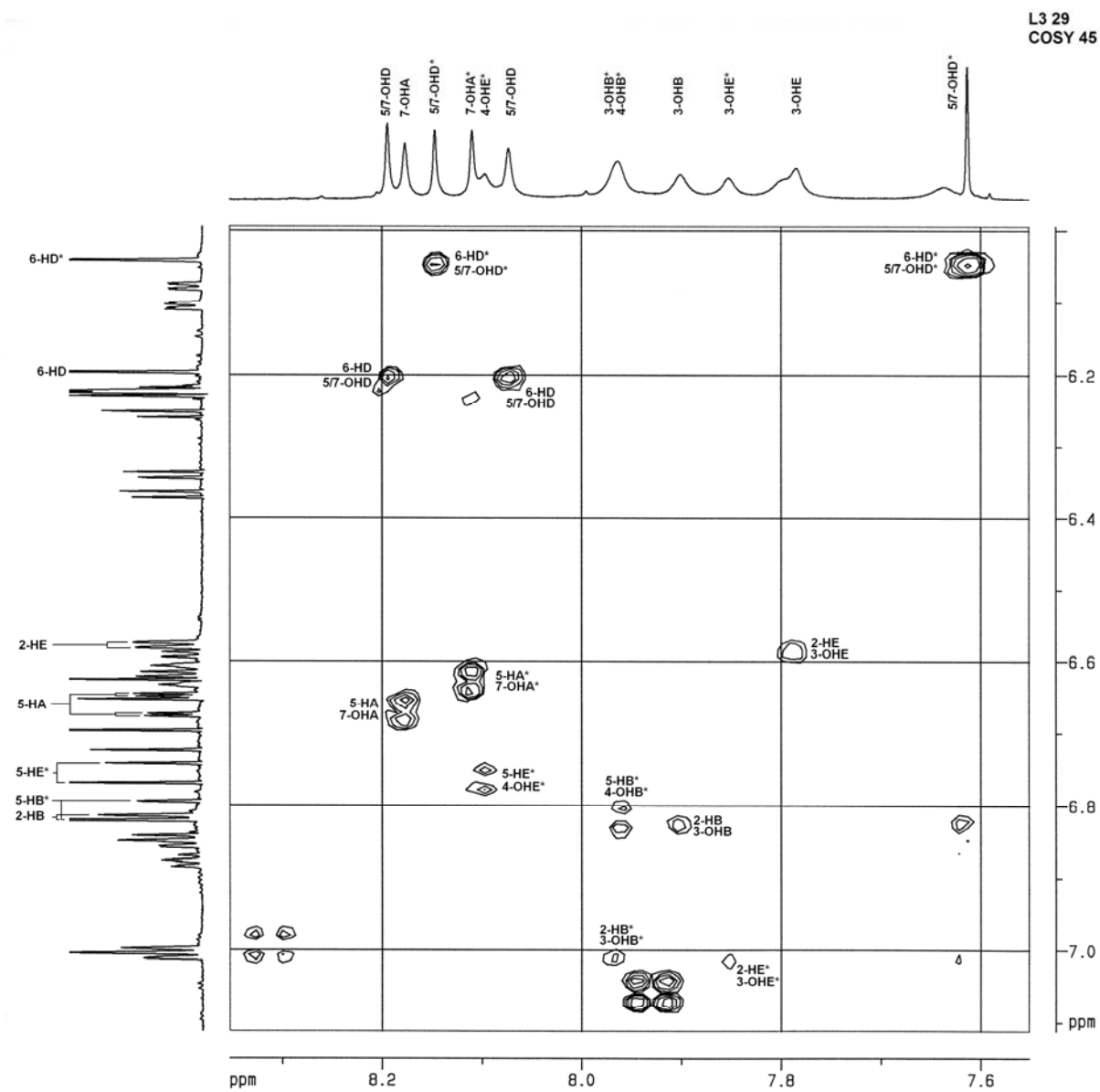


**FIGURE 6.1.16**

A NOESY PH experiment was performed to distinguish between the 5-OHD and 7-OHD resonances (Figure 6.1.17, L3-39) and to assign the heterocyclic ring hydroxy resonances (Figure 6.1.18, L3 41). Cross peaks between the 4-H$_C$ and 7-OH$_D$ resonances as well as the lower chemical shifts of the E- and B- ring resonances identified the compact rotamer as well as the extended rotamer denoted by *. This identification of the two conformers is the same as that reported.[79]
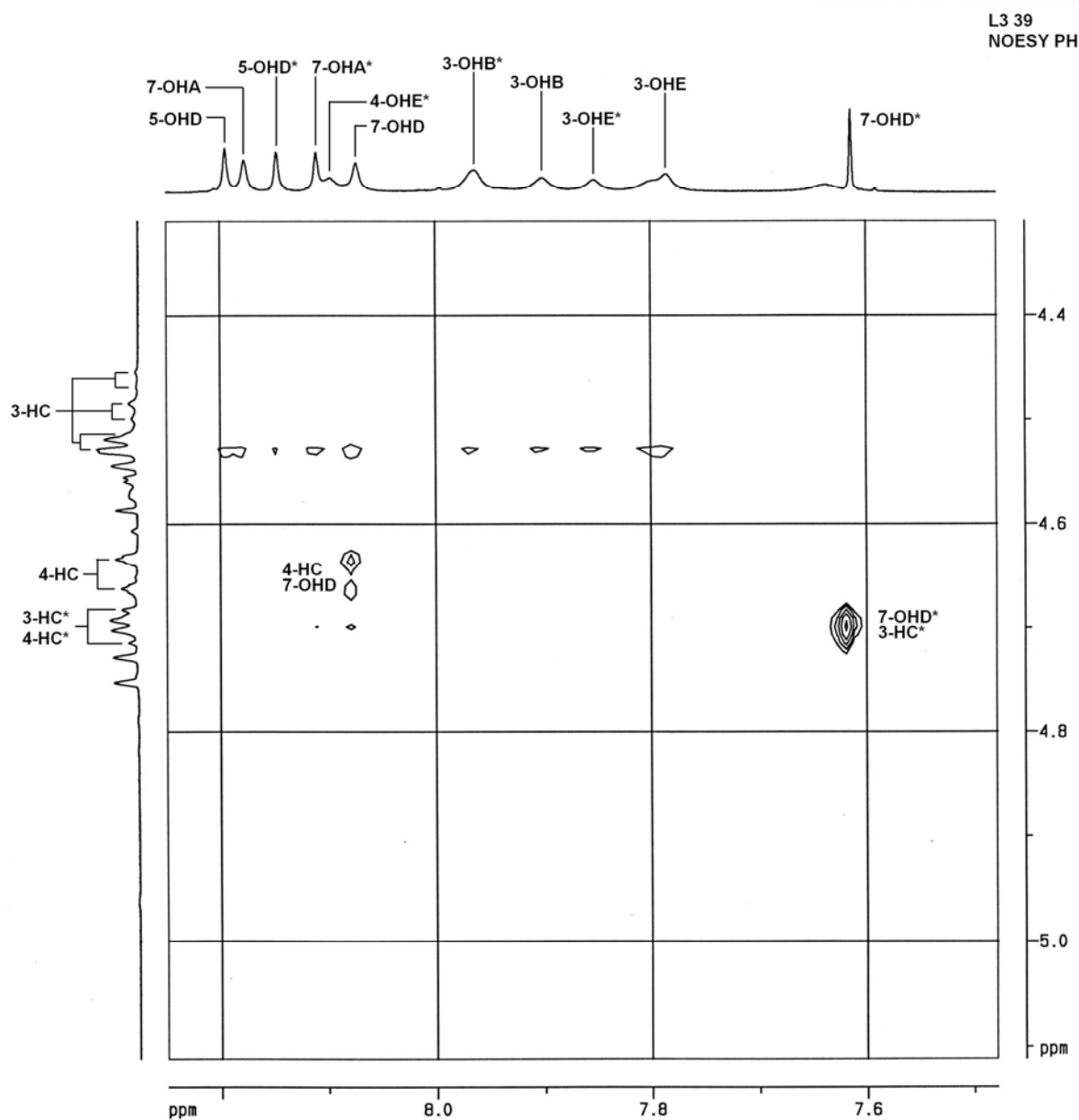


**FIGURE 6.1.17**
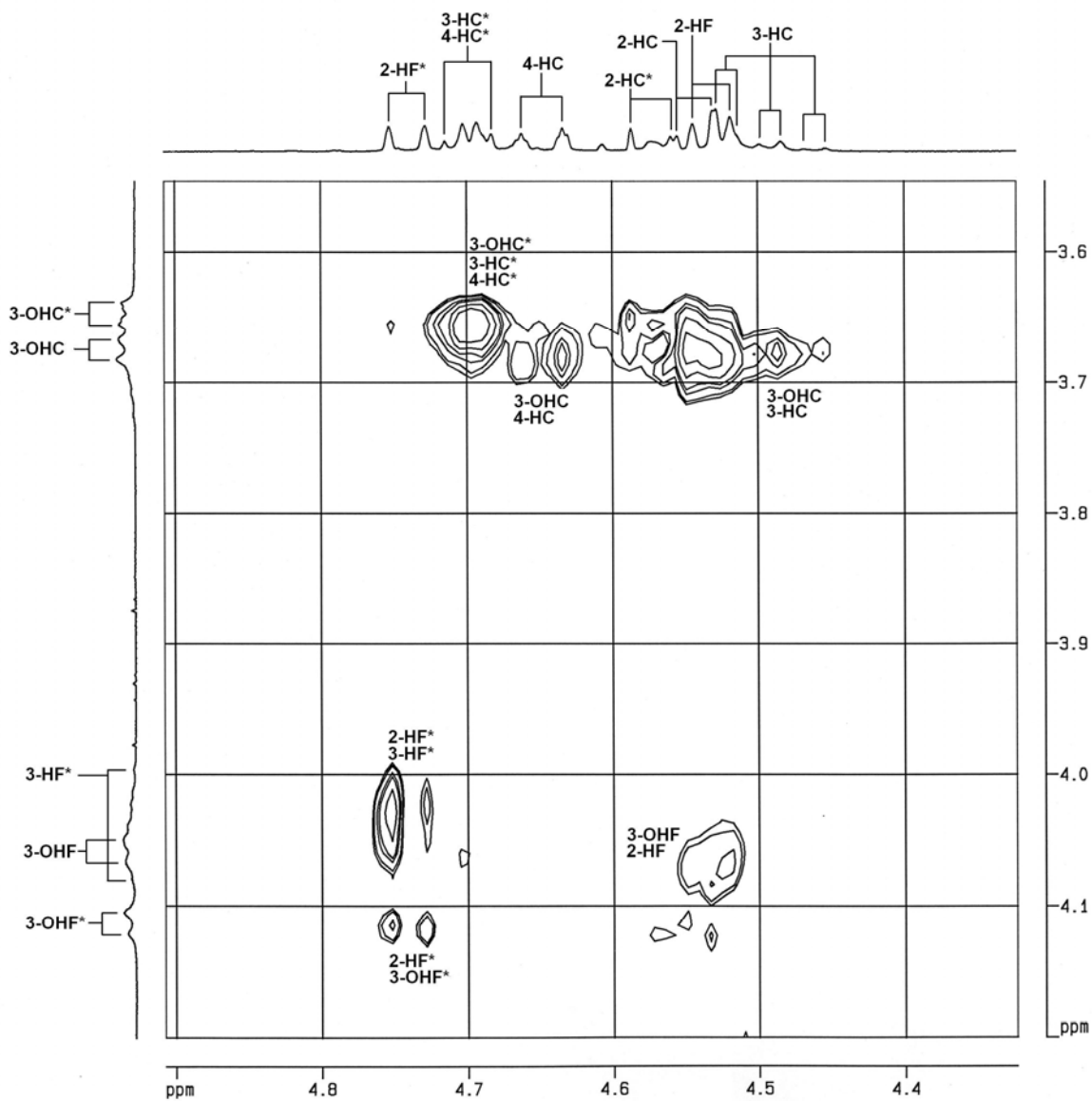
**FIGURE 6.1.18**

The presence of a small amount of water causes significant differences in the chemical shifts and coupling patterns of the heterocyclic resonances, which in turn implies changes in the C- and F-ring conformations (Table 6.1.2).

| Dry compact rotamer | C-ring | | | | F-ring | | | | |
|---|---|---|---|---|---|---|---|---|---|
| | 2 | 3 | 4 | 3-OH | 2 | 3 | 4α | 4β | 3-OH |
| chemical shift, δ | 4.55 | 4.50 | 4.66 | 3.65 | 4.53 | 3.63-3.72 | 2.856 | 2.53 | |
| multiplicity | d | dt | d | d | d | m | dd | dd | d |
| coupling constants, Hz | 6.5 | 4.5/8 | 8.5 | 4.5 | 7.5 | | 5/-16.5 | 8/-16.5 | 5 |

| "Wet" compact rotamer | C-ring | | | | F-ring | | | | |
|---|---|---|---|---|---|---|---|---|---|
| | 2 | 3 | 4 | 3-OH | 2 | 3 | 4α | 4β | 3-OH |
| chemical shift, δ | 4.53 | 4.46 | 4.63 | | 4.51 | 3.66 | 2.86 | 2.52 | |
| multiplicity | d | t | dd | | d | dq | dd | dd | |
| coupling constants, Hz | 9.5 | 8 | 1/9 | | 7.5 | 5.5/8.5 | 5.5/-16 | 8.5/-16 | |

| Dry extended rotamer | C*-ring | | | | F*-ring | | | | |
|---|---|---|---|---|---|---|---|---|---|
| | 2 | 3 | 4 | 3-OH | 2 | 3 | 4α | 4β | 3-OH |
| chemical shift, δ | 4.58 | 4.68-4.72 | 6.5 | | 4.74 | 3.99-4.08 | 2.85 | 2.66 | 4.11 |
| multiplicity | d | m | d | d | d | m | dd | dd | d |
| coupling constants, Hz | 8.5 | | 7.5 | 4.5 | 7.5 | | 8/-16.5 | 5/-16.5 | 5 |

| "Wet " extended rotamer | C*-ring | | | | F*-ring | | | | |
|---|---|---|---|---|---|---|---|---|---|
| | 2 | 3 | 4 | 3-OH | 2 | 3 | 4α | 4β | 3-OH |
| chemical shift, δ | 4.56 | 4.69 | 4.67 | | 4.73 | 4.04 | 2.92 | 2.65 | |
| multiplicity | d | t | dd | | d | dq | dd | dd | |
| coupling constants, Hz | 9 | 6.2 | 1/9 | | 7.5 | 5.5/7.5/8 | 5.5/-16 | 8/-16 | |

**TABLE 6.1.2**

The C-ring proton coupling constants for the experiment performed in dry acetone in the presence of cadmium nitrate are $J_{2,3}$ = 6.5 and 8.5Hz and $J_{3,4}$ = 8.5 and 7.5Hz (compact and extended rotamers respectively), suggesting A-E conformational exchange.

This is in contrast to the large C-ring proton coupling constants observed when there are traces of water present: $J_{2,3}$ = 9.5 and 9.0 and $J_{3,4}$ = 9.0 and 9.0 (compact and extended rotamers respectively). The C-ring thus has a preferred E-conformation in the presence of small amounts of water.

The line shapes of the 3-$H_F$ resonances in wet acetone, as well as the coupling constants

observed for the resonances in wet and dry acetone, are analogous to those described for the terminal catechin units of procyanidin dimers (Figure 6.1.6, Figure 5.2.3).[96] This indicates that the F-ring conformation in all cases is that of a skewed boat with the E-ring being in a preferentially equatorial position.

An HMQC experiment was performed on the sample in extensively dried acetone-$d_6$ with traces of cadmium nitrate monohydrate. Due to the complexity of the spectrum, resulting in overlap of many of the cross peaks, unambiguous assignments could not be made for several of the carbon atoms (Figures 6.1.18 -23, Appendix B).



**FIGURE 6.1.18**

59

**FIGURE 6.1.19**

**FIGURE 6.1.20**

**FIGURE 6.1.21**

**FIGURE 6.1.22**
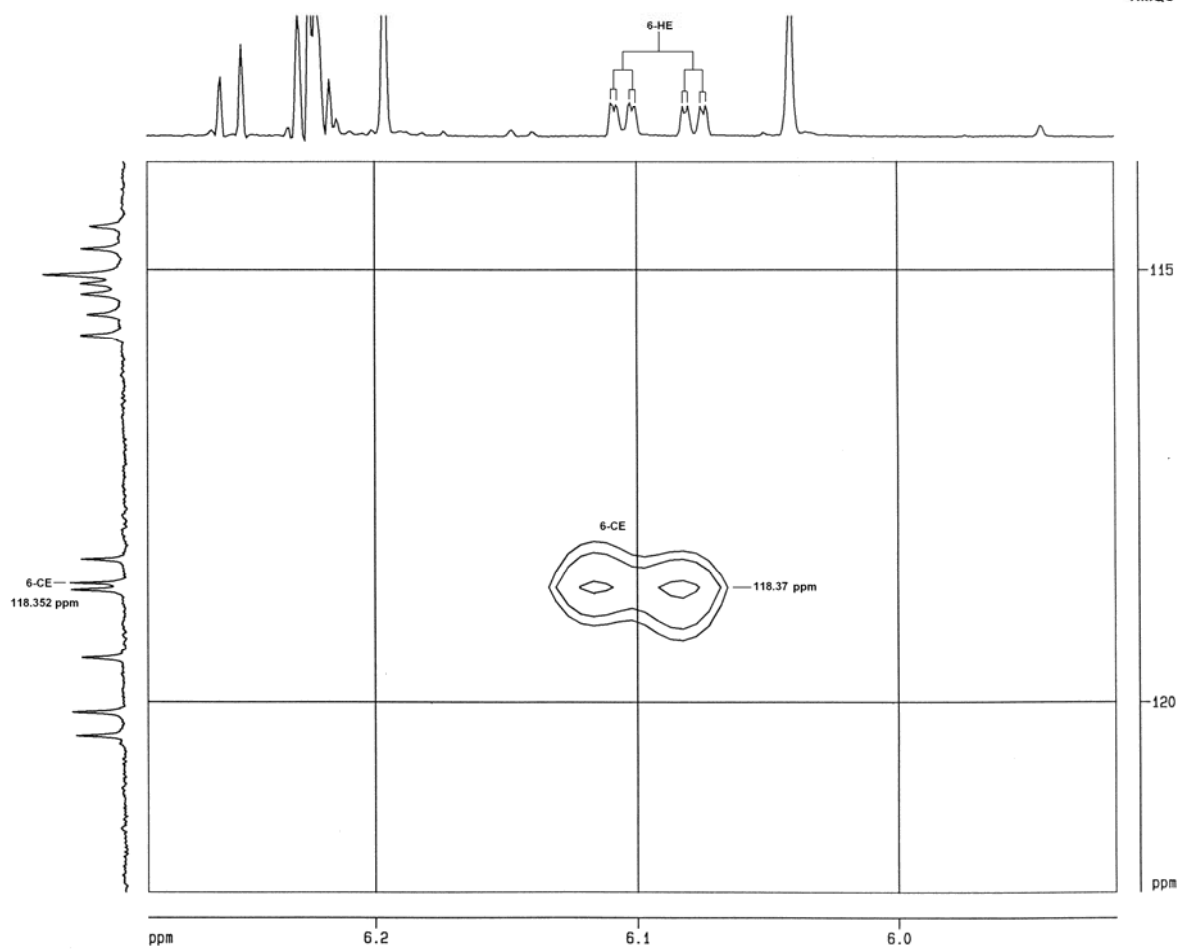
**FIGURE 6.1.23**

## 6.2. THE CONFORMATIONAL BEHAVIOUR OF FISETINIDOL-(4β→8)-CATECHIN IN ACETONE-d$_6$ AND D$_2$O.

This structure of this compound was studied with $^1$H, $^{13}$C, gradient COSY and HMQC NMR experiments in acetone-d$_6$ and D$_2$O at 293 K and 353 K (Figure 6.2.1) and CD in methanol (see Chapter 8). The $^1$H NMR spectrum in acetone-d$_6$ at 293 K displayed very broad proton resonances, except for the 5-H$_A$ and 6-H$_A$ resonances (Figure 6.2.3).

There was also no obvious duplication of resonances as is the case when two distinct rotamers are present, e.g. fisetinidol-(4α→8)-catechin (paragraph 6.1) and fisetinidol-(4α→6)-catechin (Paragraph 6.3) at 293 K. Fluorescence decay studies, however, observed a higher, but not exclusive, fraction of one of two rotamers with $f_i$ = 0.3–0.5.[16]

The broad resonances indicate either one or all of the following:

a) Slow conformational flexing that display time-averaged resonances for aromatic and heterocyclic protons.
b) Restricted rotation around the interflavanyl bond due to the presence of intramolecular hydrogen bonds.

Upon heating to 353 K, a spectrum with clearly defined resonances and coupling constants for both heterocyclic (Figure 6.2.2) and aromatic (Figure 6.2.3) proton resonances was obtained.

Resonance sharpening could be due to the breaking of intramolecular hydrogen bonds as well as faster rotation around the interflavanyl bond. An increased hydrogen exchange rate is confirmed by the disappearance of the resonances of the aromatic hydroxy resonances at 353 K.

Although heating greatly assists with the assignment of resonances and the determination of coupling constants, the conformation of the molecule at room temperature in aqueous medium (Figure 6.2.1) is of greater importance, as it is this conformation that will interact with bio-molecules and thus determine the biological activity of the compound.

**D₂O**
**293 K**
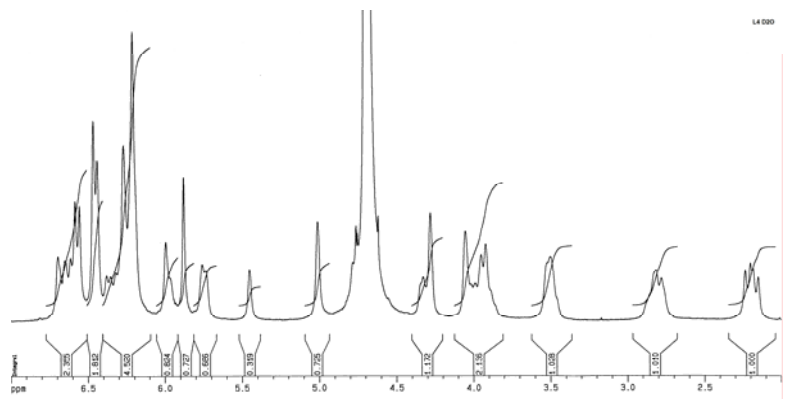
**Acetone-d₆**
**293 K**
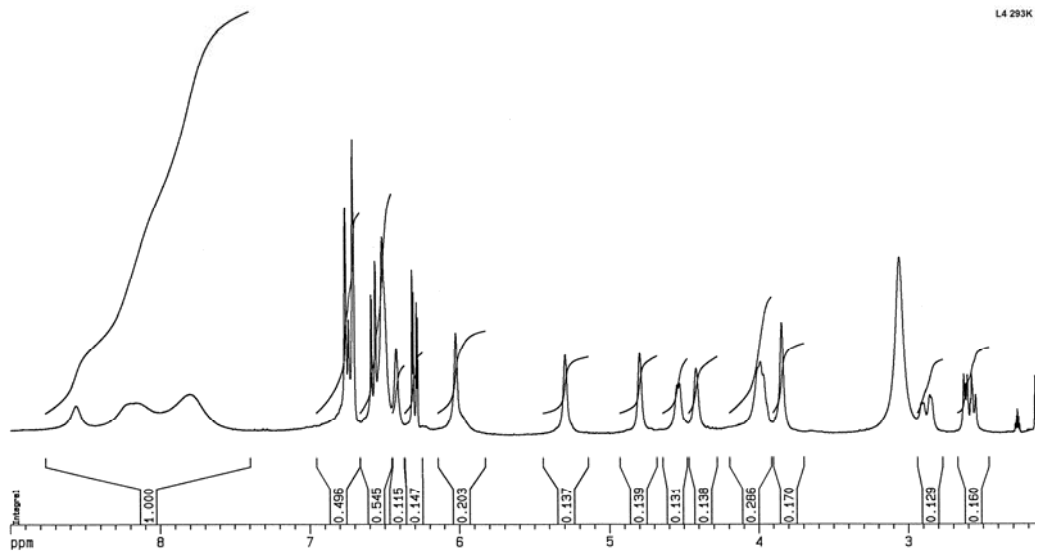
**Acetone-d₆**
**353 K**
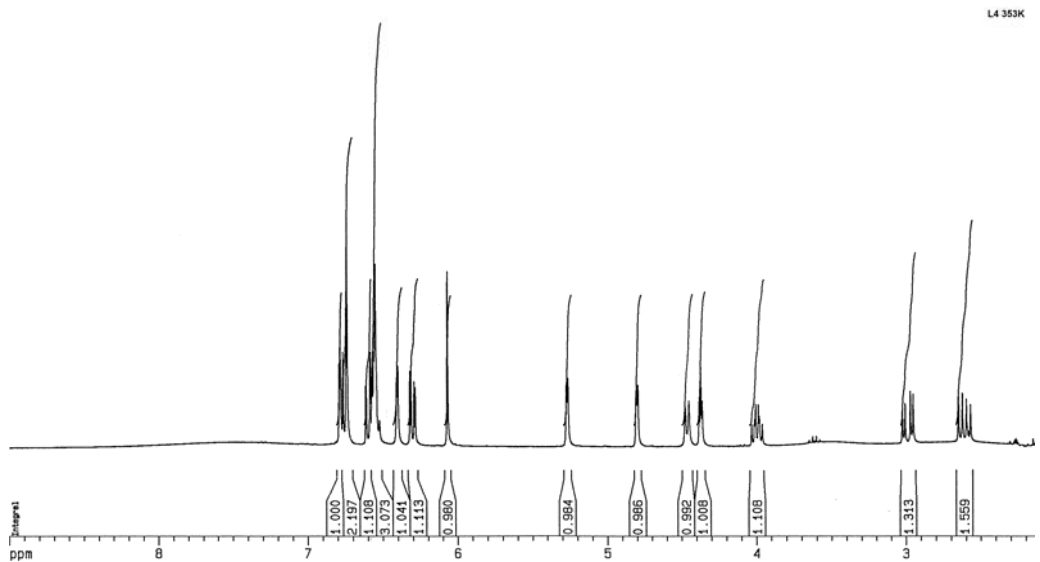
**FIGURE 6.2.1**
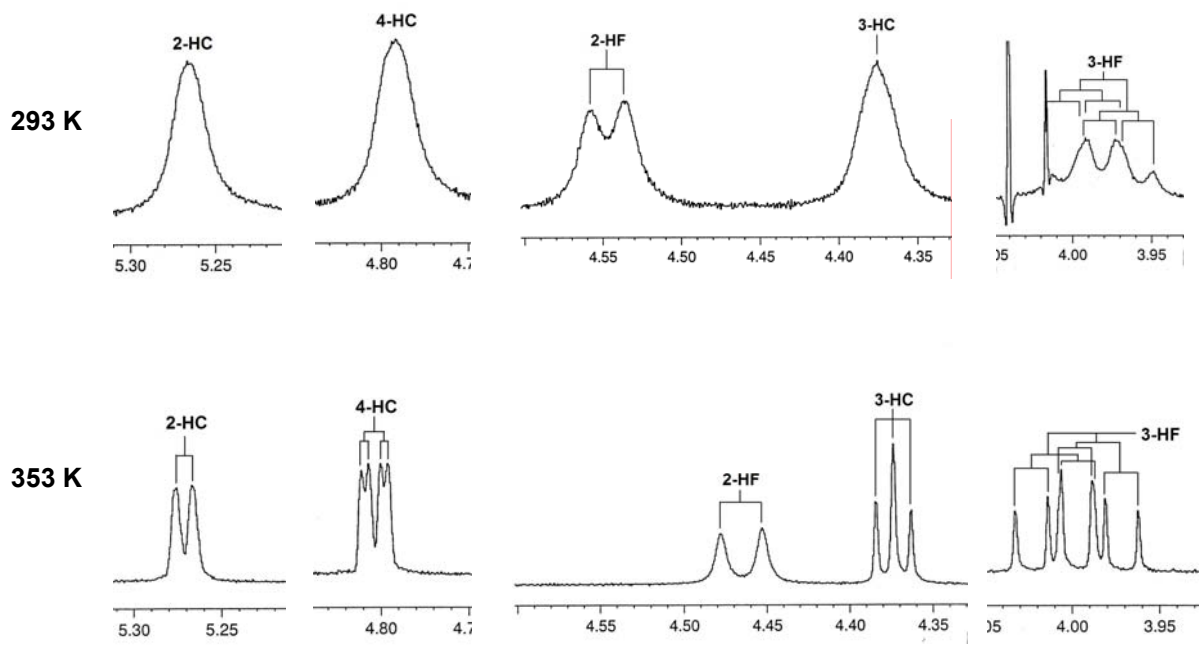
**FIGURE 6.2.2**
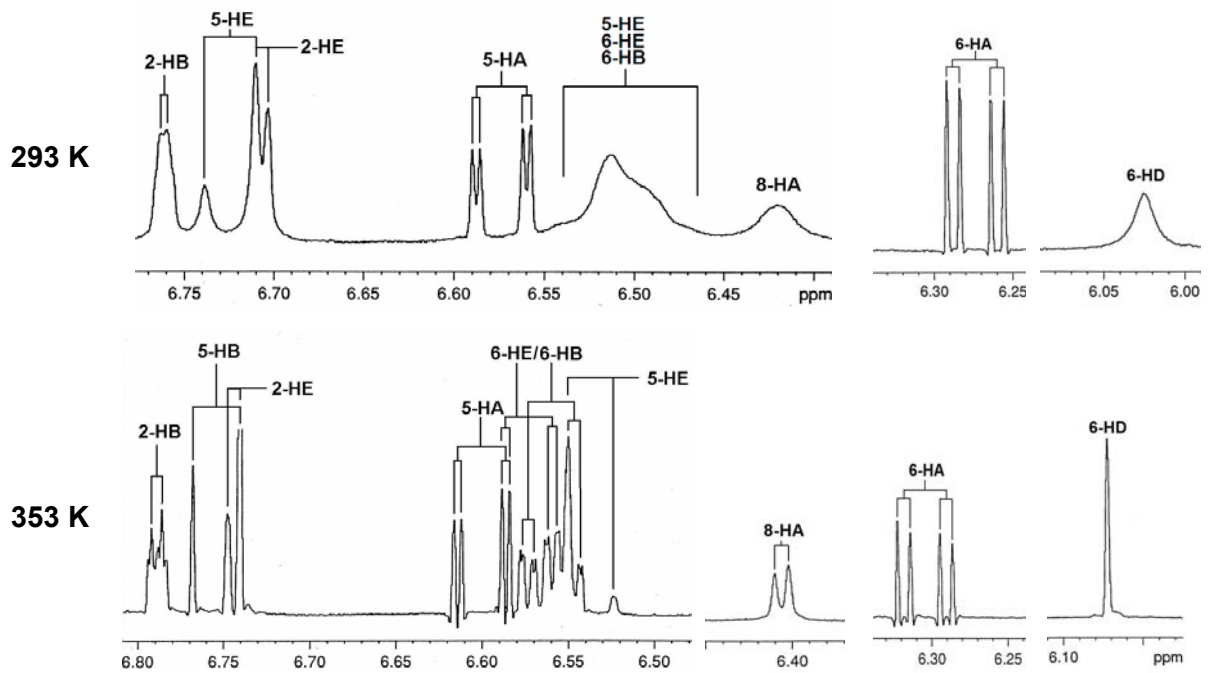


**FIGURE 6.2.3**

The gradient COSY (Figure 6.2.4, L4 22) experiment at 353 K was used to assign the proton resonances. The F-ring resonances were first assigned. The 4-H$_C$ resonances were assigned from cross peaks with the 6-H$_D$ resonance. The resonances of the other two C-ring protons were then assigned from their cross peaks with the 4-H$_C$ resonances.
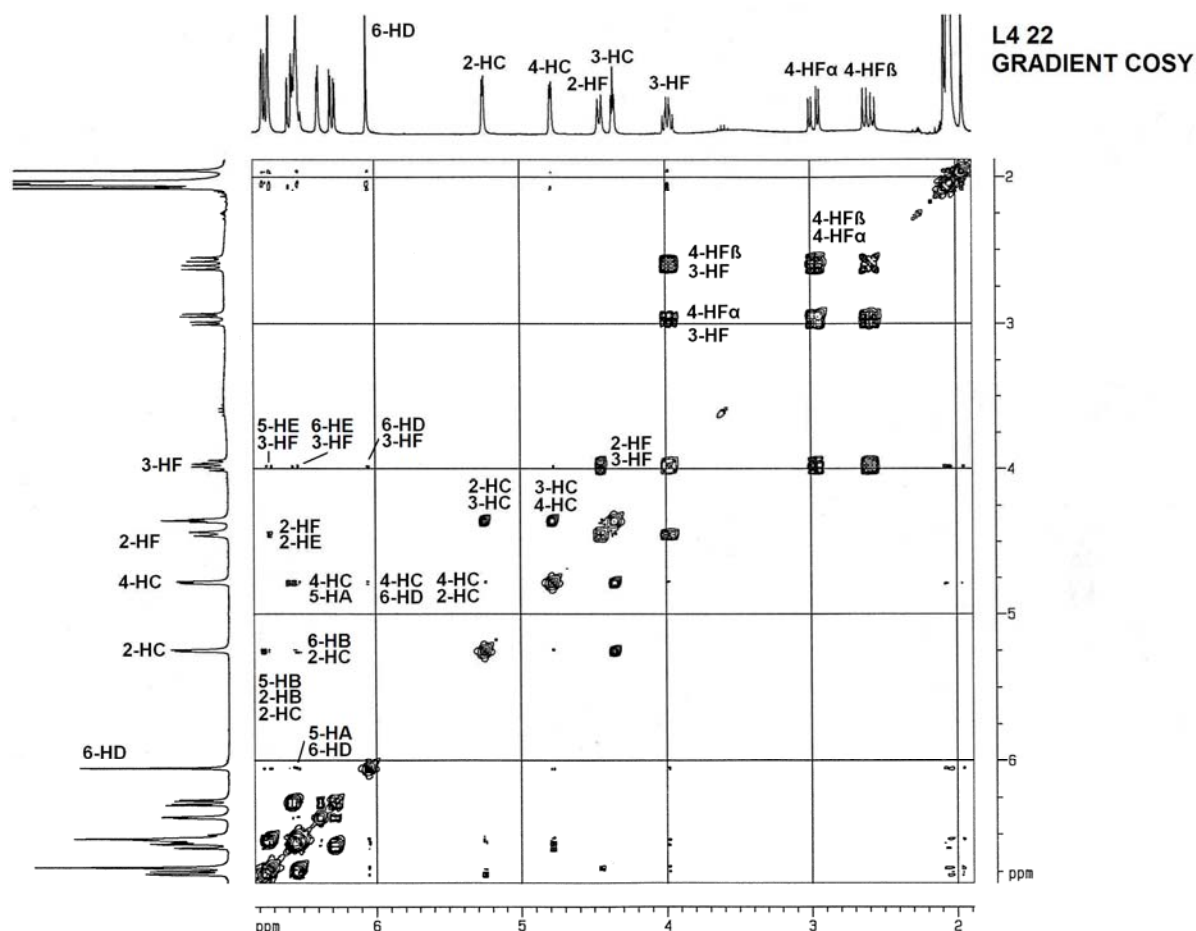


**FIGURE 6.2.4**

The resonances of the heterocyclic resonances were then used to assign some of the aromatic resonances (Figure 6.2.5, L4 26). Weak cross peaks were observed between the 6-H$_D$ resonance and the 3-H$_F$, 4-H$_{F\alpha}$ and 4-H$_C$ resonances. The 3-H$_F$ resonances displayed weak cross peaks with some of the E- and A-ring resonances. The two 4-H$_F$ resonances displayed weak cross peaks with the respective E-ring resonances.

The presence of 4-H$_{F\beta}$/H$_D$ cross peaks suggests a 90° angle between the plane of the D-ring and the 4-H$_{F\beta}$→4-C$_F$ bond. The absence of 4-H$_{F\alpha}$/H$_D$ cross peaks suggests that there is very little conformational flexing of the F-ring.

The relatively large number of heterocyclic/aromatic resonance cross peaks further confirms limited rotation around the interflavanyl bond.



**FIGURE 6.2.5**

69
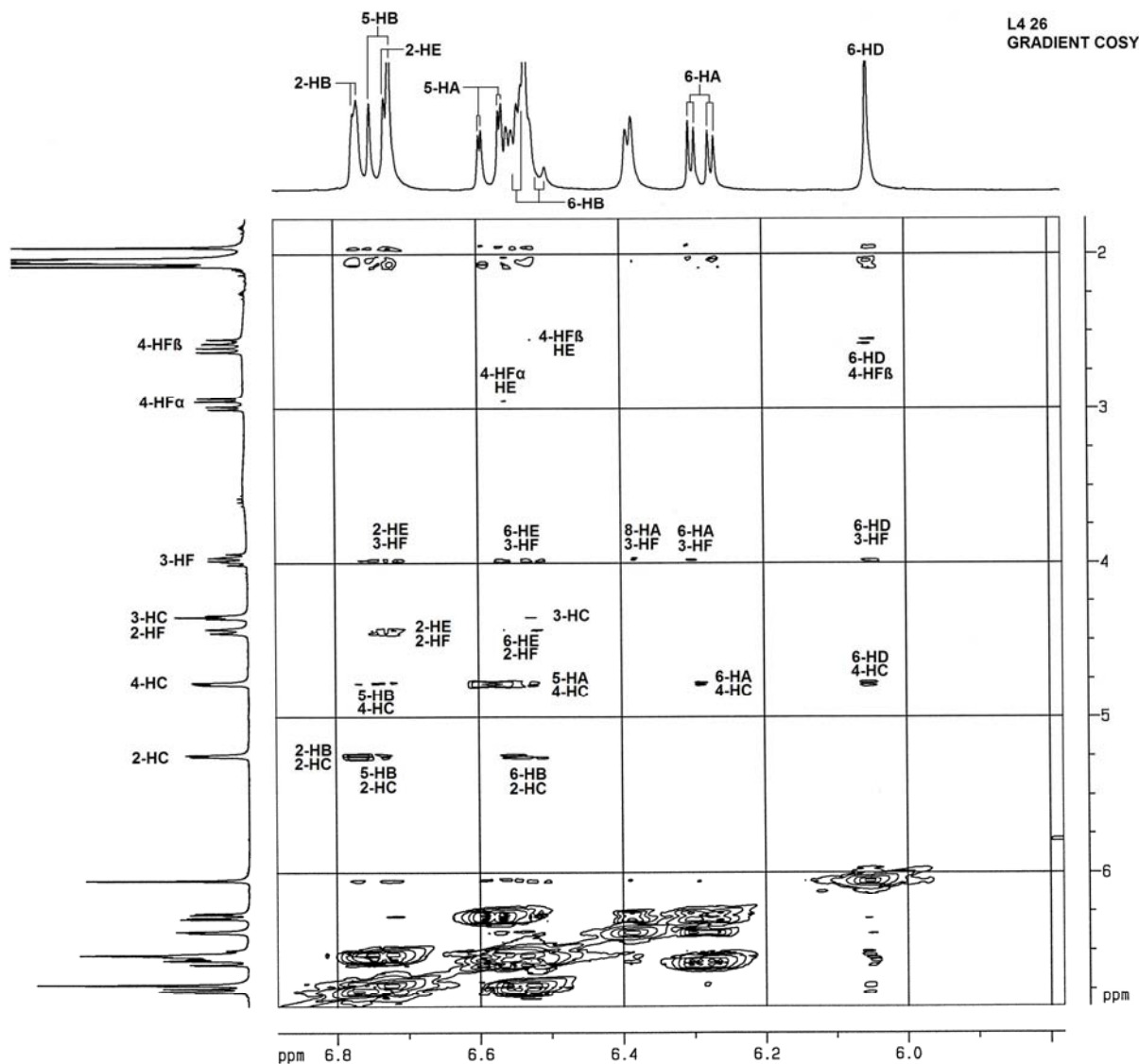
These aromatic proton assignments were then used to assign the rest of the aromatic proton resonances. The assignments of the 6-H$_B$ and 6-H$_E$ resonances are ambiguous due to their position on the gradient COSY spectrum (Figure 6.2.6, L4 24). The cross peaks of the E- and B-ring resonances also overlap. A quartet (H-5/H-6) and a doublet (H2/H6) of cross peaks are usually observed for an AMX system on a COSY spectrum, but in this case the doublet overlaps with the quartet.
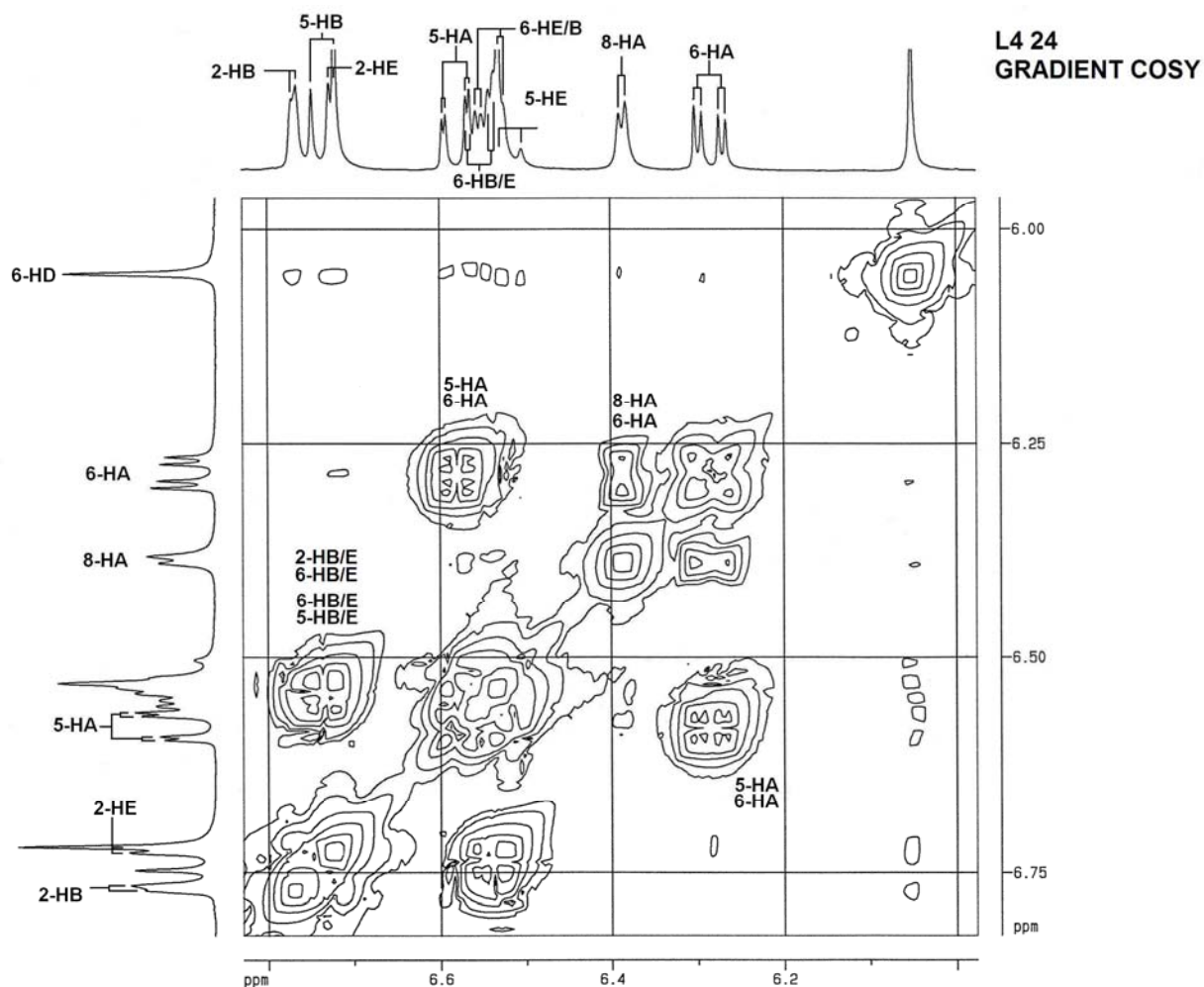


**FIGURE 6.2.6**

An HMQC experiment at 293 K (Figure 6.2.6, L4 3) yielded similar results. The assignment of the 5/6-H$_{B/E}$ resonances was further complicated by the broad ^{1}H NMR resonances as well as the proximity of the crosspeaks on the HMQC spectrum.
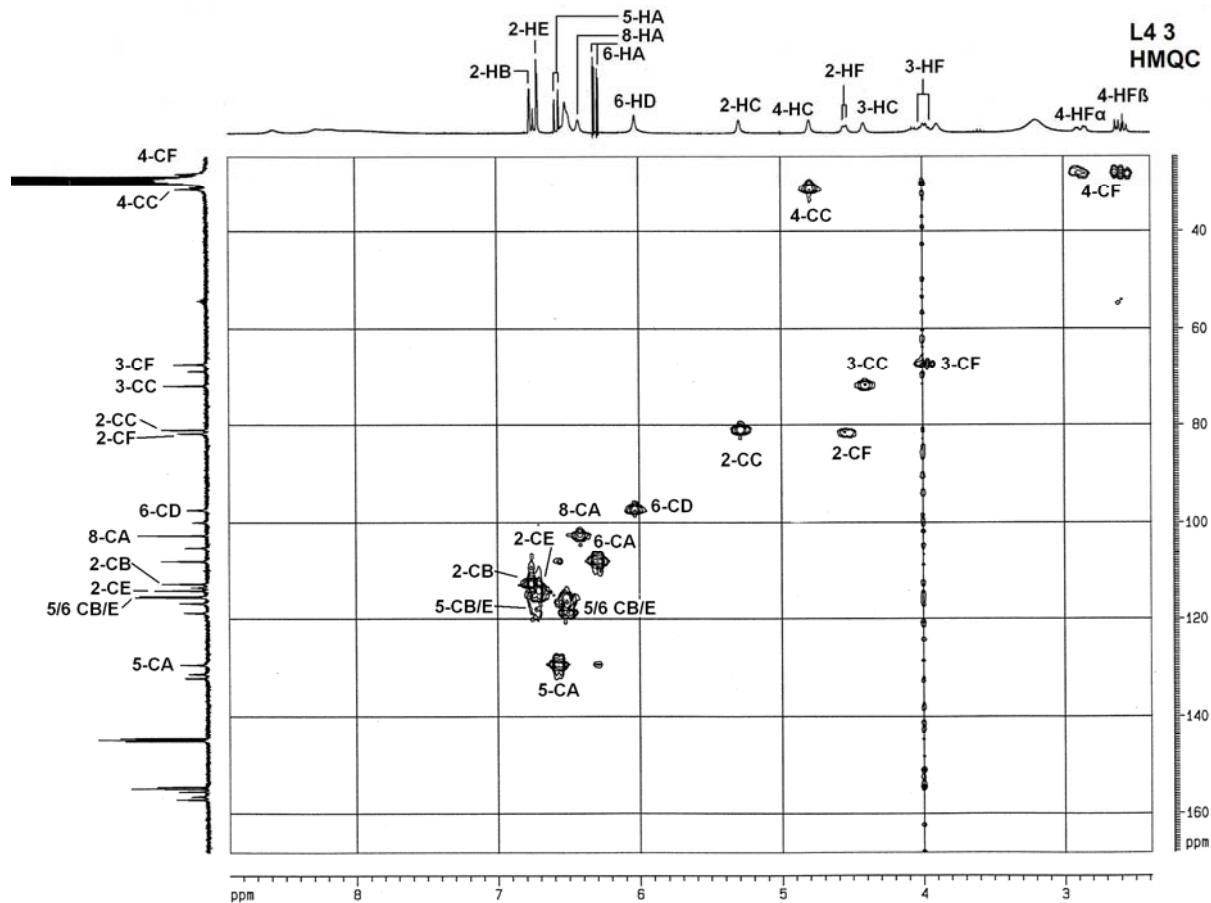


**FIGURE 6.2.7**
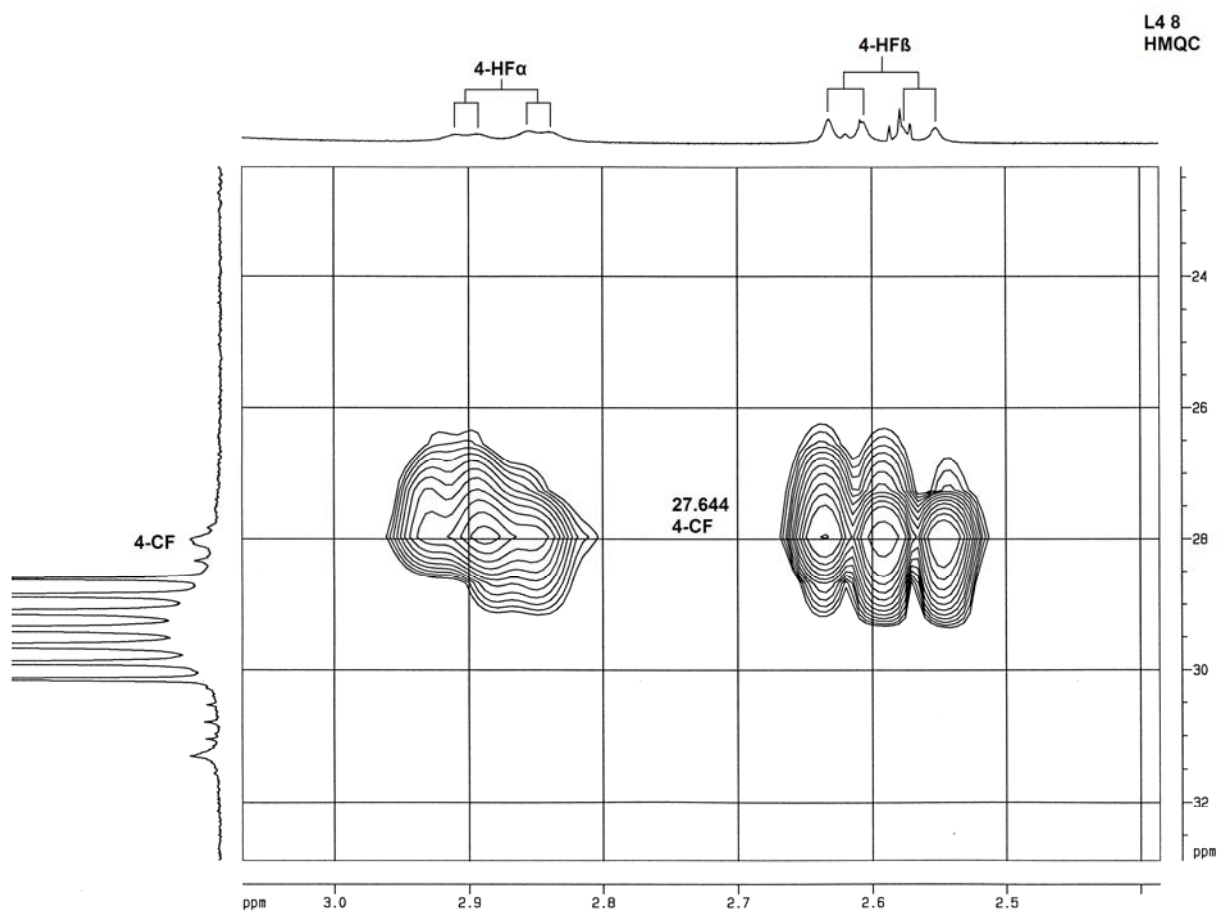
**FIGURE 6.2.8**
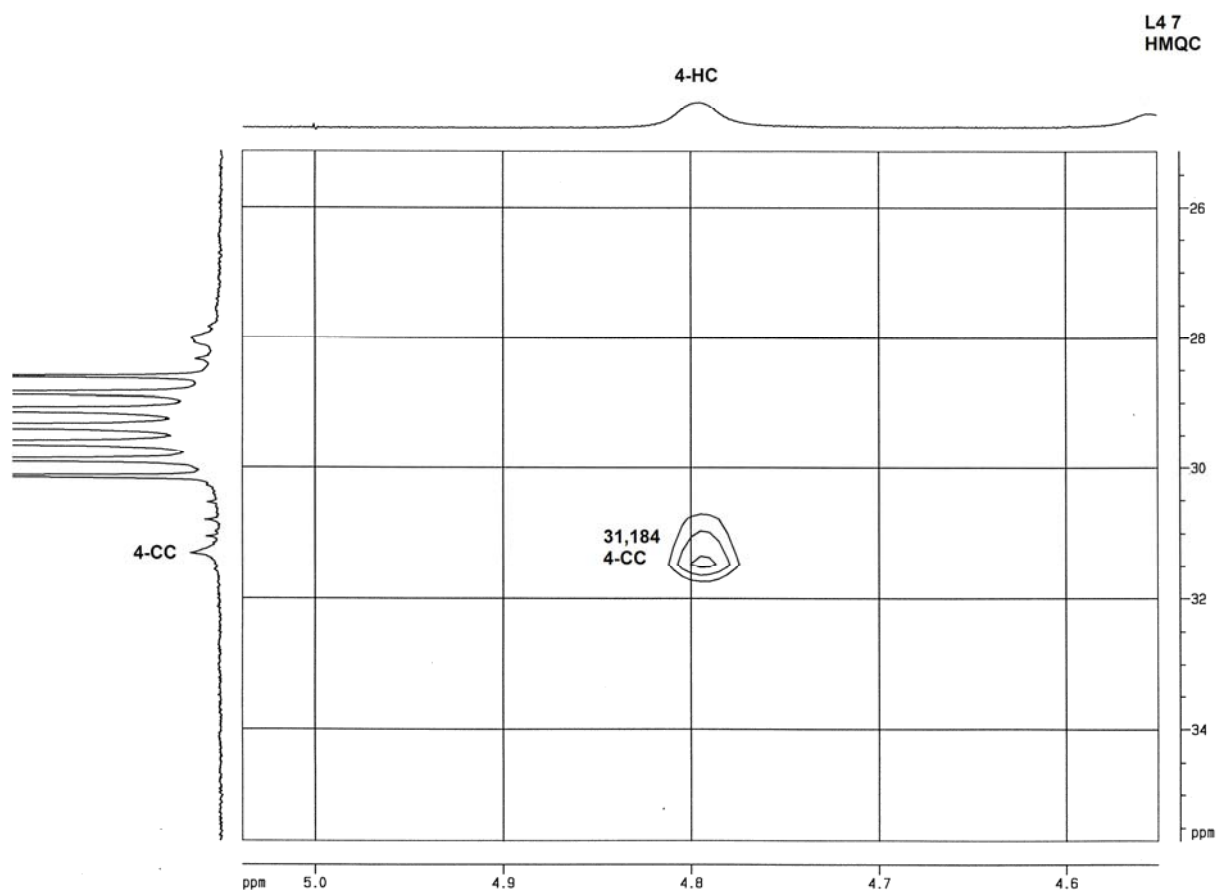
**FIGURE 6.2.9**
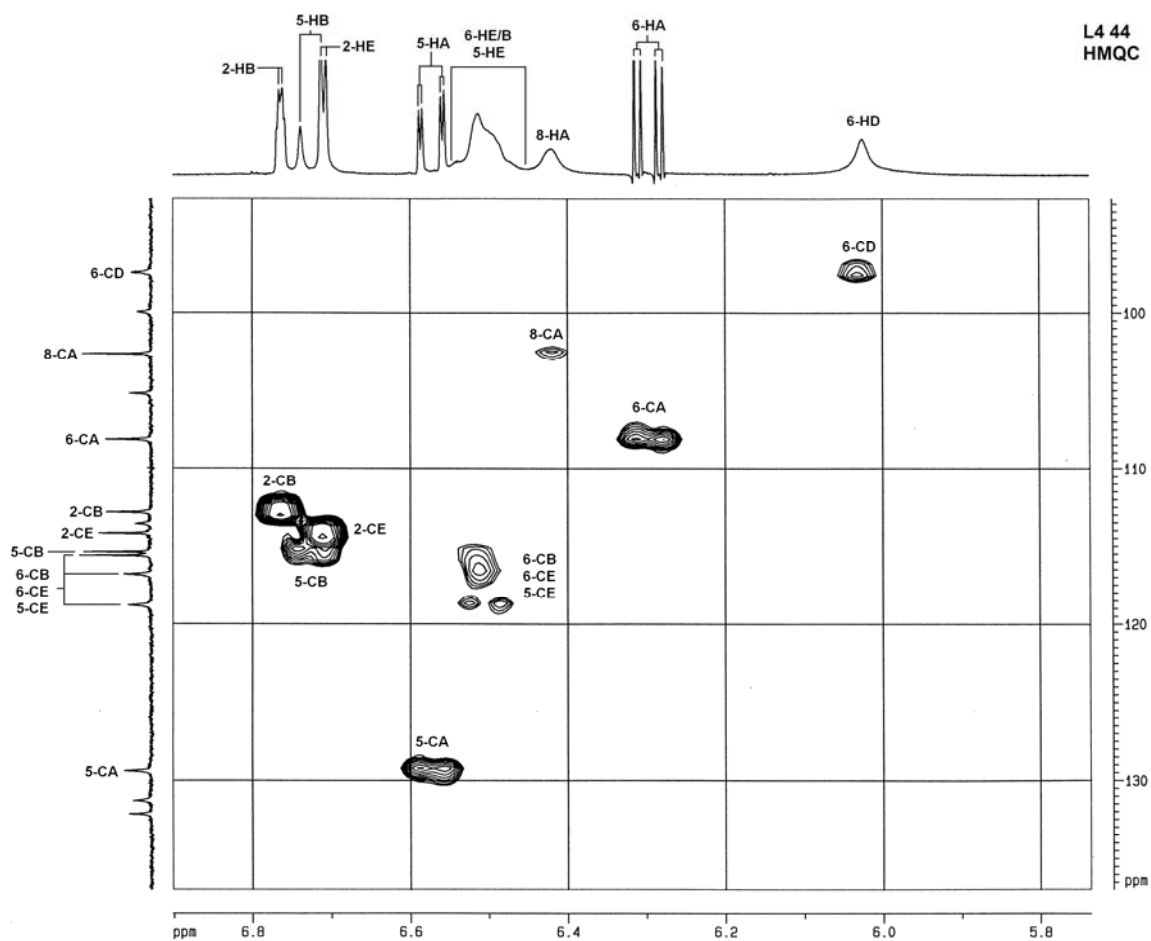
**FIGURE 6.2.10**

The results of the HMQC experiment were used to assign some of the carbon resonances

(Figure 6.2.11, L4 2, Appendix B).
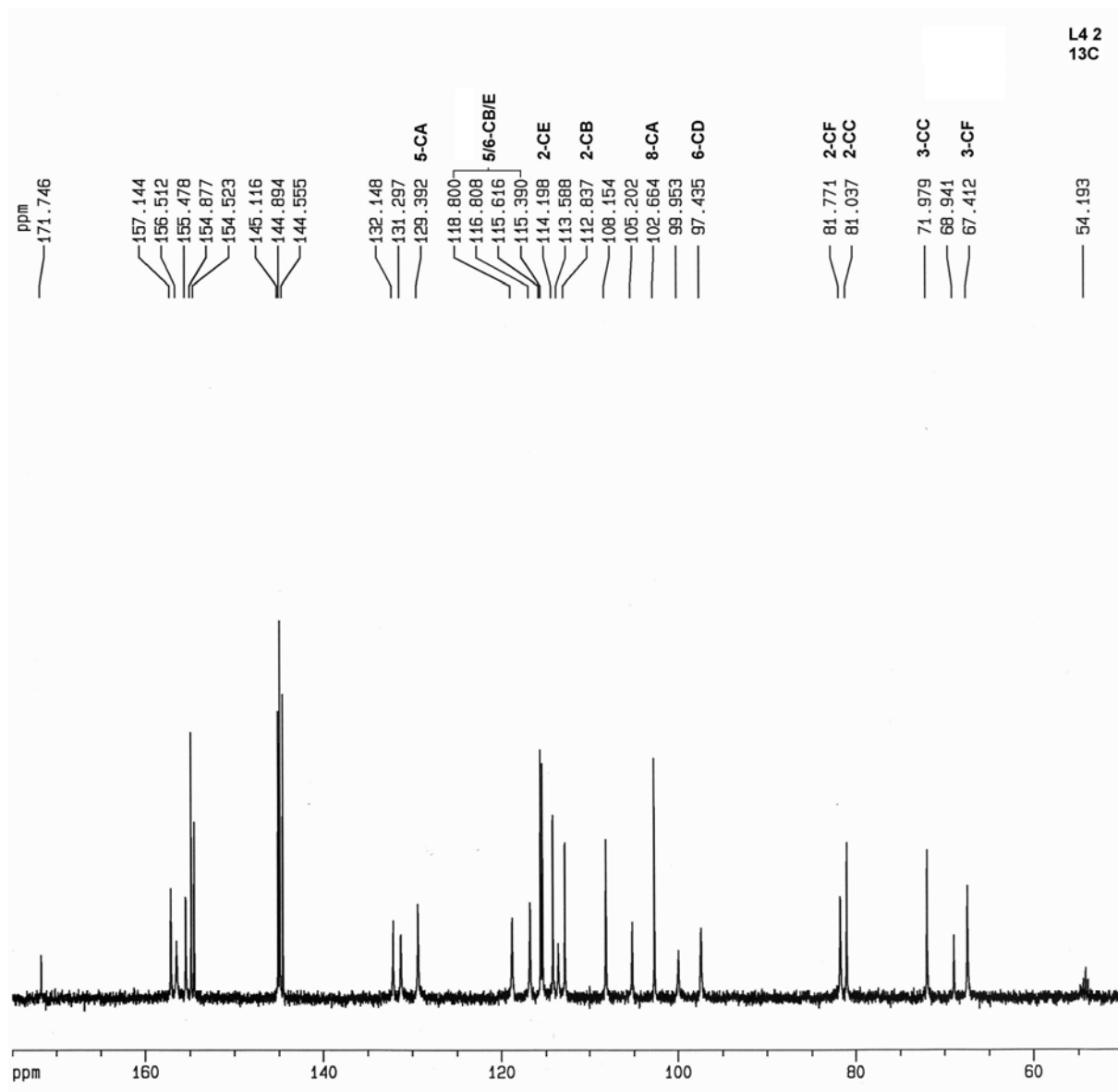


**FIGURE 6.2.11**

| HETEROCYCLIC RING DATA AT 353 K. DATA AT 293 K BRACKETS. | | | | | | | |
|---|---|---|---|---|---|---|---|
| Proton | C-ring | | | F-ring | | | |
| | 2 | 3 | 4 | 2 | 3 | 4α | 4β |
| chemical shift, δ | 5.27 (5.30) | 4.37 (4.42) | 4.08 (4.80) | 4.47 (4.54) | 4.00 (4.00) | 3 | 2.73 (2.19) |
| multiplicity | d (bs) | t (bs) | dd (bs) | d (bd) | dq (bm) | dd | dd |
| coupling constants, Hz | 2 | 3 | 1/3 | 7.5 (5.5) | 5.5/7.5 | 5.5/-16 | 7.5/-16 |

**TABLE 6.2.1**

| AROMATIC RING DATA AT 353 K. DATA AT 293 K IN BRACKETS. | | | | | | | | | | |
|---|---|---|---|---|---|---|---|---|---|---|
| Proton | A-ring | | | B-ring | | | E-ring | | | D-ring |
| | 8 | 5 | 6 | 2 | 5 | 6 | 2 | 5 | 6 | 6 |
| chemical shift, δ | 6.41 (6.42) | 6.60 (6.58) | 6.31 (6.30) | 6.79 (6.76) | 6.76 (6.72) | 6.55 | 6.743 (6.71) | 6.54 | 6.58 | 6.07 (6.02) |
| multiplicity | d (bs) | dd (dd) | dd | m (bd) | d (d) | dd | d (d) | d (m) | dd (m) | s (bs) |
| coupling constants, Hz | 2.5 (-) | 1/8 (1.2/8) | 2.5/8 (2.5/8.2) | ±2 (-) | 8 (8) | 2/8 | 2 (2) | 8 | 2/8 | |

**TABLE 6.2.2**

The relatively small coupling constants of the resonances of the C-ring (Figure 6.2.1 and Table 6.2.2) $^3J_{2,3}$=2Hz and $^3J_{3,4}$=3Hz indicate a preferred A-conformation of the C-ring. $^3J_{3,4}$ is expected to be a bit larger than $^3J_{2,3}$ in the case of an A-conformer. The possible hydrogen bond between 3-OH$_C$ and the oxygen of the pyran C-ring stabilises the conformation of the C-ring and this, together with the magnitude of the coupling constants, suggests an A/skewed boat conformation with all the C-ring hydrogen atoms in quasi-equatorial positions.

## 6.3 THE CONFORMATIONAL BEHAVIOUR OF FISETINIDOL-(4α→6)-CATECHIN IN ACETONE-d$_6$

The structure of this compound was studied by $^1$H, $^{13}$C, COSY 45, COSY 90W, HMQC and NOESY PH NMR experiments in acetone-d$_6$ on three different samples, and CD in methanol (see Chapter 8).

a)   $^1$H NMR and COSY 45 experiments were done on a sample that displayed a broad resonance at 3 ppm, indicating the presence of water (Figures 6.3.1/4).

b)   $^1$H NMR and COSY 45 experiments were done on a sample in extensively dried acetone-d$_6$ (Figures 6.3.2/5).

c)   $^1$H NMR, COSY 90W and NOESY PH experiments were done on a sample in extensively dried acetone-d$_6$ with a trace of cadmium nitrate in order to facilitate assignment of resonances of some of the hydroxy resonances (Figures 6.3.3/6).

A comparison of the $^1$H NMR spectra under the abovementioned conditions gives an indication of the effect of the presence of even trace amounts of water on the resonances and splitting patterns of the 3-H$_F$ resonances as well as the visibility and intensity of the resonances of the aromatic and aliphatic hydroxy groups. Some of these effects are similar to those observed for the fisetinidol-(4α→8)-catechin dimer discussed in paragraph 6.1.

lp152 catechin and mollisacacidin 4 alpha 6 dimer in dry
acetone

L5 102
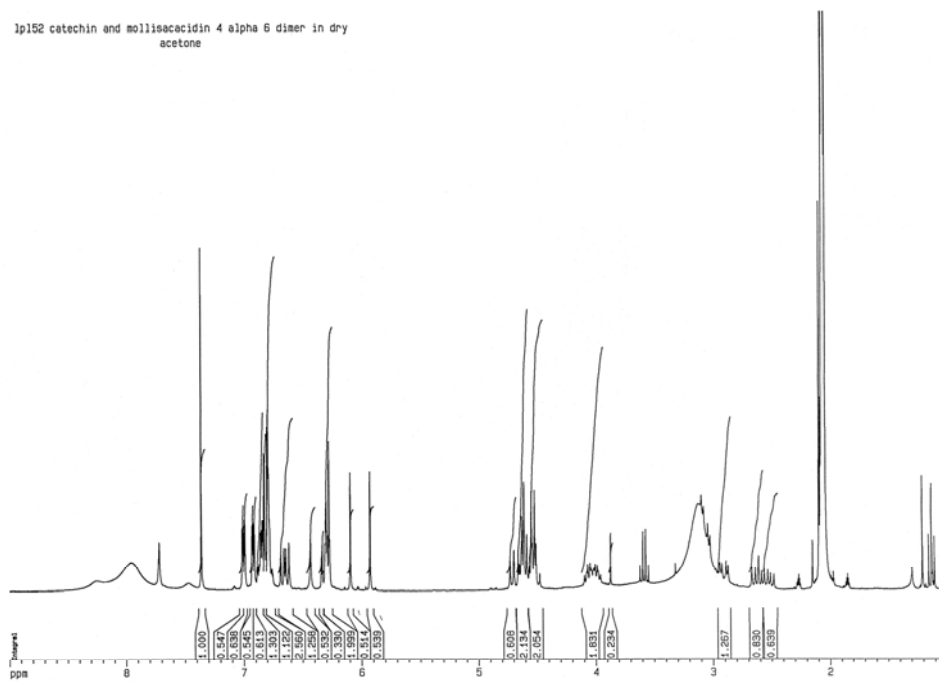
**FIGURE 6.3.1**



15temp20 in acetone from Merck vial dried
over molecular sieves for 41 hours

L5 119
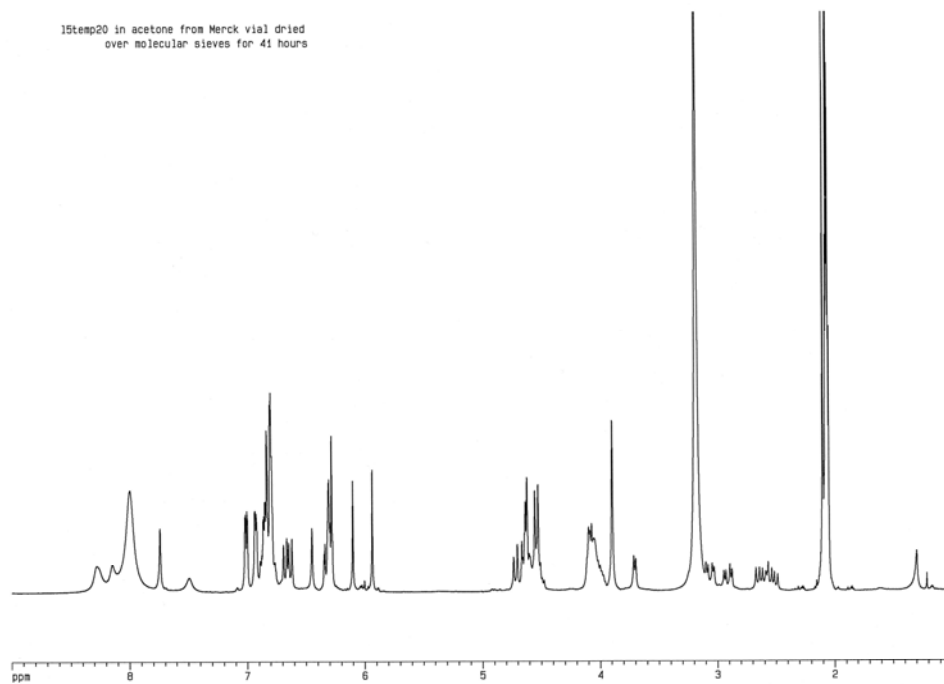
**FIGURE 6.3.2**

lpv4a6c2 4-alpha-6 dimer in acetone with cadmium nitrate
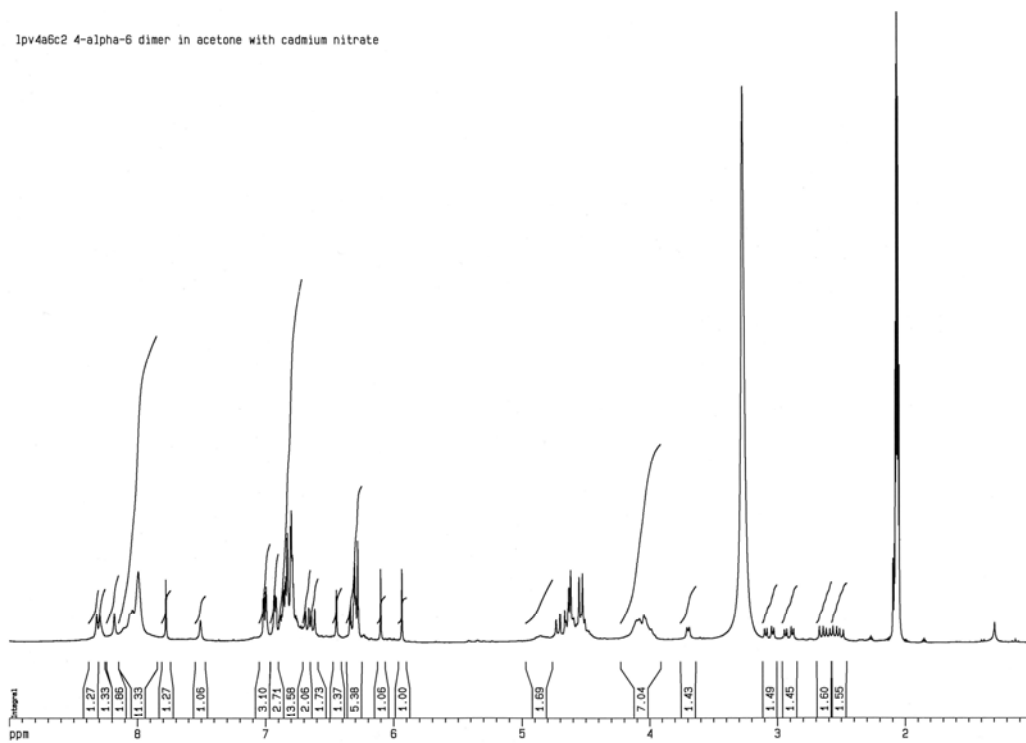
**FIGURE 6.3.3**
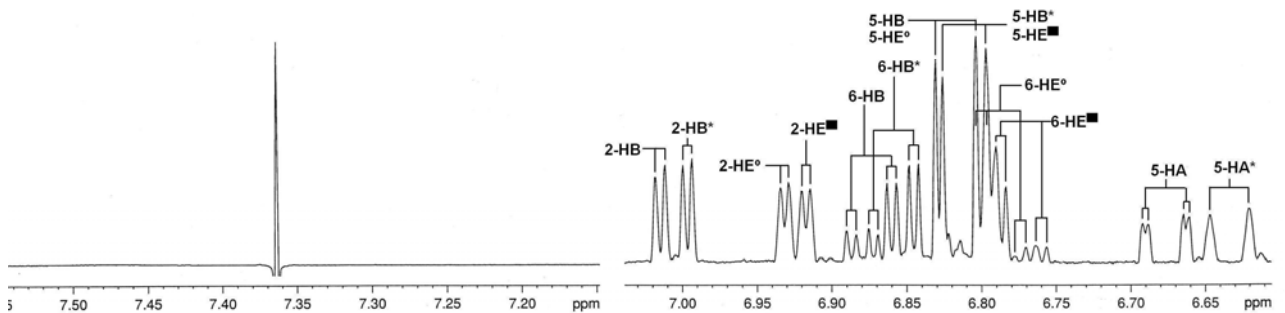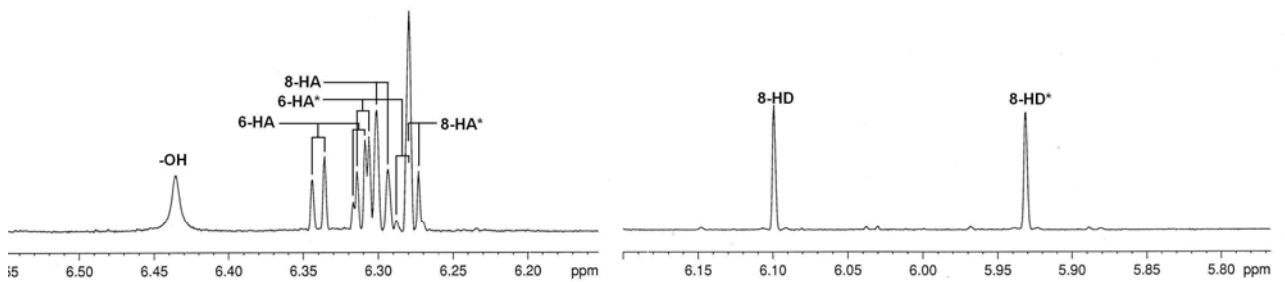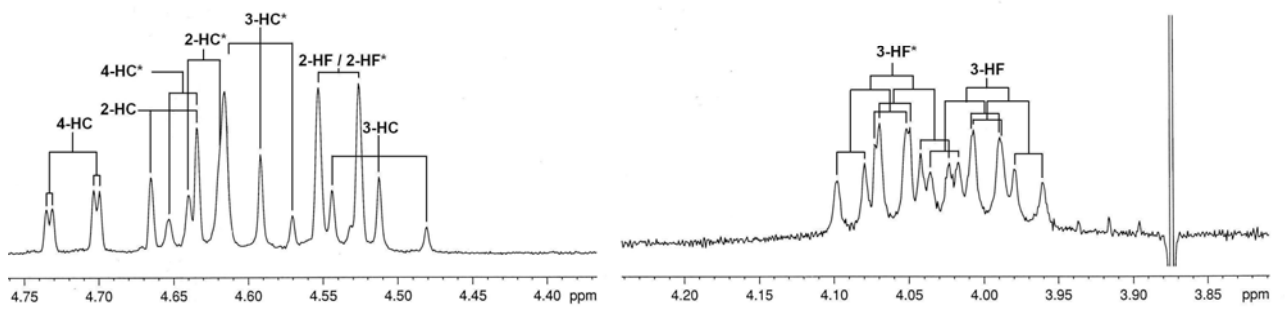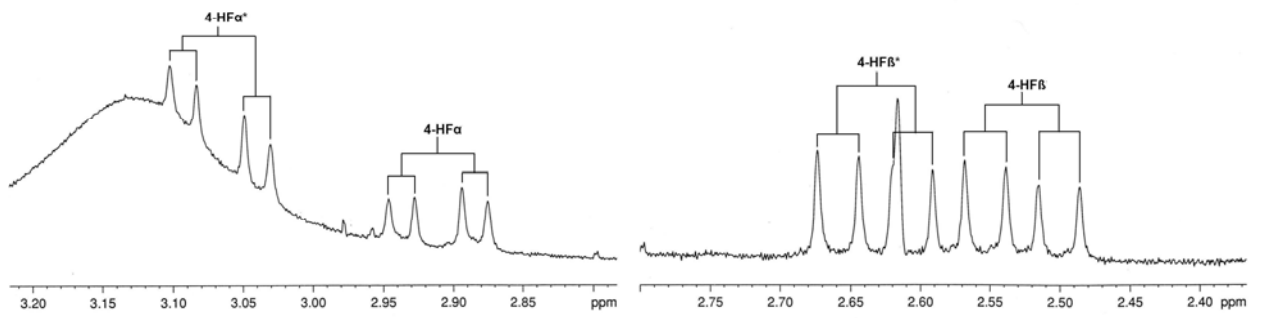
**FIGURE 6.3.4**
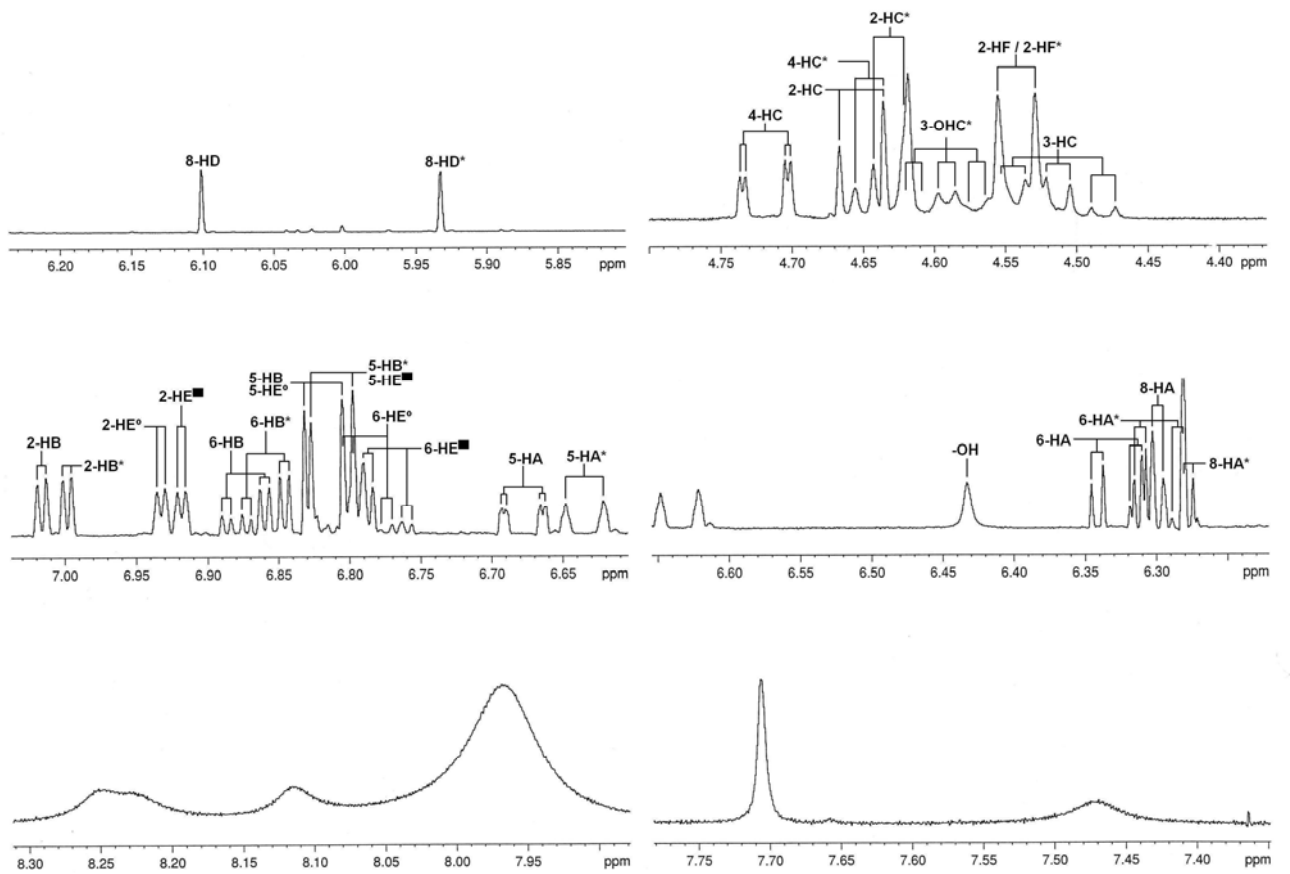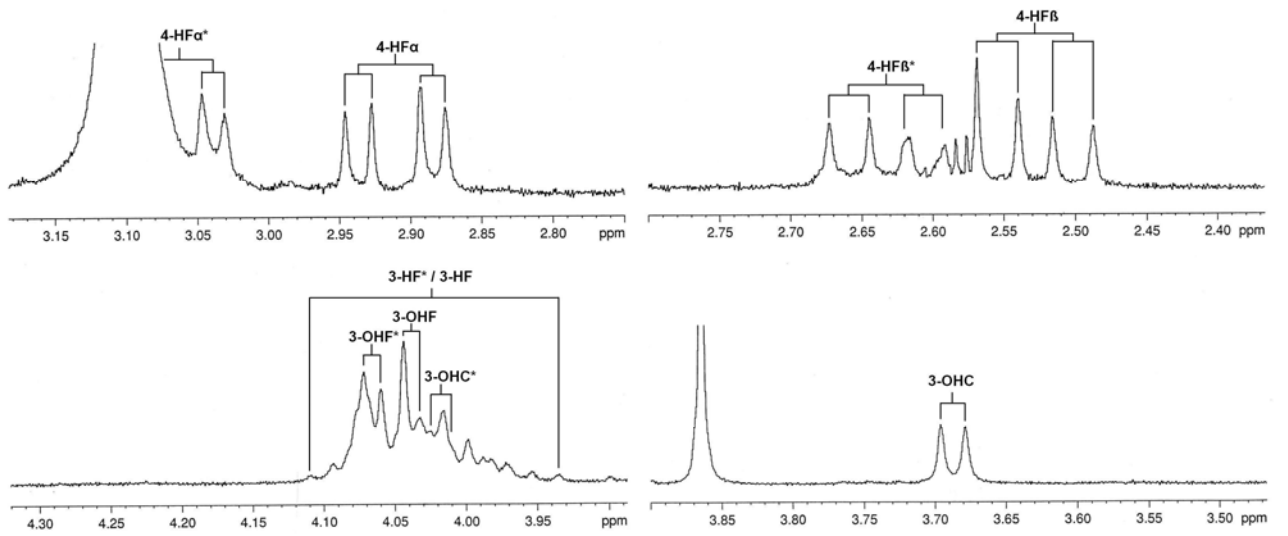
**FIGURE 6.3.5**
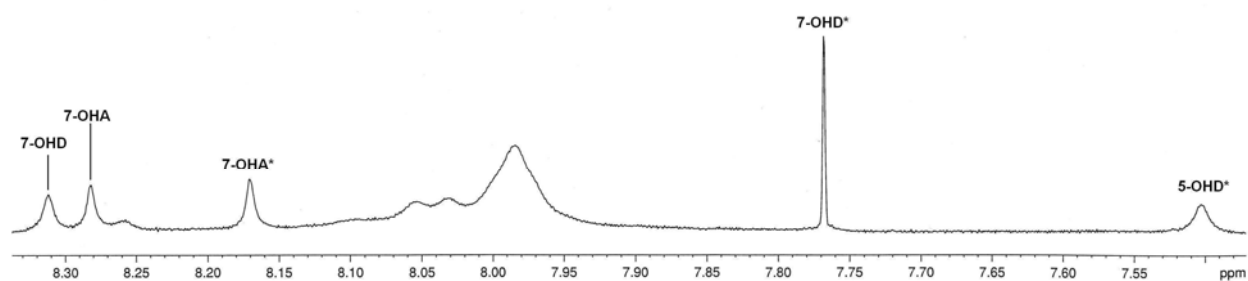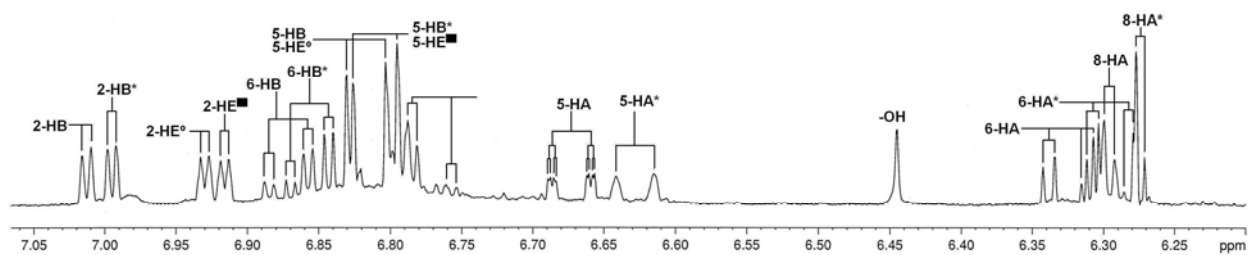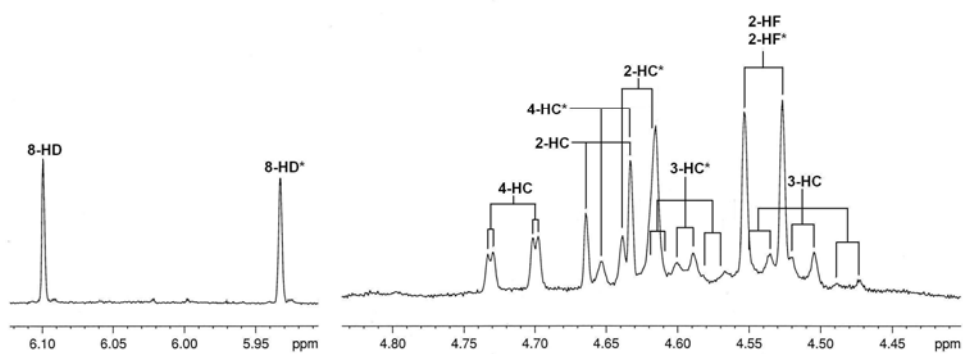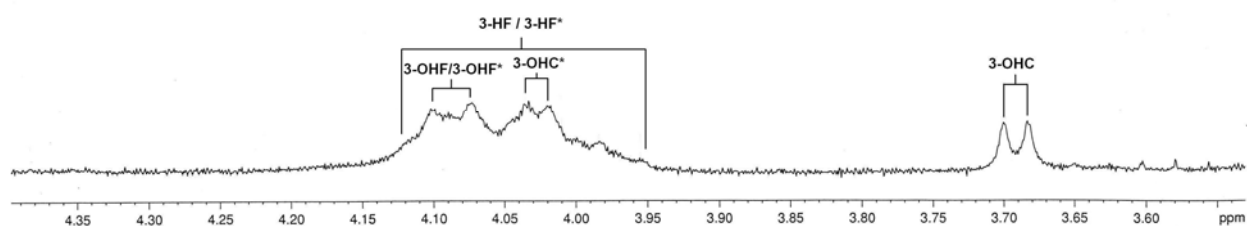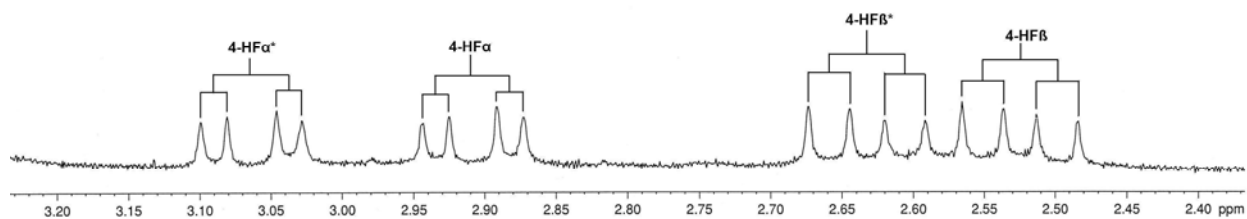
FIGURE 6.3.6

The chemical shifts of all the resonances of all three samples were essentially the same (Tables 6.3.1 and 6.3.2), the only differences being changes in splitting patterns due to differences in hydrogen ion exchange, as well as the visibility of some of the hydroxy resonances.

| "Dry" compact rotamer | C-ring | | | | F-ring | | | | |
|---|---|---|---|---|---|---|---|---|---|
| | 2 | 3 | 4 | 3-OH | 2 | 3 | 4α | 4β | 3-OH |
| chemical shift, δ | 4.65 | 4.51 | 4.72 | 3.69 | 4.54 | 3.98 | 2.91 | 2.53 | 4.04 |
| multiplicity | d | td | dd | d | d | m | dd | dd | d |
| coupling constants, Hz | 9.5 | 5.5/9.5 | 1.0/9.5 | 5.5 | 8.0 | | 5.5/-15.5 | 8.0/-15.5 | |

| "Wet" compact rotamer | C-ring | | | | F-ring | | | | |
|---|---|---|---|---|---|---|---|---|---|
| | 2 | 3 | 4 | 3-OH | 2 | 3 | 4α | 4β | 3-OH |
| chemical shift, δ | 4.65 | 5.41 | 4.72 | | 4.54 | 4.00 | 2.91 | 2.53 | |
| multiplicity | d | t | dd | | d | ddd | dd | dd | |
| coupling constants, Hz | 9.5 | 9.5 | 1.0/9.5 | | 8.0 | 5.5/8.5/8.0 | 5.5/-16.0 | 8.5/-16.0 | |

| "Dry" extended rotamer | C*-ring | | | | F*-ring | | | | |
|---|---|---|---|---|---|---|---|---|---|
| | 2 | 3 | 4 | 3-OH | 2 | 3 | 4α | 4β | 3-OH |
| chemical shift, δ | 4.63 | 4.59 | 4.65 | 4.02 | 4.54 | 4.07 | 3.06 | 2.63 | 4.07 |
| multiplicity | dd | td | dd | d | d | m | dd | dd | d |
| coupling constants, Hz | 6.0 | 4.5/6.0 | 6.0 | | 8.0 | | 4.5/-15.5 | 8.5/-15.5 | |

| "Wet" extended rotamer | C*-ring | | | | F*-ring | | | | |
|---|---|---|---|---|---|---|---|---|---|
| | 2 | 3 | 4 | 3-OH | 2 | 3 | 4α | 4β | 3-OH |
| chemical shift, δ | 4.63 | 4.60 | 4.64 | | 4.54 | 4.06 | 3.06 | 2.63 | |
| multiplicity | d | t | d | | d | ddd | dd | dd | |
| coupling constants, Hz | 6.2 | 6.2 | 6.2 | | 8.0 | 5.5/8.5/8/0 | 5.5/-16.0 | 8.5/-16.0 | |

**TABLE 6.3.1**

| "Dry" compact rotamer | A-ring | | | B-ring | | | E-ring | | | D-ring |
|---|---|---|---|---|---|---|---|---|---|---|
| | **8** | **5** | **6** | **2** | **5** | **6** | **2** | **5** | **6** | **8** |
| chemical shift, δ | 6.28 | 6.68 | 6.33 | 7.02 | 6.82 | 6.87 | 6.94 | 6.82 | 6.79 | 5.93 |
| multiplicity | d | dd | dd | dd | d | dd | d | d | dd | s |
| coupling constants, Hz | 2.2 | 8.0 | 2.2/8.0 | 2.0 | 8.0 | 2.0/8.0 | 2.0 | 8.0 | 2.0/8.0 | |

| "Wet" compact rotamer | A-ring | | | B-ring | | | E-ring | | | D-ring |
|---|---|---|---|---|---|---|---|---|---|---|
| | **8** | **5** | **6** | **2** | **5** | **6** | **2** | **5** | **6** | **8** |
| chemical shift, δ | 6.30 | 6.68 | 6.33 | 7.02 | 8.82 | 6.87 | 6.94 | 6.82 | 6.79 | 6.10 |
| multiplicity | d | dd | dd | d | d | dd | d | d | dd | s |
| coupling constants, Hz | 2.5 | 1.0/8.2 | 2.5/8.2 | 2.0 | 8.0 | 2.0/8.0 | 2.0 | 8.0 | 2.0/8.0 | |

| "Dry" extended rotamer | A*-ring | | | B*-ring | | | E*-ring | | | D*-ring |
|---|---|---|---|---|---|---|---|---|---|---|
| | **8** | **5** | **6** | **2** | **5** | **6** | **2** | **5** | **6** | **8** |
| chemical shift, δ | 6.30 | 6.63 | 6.30 | 7.00 | 6.81 | 6.86 | 6.92 | 6.81 | 6.77 | 6.10 |
| multiplicity | d | bd | dd | dd | d | dd | d | d | dd | s |
| coupling constants, Hz | 2.0 | 8.0 | 2.0/8.0 | 2.0 | 8.0 | 2.0/8.0 | 2.0 | 8.0 | 2.0/8.0 | |

| "Wet" extended rotamer | A*-ring | | | B*-ring | | | E*-ring | | | D*-ring |
|---|---|---|---|---|---|---|---|---|---|---|
| | **8** | **5** | **6** | **2** | **5** | **6** | **2** | **5** | **6** | **8** |
| chemical shift, δ | 6.28 | 6.63 | 6.30 | 7.00 | 6.81 | 6.86 | 6.92 | 6.81 | 6.77 | 5.93 |
| multiplicity | d | bd | dd | dd | d | dd | d | d | dd | s |
| coupling constants, Hz | 2.0 | 8.0 | 2.0/8.0 | 2.0 | 8.0 | 2.0/8.0 | 2.0 | 8.0 | 2.0/8.0 | |

**TABLE 6.3.2**

The COSY 45 experiment done on the extensively dried sample without cadmium nitrate was used to assign the 4-H$_{F\alpha}$ and 4-H$_{F\beta}$ resonances (Figure 6.3.7, L5 113). Since half the responses are missing, the lean of the cross peaks confirms the magnitude and the negative sign of the $^2J_{4HF\alpha,4HF\beta}$ vicinal coupling constant.



**FIGURE 6.3.7**

85
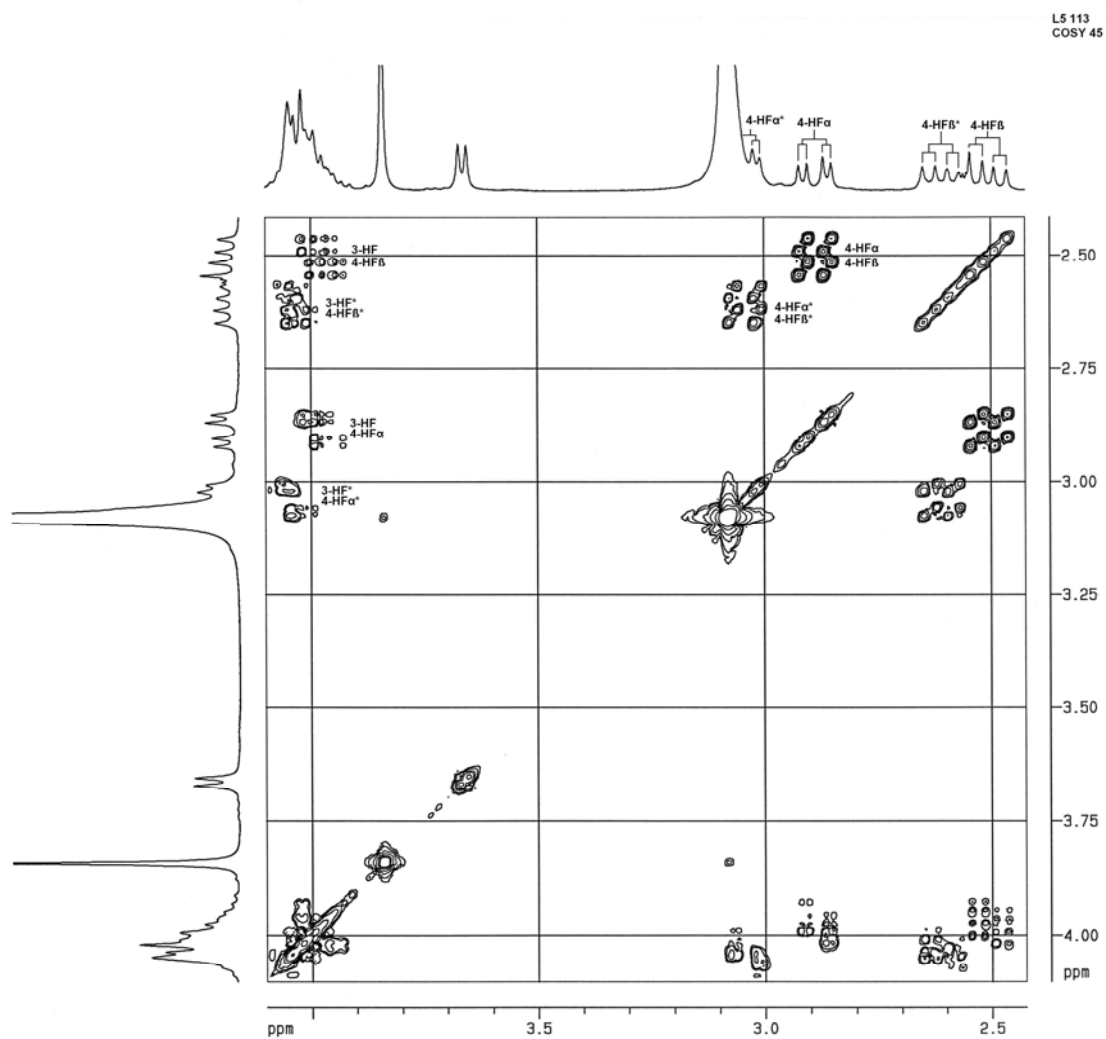
These assignments were then used to assign the resonances of the 3-H$_F$ protons in the dry sample (Figure 6.3.7, L5 113) as well as in the slightly wet sample (Figure 6.3.8, L72). Cross peaks are also observed between the 4-H$_{F\beta}$ and the 2-H$_F$ protons (Figure 6.3.7, L5 72). Half the responses are missing and the lean of the cross peaks confirms the magnitude and positive sign of the $^4J_{4HF,2HF}$ coupling constant.
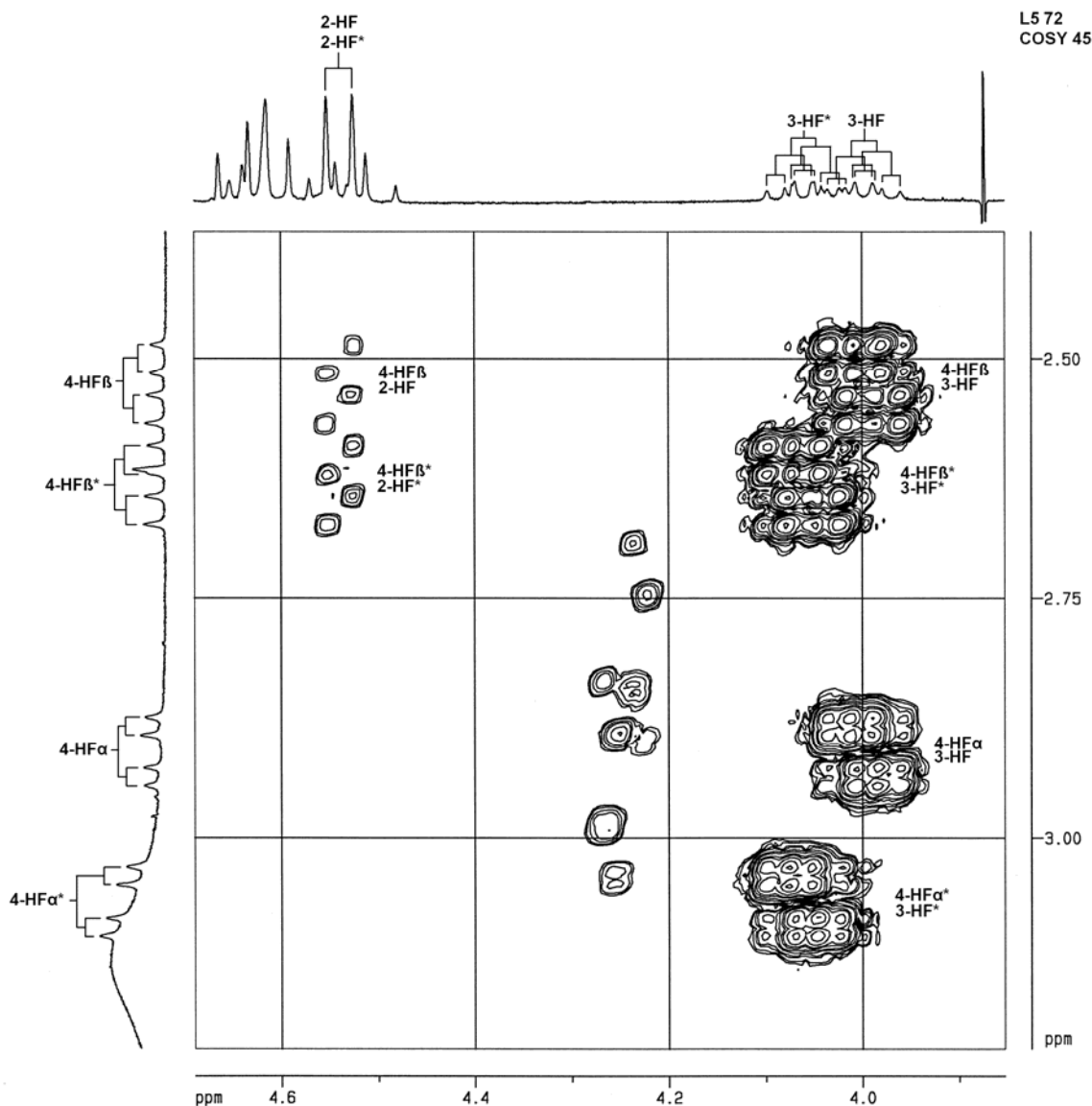


**FIGURE 6.3.8**

The 3-H$_F$ resonances were used to assign the 2-H$_F$ resonances (Figure 6.3.9, L5 5).
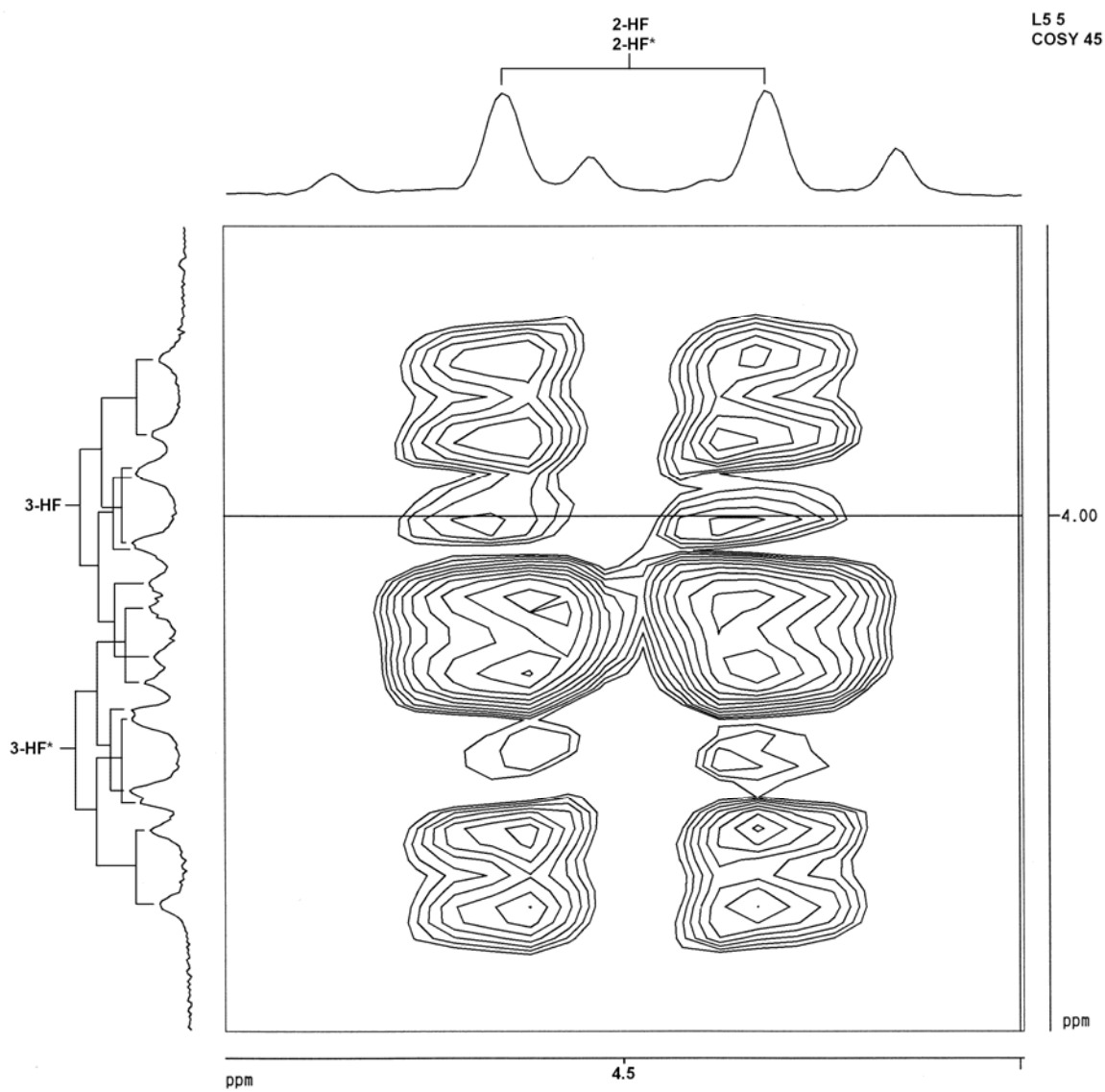


**FIGURE 6.3.9**

Cross peaks are also observed between the 4-H$_F$ and 8-H$_D$ resonances of each rotamer (Figure 6.3.10, L5 64b). Strong coupling between a 4-H$_F$ proton and the 8-H$_D$ proton implies that the 4-H$_F$→4C$_4$ bond is at an approximately 90$^o$ angle with the 8-H$_D$→8C$_D$ bond and therefore also with respect to the plane of the D-ring. Due of the apparent similarity in intensity between the cross peaks of both sets of 4-H$_{F\alpha}$ and 4-H$_{F\beta}$ resonances with their respective 8-H$_D$ resonances, it can be concluded that the F-rings of both conformers undergo conformational exchange, with the 4-H$_{F\alpha}$→4C$_4$ and 4-H$_{F\beta}$→4C$_4$ bonds forming approximately 90$^o$ angles with the 8-H$_D$→8C$_A$ bonds and therefore also with the planes of the respective D-rings.
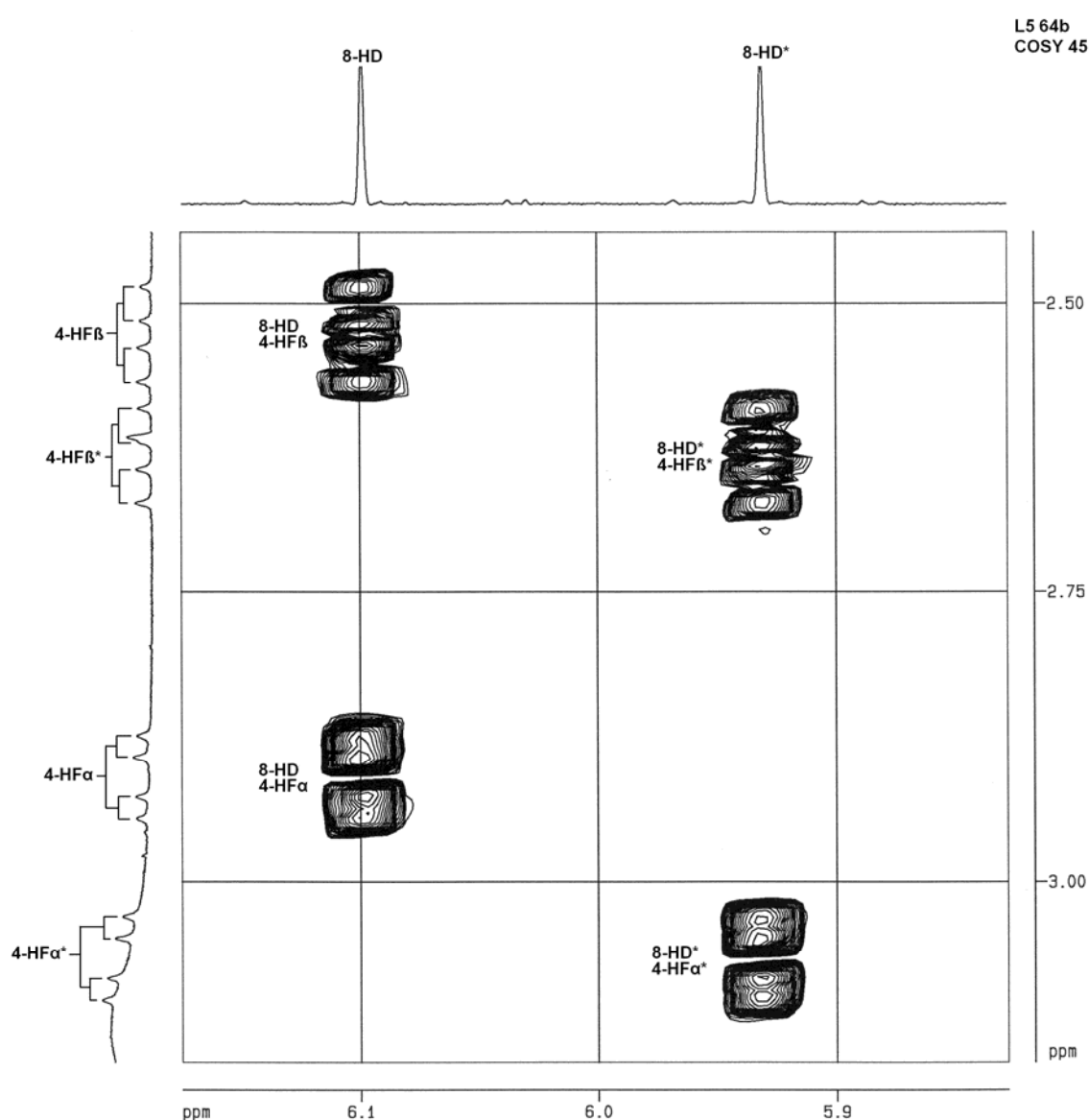
FIGURE 6.3.10

The resonances of both sets of C-ring protons are all in the 4.4 - 4.8 ppm region (Figure 6.3.11, L5 62) Unambiguous assignments of the resonances of the C*-ring protons were not possible due to their proximity to the diagonal.
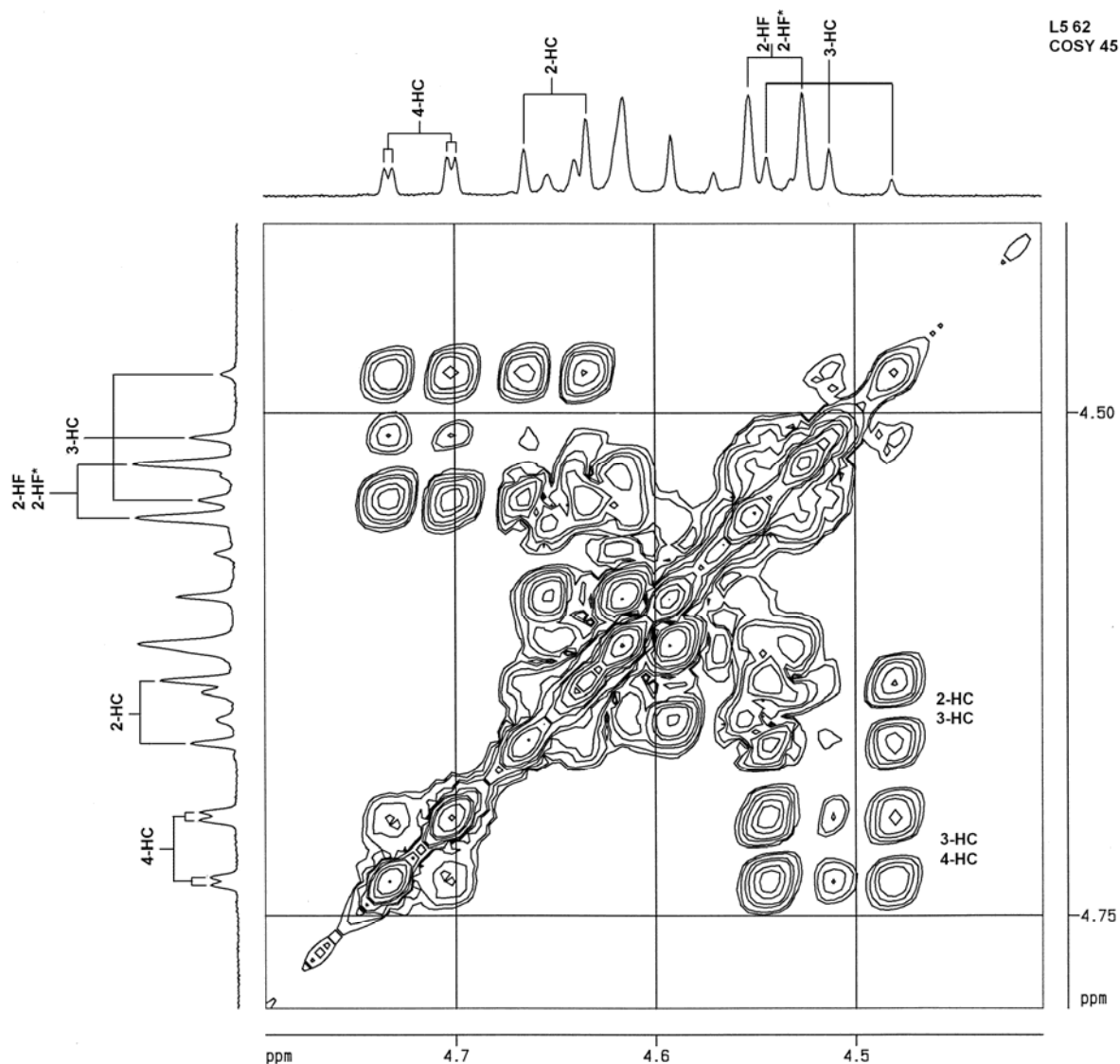


**FIGURE 6.3.11**

The COSY 90W experiment showed cross peaks between the 2-H$_C$, 3-H$_C$, 4-H$_C$ and 3-OH$_C$ resonances (Figure 6.3.12, L5 15). The magnitude of the coupling constants of all the C-ring protons further confirms their assignments. (Table 6.3.3) The presence of cross peaks between the 3-OH$_C$* and C*-ring proton resonances still did not facilitate unambiguous assignments.

| Coupling constant | Sample | Magnitude (Hz) |
|---|---|---|
| $^3J_{2-HC,3-HC}$ | Wet and dry | 9.5 |
| $^3J_{3-HC,3-OHC}$ | Dry | 5.0 |
| $^3J_{3-HC,4-HC}$ | Wet and dry | 9.5 |
| $^3J_{4-HC,5-HA}$ | Wet and dry | 1.0 |

**TABLE 6.3.3**
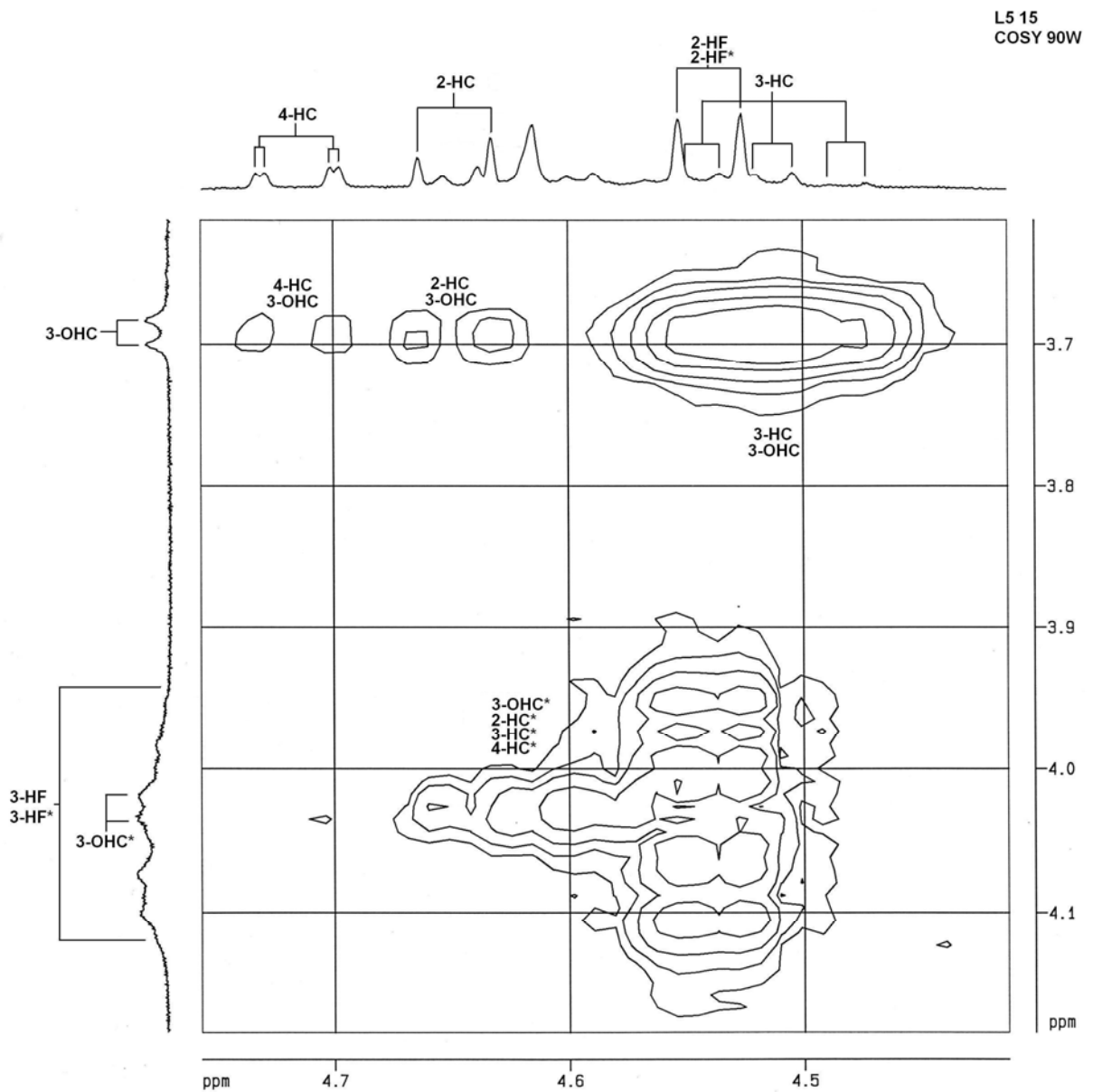


**FIGURE 6.3.12**

The coupling of the 3-H$_C$ and 3-H$_C$* resonances with the respective 3-OH$_C$ and 3-OH$_C$* resonances in the extensively dried sample, results in further splitting of the triplets of both sets of 3-H$_C$ resonances displayed for the wet sample (Figure 6.3.13 from Figure 6.3.4) into doublets of triplets (Figure 6.3.14 from Figures 6.3.5/6). The chemical shifts of these resonances and the magnitude of the $^3J_{3-HC,3-OHC}$ coupling constants (5.0 Hz) of both the 3-H$_C$ (4.513ppm) and the 3-H$_C$* (4.592ppm) resonances, confirm their assignments.
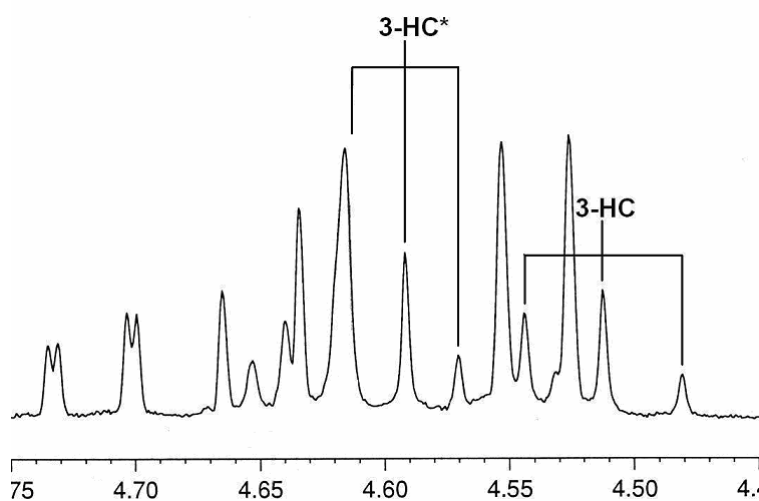


**FIGURE 6.3.13**
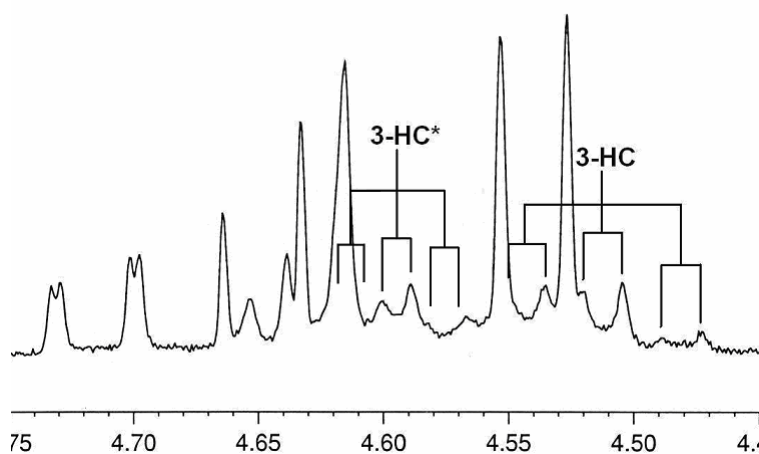


**FIGURE 6.3.14**

Strong coupling in the same COSY 45 experiment between the 4-H$_C$ and respective 8-H$_D$ resonances implies that the 4-H$_C$→4C$_C$ bonds of both rotamers are at approximately 90° angles with the 8-H$_D$→8C$_D$ bonds and therefore also with respect to the plane of the D-rings (Figure 6.3.15, L5 78).

The 6-H$_A$, 8-H$_A$, 6-H$_A$* and 8-H$_A$* resonances were assigned from their cross peaks with the respective 4-H$_C$ and 4-H$_C$* resonances.
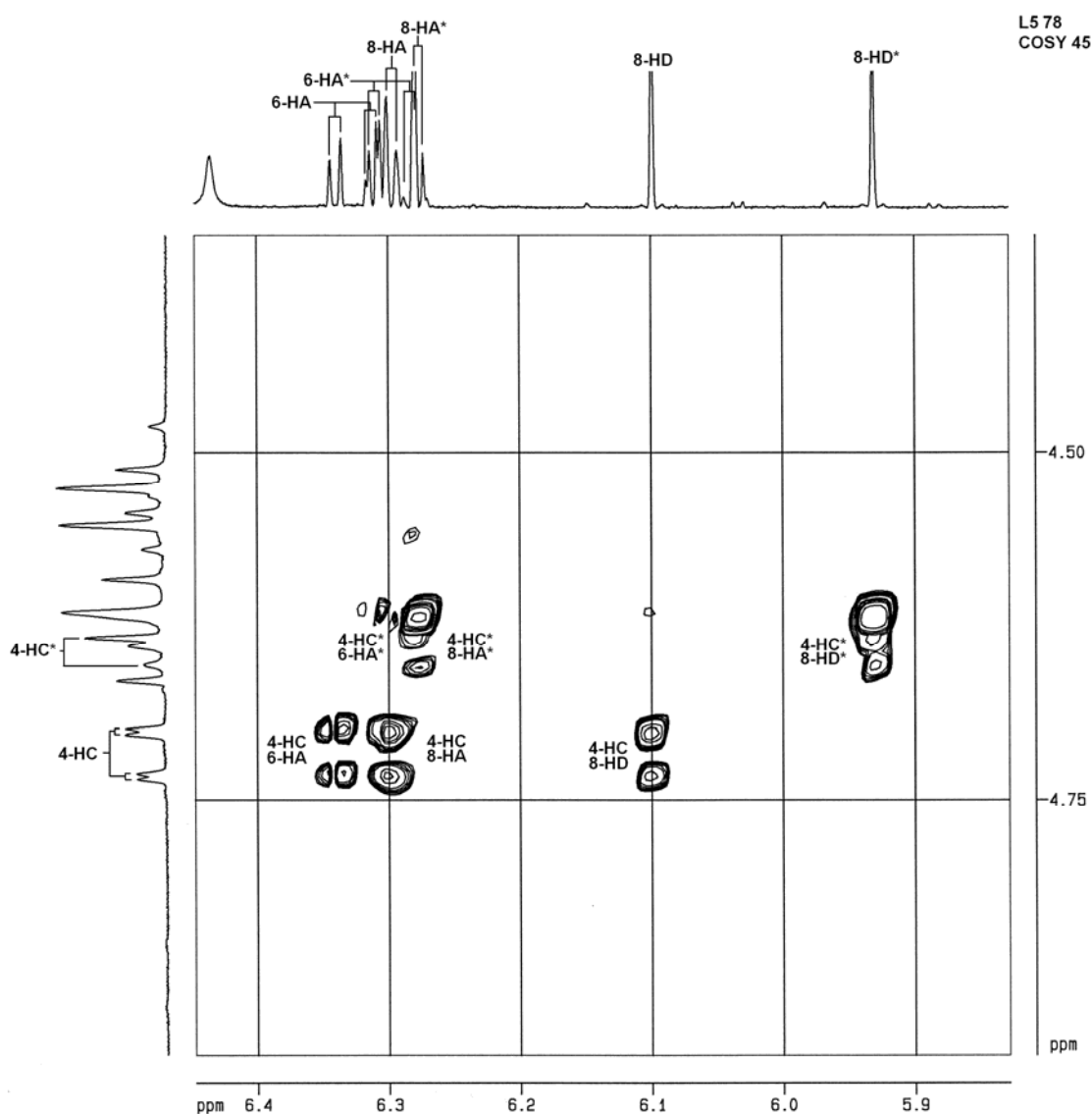


**FIGURE 6.3.15**

The 2-H$_C$* resonance was assigned from its cross peaks with the 2-H$_B$* and 6-H$_B$* resonances (Figure 6.3.19, L5 9c)

The 4-H$_C$* resonance could not be unambiguously assigned by its cross peaks with the 8-H$_D$* resonance in the COSY 45 experiment of the wet sample (Figure 6.3.15, L5 78). Two sets of resonances with different coupling constants were considered as a result of the appearance of these cross peaks (Figures 6.3.15, 6.3.16 and 6.3.17). A comparison of the coupling constants of the HC* protons favours the assignments in Figure 6.3.17.
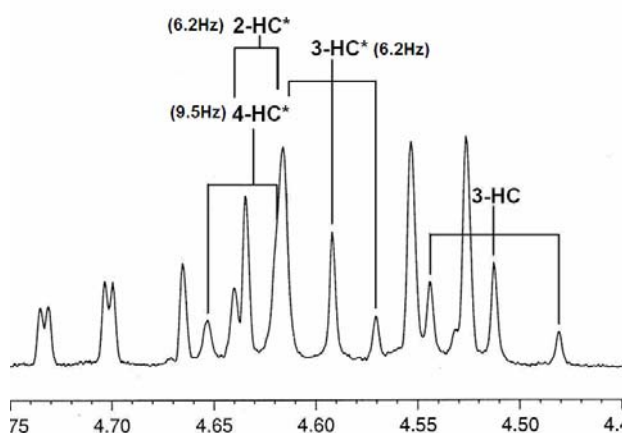


**FIGURE 6.3.16**
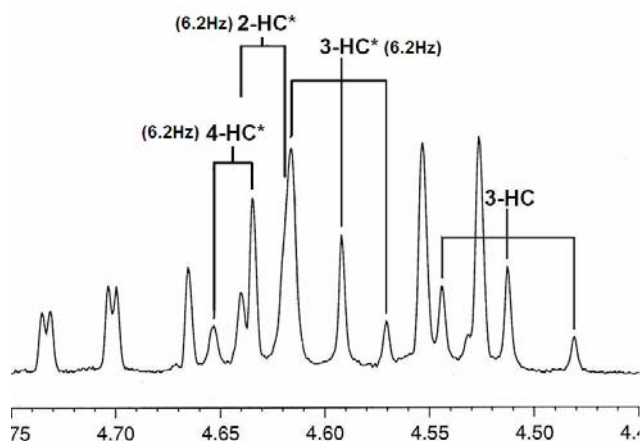


**FIGURE 6.3.17**

However, the appearance of the 4-H$_C$*/5-H$_A$* cross peaks (Figure 6.3.19) as well as the 4-H$_C$*/5-C$_A$* cross peaks (Figure 6.3.25) favours the assignment in Figure 6.3.16.

The 5-H$_A$ resonances were assigned from their cross peaks with the respective 6-H$_A$ and 8-H$_A$ resonances (Figure 6.3.18, L5 81)
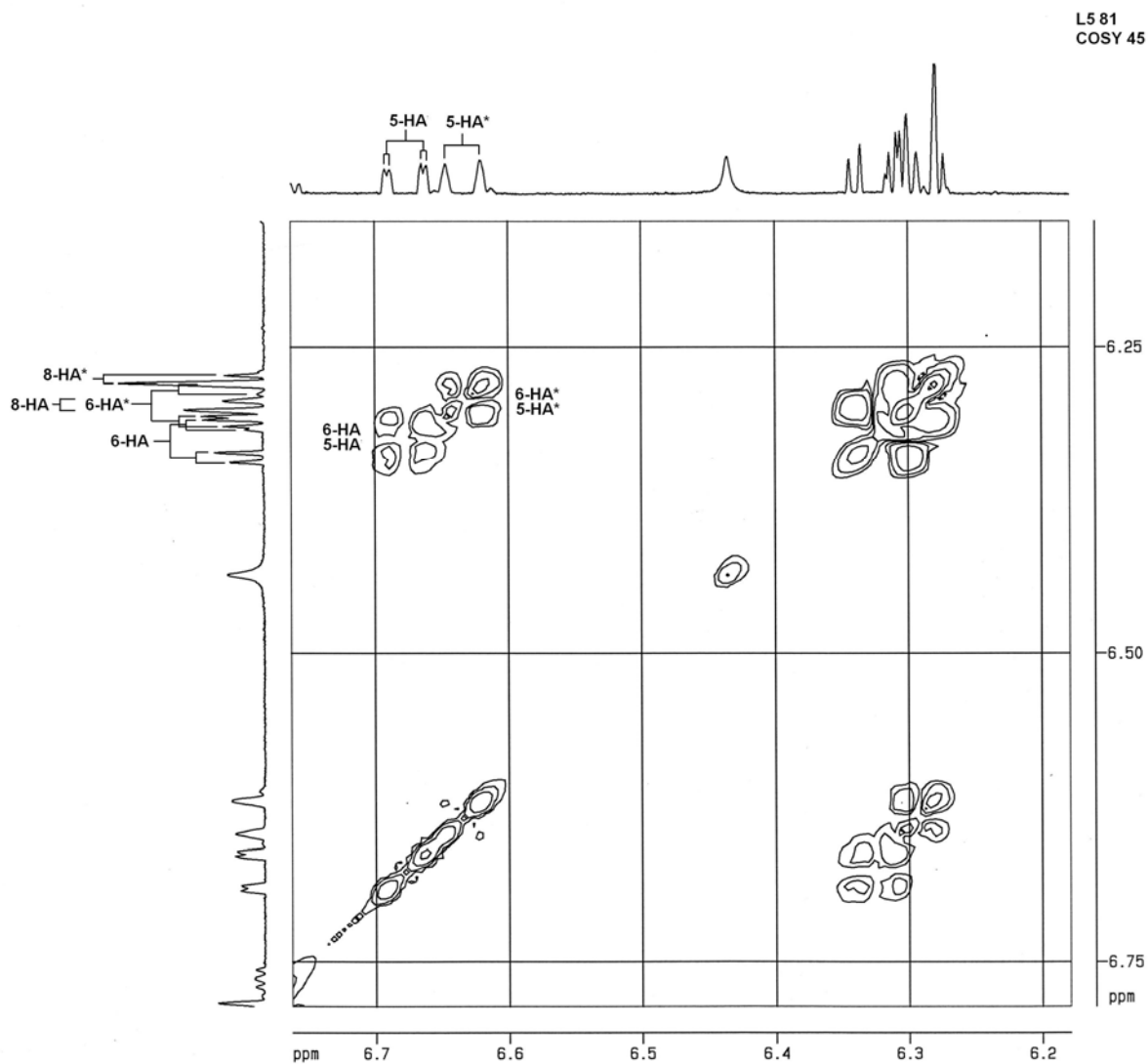


**FIGURE 6.3.18**

Because of the coincidental 2-H$_F$ resonances of both rotamers, unambiguous assignments of the H$_E$ resonances of each rotamer were not possible. The 2-H$_B$ and 6-H$_B$ resonances were assigned from their cross peaks with the resonances of the C-ring protons (Figure 6.3.19, L5 9c).
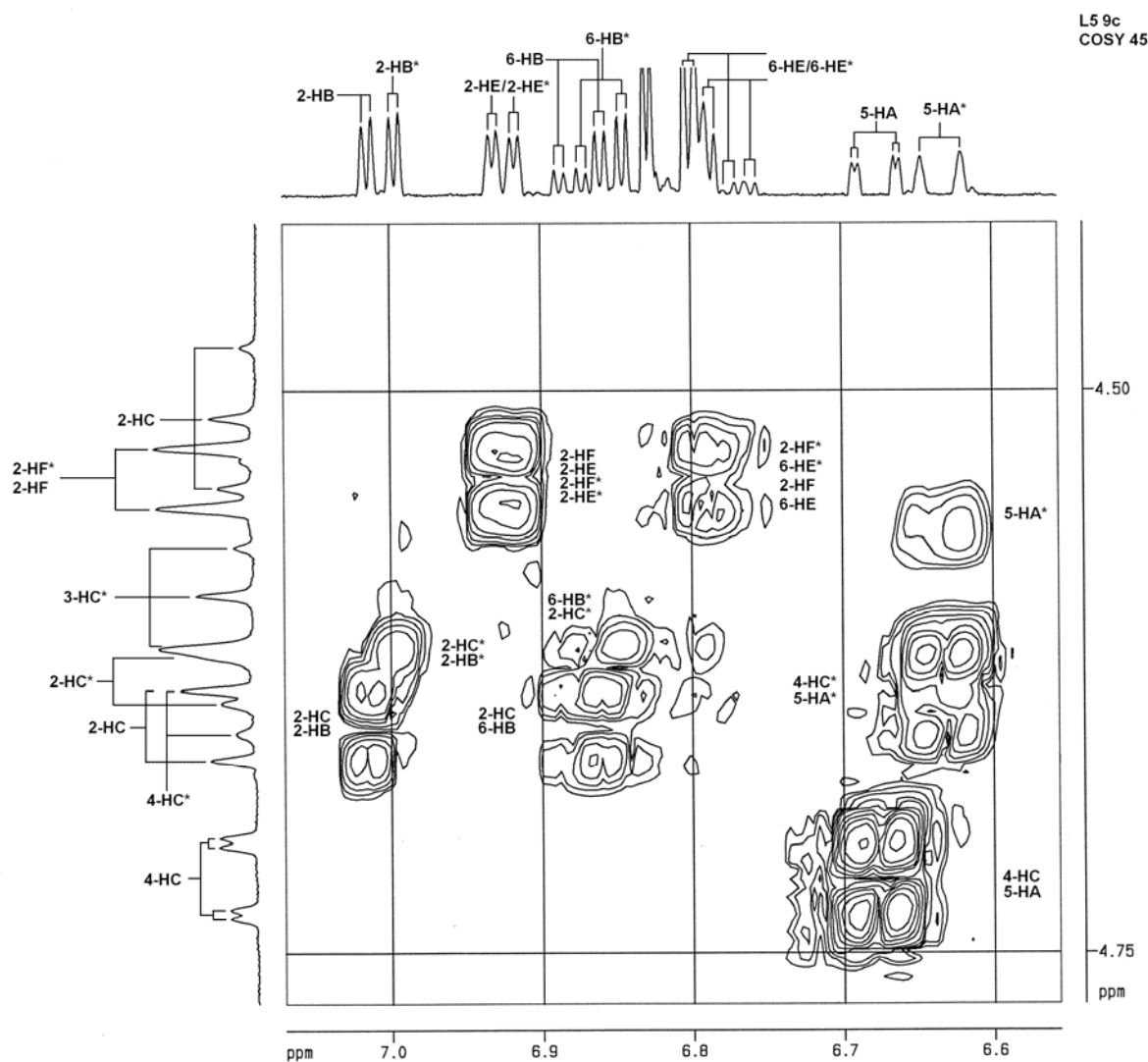


**FIGURE 6.3.19**

Both sets of 5-H$_B$ resonances were assigned from their cross peaks with the 6-H$_B$ resonances (Figure 6.3.20, L5 76).

Both sets of H$_E$ resonances were assigned from their cross peaks with each other (° and ■), but it was not possible to assign each set to a specific rotamer. Unambiguous assignments of the 5-H$_E$ resonances were not possible due to their proximity to the diagonal (Figure 6.3.20, L5 76).
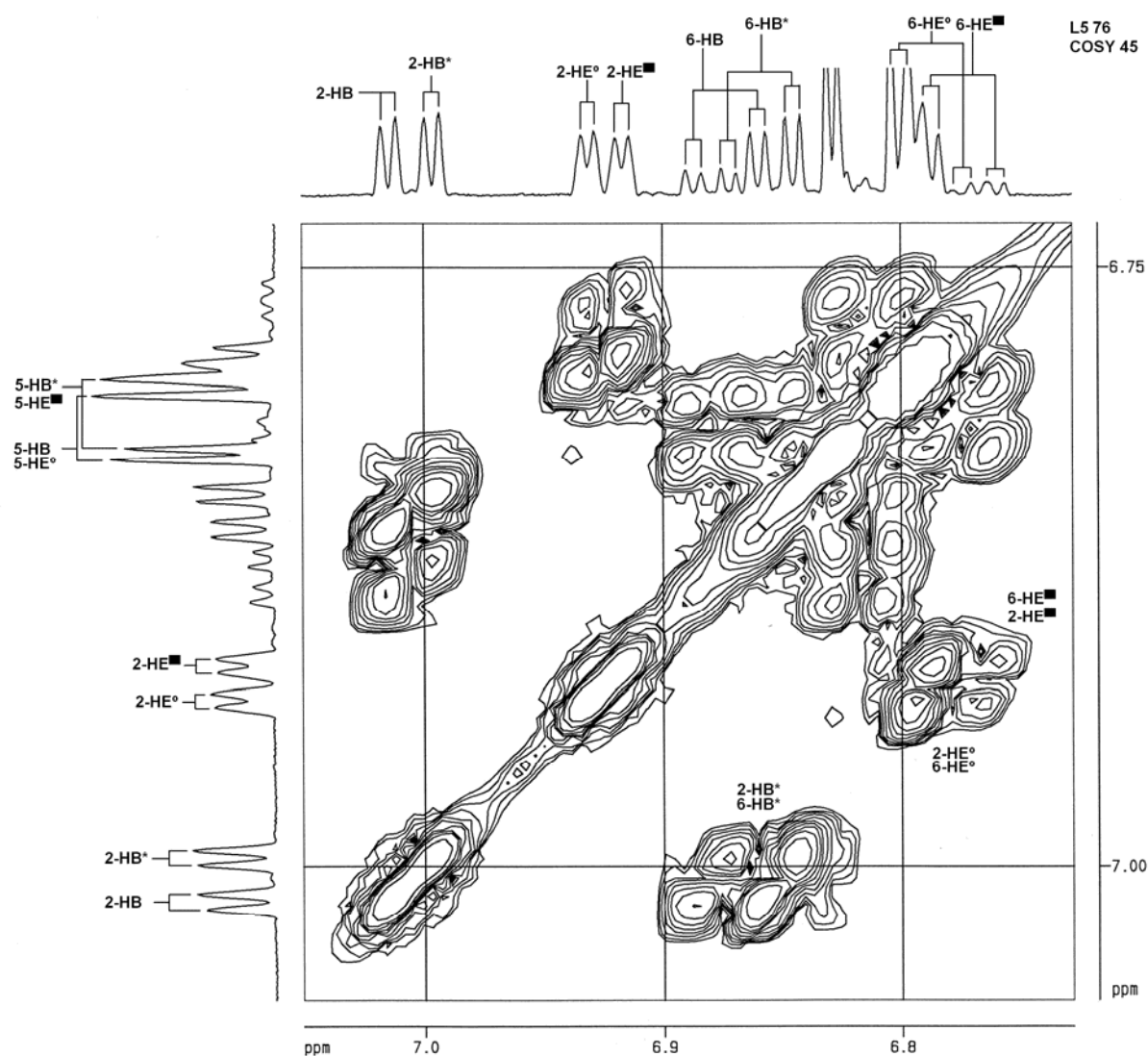


**FIGURE 6.3.20**

The resonances of some of the aromatic hydroxy groups were assigned from their cross peaks with some of the aromatic proton resonances (Figure 6.3.21, L5 5).
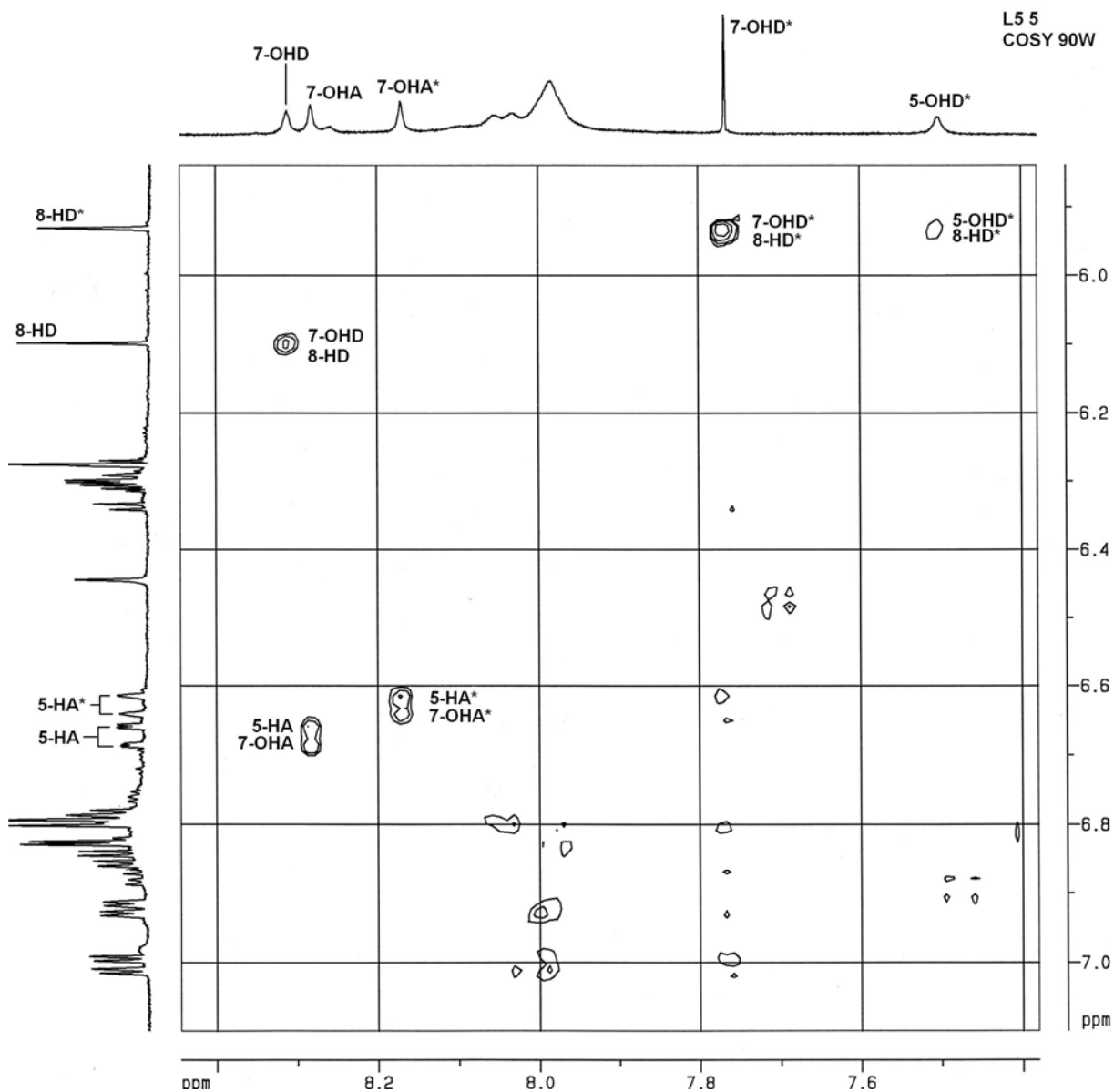


**Figure 6.3.21**

Cross peaks between the 4-H$_C$ and 7-OH$_D$ resonances in the COSY 90W experiment (Figure 6.3.22, L5 4) are similar to those observed in the NOESY PH experiment (Figure 6.3.23, L5 44).
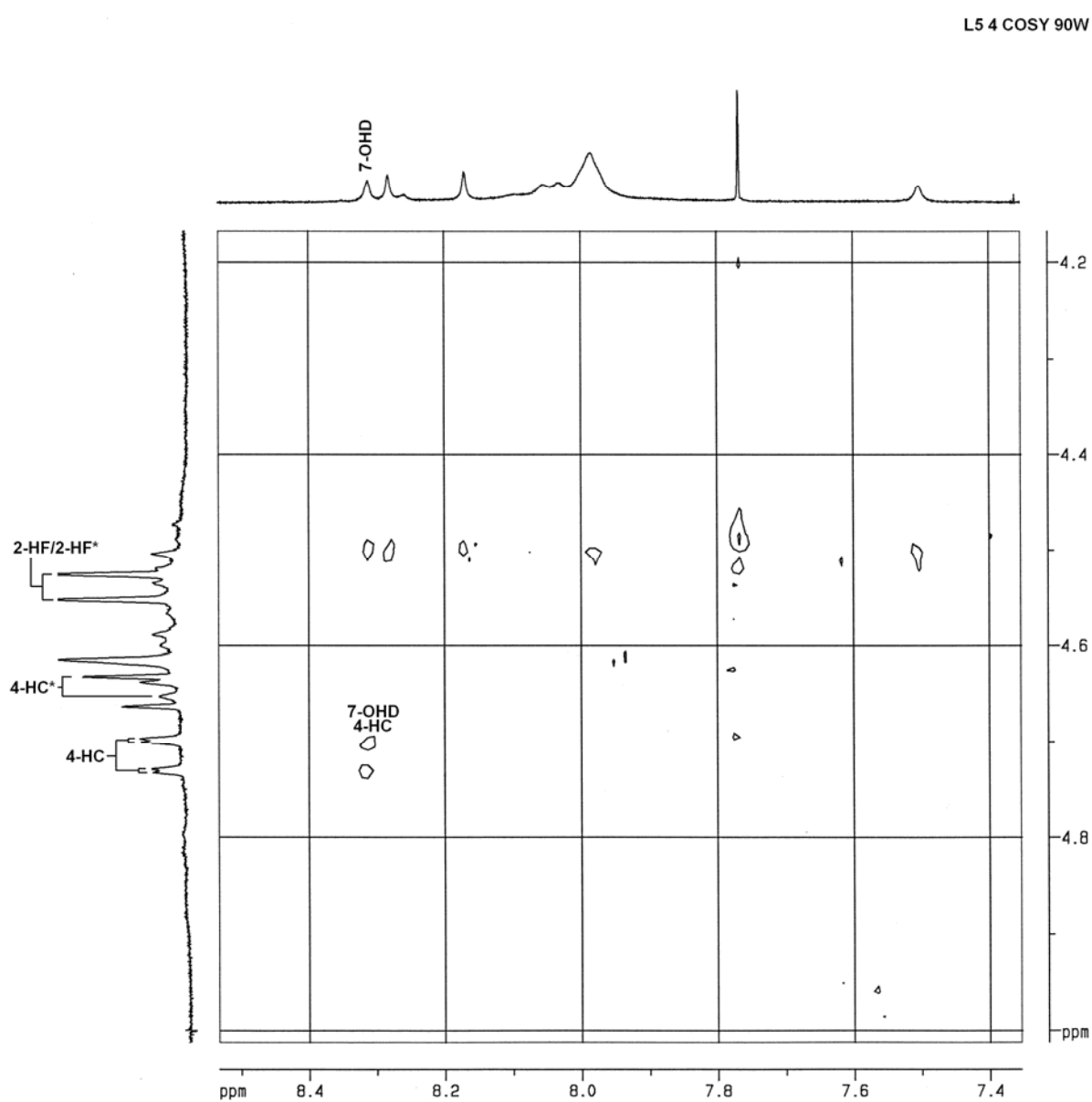


**FIGURE 6.3.22**
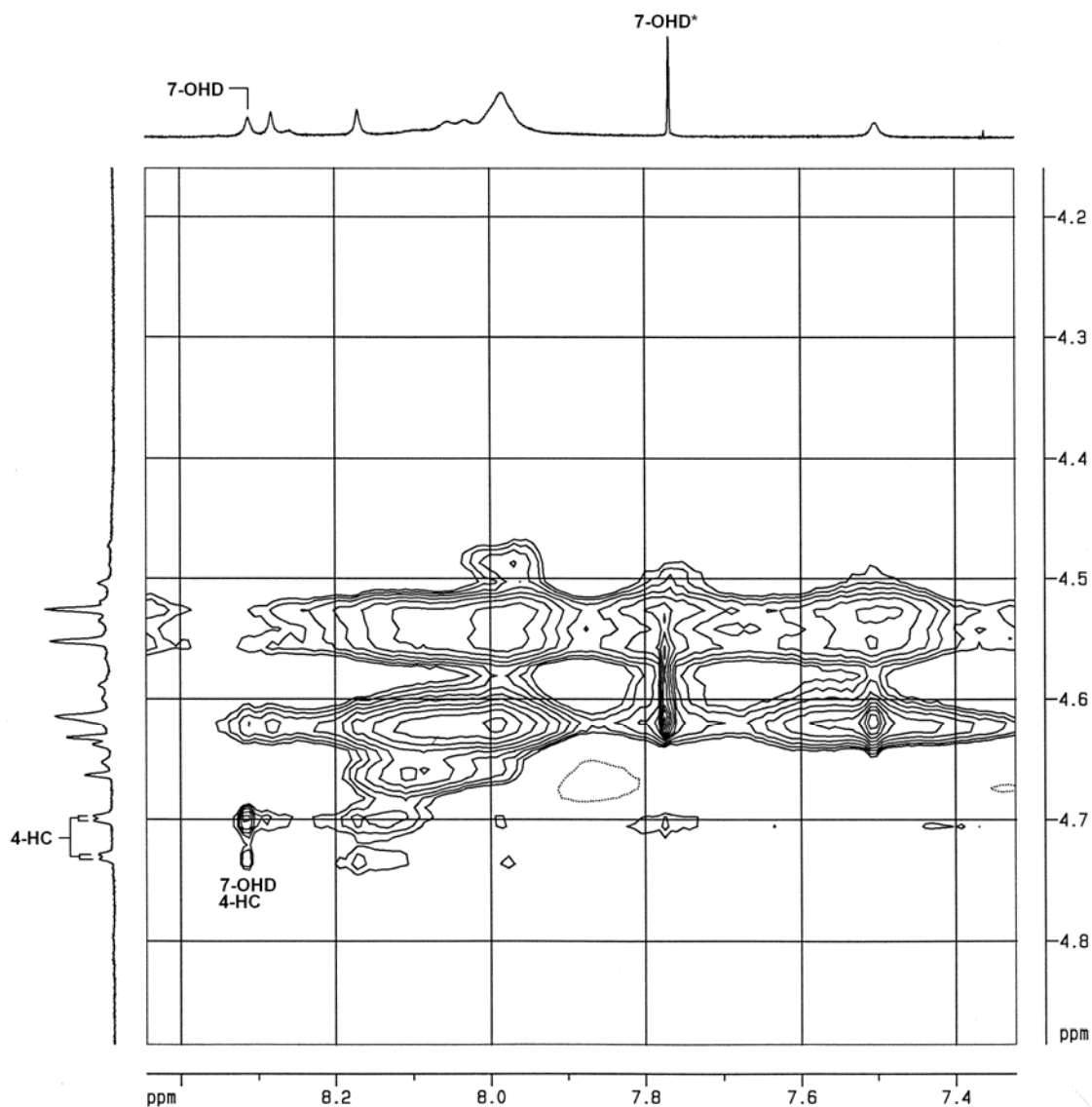
**FIGURE 6.3.23**

The identification of the rotamers as either "compact" or "extended" as in the case of fisetinidol-(4α→8)-catechin (Paragraph 6.1) as well as catechin-(4α→8)-catechin and catechin-(4α→8)-epicatechin[98], cannot be applied to the 4α→6 linked dimer, as both rotamers have shapes that resemble those of the "extended" conformations of the 4α→8 linked dimers.

99

All the 4α→8 linked dimers have significant chemical shift differences between the resonances of the B- and E-ring protons of each of the two rotamers[98] (Paragraphs 6.1/2).. In contrast, there are only small differences in chemical shifts of the proton resonances of the aromatic rings of both rotamers of the 4α→6 linked dimer. This is due to the similar magnetic environments of the aromatic rings of both rotamers. Hence, it is not always possible to unambiguously assign resonances to some of the protons, as well as to assign them to a specific rotamer. The same holds true for the carbon resonances (Figure 6.3.25).
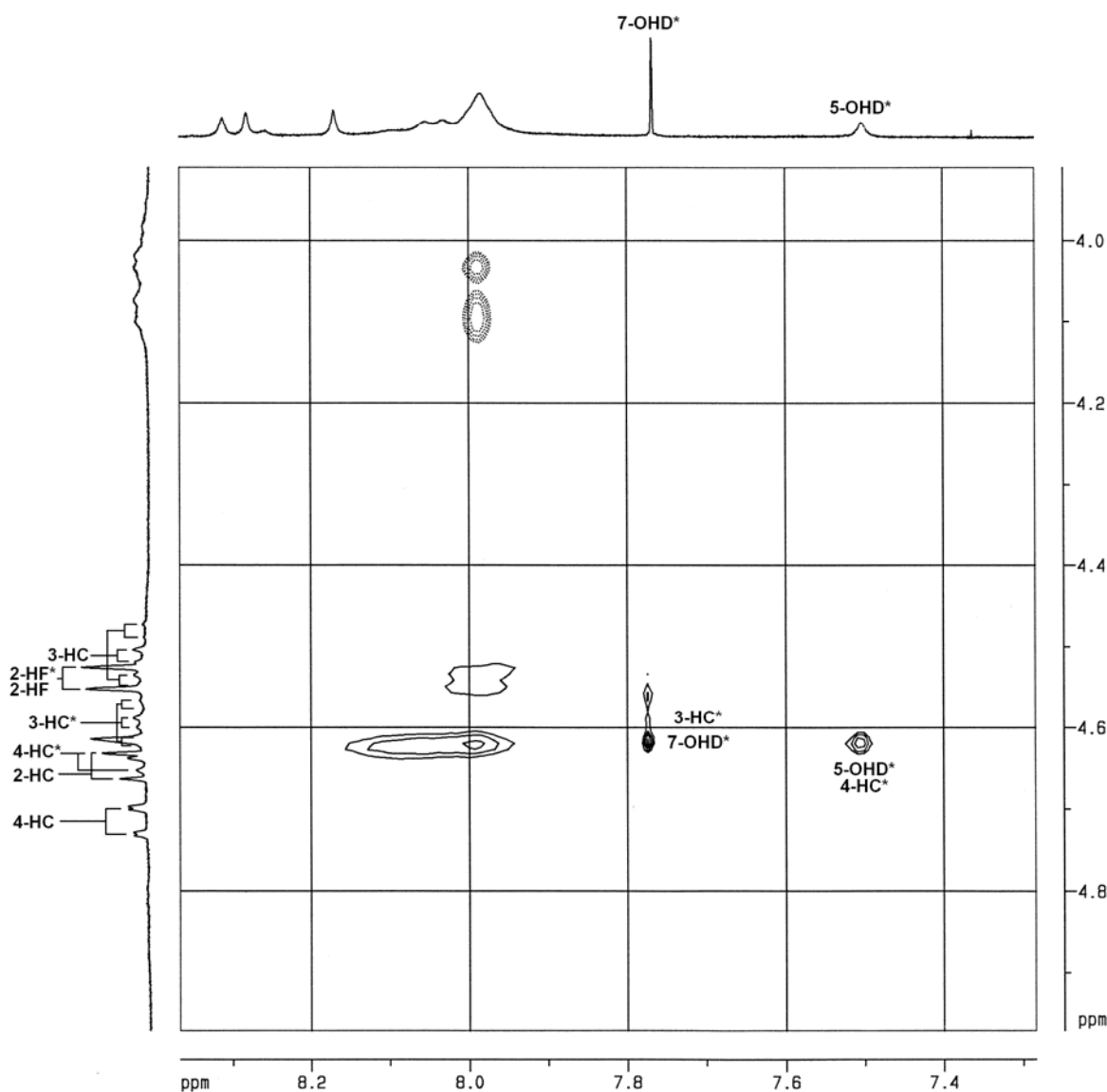


**FIGURE 6.3.24**

The *-rotamer is identified by cross peaks between the $4\text{-H}_C^*$ and $7\text{-OH}_D^*$ resonances well as the cross peaks between the $3\text{-H}_C^*$ and $5\text{-OH}_D^*$-resonances (Figure 6.3.24, L5 46).

The cross peaks between the $4\text{-H}_C$ and $7\text{-OH}_D$ resonances are weaker (Figure 6.3.23, L5 44) than the two sets of cross peaks identifying the *-rotamer. The distance between $4\text{-H}_C$ and $7\text{-OH}_D$ proton is therefore larger than the distances between $4\text{-H}_C^*$ and $7\text{-OH}_D^*$, as well as between $3\text{-H}_C^*$ and $5\text{-OH}_D^*$.

The intensities of the cross peaks between the $4\text{-H}_C^*$ and $8\text{-H}_D^*$ resonances as well as the $4\text{-H}_C$ and $8\text{-H}_D$ resonances (Figure 6.3.15) seem to be similar in magnitude and suggest an approximately 90° angle between the $4\text{-H}_C{\rightarrow}4C_C$ bonds and the planes of the respective D-rings. The different intensities of the cross peaks in the NOESY PH experiment identifying the two rotamers, however, indicate that the angle between the $4\text{-H}_C{\rightarrow}4C_C$ bond and the plane of the D-ring is larger than the angle between the $4\text{-H}_C^*{\rightarrow}4C_C^*$ bond and the plane of the $D^*$-ring.

The $^{13}\text{C}$ NMR and HMQC experiments (Figures 6.3.25-28, Appendix B) display very small chemical shift differences between the carbon resonances of the two rotamers, as well as substantial overlap of C/H cross peaks.
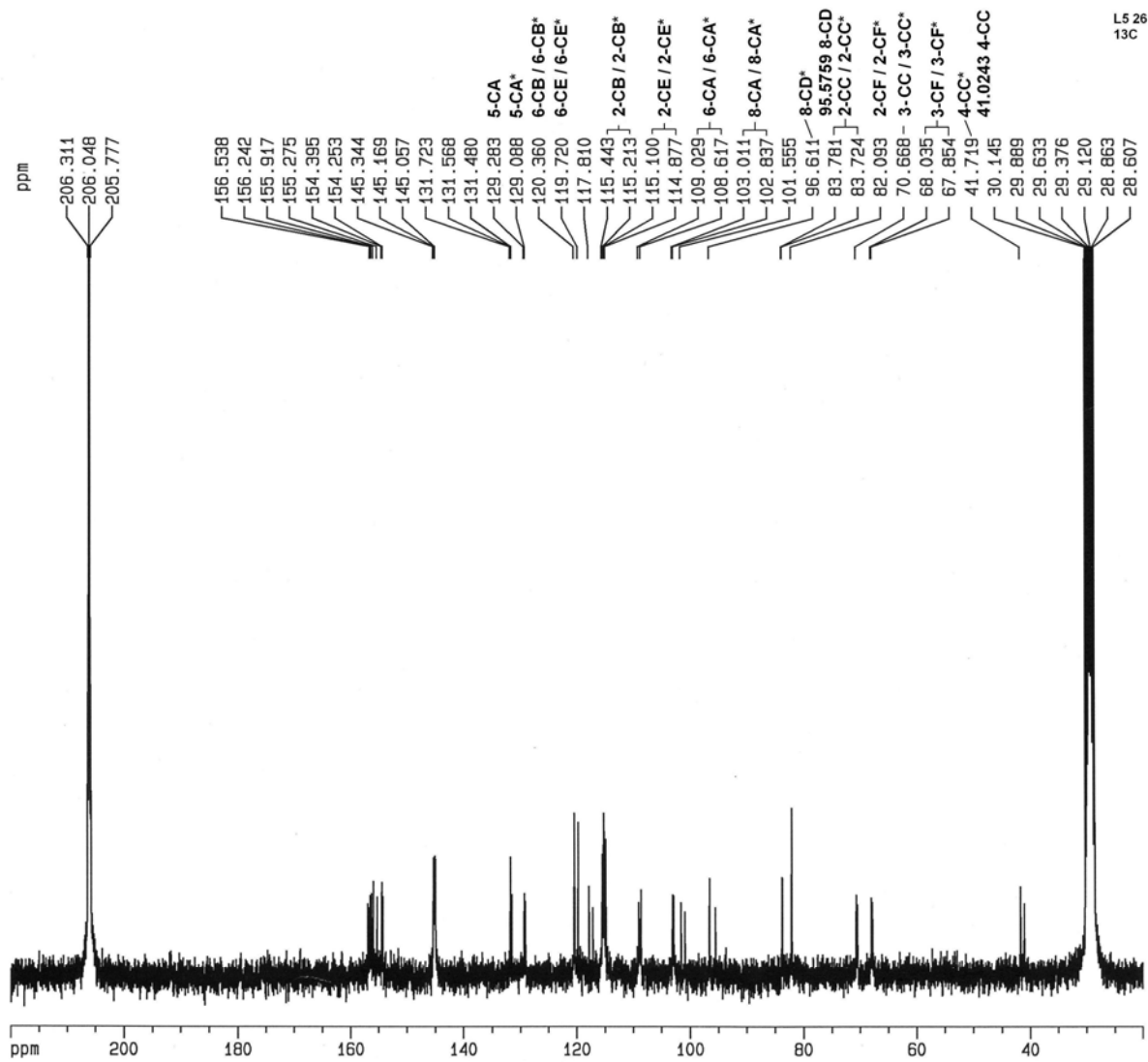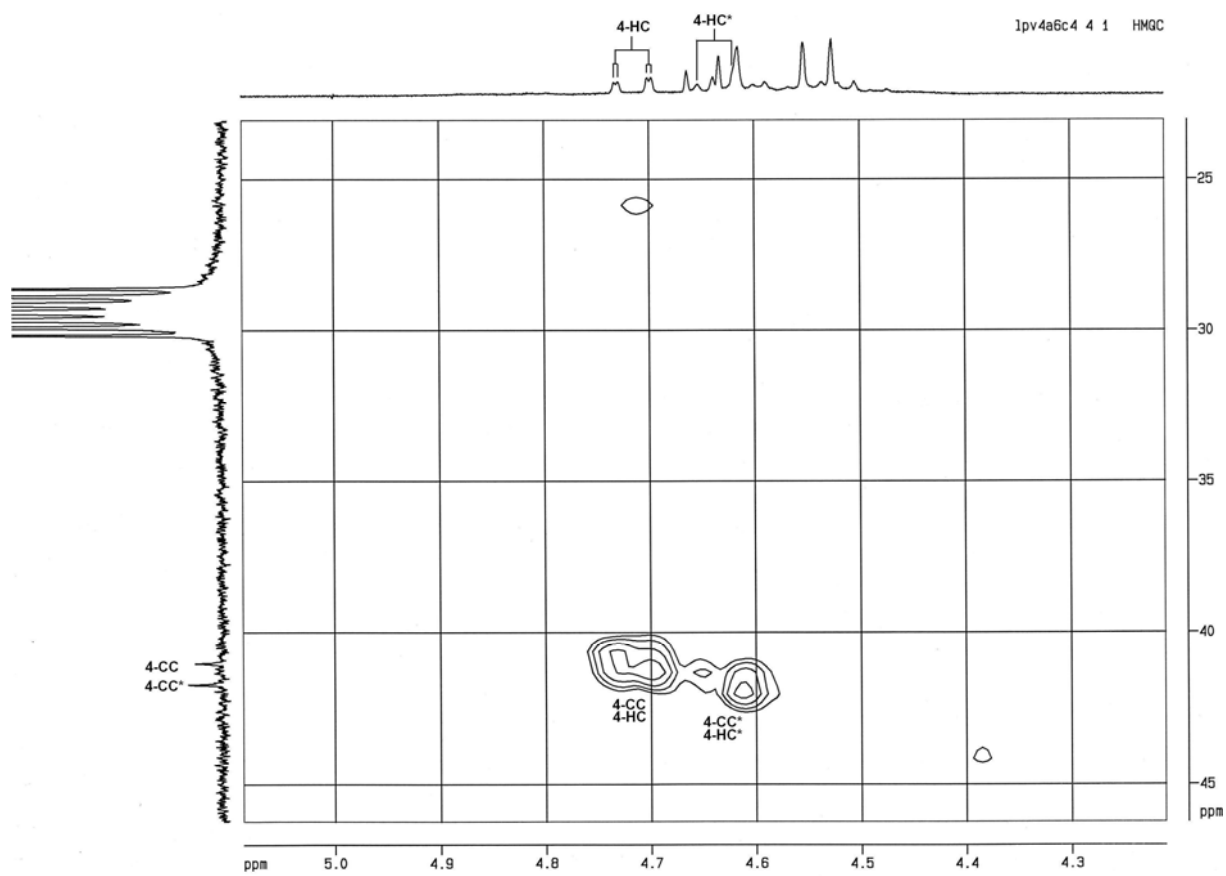
**FIGURE 6.3.25**

**FIGURE 6.3.25**
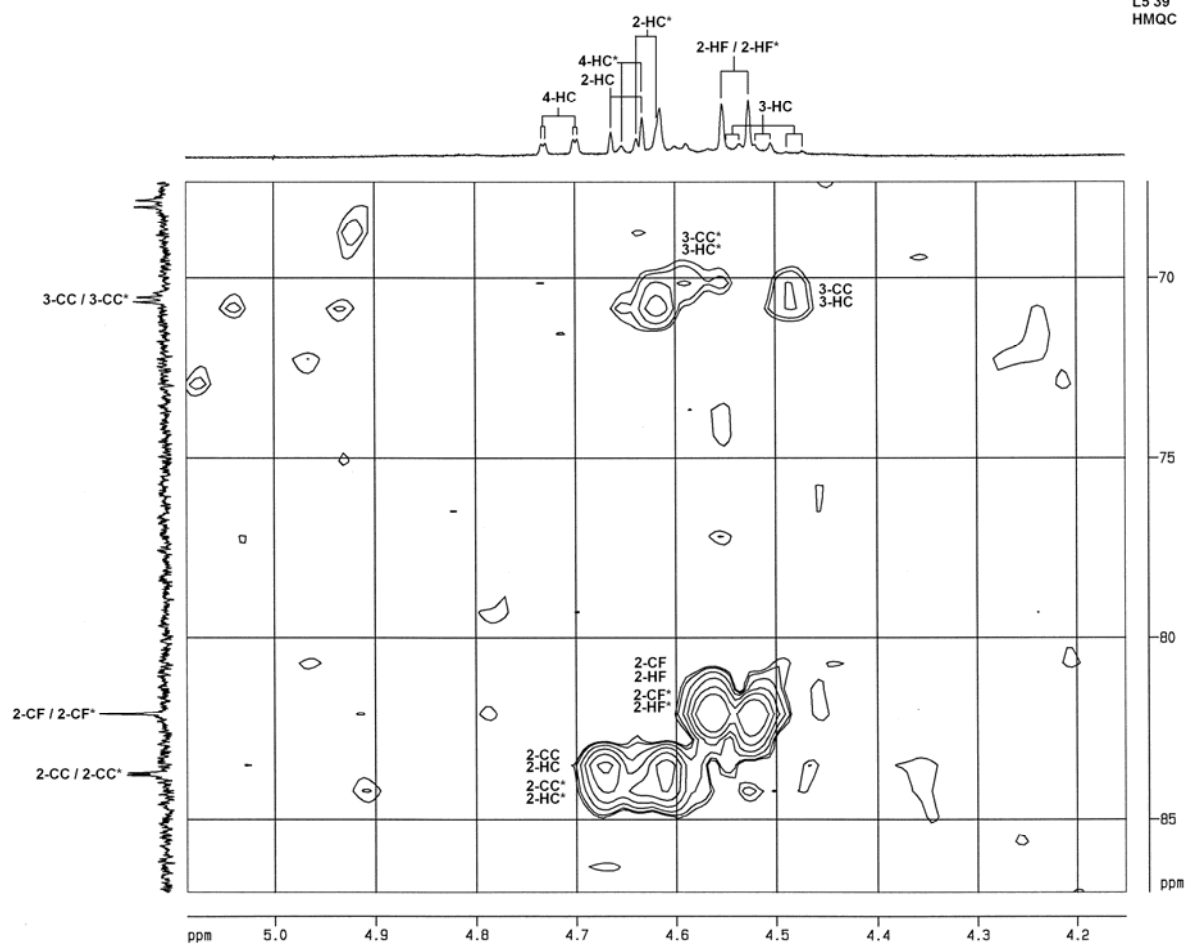
**FIGURE 6.3.26**
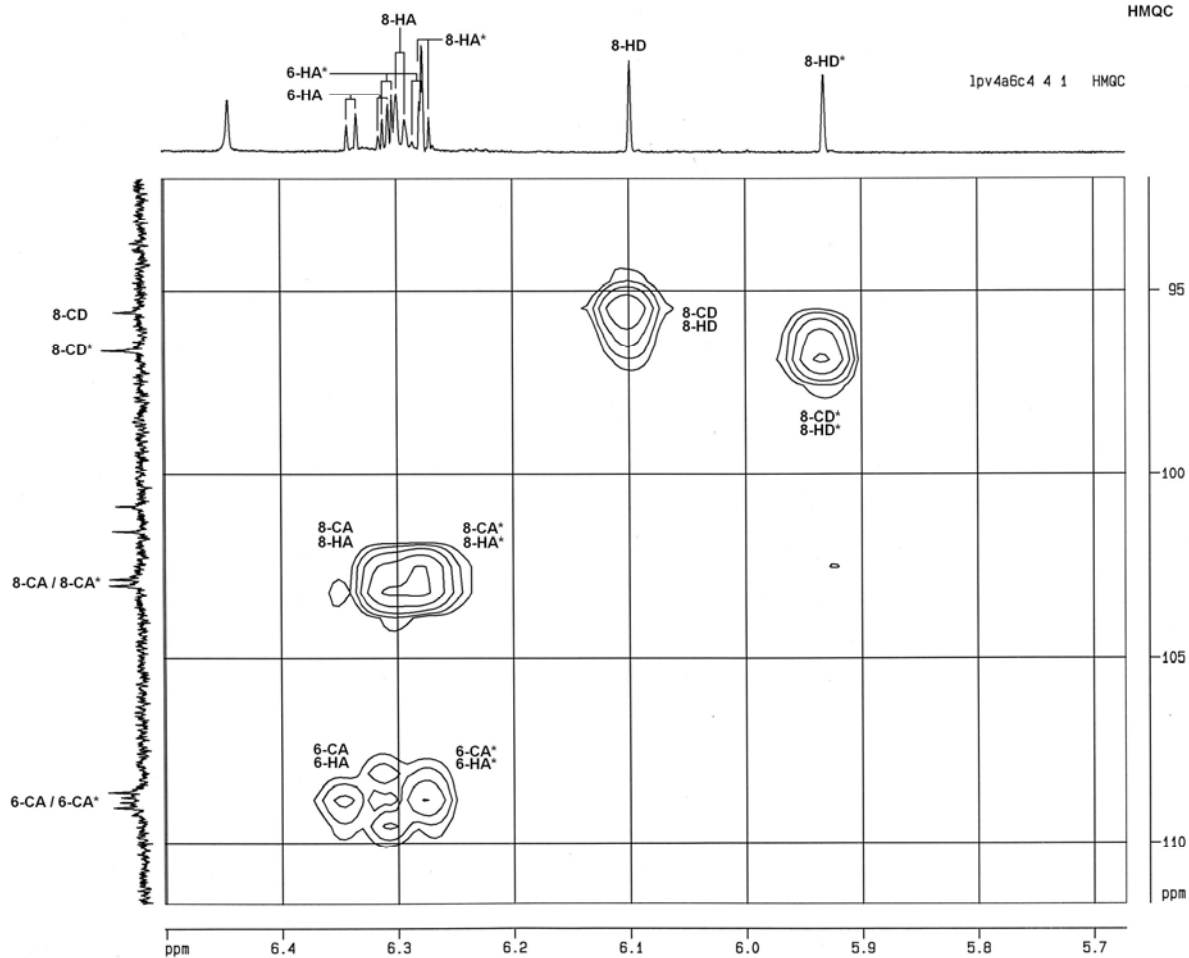
**FIGURE 6.3.27**
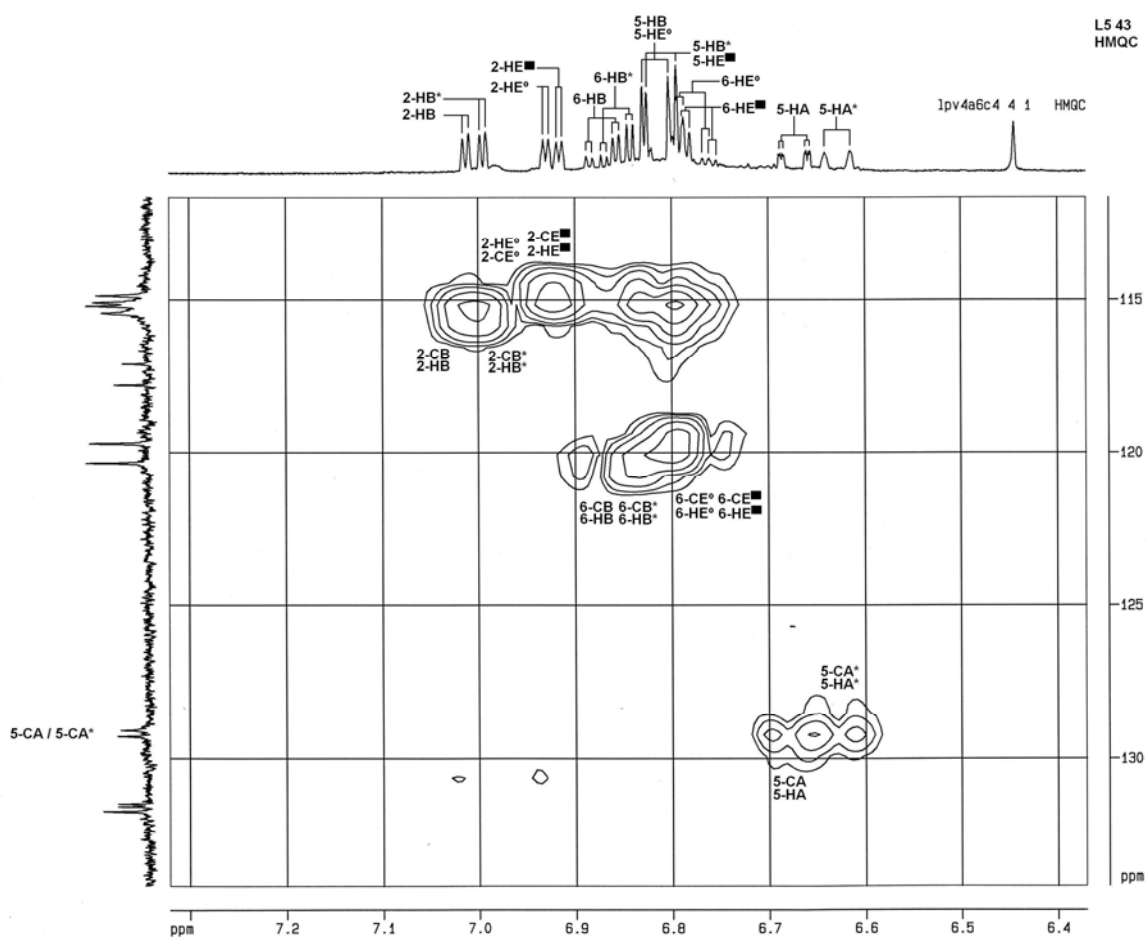
**FIGURE 6.3.28**

## 6.4 THE CONFORMATIONAL BEHAVIOUR OF FISETINIDOL-(4β→6)-CATECHIN IN ACETONE-d₆

The structure of this compound was studied by CD in methanol (see Chapter 8), ^{1}H NMR, ^{13}C NMR, COSY 45 and HMQC experiments (Tables 6.4.1/2) in extensively dried acetone acetone-d$_6$.The ^{1}H NMR spectrum (Figures 6.4.1/2) displayed only one set of resonances, indicating either fast rotation around the interflavanyl bond or the presence of intramolecular hydrogen bonds, arresting rotation around the interflavanyl bond.

Resonances at δ = 2.61, 3.84 and 3.88 were impurities present as a result of the extensive drying process of acetone-d$_6$ (Paragraph 9.3, Appendix D)
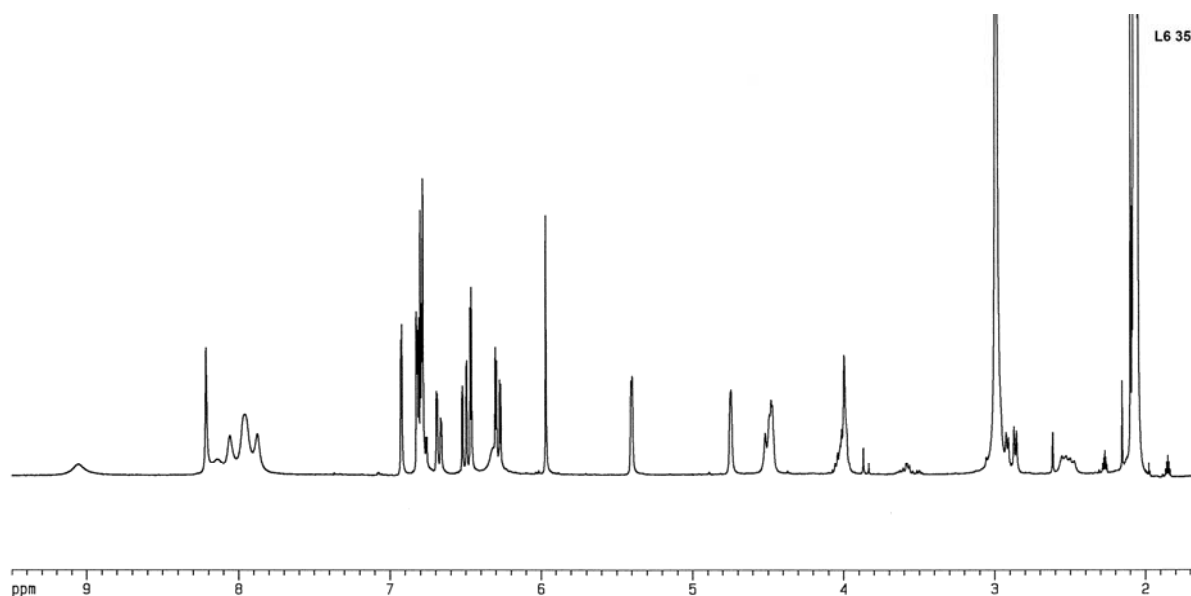


**FIGURE 6.4.1**
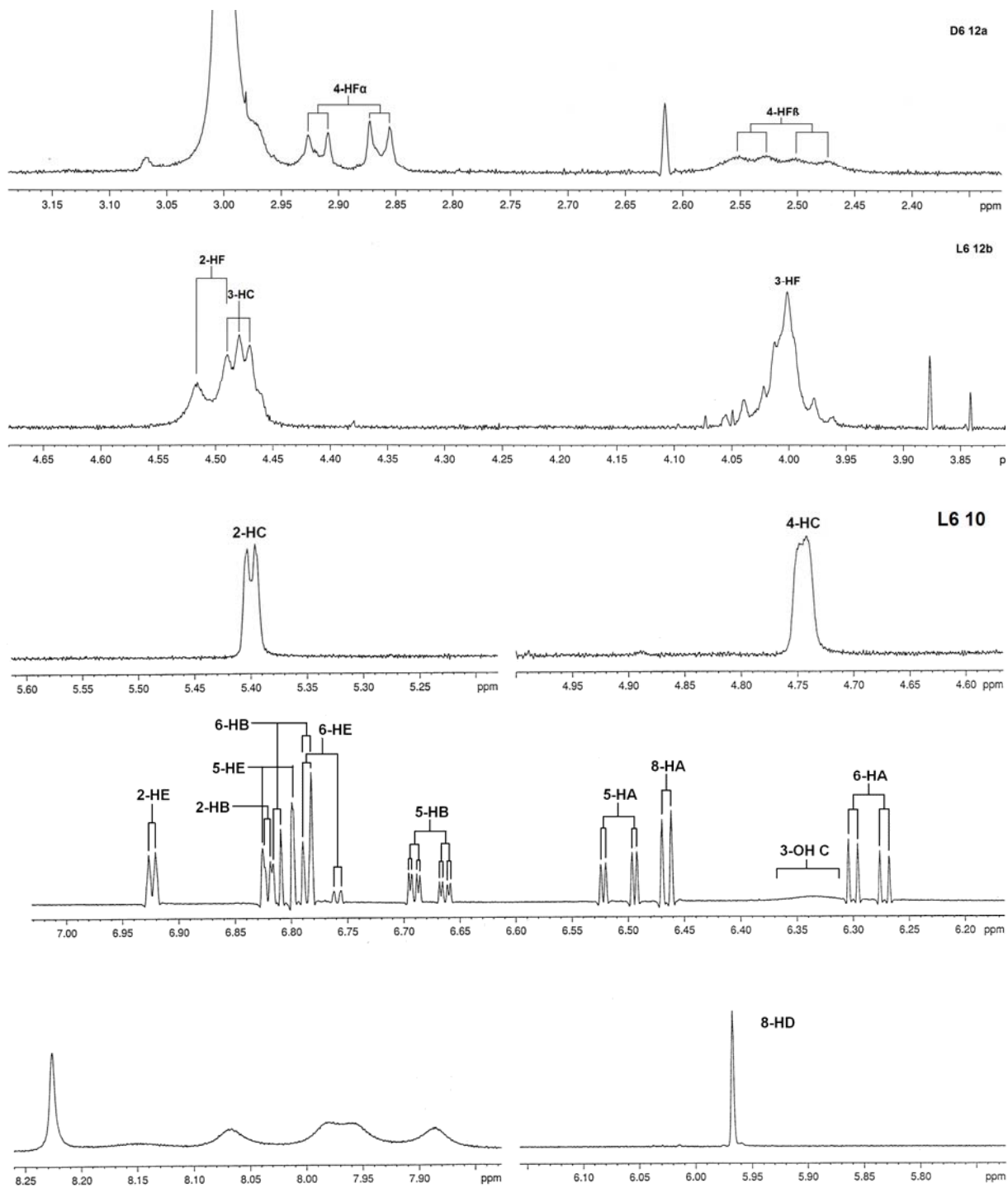
**FIGURE 6.4.2**

The 2-H$_C$ and 4-H$_C$ resonances were assigned by COSY 45 cross peaks (Figure 6.4.4, L6-

26) as well as HMQC cross peaks (Figure 6.4.3, L6 1). This is unusual, as 4-$H_C$ is usually more deshielded than 2-$H_C$ in the 4α-linked dimers. The resonance of 4-$C_C$ has a slightly higher chemical shift than 4-$C_F$, which is obscured by the acetone-$d_6$ resonance on the HMQC spectrum (Figure 6.4.2, L6 12; Figure 6.4.3 L6 1 and Figure 6.4.13, L6 5).
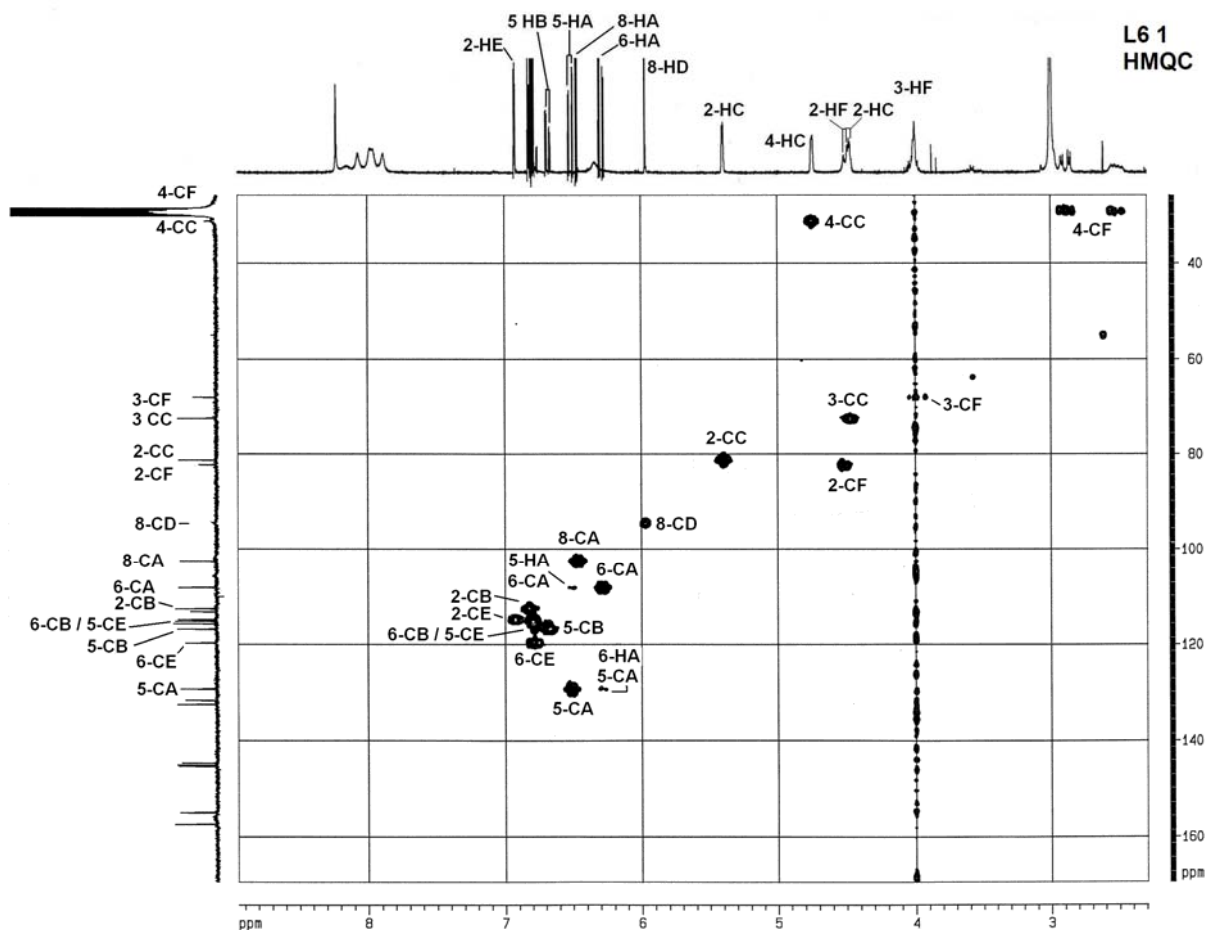


**FIGURE 6.4.3**

The small coupling constants (0.8 to 4Hz) observed for the heterocyclic C-ring proton resonances as well as the 2-$H_C$/4-$H_C$ cross peaks (Figure 6.4.4, L 26) suggested a preferred A-conformation for the C-ring (Figure 6.4.2, L6 10/12).

Although the coupling constants of 3-$H_F$ could not be determined due to the broadness and

lack of definition of its resonance (Figure 6.4.2, L6-10/12), even in the COSY 45 experiment (Figure 6.4.5, L6-20), the coupling constant $J_{2,3}$ = 8Hz obtained from the 2-$H_F$ resonance and $J_{3,4\alpha}$ = 5.5Hz and $J_{3,4\beta}$ = ±8Hz from the 4-$H_F$ proton resonances indicate that the F-ring most probably displays conformational interchange, with the E-conformer being the more dominant contributor.
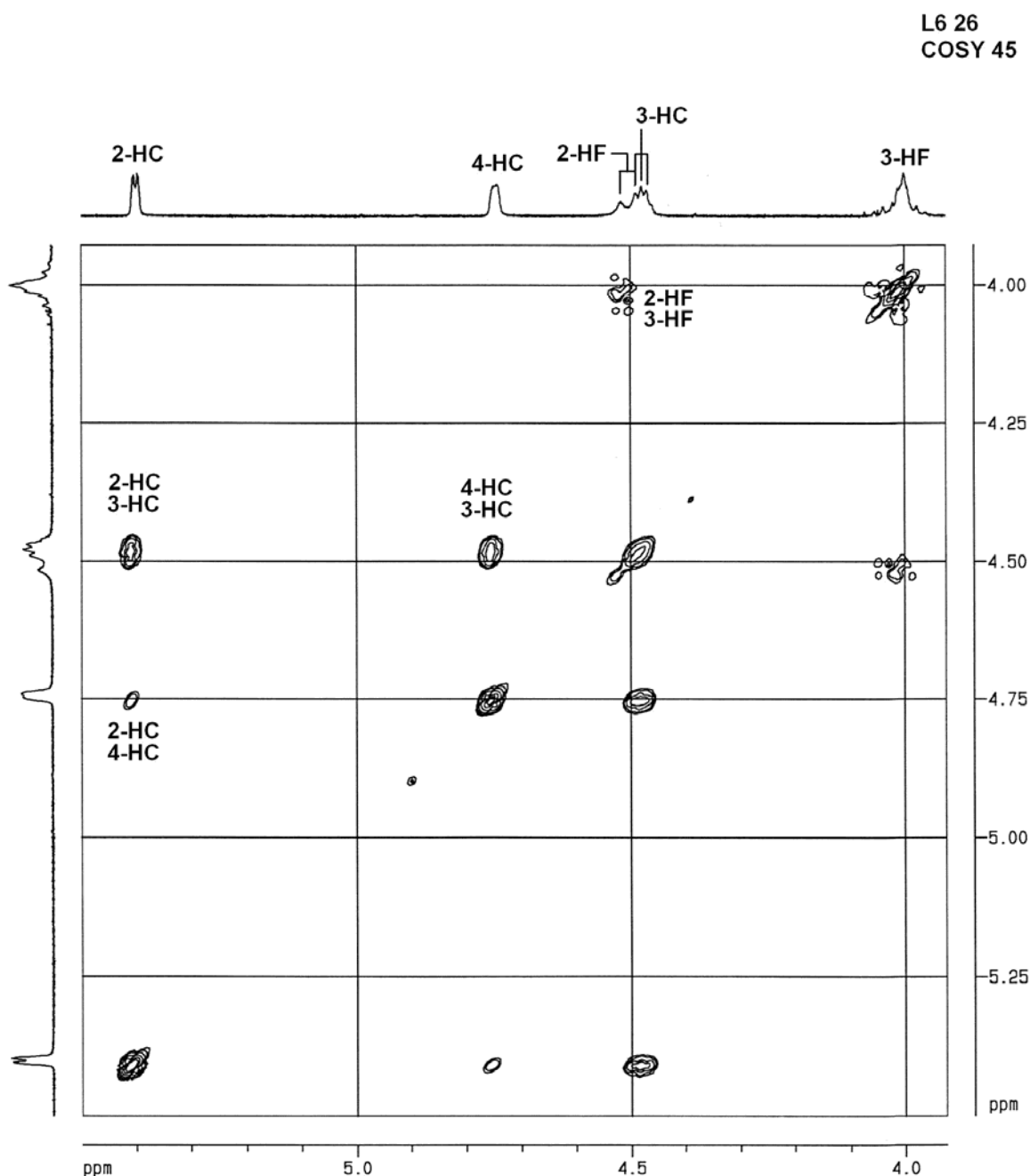


**FIGURE 6.4.4**

Due to the overlap and broadening of the 3-$H_F$ and possibly a 3-OH resonance (Figures 6.4.4/5, L6 26/20), the line shape of the 3-$H_F$ resonance could not be compared to the

published 3-H$_F$ line shapes.[97]
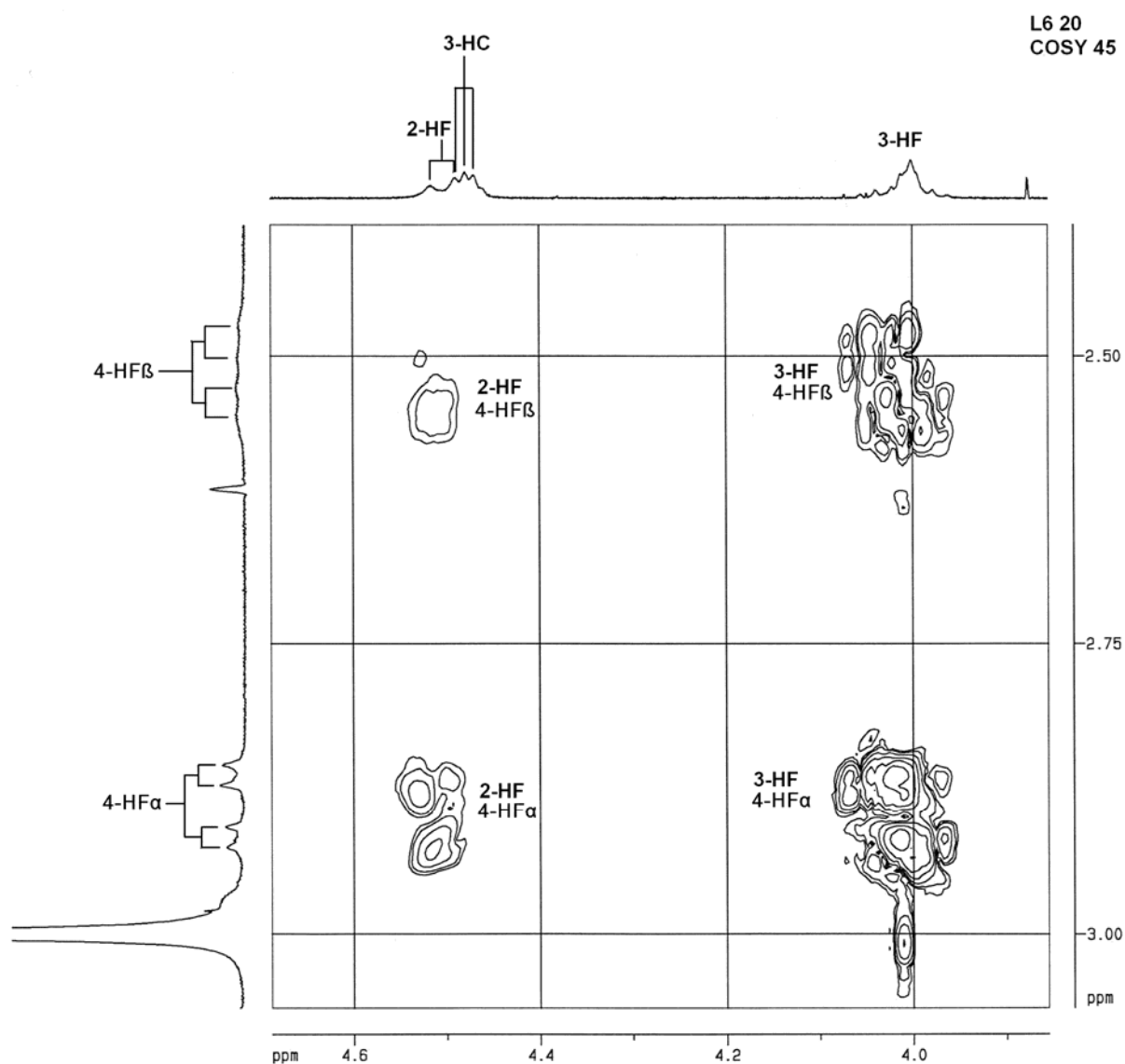


**FIGURE 6.4.5**

Analysis with a Dreiding model confirmed that if the C-ring were to exist mainly as an E-conformer, the D-ring of the bottom unit would be rotating right above and into the 1,3 diaxial space of the C-ring (the more compact conformer of the dimer), which makes it an

energetically very unfavourable conformation. This is further proof of the preferred A-conformation of the C-ring, which could be unambiguously assigned if NOE would be observed between H-$C_4$ and 2/6-$H_B$. A further contribution to the stability of the extended conformer would be the formation of hydrogen bonds between 3-$OH_C$ and the pyran ring oxygen of the C-ring, and/or 3-$OH_C$ and 5/7-$OH_D$.

The resonances of the B- and E-ring protons have higher chemical shifts than those of the A- and D-rings. The 8-$H_D$ resonance had the lowest chemical shift as is the case with all the dimers studied so far (Figure 6.4.2, L6-10).

Strong cross peaks between 2-$H_C$ and all the B ring protons were observed (Figure 6.4.6, L6-23), with the cross peak between 2-$H_C$ and 5-$H_B$ being the strongest. The sharp and well defined resonances of the B-ring protons, showing *p*-coupling between 2-$H_B$ and 5-$H_B$, further confirm that there is little conformational exchange of the C-ring with limited rotation around the 2-$C_C \rightarrow$1-$C_B$ bond, indicating a preferred $90^o$ angle between the 2-$C_C \rightarrow$1-$C_B$ bond and the plane of the B-ring. This is contrary to the results obtained for the B-ring of both the E-and A-conformers of tetra-O-methylated (+)-catechin and (-)-epicatechin.[22,80,81]

There were strong cross peaks in the COSY experiment between 4-$H_C$ and all three A-ring proton resonances. 5-$H_A$ formed the strongest cross peak, indicating a $90^o$ angle between the 4-$H_C \rightarrow$4-$C_C$ bond and the plane of the A-ring. This further supports the limited conformational flexibility of the C-ring.

Cross peaks between some heterocyclic and aromatic resonances afforded unambiguous assignments of some of the aromatic proton resonances. Strong cross peaks between 2-$H_F$ and 2-$H_E$/6$H_E$ (Figure 6.4.6, L6-23) were observed, with the 2-$H_E$ cross peak being the

strongest. This could indicate a preferential $90^{\circ}$ angle between the 2-$H_F$→2-$C_F$ bond and the plane of the E-ring, which is also different to results obtained for both A- and E-conformers of (+)-catechin and (-)-epicatechin derivatives.[22,80,81]
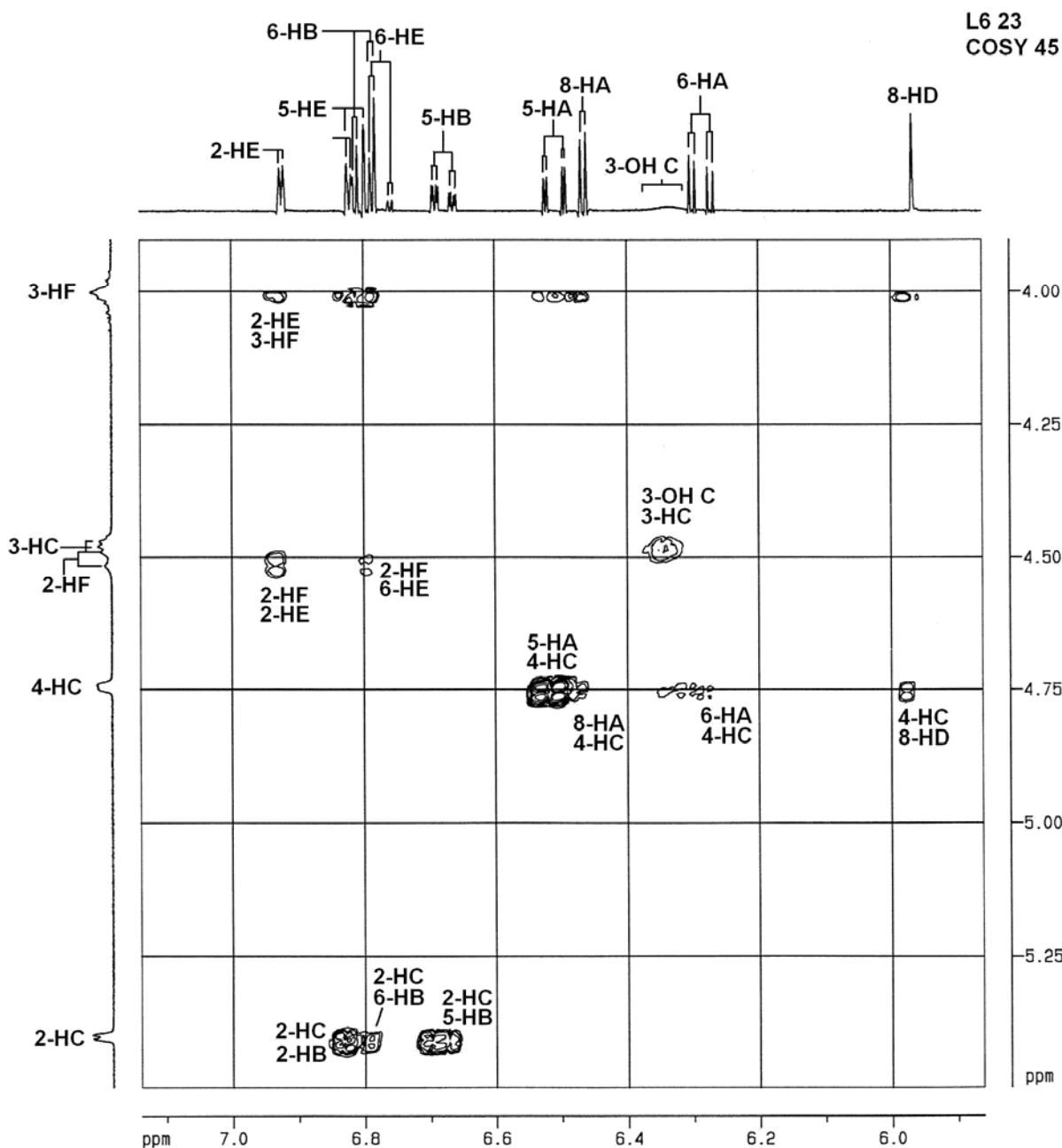


**FIGURE 6.4.6**

These assignments were then used to afford complete assignment of all aromatic proton resonances (Figures 6.4.7/8, L6-17/29). The quartet of cross peaks between 5-$H_B$ and 6-$H_B$ partially overlap the cross peaks between 2-$H_B$ and 5-$H_B$.
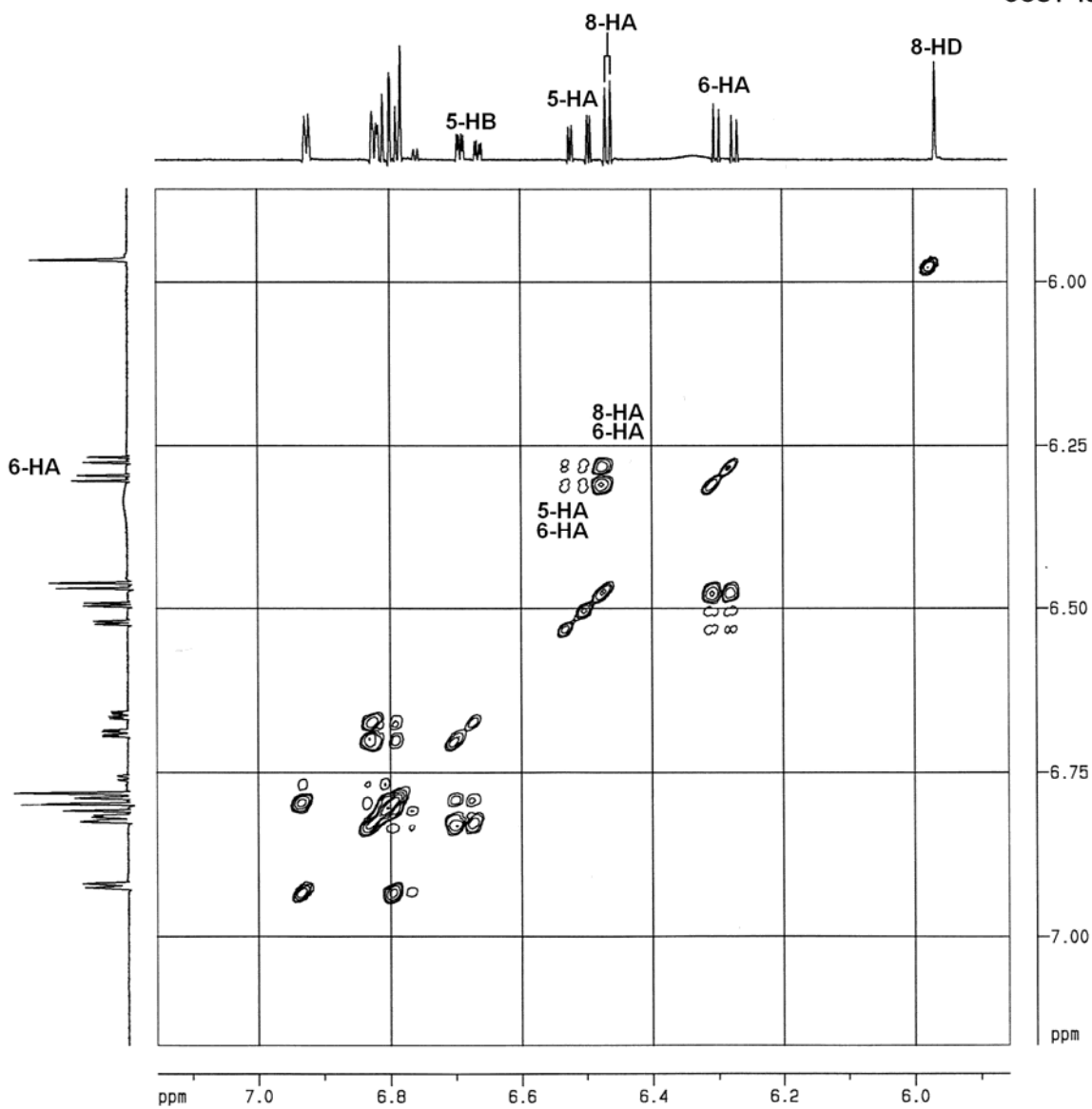
**FIGURE 6.4.7**
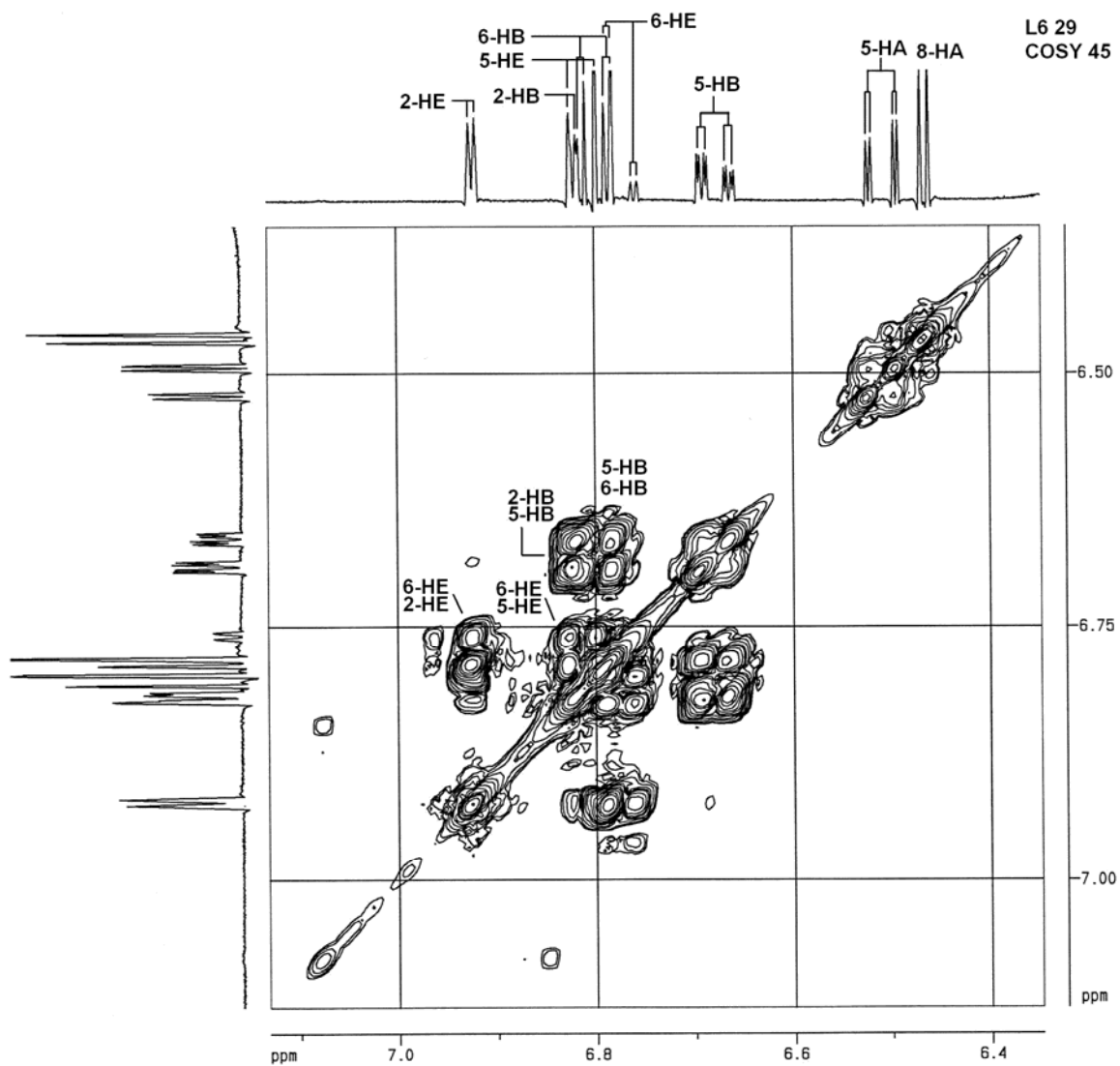
**FIGURE 6.4.8**

Strong cross peaks were also observed between 4-HF$_\alpha$ and 8-H$_D$ (Figure 6.4.9, L6-30),

suggesting a preferred $90^o$ angle between the plane of the D-ring and the $4\text{-HF}_\alpha \rightarrow 4\text{-C}_F$ bond. This is permitted only if the conformation of the F-ring has a more skewed-boat than C-2 sofa character with the E-ring in a quasi-equatorial position. Strong cross peaks between 4-$HF_\beta$ and 8-$H_D$ would indicate a more skewed boat/C-3-sofa character.[66,67,97]
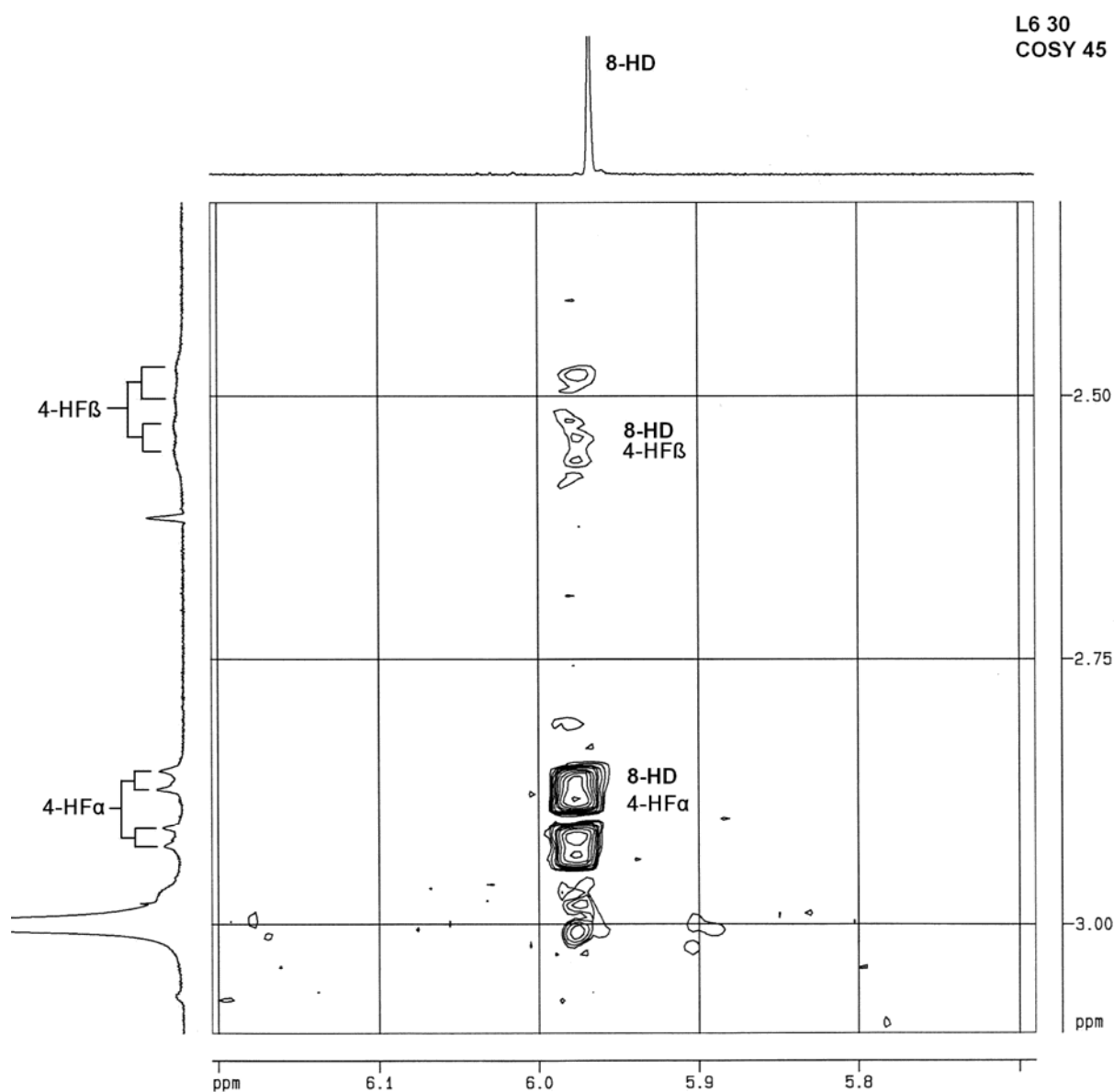


**FIGURE 6.4.9**

An HMQC experiment (Figure 6.4.3, L6 1) was performed to assign some of the carbon resonances (Figure 6.4.10, L6 9, Appendix B). An anomalous result observed for all the

compounds in this study is the very high chemical shift (129,28 ppm) of 5-C$_A$, (Figure 6.4.11, L6-4). This is not commensurate with the chemical shift of 5-H$_C$ relative to the other A- B and E-ring protons as observed on the ^{1}H NMR spectrum.

Due to overlap of resonances, unambiguous assignments for 2-C$_B$ and 5-C$_E$ were not possible (Figure 6.4.11, L6-4).
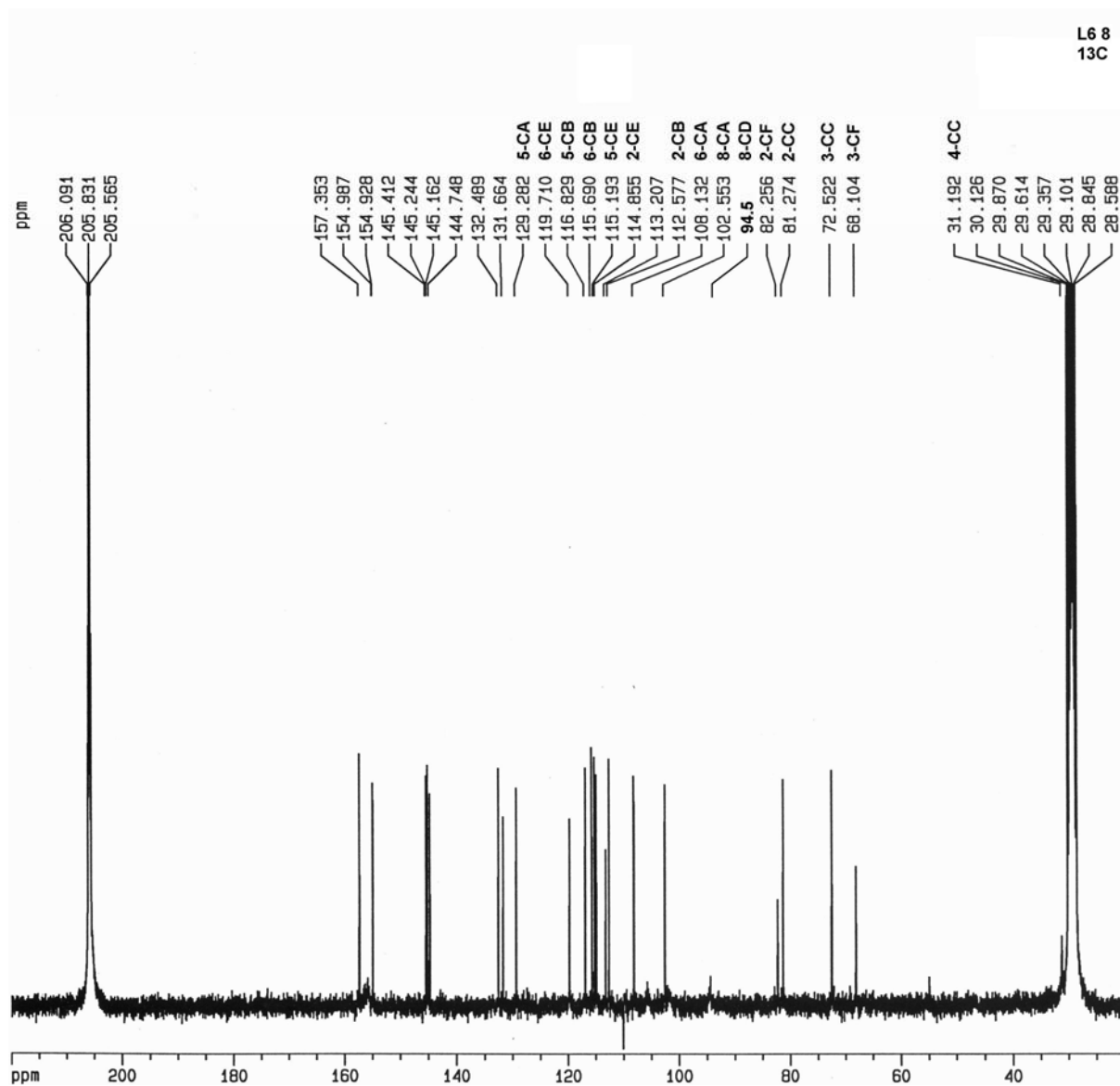


**FIGURE 6.4.10**
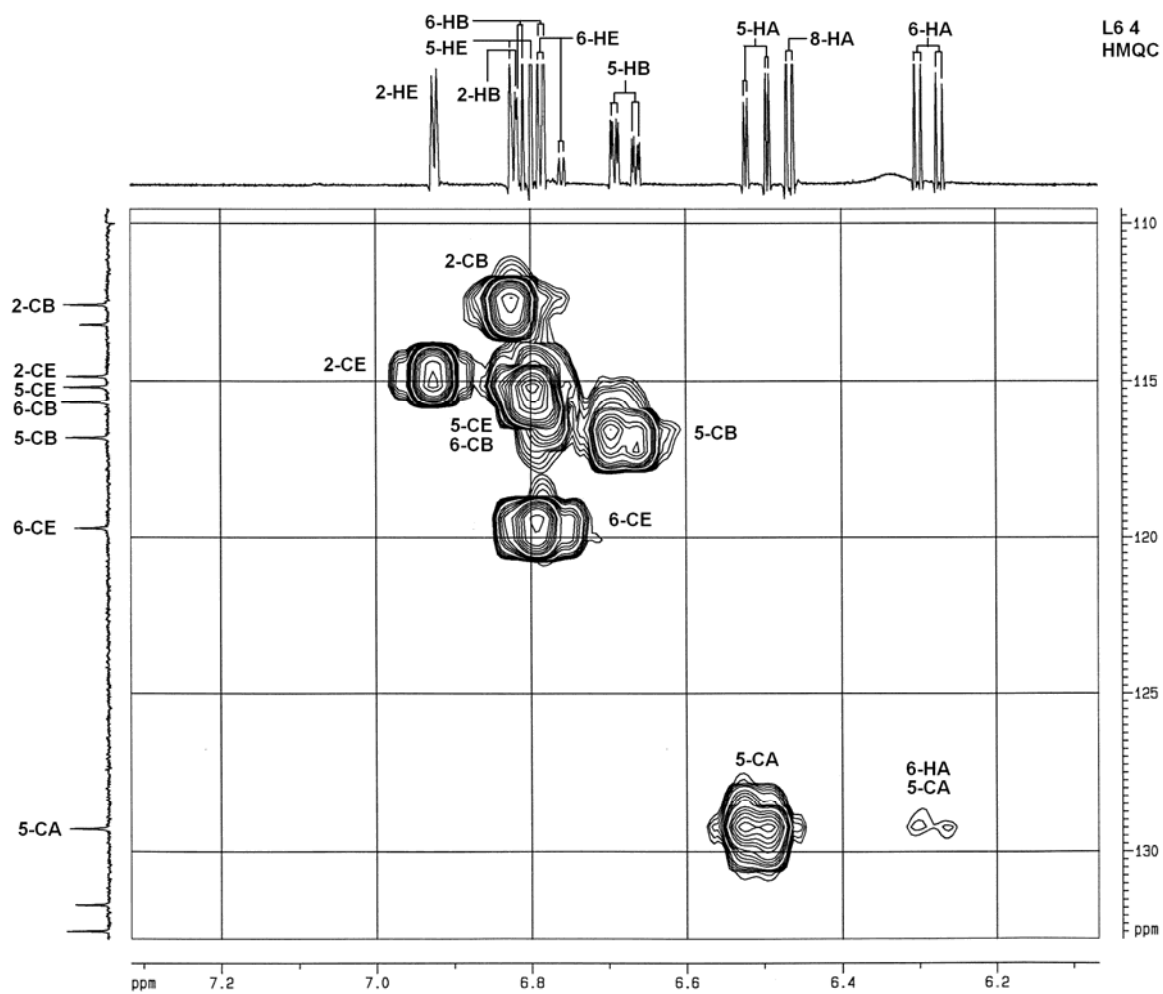
**FIGURE 6.4.11**
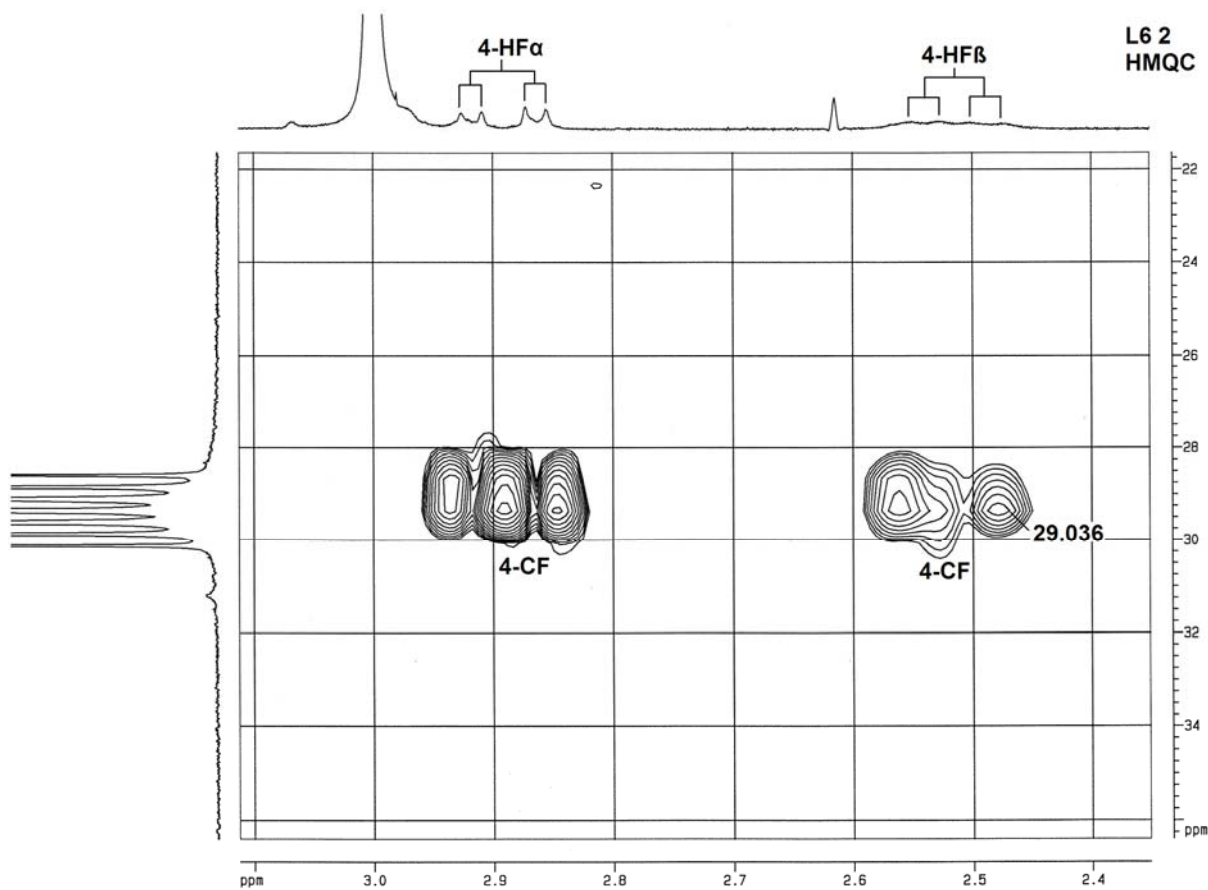
**FIGURE 6.4.12**
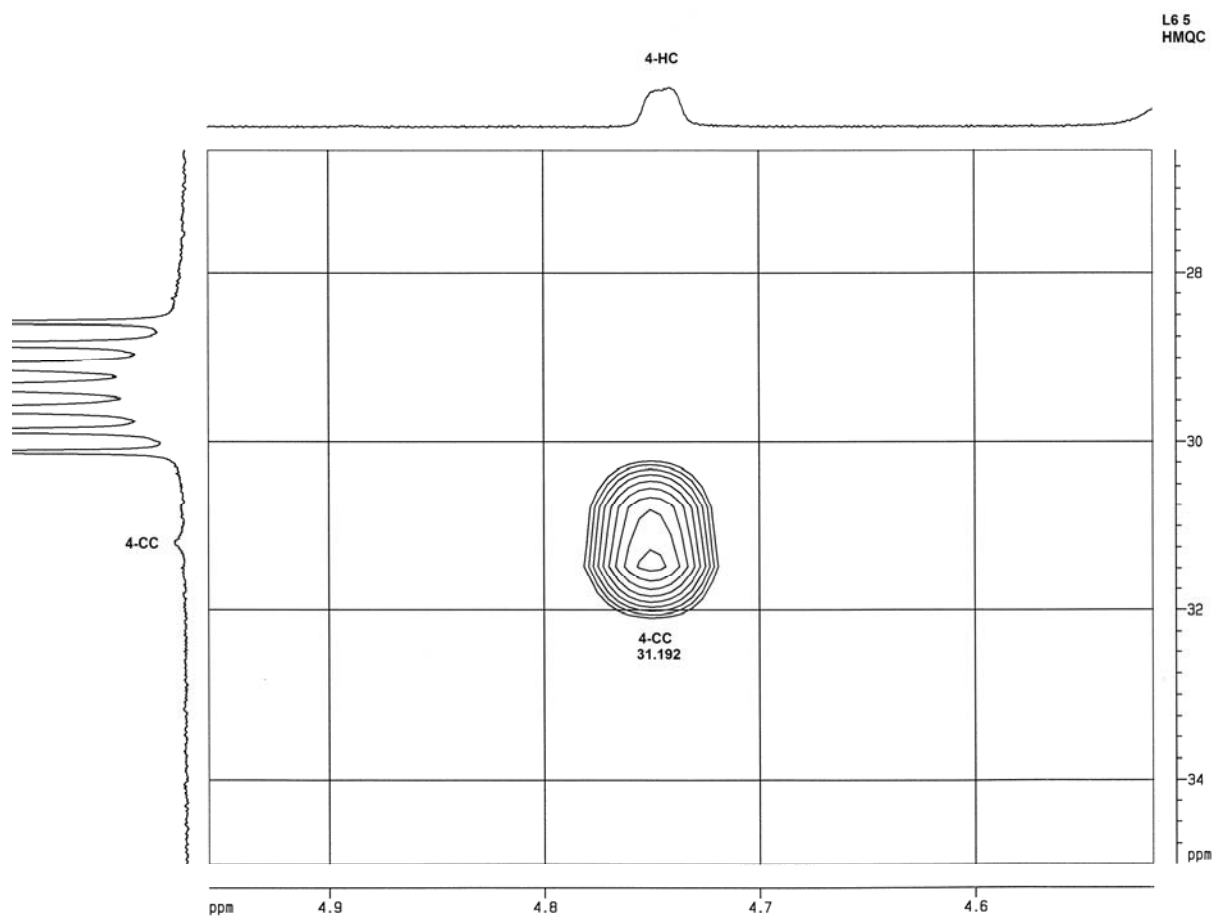
**FIGURE 6.4.13**

| AROMATIC RING DATA FOR FISETINIDOL-(4ß→6)-CATECHIN | | | | | | | | | | |
|---|---|---|---|---|---|---|---|---|---|---|
| Proton | A-ring | | | B-ring | | | E-ring | | | D-ring |
| | 8 | 5 | 6 | 2 | 5 | 6 | 2 | 5 | 6 | 8 |
| chemical shift, δ | 6.47 | 6.51 | 6.29 | 6.82 | 6.68 | 6.80 | 6.93 | 6.38 | 6.77 | 5.96 |
| multiplicity | d | dd | dd | dd | ddd | dd | d | dd | dd | s |
| coupling constants, Hz | 2.5 | 1.2 8.2 | 2.5 8.2 | 2.2 0.8 | 0.8 2.2 8.0 | 8.22 | 1.9 | 0.8 8 | 1.9/8 | |

**TABLE 6.4.1**

| HETEROCYCLIC RING DATA FOR FISETINIDOL-(4ß→6)-CATECHIN | | | | | | | |
|---|---|---|---|---|---|---|---|
| Proton | C-ring | | | F-ring | | | |
| | 2 | 3 | 4 | 2 | 3 | 4α | 4β |
| chemical shift, δ | 5.40 | 4.45 | 4.75 | 4.51 | 3.96-4.05 | 2.89 | 2.52 |
| multiplicity | dd | m | m | d | m | dd | dd |
| coupling constants, Hz | 0.8/2.5 | 2.5 | 3 broad | 8 | | 5.0/-16 | 8.0/-16 |

**TABLE 6.4.2**

# The conformational behaviour of free phenolic profisetinidin dimers from *Schinopsis balansae*

## 7.1    THE CONFORMATIONAL BEHAVIOUR OF *ENT*-FISETINIDOL-(4α→8)-CATECHIN IN ACETONE-d$_6$.

The structure of this compound was studied by $^1$H, $^{13}$C, gradient COSY and HMQC NMR experiments in wet acetone-d$_6$ and CD in methanol (see Chapter 8). There is also no obvious duplication of resonances as is the case when two distinct rotamers are present. The $^1$H NMR spectrum in acetone-d$_6$ at 293 K displayed broad resonances (Figure 7.1.1). This indicates either slow rotation around the interflavanyl bond due to intramolecular hydrogen bonding and/or slow conformational flexing of the heterocyclic rings that display time-averaged resonances for aromatic as well as heterocyclic protons.
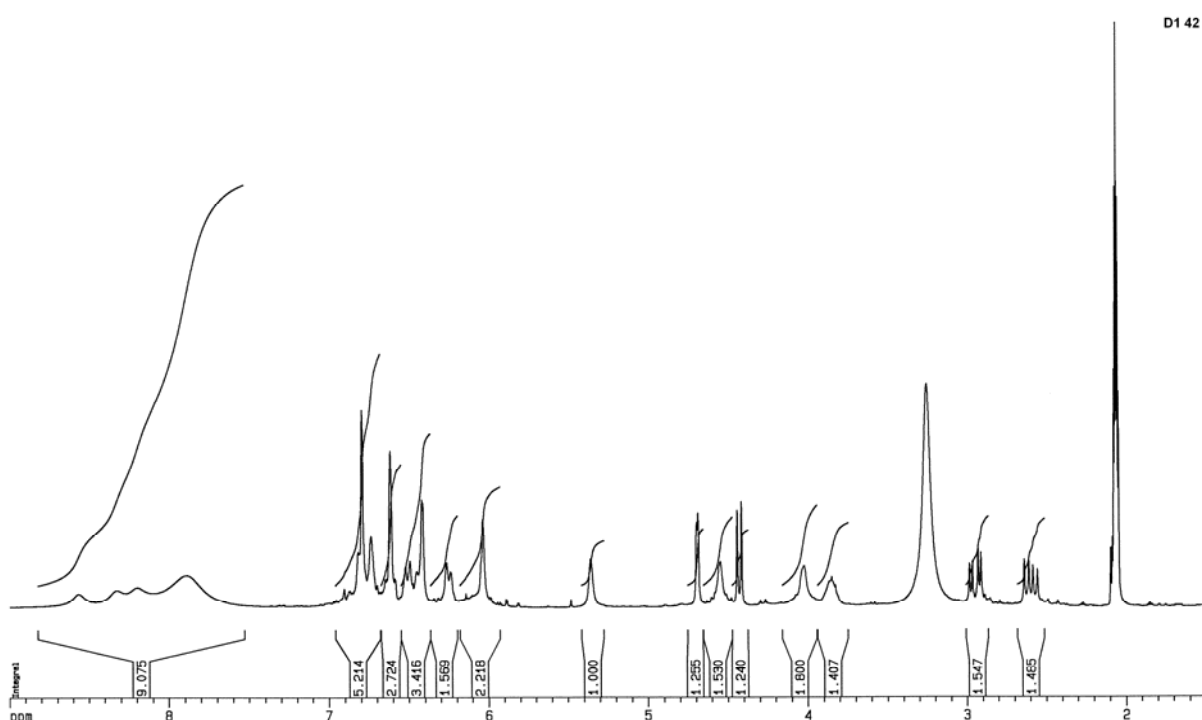


**FIGURE 7.1.1**

A $^1$H NMR spectrum with clearly defined resonances and coupling constants for both heterocyclic and aromatic proton resonances was obtained at 333 K (Figures 7.1.2/3) (Tables 7.1.1 and 7.1.2). Hydrogen exchange, however, was still slow enough to display very broad resonances for some of the aromatic- and heterocyclic-ring hydroxy groups.
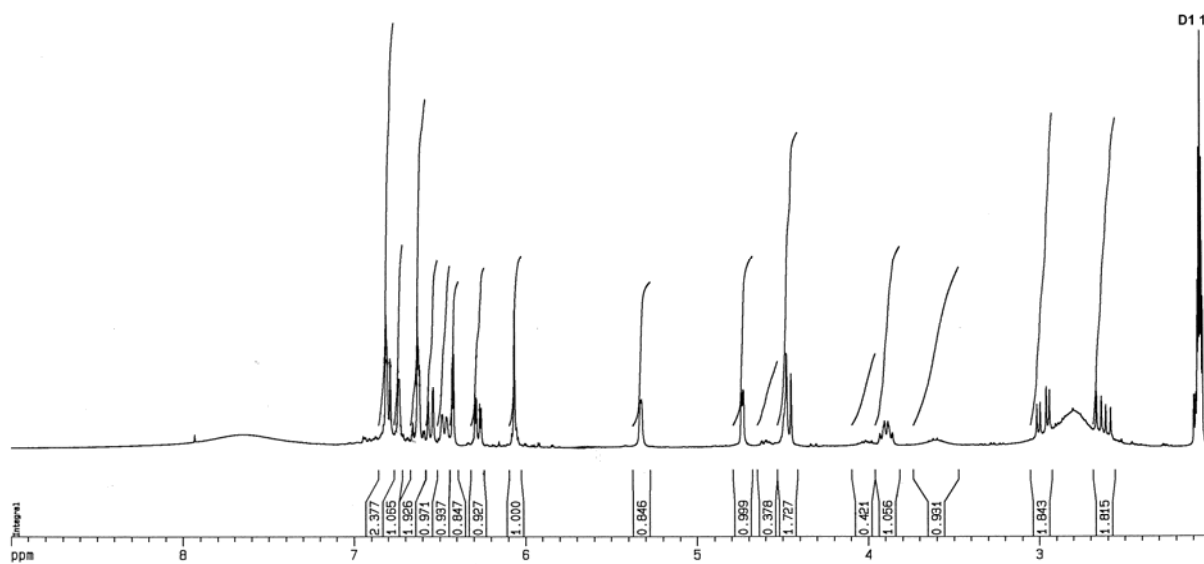


**FIGURE 7.1.2**
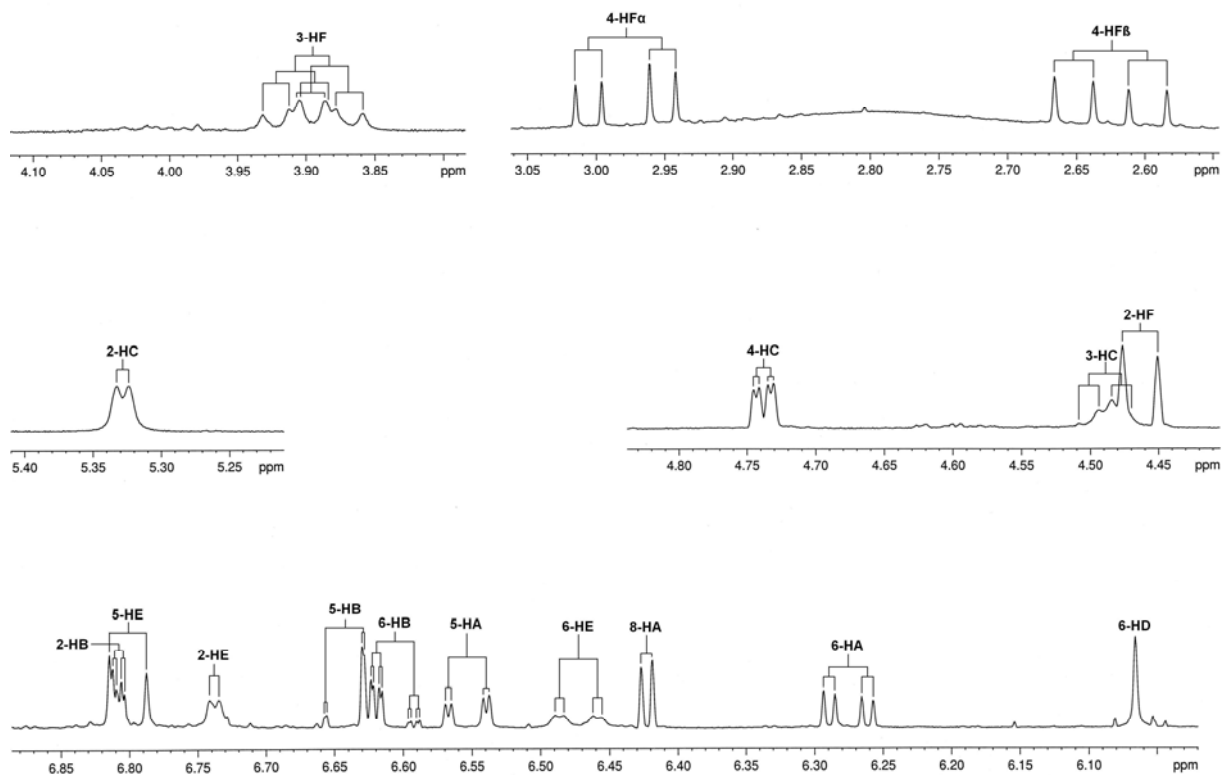
**FIGURE 7.1.3**

A gradient COSY experiment was performed at 333 K to assign the 4-H$_{F\alpha}$ and 4-H$_{F\beta}$ resonances (Figure 7.1.4, D1 17). The lean of the cross peaks confirmed the magnitude and the negative sign of the $^2J_{4HF\alpha,4HF\beta}$ vicinal coupling constant.
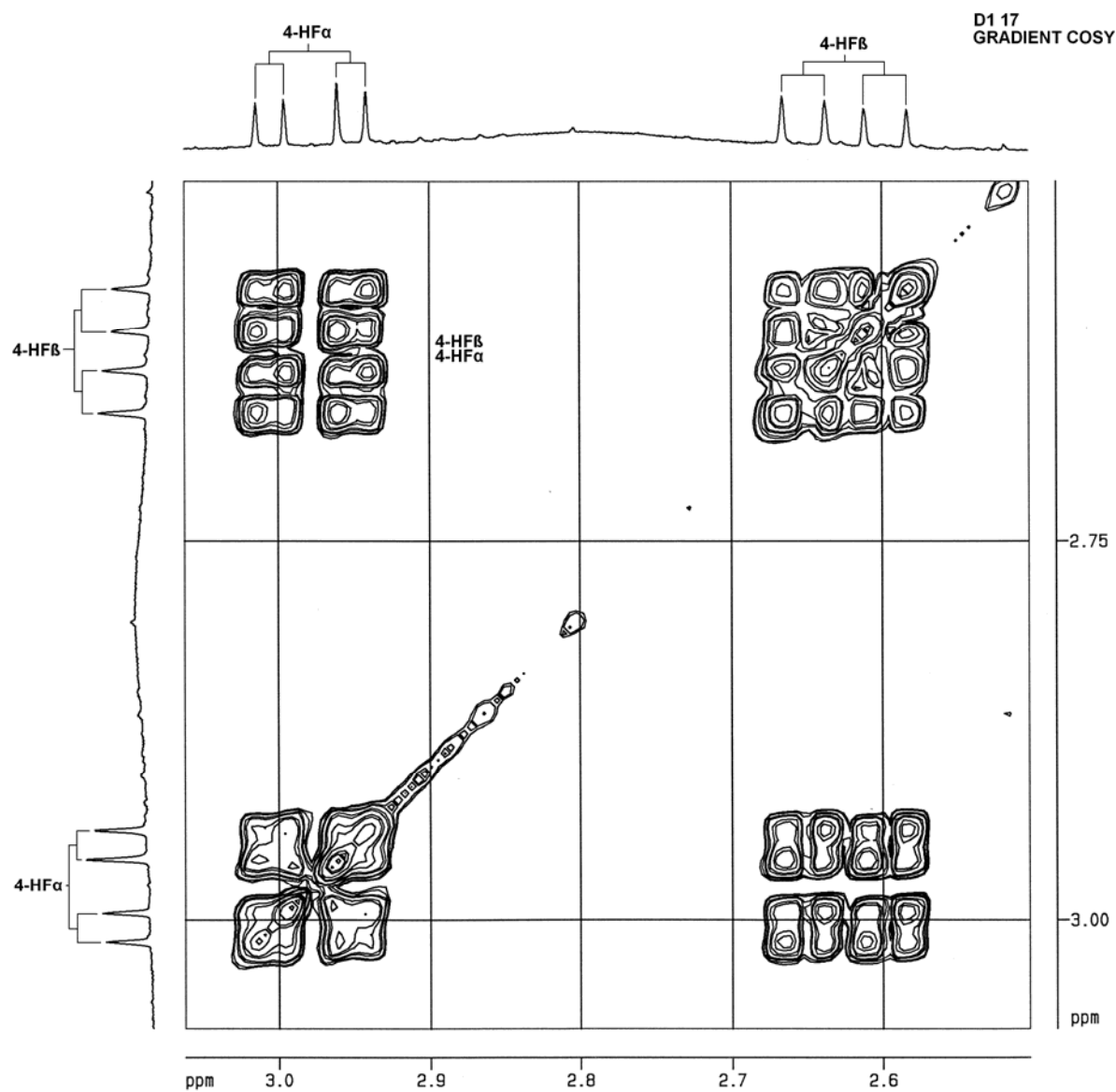


**FIGURE 7.1.4**

These assignments were used to assign the 3-H$_F$ resonance (Figure 7.1.5, D1 18).



**FIGURE 7.1.5**

126
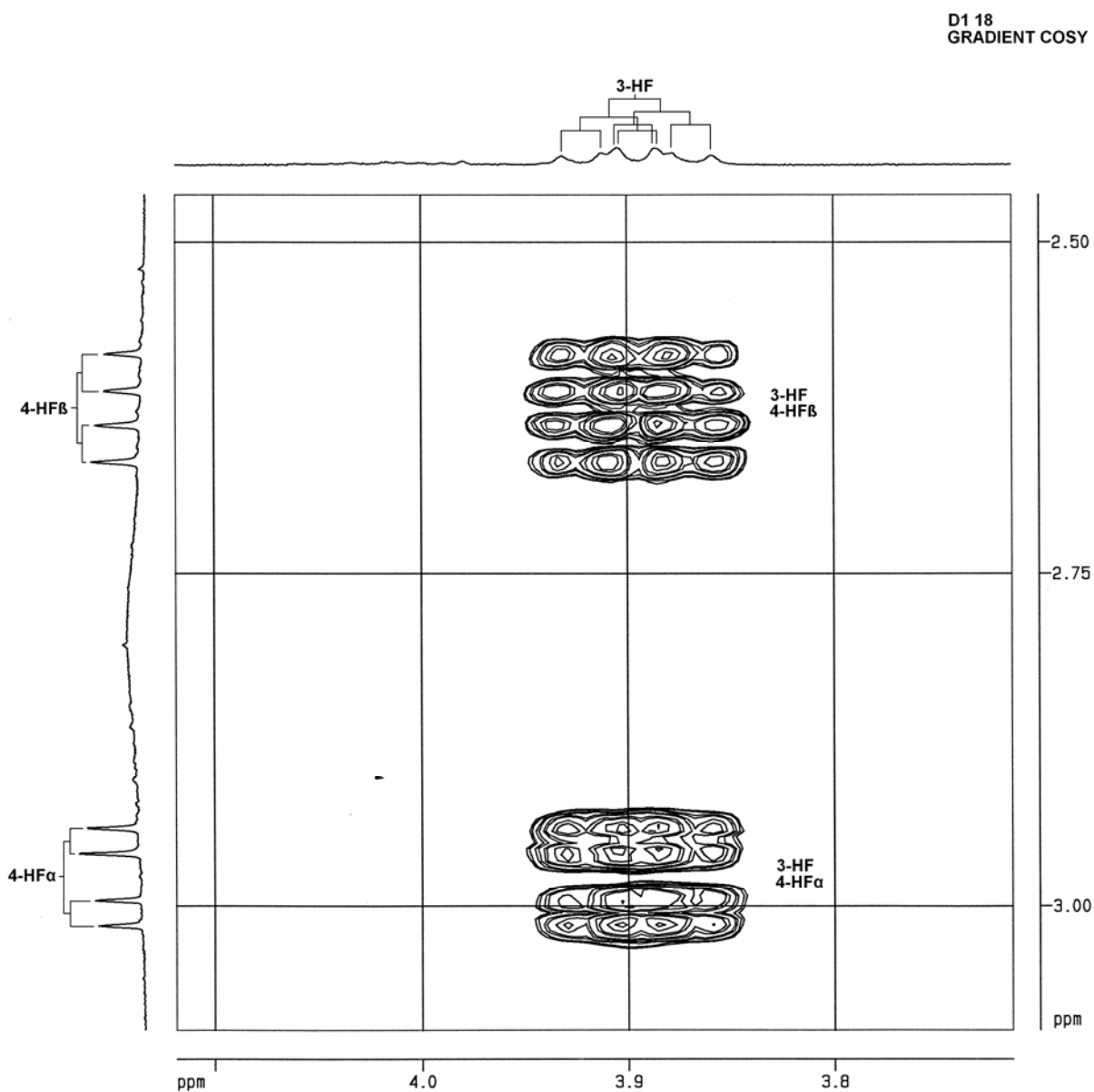
The 3-HF resonance was used to assign the 2-H_F resonance (Figure 7.1.6, D1 19).
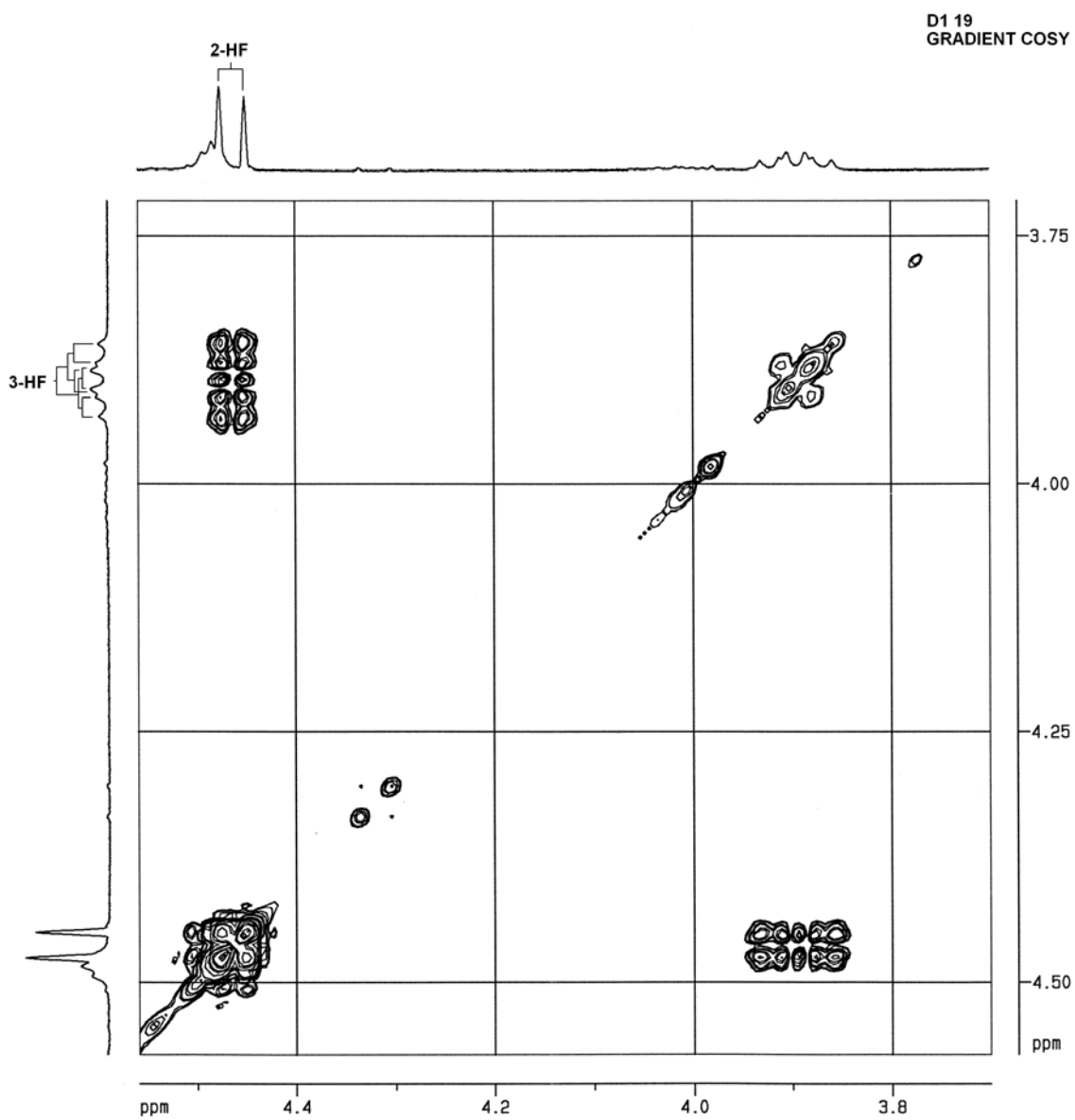


**FIGURE 7.1.6**

Strong 4-H$_F$/6-H$_D$ cross peaks imply that the 4-H$_F$→4C$_F$ bond is at an approximately 90$^o$ angle with the 6-H$_D$→6C$_D$ bond and therefore also with respect to the plane of the D-ring (Figure 7.1.7, D1 29). Because of the apparent similarity in intensity between the cross peaks of both the 4-H$_{F\alpha}$ and 4-H$_{F\beta}$ resonances with the 6-H$_D$ resonance, it can be interpreted that the F-ring undergoes conformational exchange, with both the 4-H$_{F\alpha}$→4C$_F$ and 4-H$_{F\beta}$→4C$_F$ bonds forming angles of similar magnitude to the plane of the D-ring.
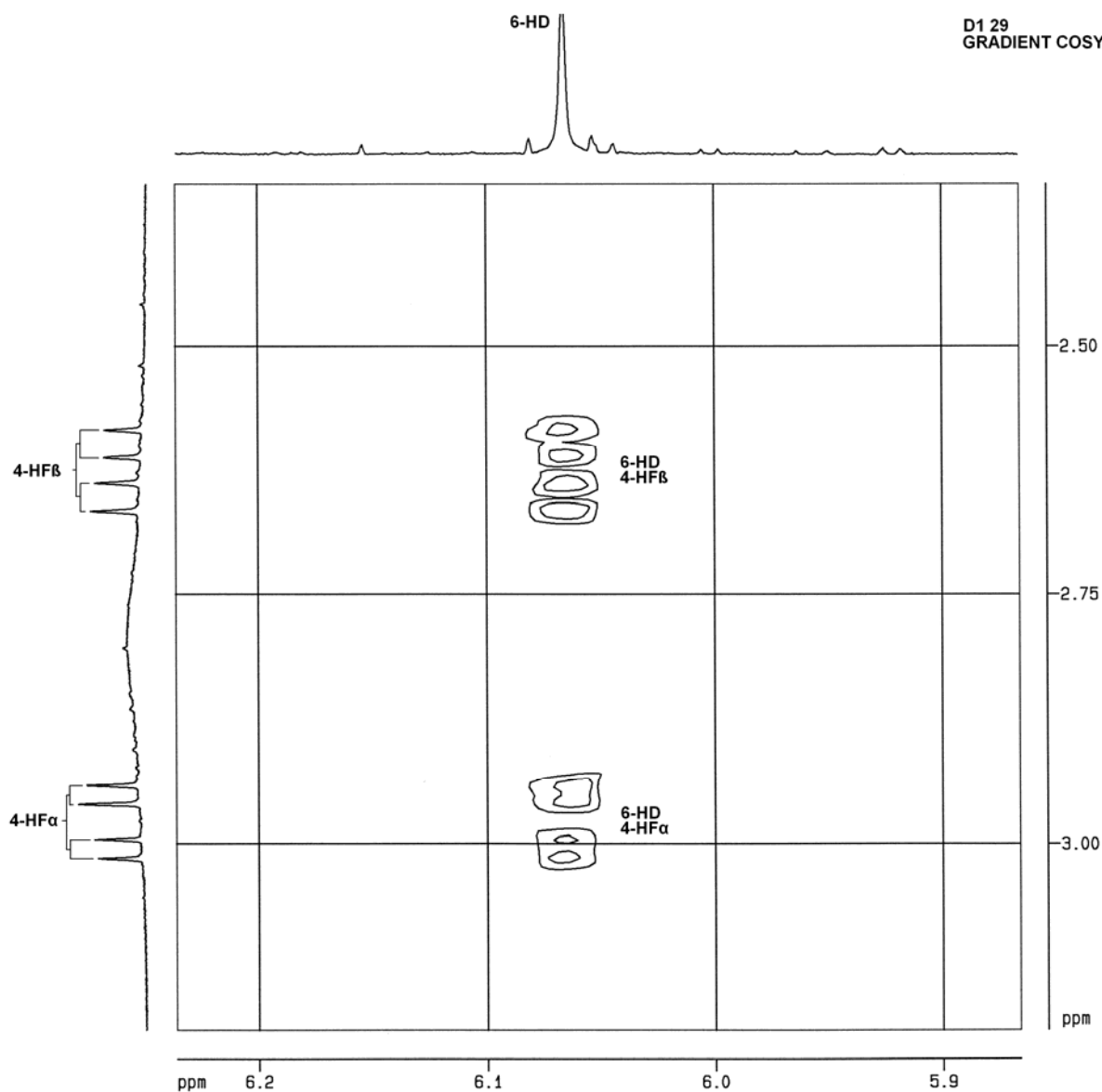


**FIGURE 7.1.7**

Strong 4-H$_C$/6-H$_D$ cross peaks imply that the 4-H$_C$→4C$_C$ bond is at an approximately 90$^o$ angle with the 6-H$_D$→6C$_D$ bond and therefore also with respect to the plane of the D-ring. The 4-H$_C$/6-H$_D$ cross peaks were relatively weak, indicating an angle of less or more than 90$^o$ between the 4-H$_C$→4C$_C$ bond and the plane of the D-ring (Figure 7.1.8, D1 34).[97] The 4-H$_C$ / 6-H$_D$ cross peaks were used to unambiguously assign the 4-H$_C$ resonance.
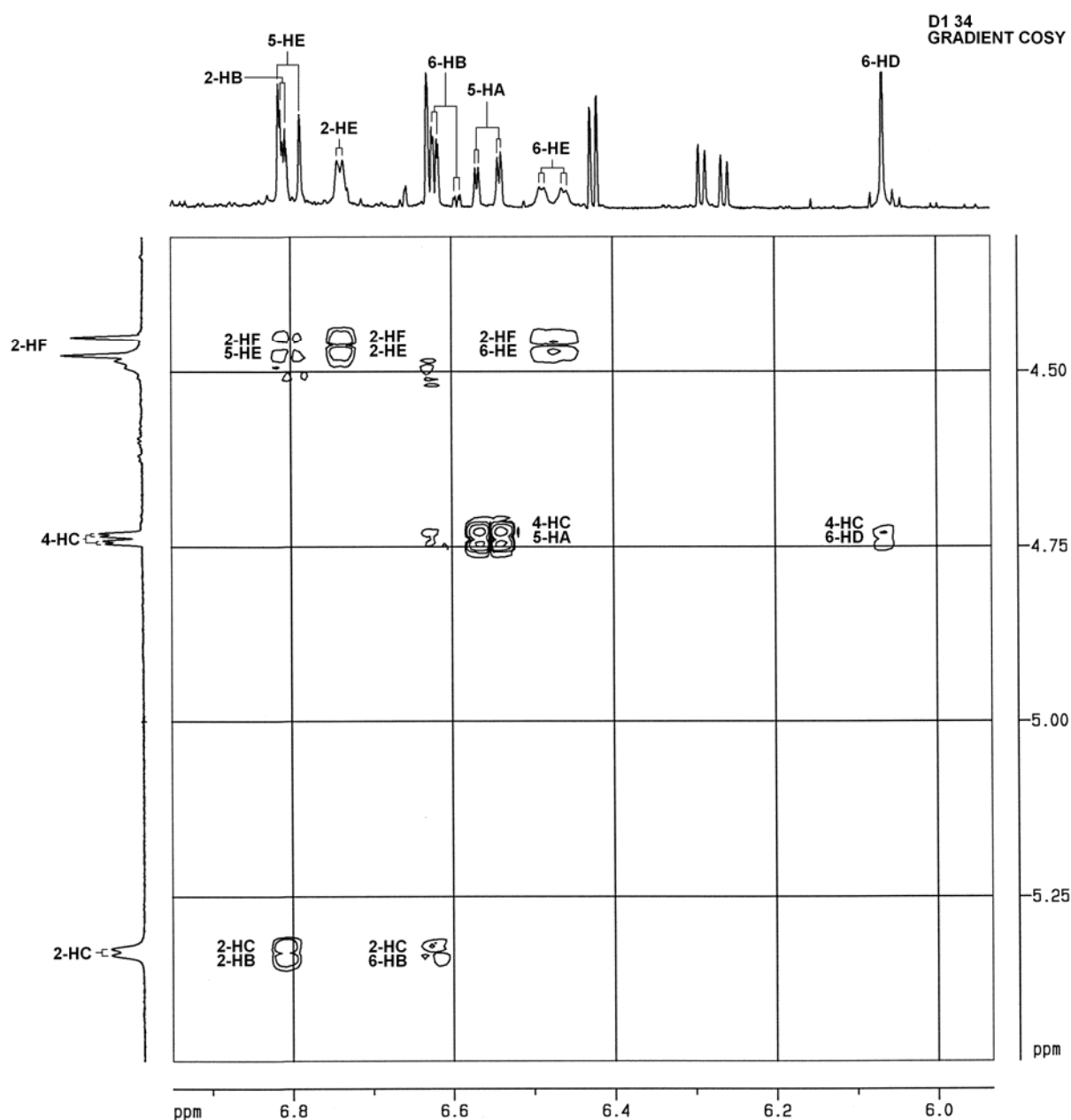


**FIGURE 7.1.8**

The 4-H$_C$ resonance was used to assign the 2-H$_C$ and 3-H$_C$ resonances (Figure 7.1.9, D1

20). Due to the overlap of the 3-H$_C$ and 2-H$_F$ resonances, as well as small C-ring proton coupling constants, an unambiguous analysis of the multiplicity of the 3-H$_C$ resonance could not be made.
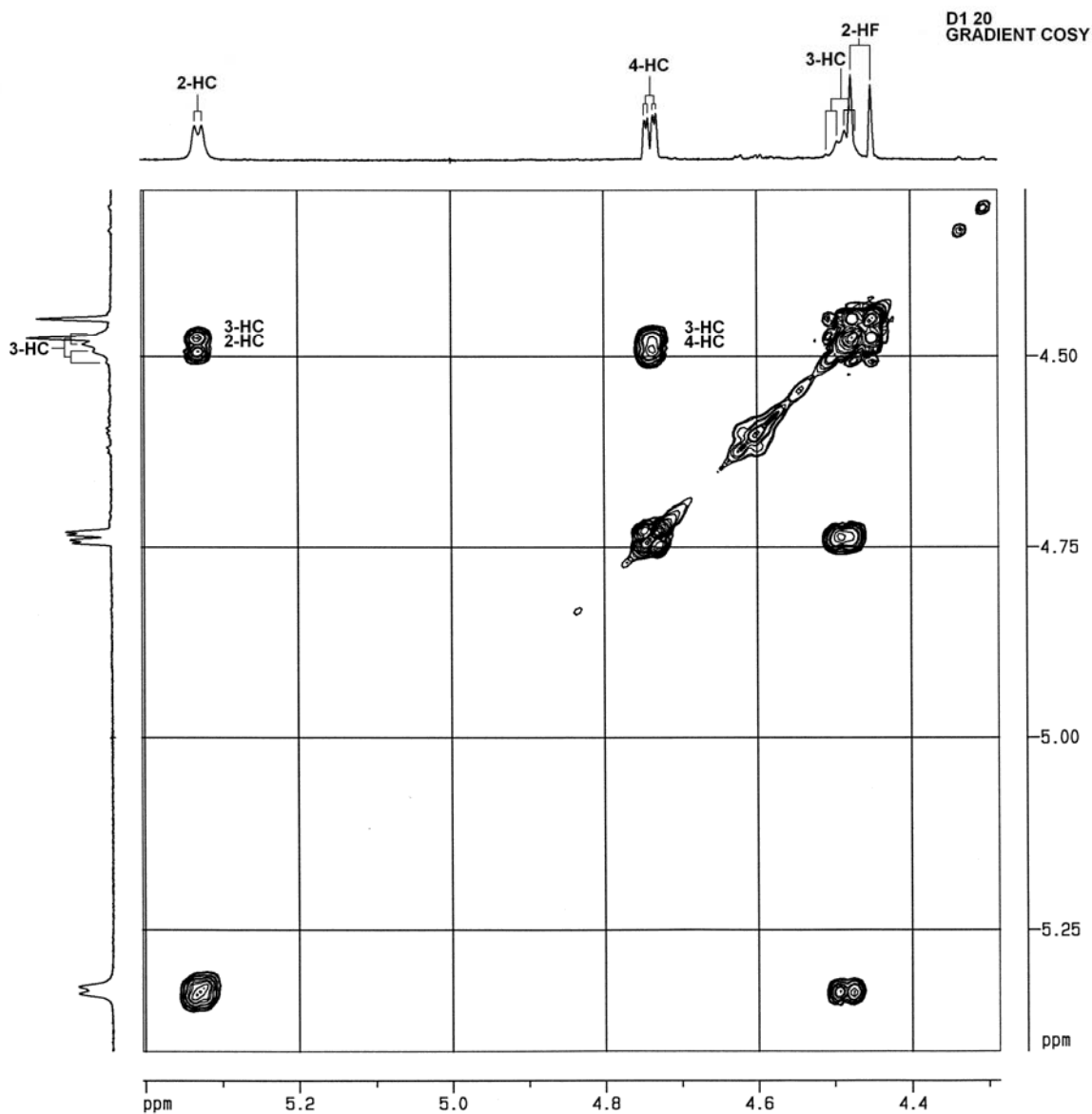


**FIGURE 7.1.9**

Coupling 2-H$_F$ resonance was used to assign the 2-H$_E$, 5-H$_E$ and 6-H$_E$ resonances. The 2-H$_C$ resonance was used to assign the 2-H$_B$ and 6-H$_B$ resonances. The 4-H$_C$ resonance was used to assign the 5-H$_A$ resonances (Figure 7.1.8).

These assignments were then used to complete the assignments of all the aromatic ring protons (Figure 7.1.10, D1 21).
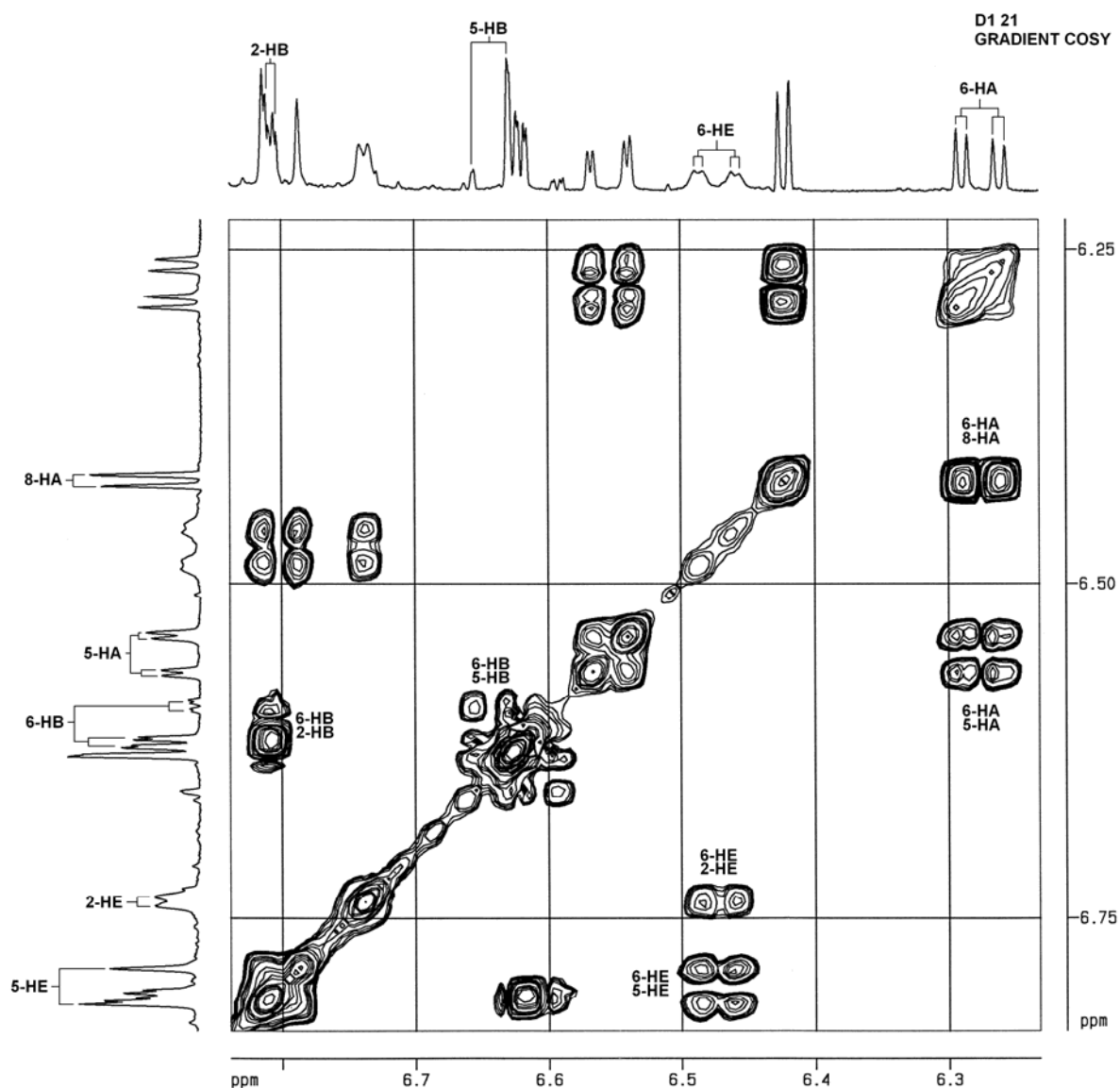


**FIGURE 7.1.10**

A deeper cut of the Gradient COSY spectrum in the heterocyclic-aromatic region confirmed

these assignments (Figure 7.1.11, D1 24). Cross peaks between the 4-$H_C$ resonances and the 2-$H_A$, 5-$H_A$ and 6-$H_A$ resonances were observed. There were also cross peaks between the 3-$H_C$ resonances and the 5-$H_A$ and 6-$H_A$ resonances, indicating the 3-$H_C$ resonance could appear as a doublet of triplets.
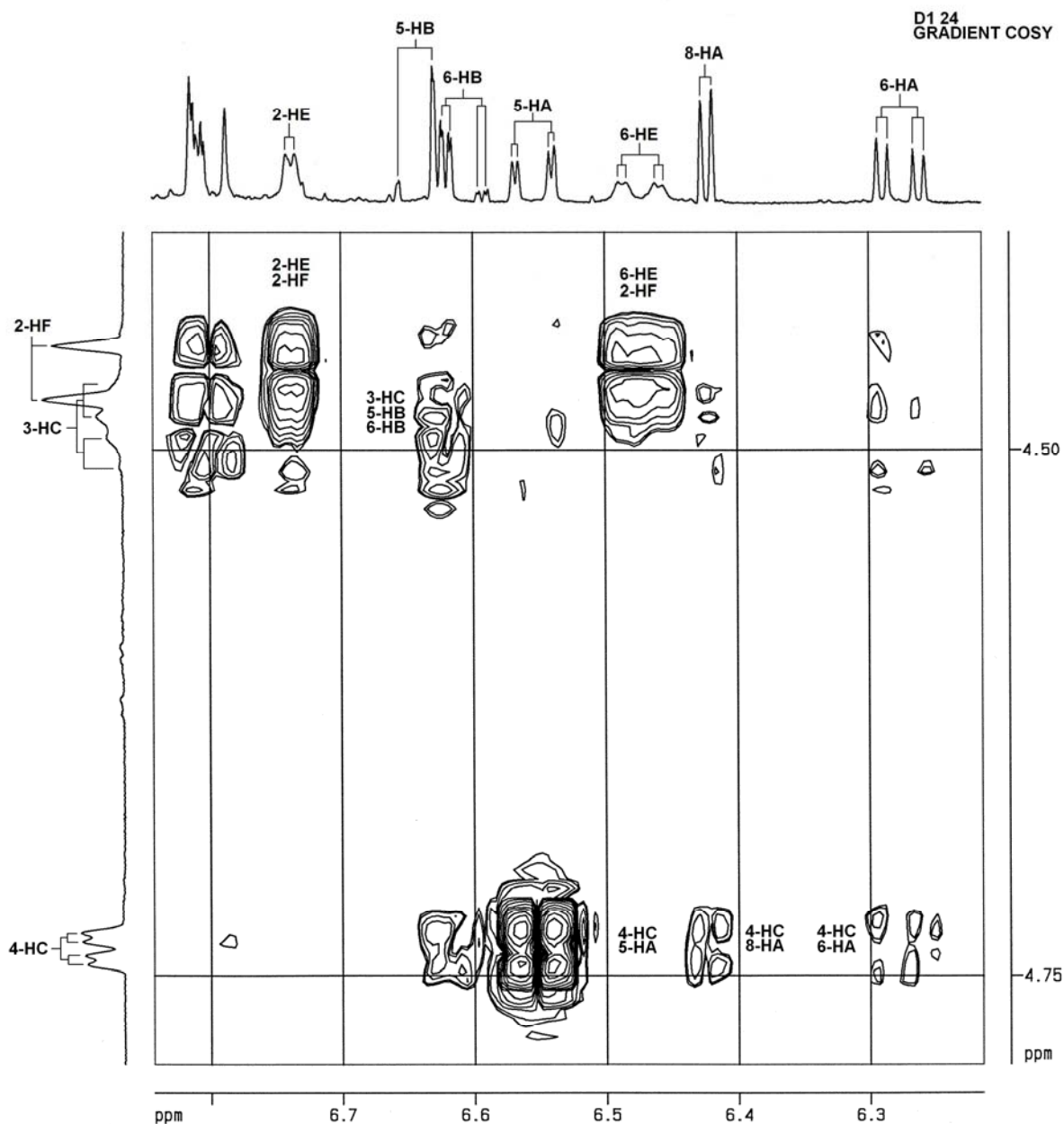


**FIGURE 7.1.11**

An HMQC experiment at 293 K (Figures 7.1.13/14) was used to assign some of the carbon resonances (Figure 7.1.12, D1 20), even though some of the peaks at this temperature were

broader with slightly different chemical shifts than at 333 K.



**FIGURE 7.1.12**

133
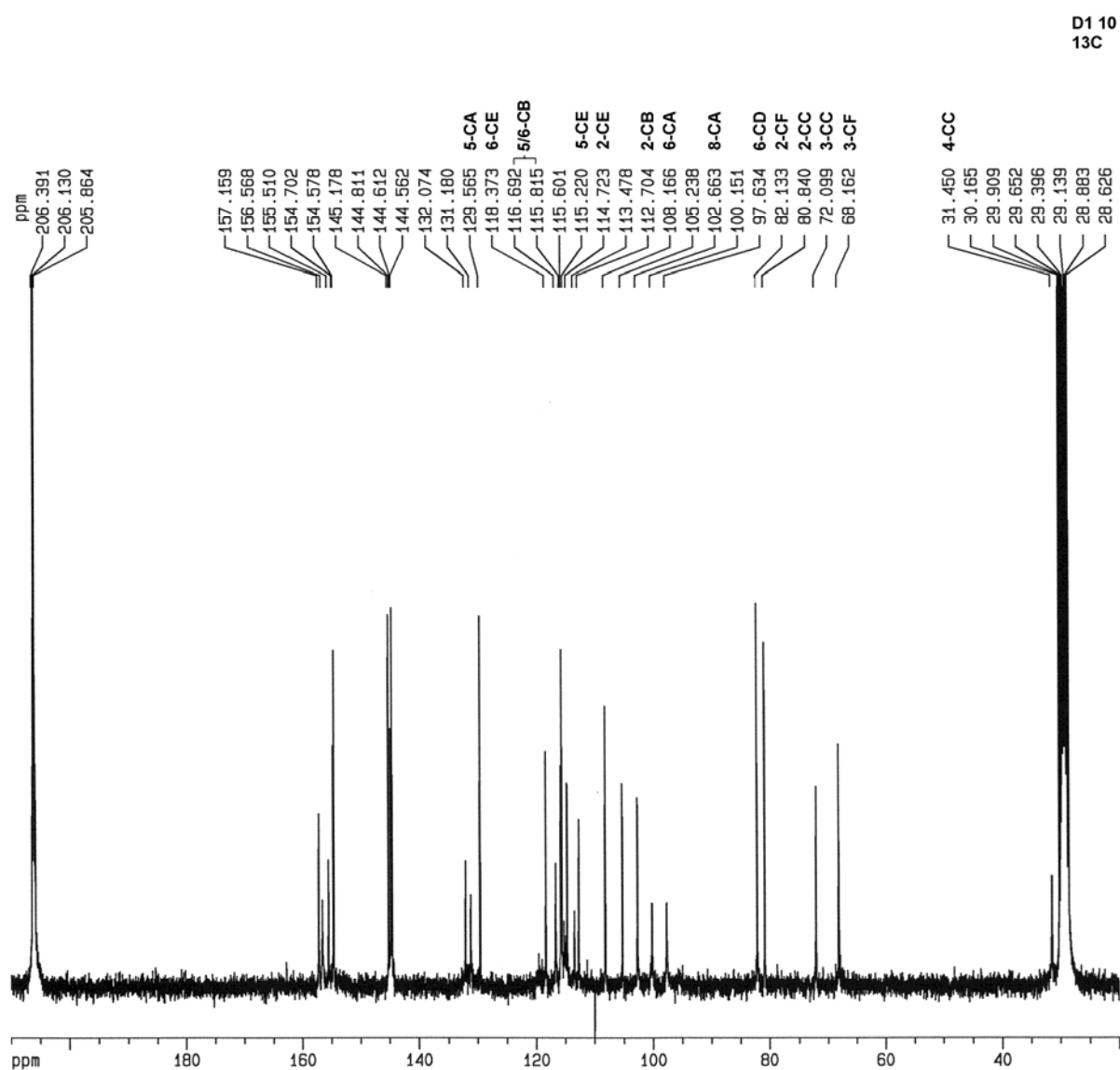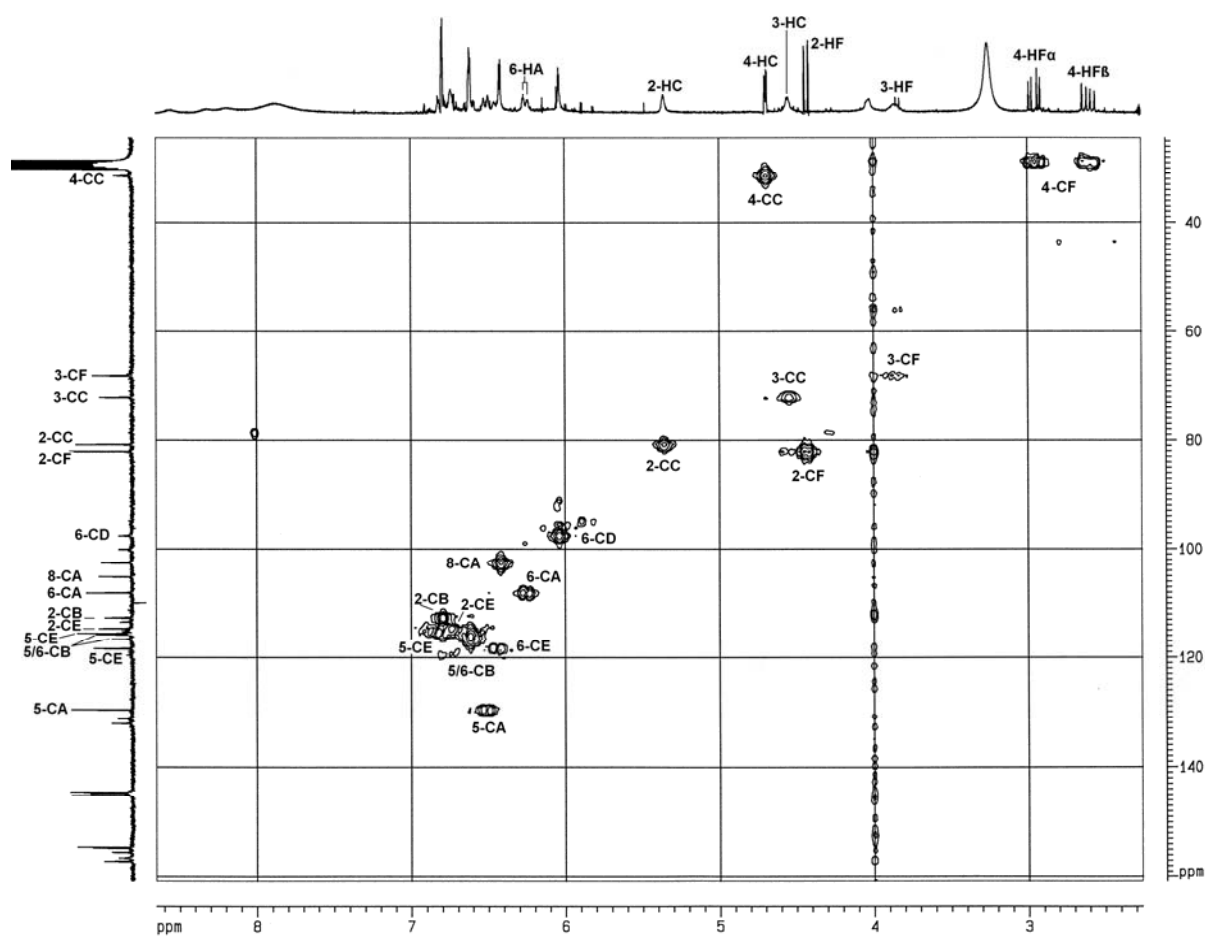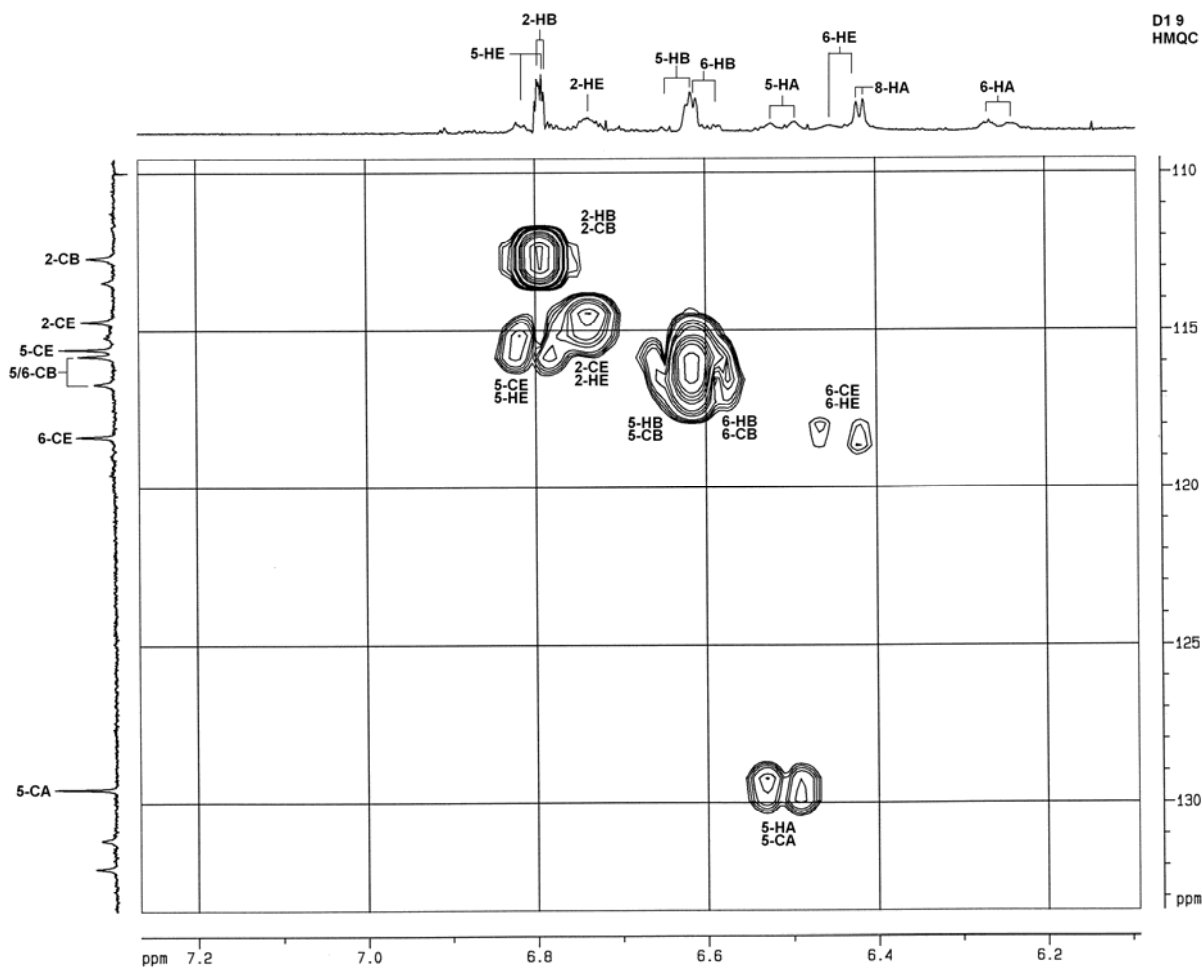
**FIGURE 7.1.13**

**FIGURE 7.1.14**

| HETEROCYCLIC RING DATA FOR *ENT*-FISETINIDOL-(4α→8)-CATECHIN AT 333 K. | | | | | | | |
|---|---|---|---|---|---|---|---|
| | C-ring | | | F-ring | | | |
| | 2 | 3 | 4 | 2 | 3 | 4α | 4β |
| chemical shift, δ | 5.33 | 4.49 | 4.74 | 4.46 | 3.90 | 3.00 | 2.63 |
| multiplicity | d | t or q | dd | d | ddd | dd | dd |
| coupling constants, Hz | 3.0 | broad | 1.2/3.0 | 7.5 | 5.5/7.5/8.5 | 5.5/-16.2 | 8.5/-16.2 |

**TABLE 7.1.1**

| AROMATIC RING DATA FOR *ENT*-FISETINIDOL-(4α→8)-CATECHIN AT 333 K. | | | | | | | | | |
|---|---|---|---|---|---|---|---|---|---|
| | A-ring | | | B-ring | | | E-ring | | | D-ring |
| | 8 | 5 | 6 | 2 | 5 | 6 | 2 | 5 | 6 | 6 |
| chemical shift, δ | 6.42 | 6.55 | 6.28 | 6.81 | 6.64 | 6.61 | 6.74 | 6.80 | 6.47 | 6.07 |
| multiplicity | d | dd | dd | dd | dd | ddd | dd | d | dd | s |
| coupling constants, Hz | 2.5 | 1.2/8.2 | 2.5/8.2 | 0.5/2.0 | 0.5/8.0 | 0.5/2.0/8.0 | 2.0/8.0 | 8.0 | 2.0/8.0 | |

**TABLE 7.1.2**

The relatively small coupling constants of the protons of the C-ring (Figure 7.1.3, D1 36, Table 7.1.1) $^3J_{2,3}$=3Hz and $^3J_{3,4}$=3Hz indicate an almost exclusive contribution of the A-conformer of the C-ring. $^3J_{3,4}$, however, is expected to be slightly larger than $^3J_{2,3}$ in the case of an A-conformer. The possible hydrogen bonding between 3-OH$_C$ and the oxygen of the pyran C-ring further stabilises the conformation of the C-ring and this, together with the magnitude of the coupling constants, suggests an A/skewed boat conformation with all the C-ring hydrogen atoms in quasi-equatorial positions.

## 6.4 THE CONFORMATIONAL BEHAVIOUR OF *ENT*-FISETINIDOL-(4β→6)-CATECHIN IN ACETONE-d$_6$

The structure of this compound was studied by $^1$H, $^{13}$C, COSY 45, HMQC and NOESY PH NMR experiments in extensively dried acetone-d$_6$ and CD in methanol (see Chapter 8). The $^1$H NMR spectrum (Figures 7.2.1/2, Table 7.2.1/2) differs only slightly from the corresponding $^1$H NMR spectra of fisetinidol-(4α→6)-catechin (Figures 6.3.2 and 6.3.3).
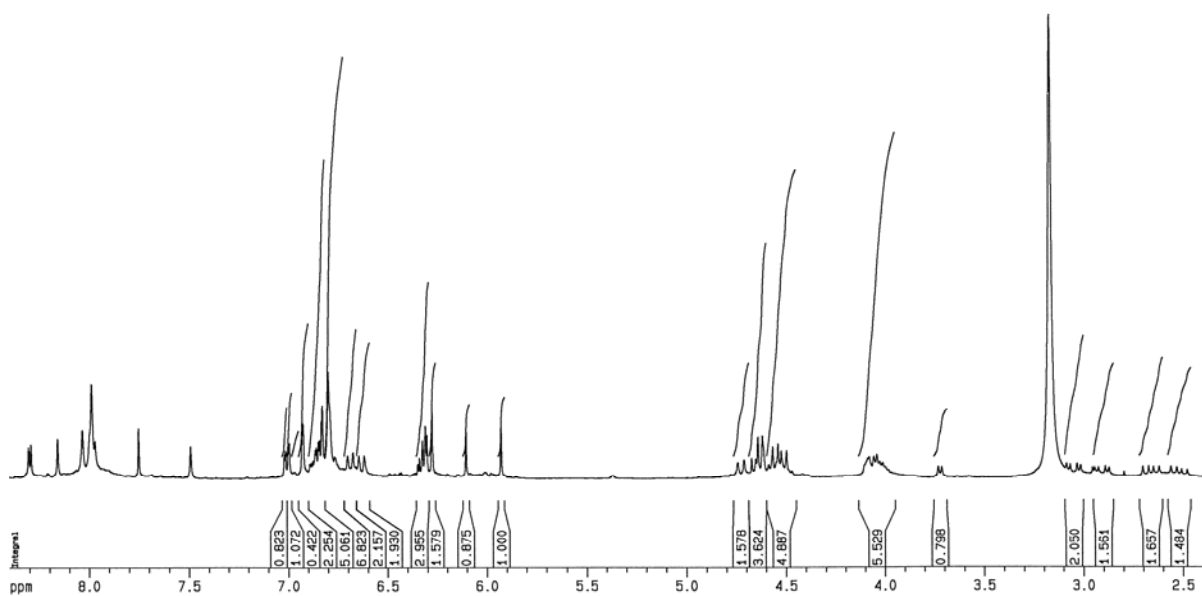


**FIGURE 7.2.1**

**FIGURE 7.2.2**

138
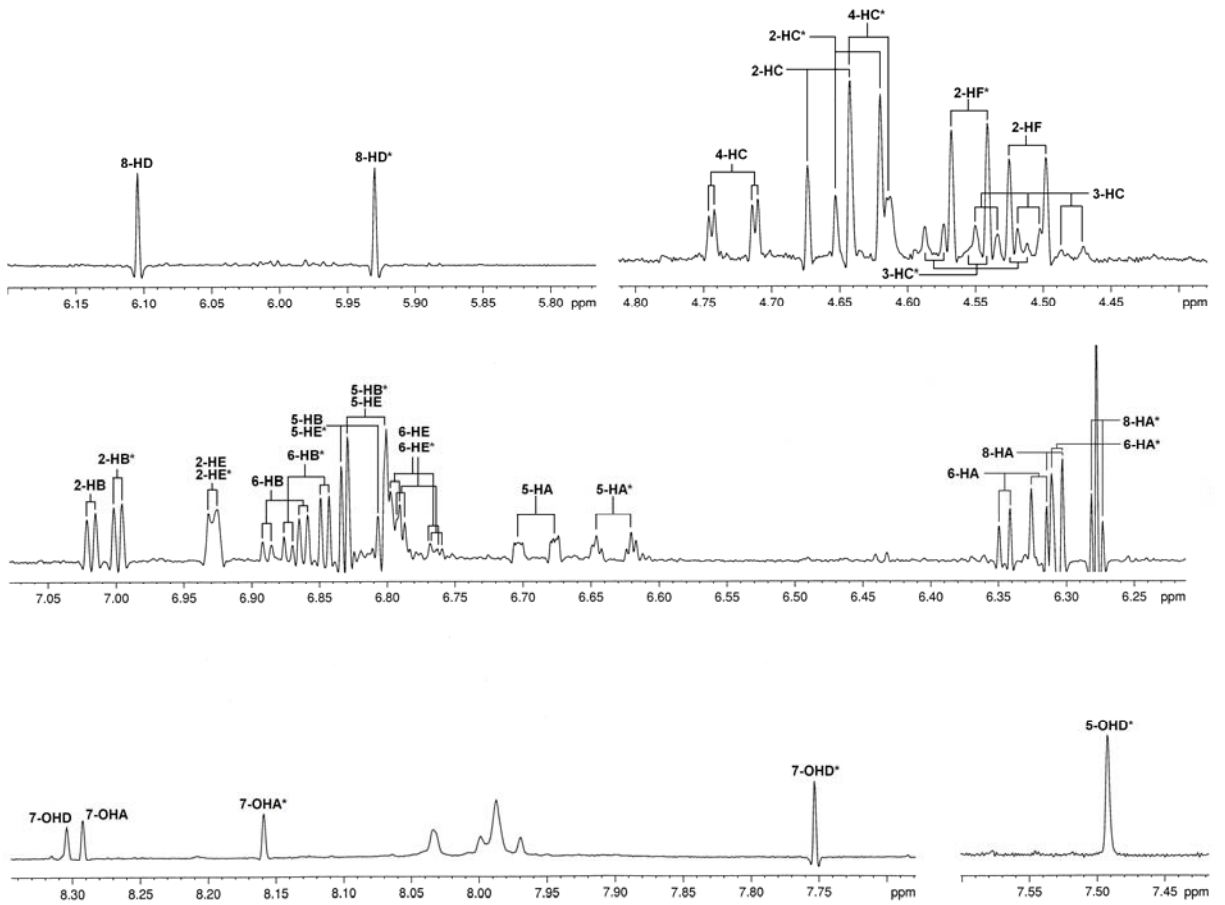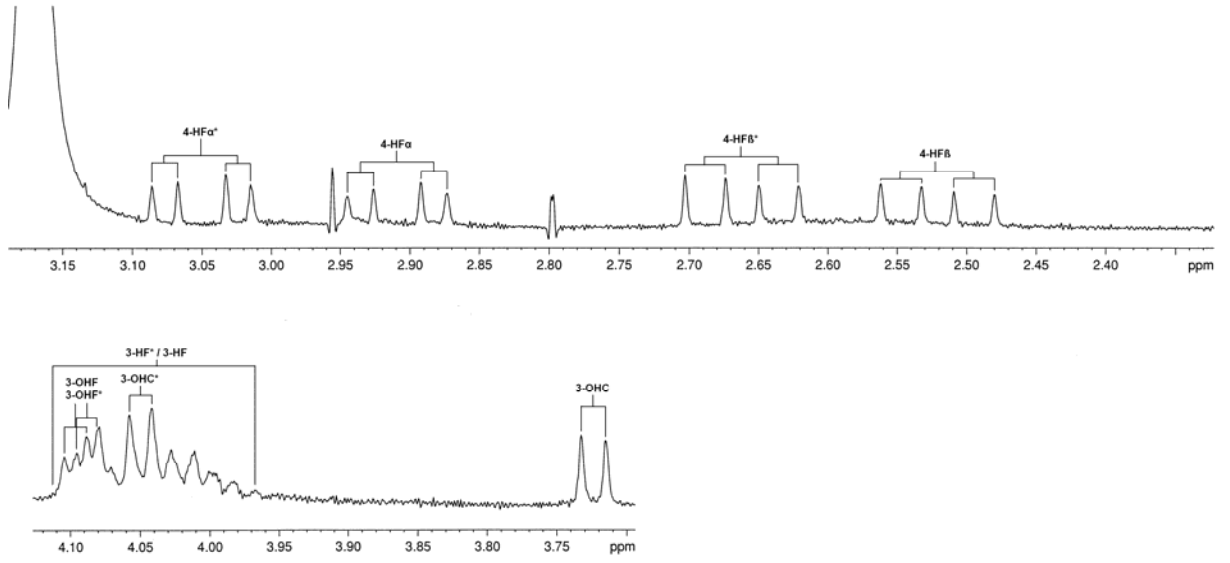
| "Compact" rotamer | C-ring | | | | F-ring | | | | |
|---|---|---|---|---|---|---|---|---|---|
| | 2 | 3 | 4 | 3-OH | 2 | 3 | 4α | 4β | 3-OH |
| chemical shift, δ | 4.66 | 4.51 | 4.73 | 3.72 | 4.51 | 3.97 to 4.11 | 2.91 | 2.52 | 4.10 |
| Multiplicity | d | td | dd | d | d | m | dd | dd | d |
| coupling constant, Hz | 9.5 | 5.2 9.5 | 1.2 9.5 | 5.2 | 8.0 | broad | 5.5 -15.8 | 8.8 -15.8 | 5.0 |
| | | | | | | | | | |
| *-Rotamer | C*-ring | | | | F*-ring | | | | |
| | 2 | 3 | 4 | 3-OH | 2 | 3 | 4α | 4β | 3-OH |
| chemical shift, δ | 4.64 | 4.55 | 4.63 | 4.05 | 4.56 | 3.97 to 4.11 | 3.05 | 2.67 | 4.09 |
| Multiplicity | dd | td | dd | d | d | m | dd | dd | d |
| coupling constant, Hz | 10.0 | 4.5 10.0 | 1.0 10.0 | 4.8 | 8.0 | broad | 4.5 -15.5 | 8.5 -15.5 | 5.0 |

**TABLE 7.2.1**

| "Compact" rotamer | A-ring | | | B-ring | | | E-ring | | | D-ring |
|---|---|---|---|---|---|---|---|---|---|---|
| | 8 | 5 | 6 | 2 | 5 | 6 | 2 | 5 | 6 | 8 |
| chemical shift, δ | 6.31 | 6.69 | 6.33 | 7.02 | 6.82 | 6.88 | 6.93 | 6.81 | 6.78 | 5.93 |
| multiplicity | d | ddd | dd | dd | d | dd | d | d | dd | s |
| coupling constant, Hz | 2.5 | 0.5 2.5 8.0 | 2.5 8.0 | 2.0 | 8.0 | 2.0 8.0 | 2.0 | 8.0 | 2.0 8.0 | |
| | | | | | | | | | | |
| *- Rotamer | A*-ring | | | B*-ring | | | E*-ring | | | D*-ring |
| | 8 | 5 | 6 | 2 | 5 | 6 | 2 | 5 | 6 | 8 |
| chemical shift, δ | 6.28 | 6.64 | 6.29 | 7.00 | 6.81 | 6.86 | 6.93 | 6.82 | 6.78 | 6.10 |
| multiplicity | d | dt | dd | dd | d | dd | d | d | dd | s |
| coupling constant, Hz | 2.5 | 1.0 8.0 | 2.5 8.0 | 2.0 | 8.0 | 2.0 8.0 | 2.0 | 8.0 | 2.0 8.0 | |

**TABLE 7.2.2**

The COSY 45 experiment was used to assign all proton resonances. Cross peaks between 4-H$_{F\alpha}$ and 4-H$_{F\beta}$ (Figure 7.2.3, D4 16) had half the responses missing. The lean of the cross peaks confirmed the magnitude and the negative sign of the $^2J_{4HF\alpha,4HF\beta}$ vicinal coupling constant.
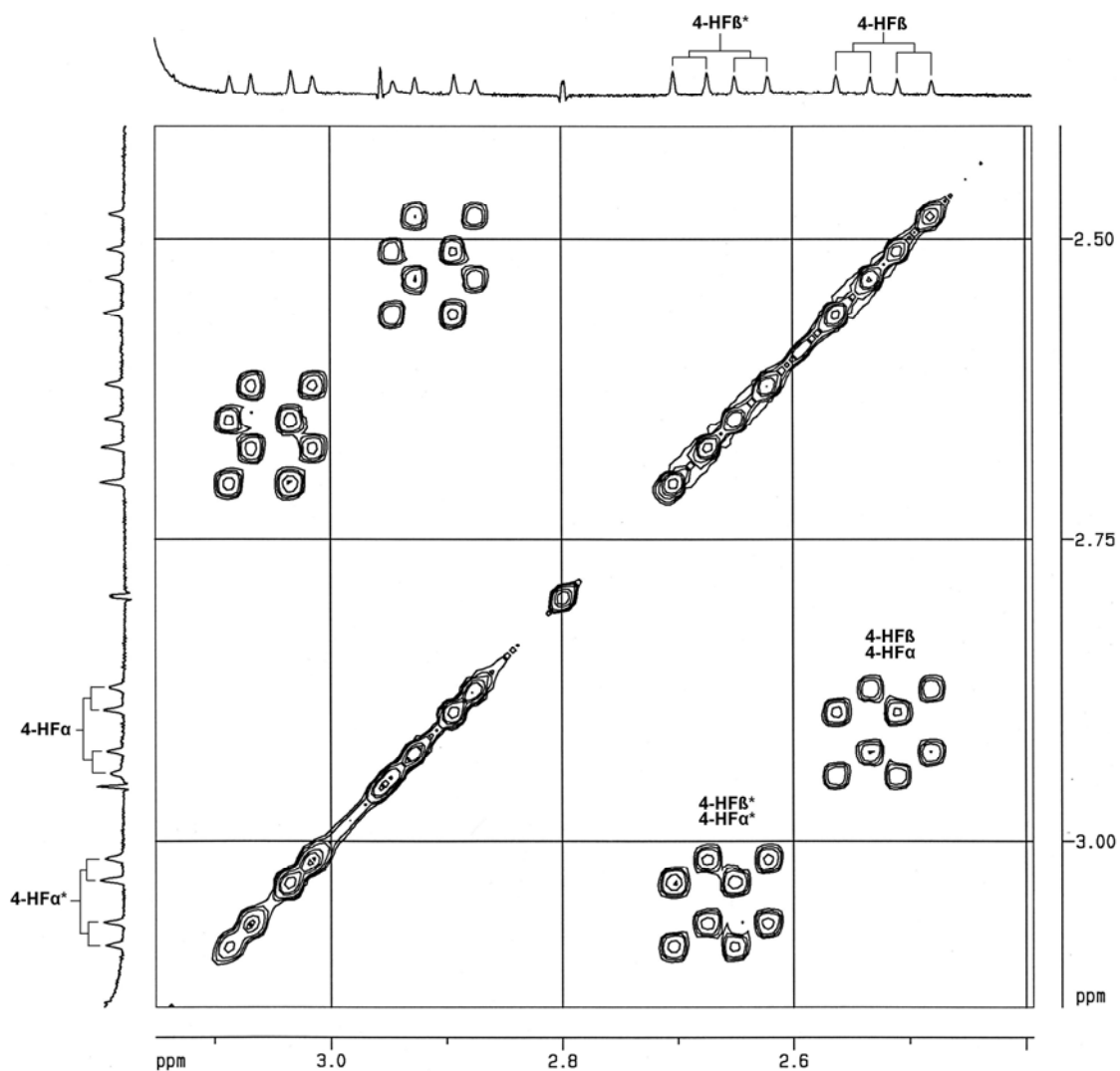


**FIGURE 7.2.3**

These assignments were used to assign the 3-H$_F$ resonance (Figure 7.2.4, D4 17).



**FIGURE 7.2.4**

Cross peaks were also observed between the 4-$H_F$ and 8-$H_D$ (Figure 7.2.5, D4 20). Because of the apparent similarity in intensity between these cross peaks, it can be interpreted that the F-ring of both conformers undergoes conformational exchange, with both the 4-$H_{F\alpha}{\rightarrow}4C_4$ and 4-$H_{F\beta}{\rightarrow}4C_4$ bonds forming approximately $90^o$ angles with planes of their respective D-rings.
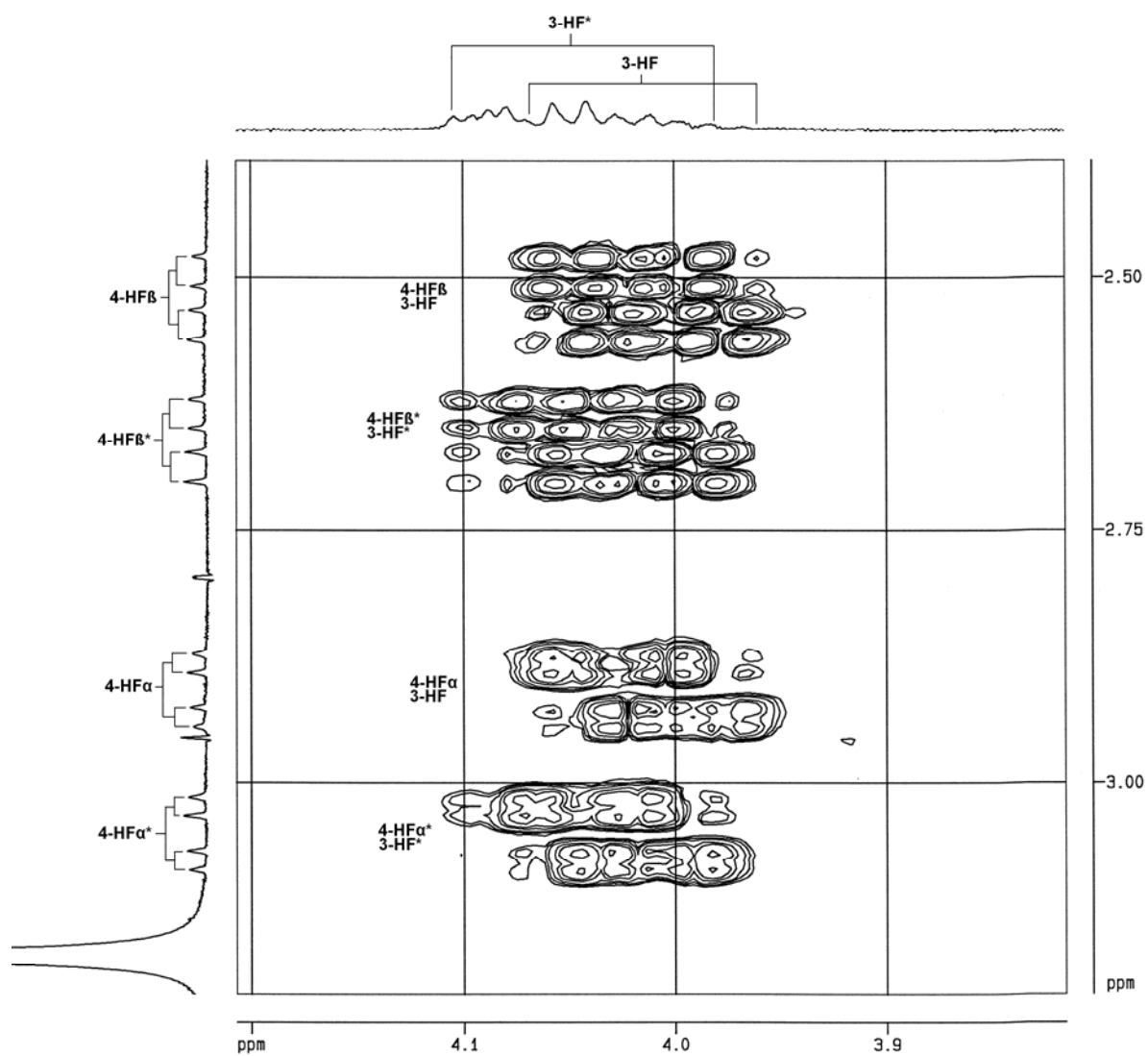


**FIGURE 7.2.5**

3-HF was used to assign the 2-H$_F$ and 3-OHF resonances (Figure 7.2.6, D4 21).
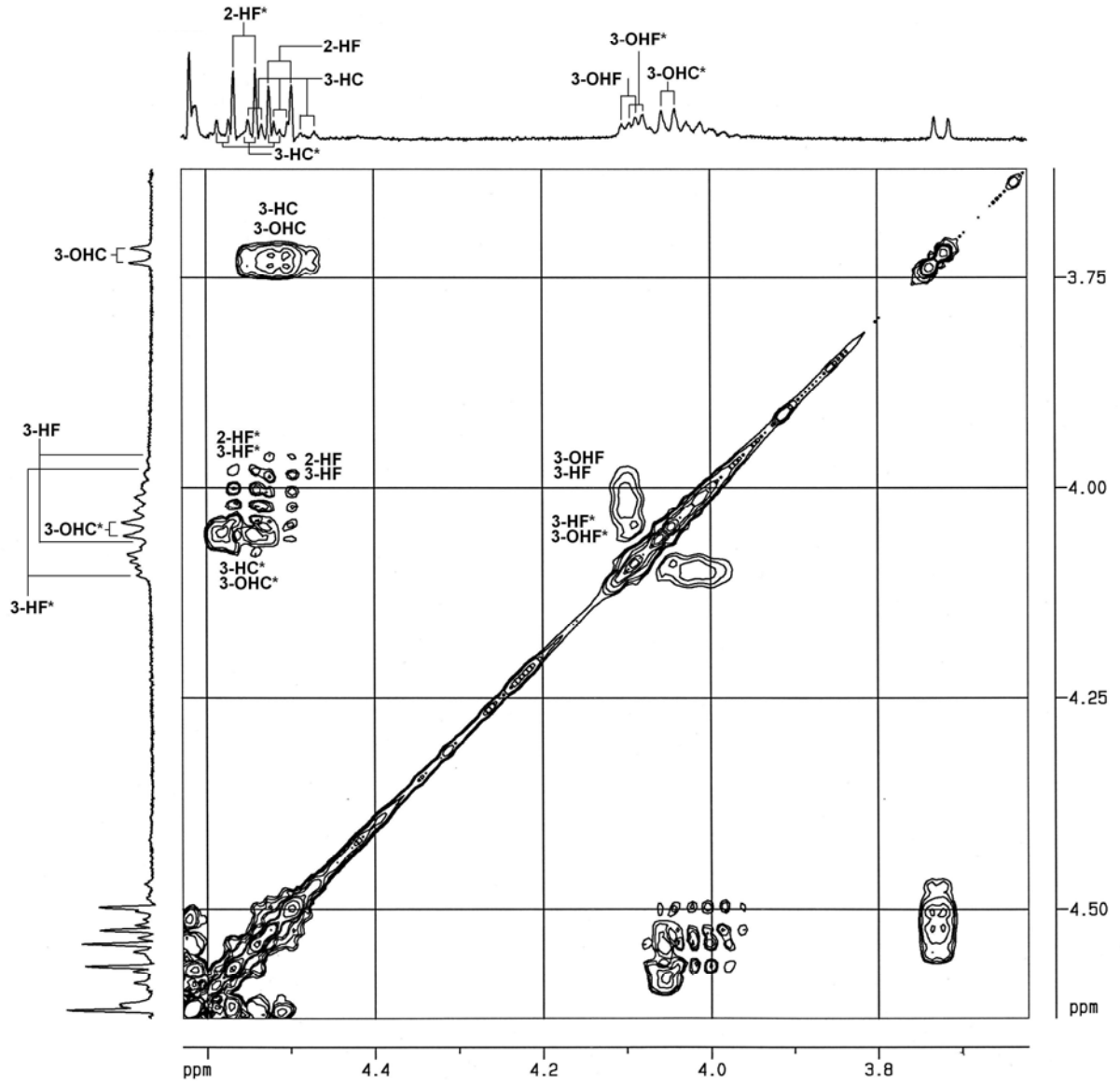


**FIGURE 7.2.6**

143

The resonances of both sets of C-ring protons are all in the 4.4 - 4.8 ppm region (Figure 7.2.7, D4 31) Unambiguous assignments of the resonances of the C*-ring protons were not possible due to their proximity to the diagonal.
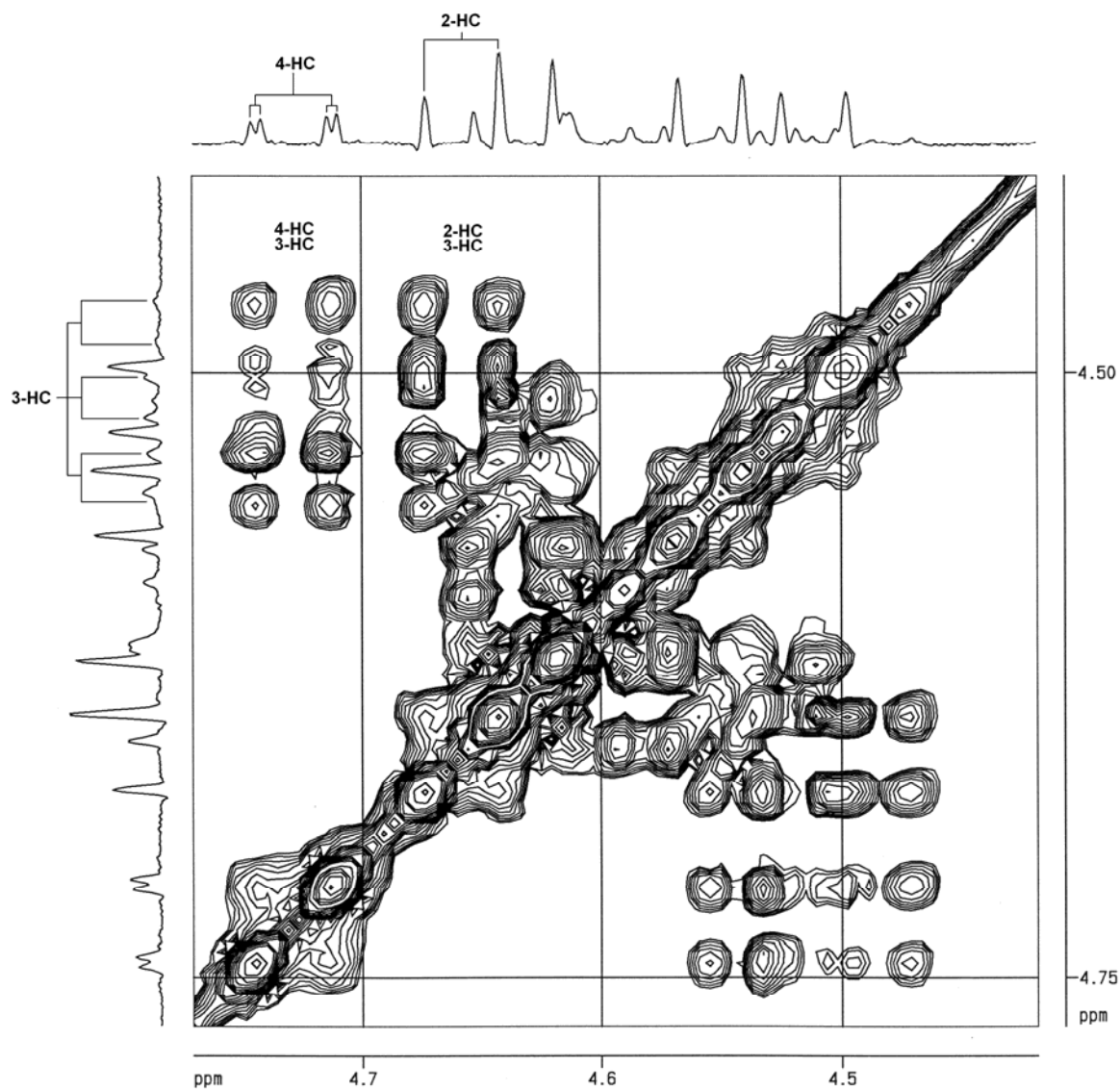


**FIGURE 7.2.7**

Both 3-H$_C$ resonances were confirmed by their cross peaks with the respective 3-OH$_C$ resonances (Figures 7.2.6/8, D4 21/24). Cross peaks between 3-H$_C$ and 3-H$_C$*, and the 3-OH$_C$ and 3-OH$_C$* resonances, respectively, as well as the magnitude of the $^3J_{3\text{-}HC,3\text{-}OHC}$ coupling constants (Table 7.2.1), confirmed their assignments.
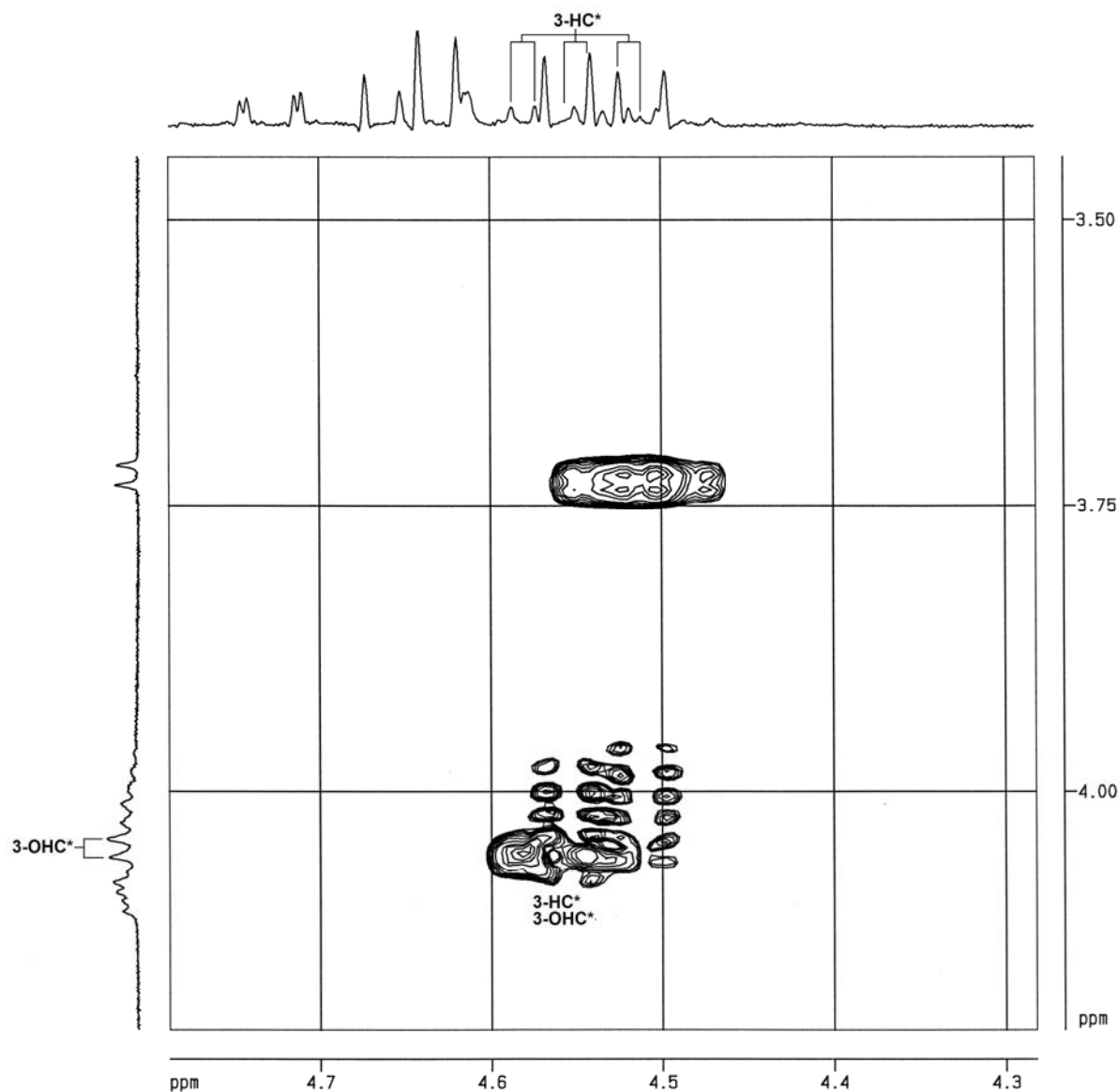


**FIGURE 7.2.8**

The 4-H$_C$* resonances were assigned by their cross peaks with 8-H$_D$* (Figure 7.2.9). Relatively strong coupling between 4-H$_C$ and the respective 8-H$_D$ resonances implies that the 4-H$_C$→4C$_C$ bonds are both at approximately 90$^o$ or slightly larger or smaller angles with the planes of the respective D-rings.



D4 34
COSY 45
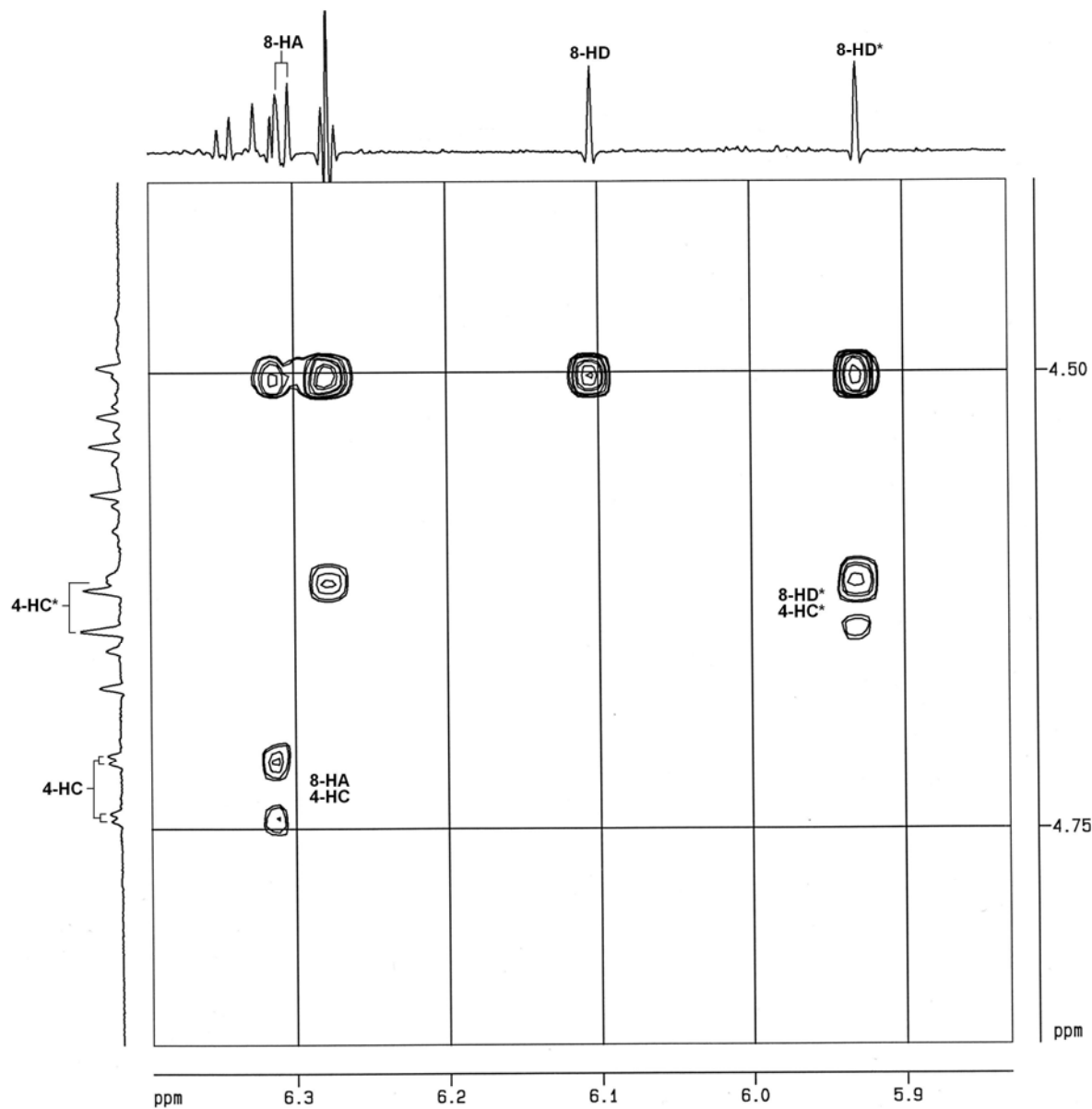
**FIGURE 7.2.9**

The 5-H$_A$ resonances were assigned from their cross peaks with the respective 4-H$_C$ resonances (Figure 7.2.10, D4 35). The 2-H$_B$ and 6-H$_B$ resonances were assigned from their cross peaks with the C-ring resonances. The 2-H$_F$ resonances of the two rotamers are not coincidental as in the case of fisetinidol-(4α→6)-catechin, and they were used to assign the coincidental 2-H$_E$ resonances. They were also used to make preliminary assignments of one 5-H$_E$ and both 6-H$_E$ resonances.
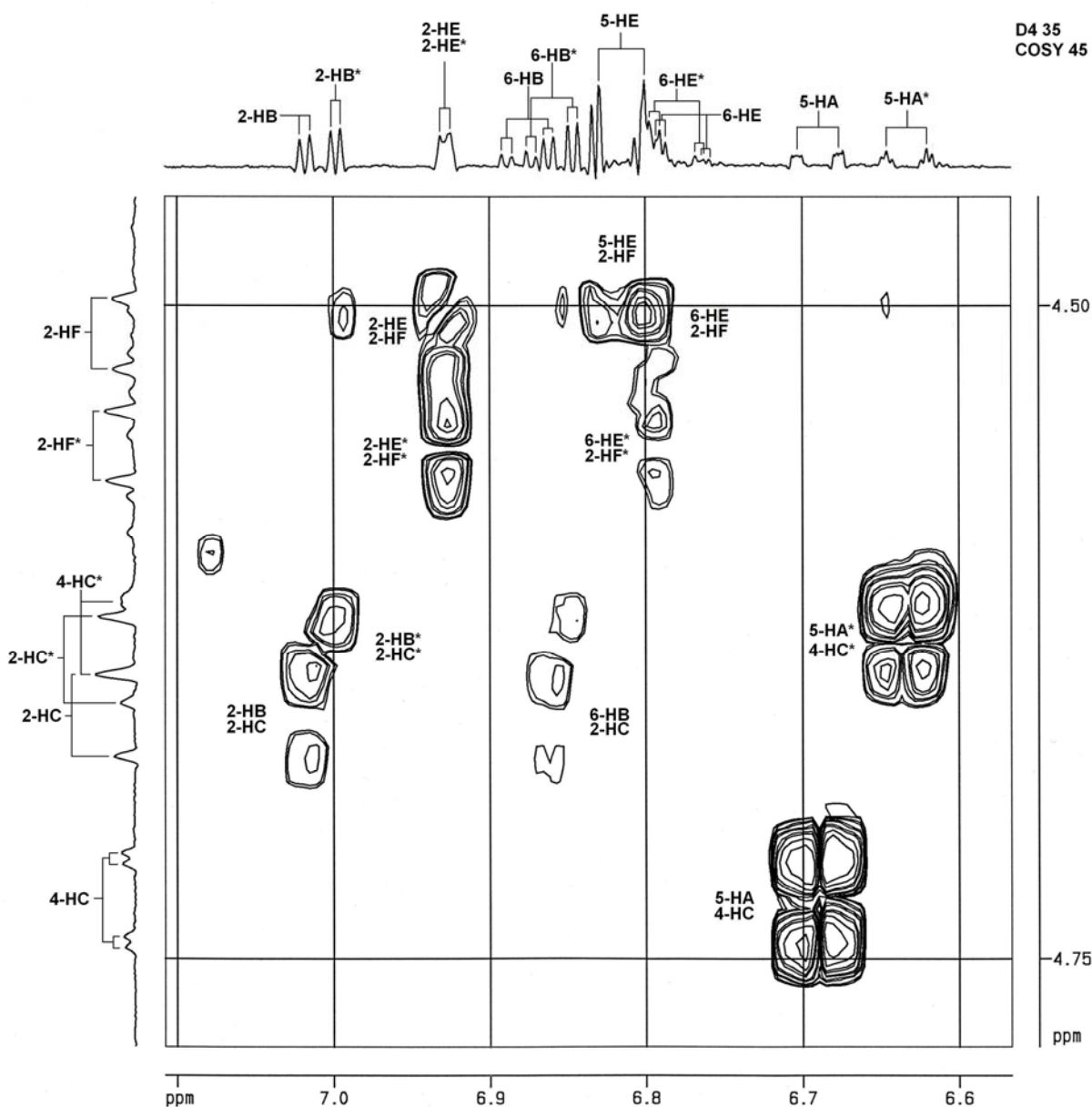


**FIGURE 7.2.10**

Due to the pronounced skewness of the 6-H$_A$, 6-H$_B$ and 6-H$_E$ resonances, the responses of

their cross peaks with other proton resonances do not have they same intensities, and are often missing depending on the depth of the particular plot of the COSY 45 experiment.

The 6-$H_A$ and 8-$H_A$ resonances were assigned from their cross peaks with the respective 5-$H_A$ resonances.
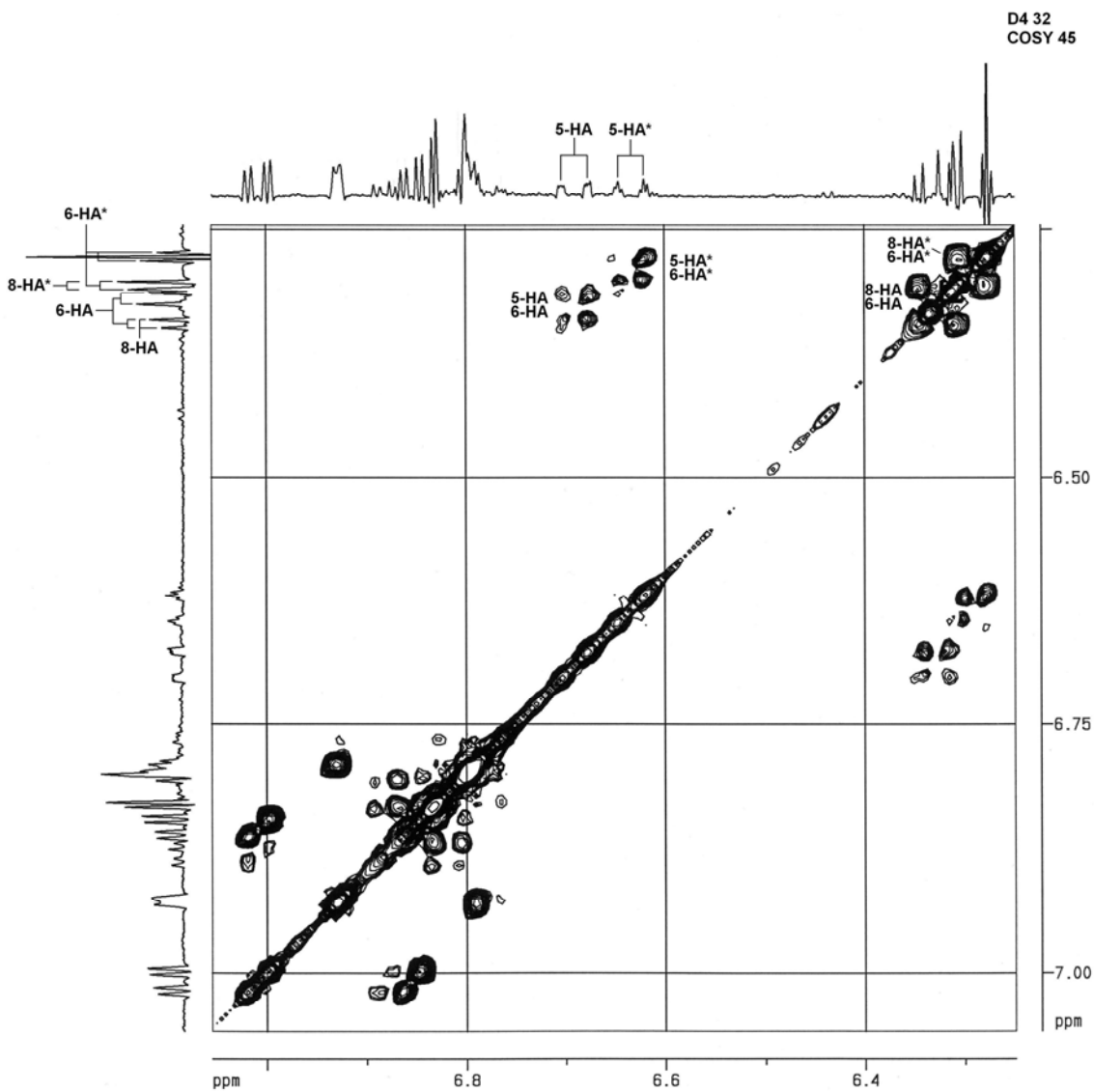


**FIGURE 7.2.11**

Both 5-$H_B$ resonances were assigned from their cross peaks with the respective 6-$H_B$

resonances (Figure 7.2.12, D4 33). Unambiguous assignment of the 5-H$_E$* resonance was not possible due to its proximity to 5-H$_E$ and to the diagonal.
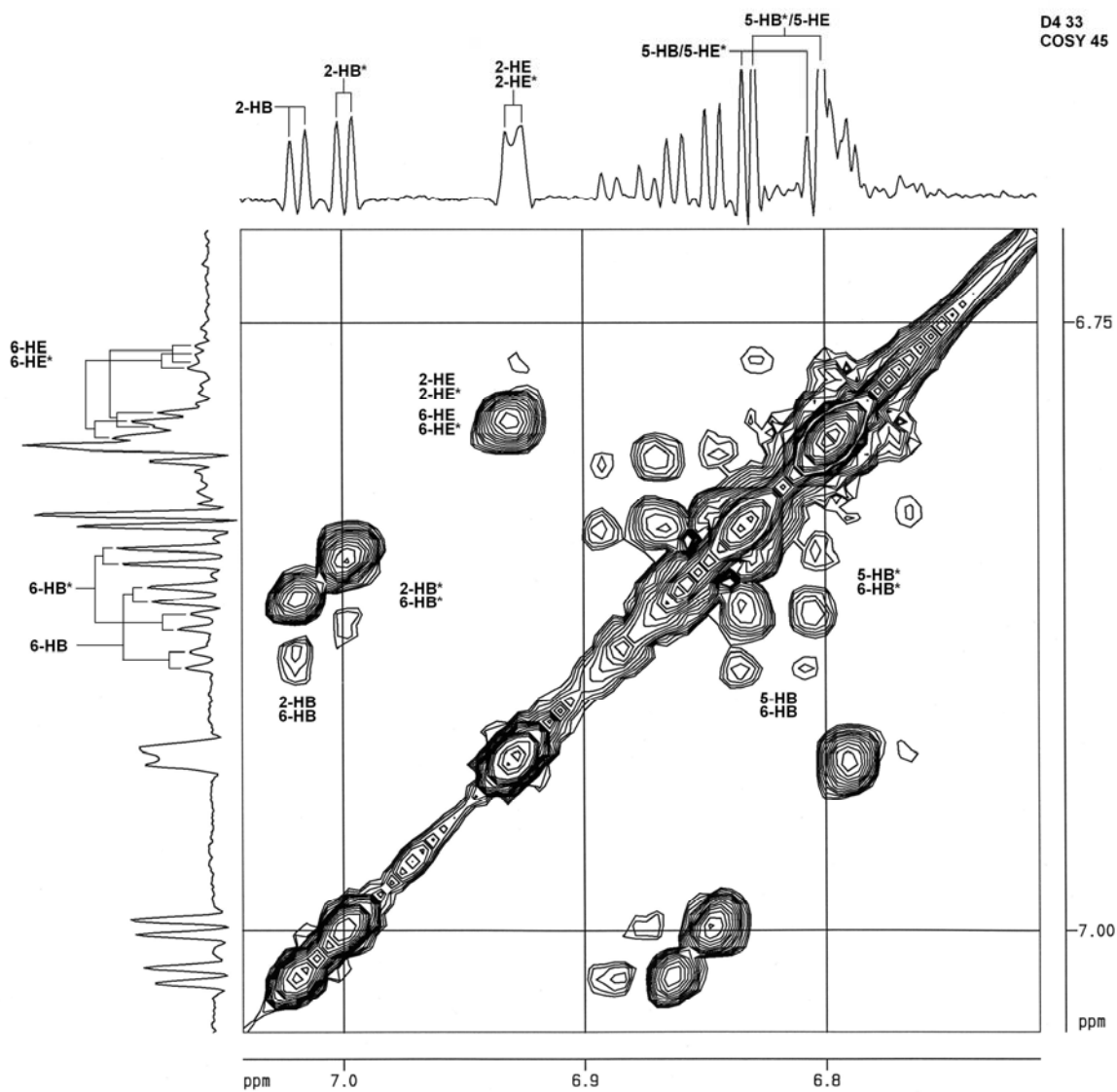


**FIGURE 7.2.12**

The resonances of some of the aromatic hydroxy groups were assigned from their cross

peaks with the resonances of some of the aromatic protons (Figure 7.2.13, D4 28).
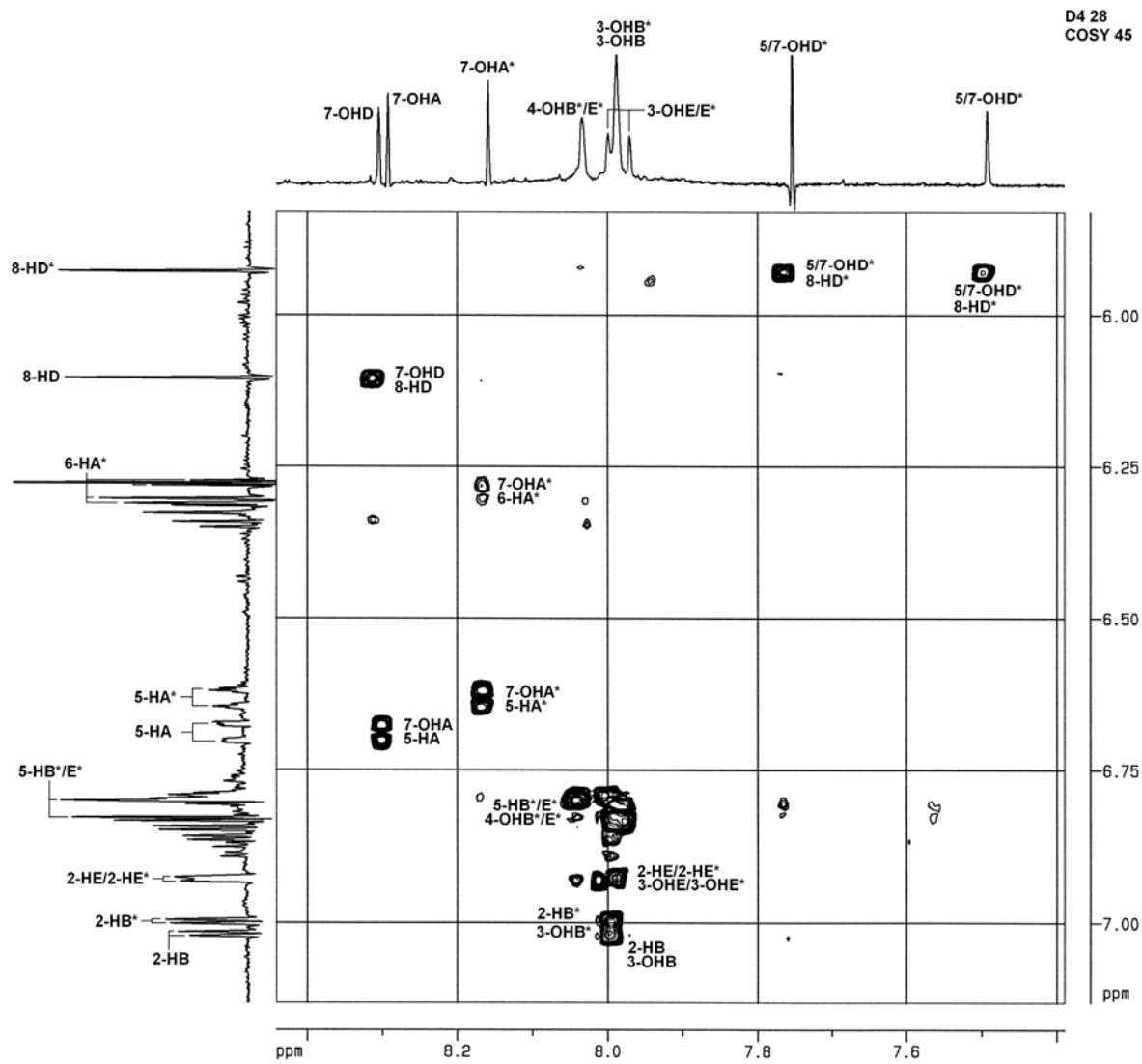


**FIGURE 7.2.13**

The identification of the rotamers as either "compact" or "extended", as is the case with the

fisetinidol-(4α→8)-catechin (Paragraph 6.1), catechin-(4α→8)-catechin and catechin-(4α→8)-epicatechin dimers,[98] could not be done. As demonstrated in the case of the fisetinidol-(4α→6)-catechin dimer (Paragraph 6.3), both rotamers have shapes more similar to those of the "extended" conformers of the 4α→8 linked dimers.
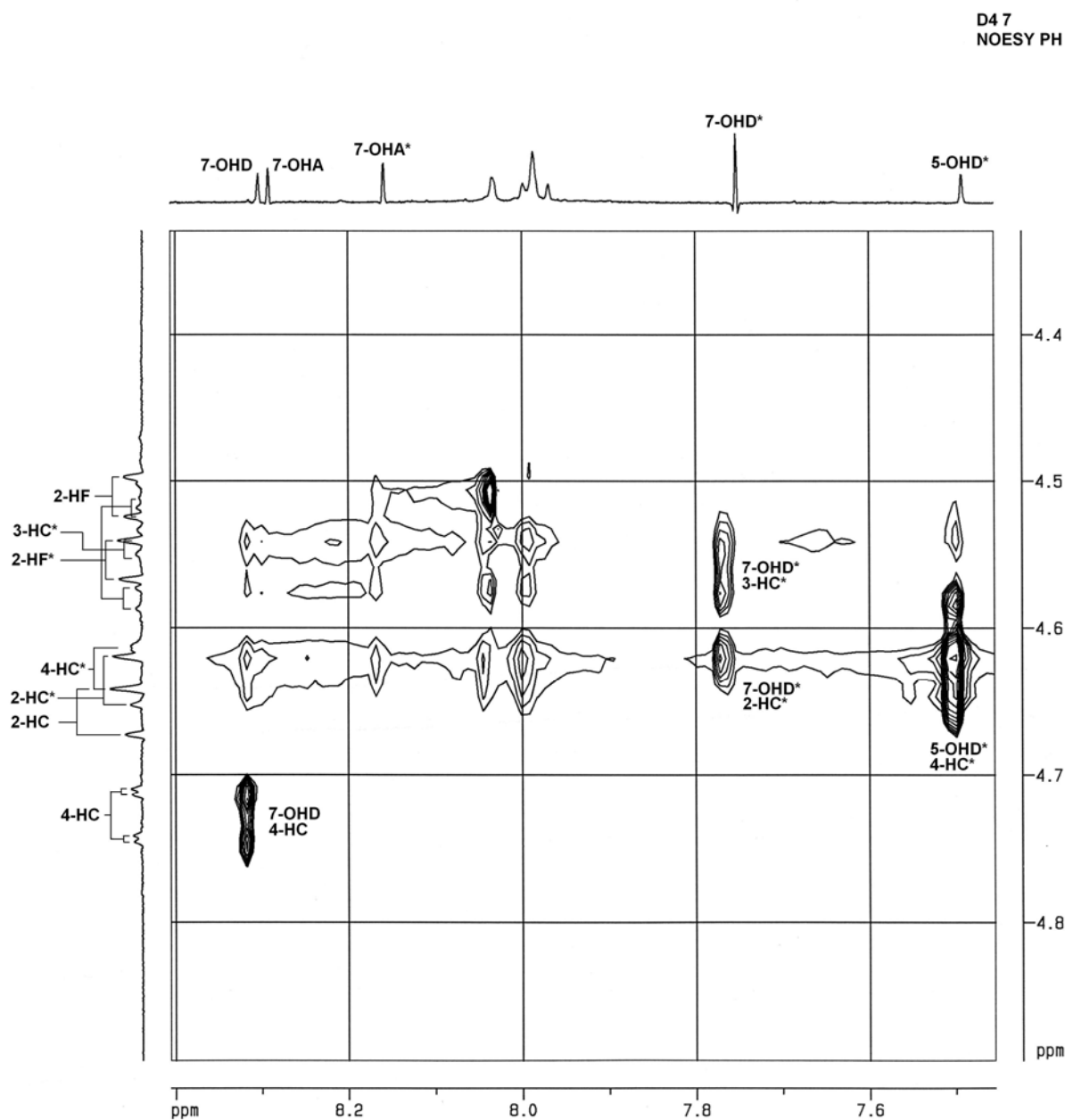


**FIGURE 7.2.14**

The *-rotamer was identified by cross peaks between the 3-H$_C$* and 7-OH$_D$* resonances as

well as between the 4-H$_C$* and 5-OH$_D$* resonances (Figure 7.2.14, D4 7).

There is an approximately 0º angle between the 4-H$_C$→4C$_C$ bond and the plane of the D-ring, and an approximately 90º angle between the 4-H$_C$*→4C$_C$* bond and the plane of the D*-ring. This is supported by the following two observations:

a)      The cross peaks between the 4-H$_C$ and 7-OH$_D$ resonances in the NOESY PH experiment are stronger than the two sets of cross peaks identifying the *-rotamer. The distance between 4-H$_C$ and the 7-OH$_D$ is therefore smaller than the distances between 4-H$_C$* and 7-OH$_D$*, as well as 3-H$_C$* and 5-OH$_D$*.

b)      There are cross peaks between the 4-H$_C$* and 8-H$_D$* resonances in the COSY 45 experiment, whereas no cross peaks were observed between 4-H$_C$ and 8-H$_D$ (Figure 7.2.9, D4 34). This indicates that the angle between the 4-H$_C$→4C$_C$ bond and the plane of the D-ring is smaller than the angle between the 4-H$_C$*→4C$_C$* bond and the plane of the D*-ring.

The $^{13}$C NMR and HMQC spectra (Figures 7.2.15 – 19, Appendix B) display very small

chemical shift differences between the carbon resonances of the two rotamers, as well as substantial overlap of C/H cross peaks.
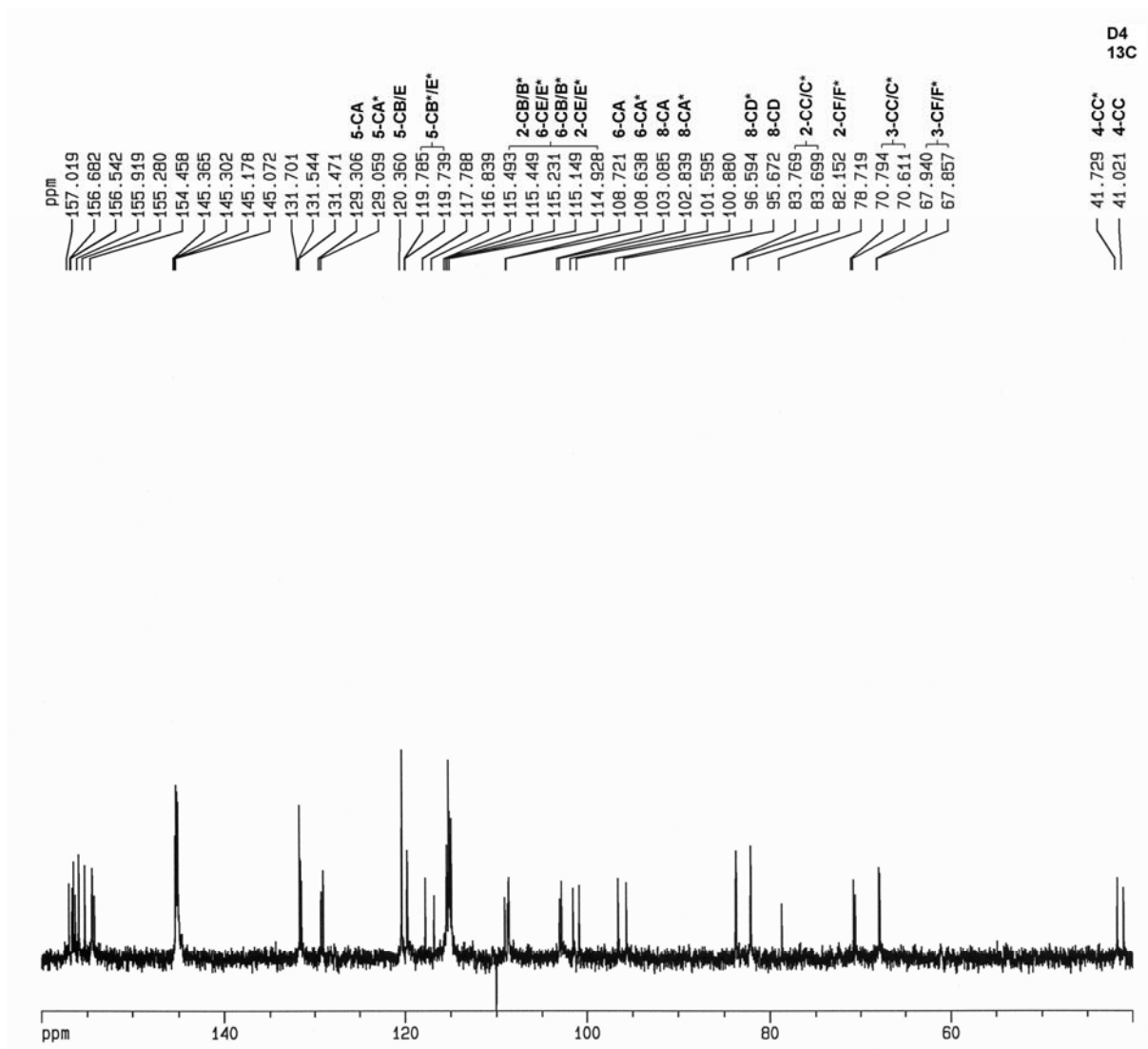


**FIGURE 7.2.15**
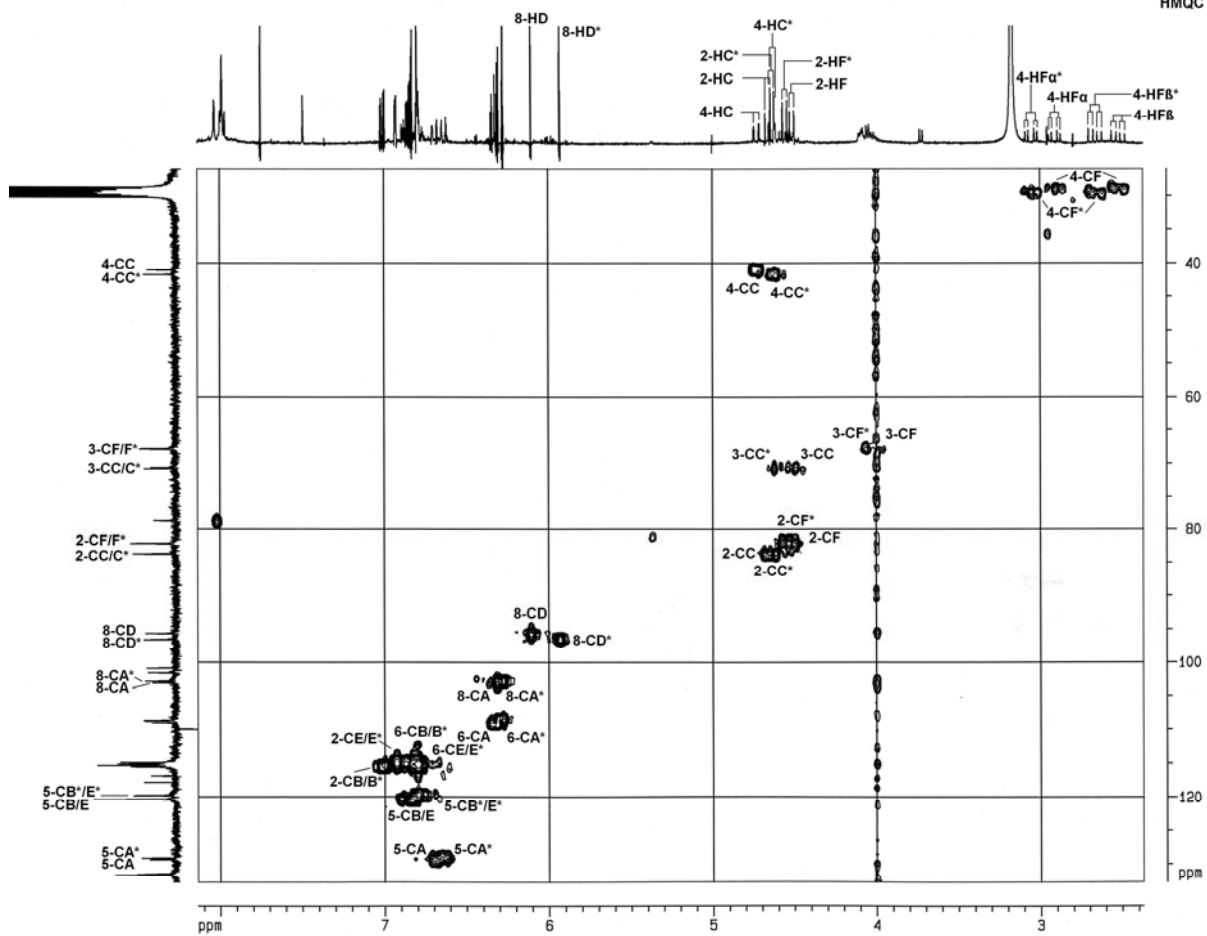
**FIGURE 7.2.16**
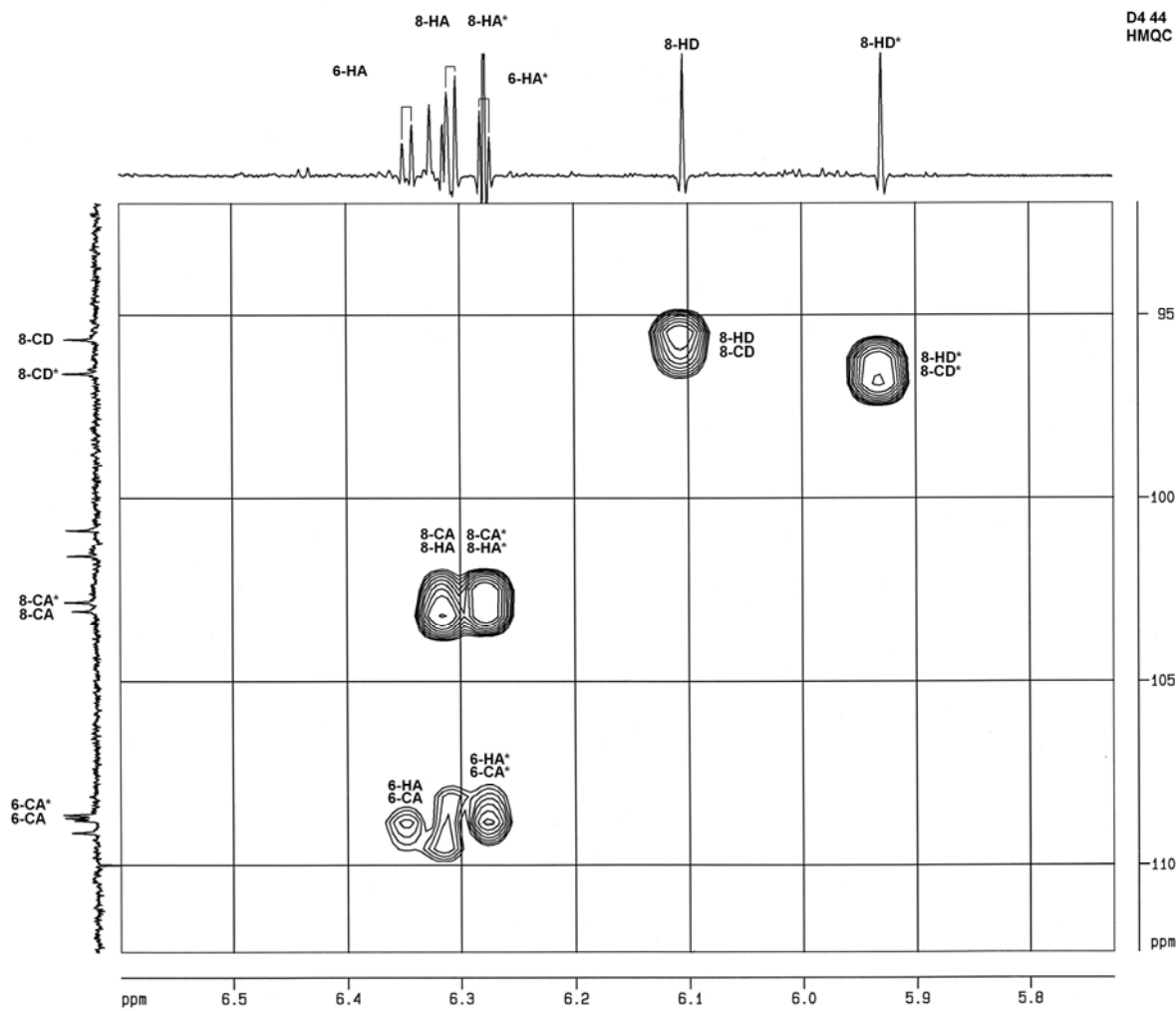
**FIGURE 7.2.17**
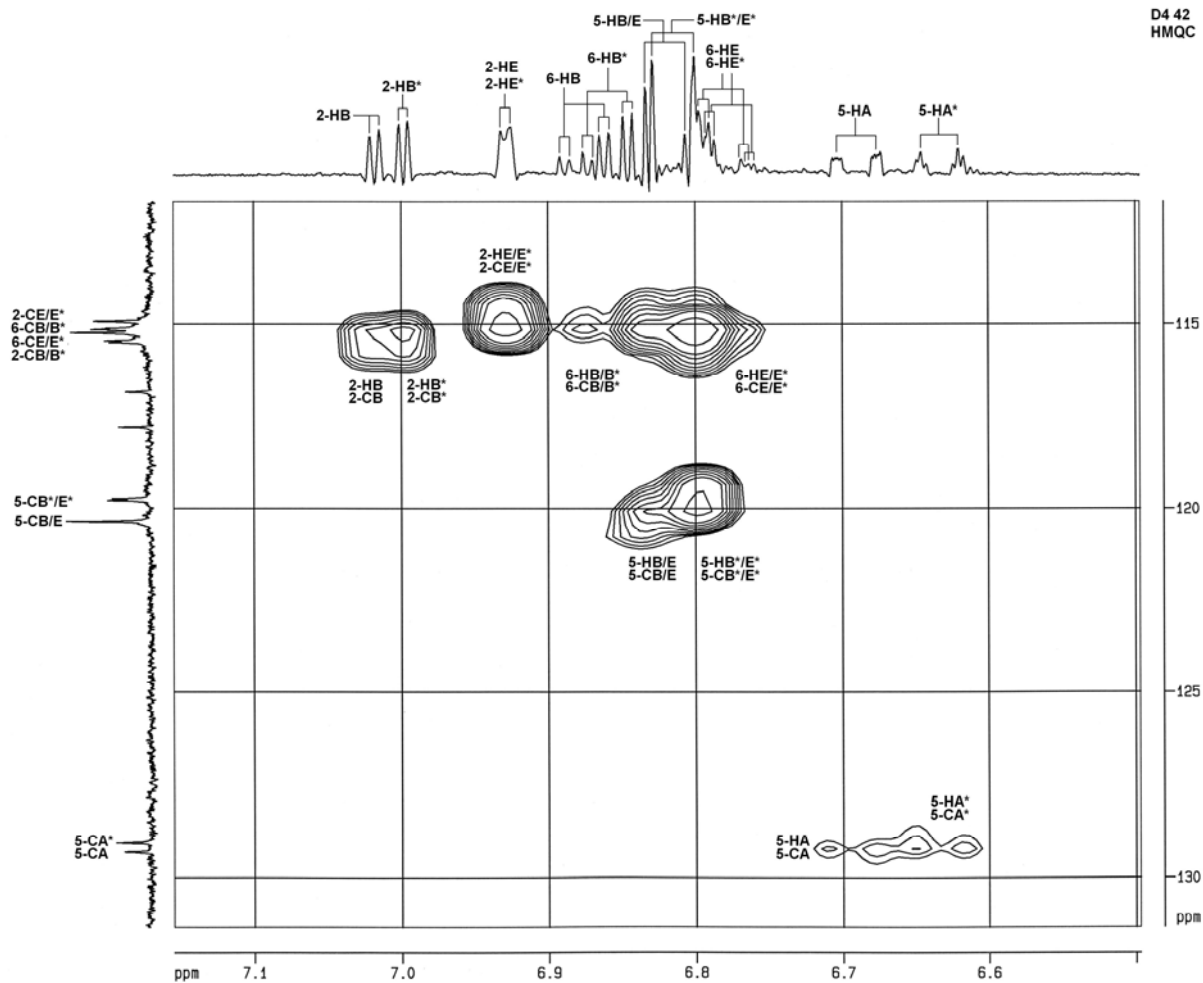
**FIGURE 7.2.18**
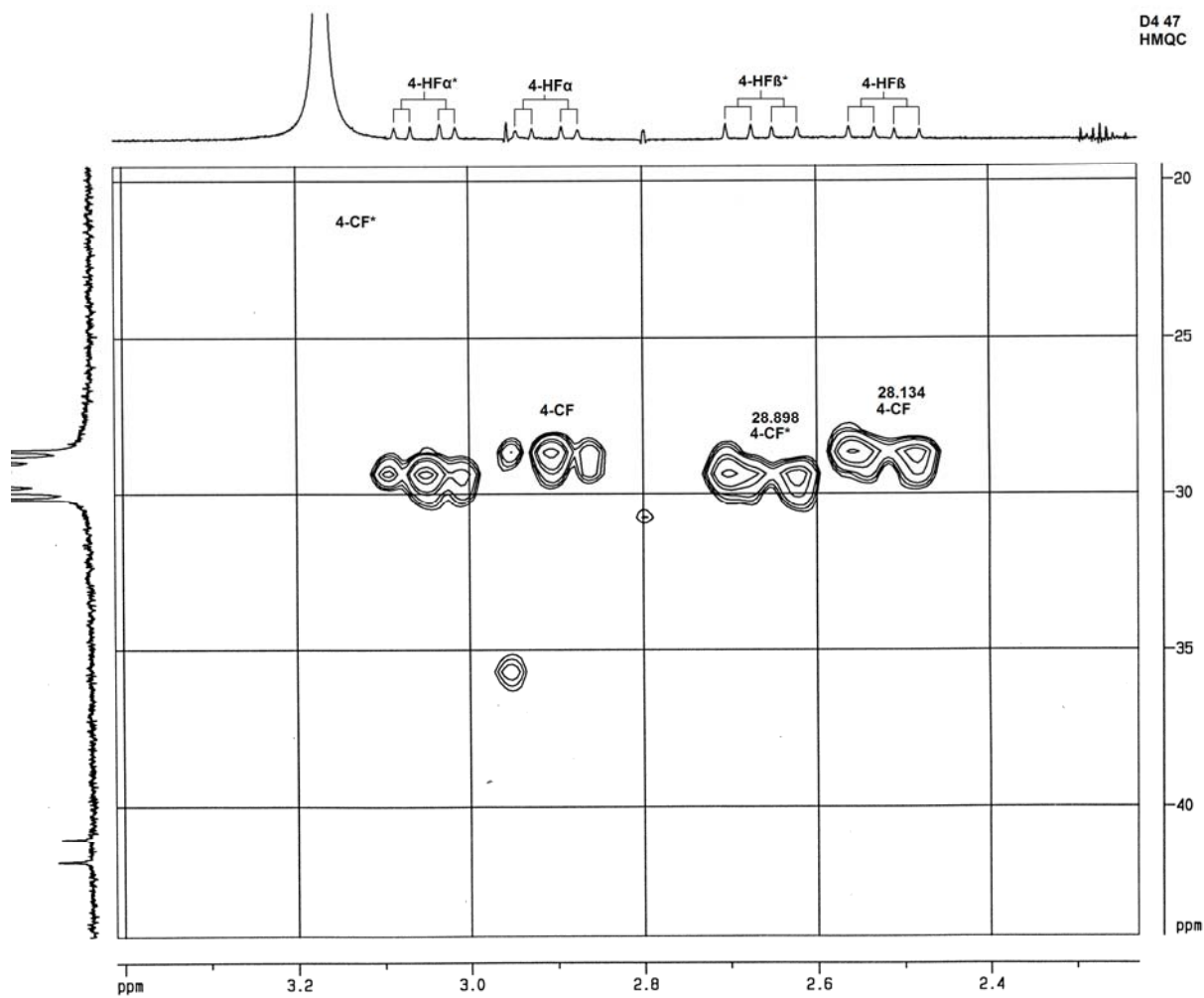
**FIGURE 7.2.19**

## 7.3    THE CONFORMATIONAL BEHAVIOUR OF *ENT*-FISETINIDOL-(4β→8)-CATECHIN IN ACETONE-D$_6$

The structure of this compound was studied by $^1$H, $^{13}$C, COSY 45, HMQC and NOESY PH NMR experiments in extensively dried acetone-d$_6$ and CD in methanol (see Chapter 8). The $^1$H NMR spectrum indicates the presence of two distinct rotamers (Figures 7.3.1/2).
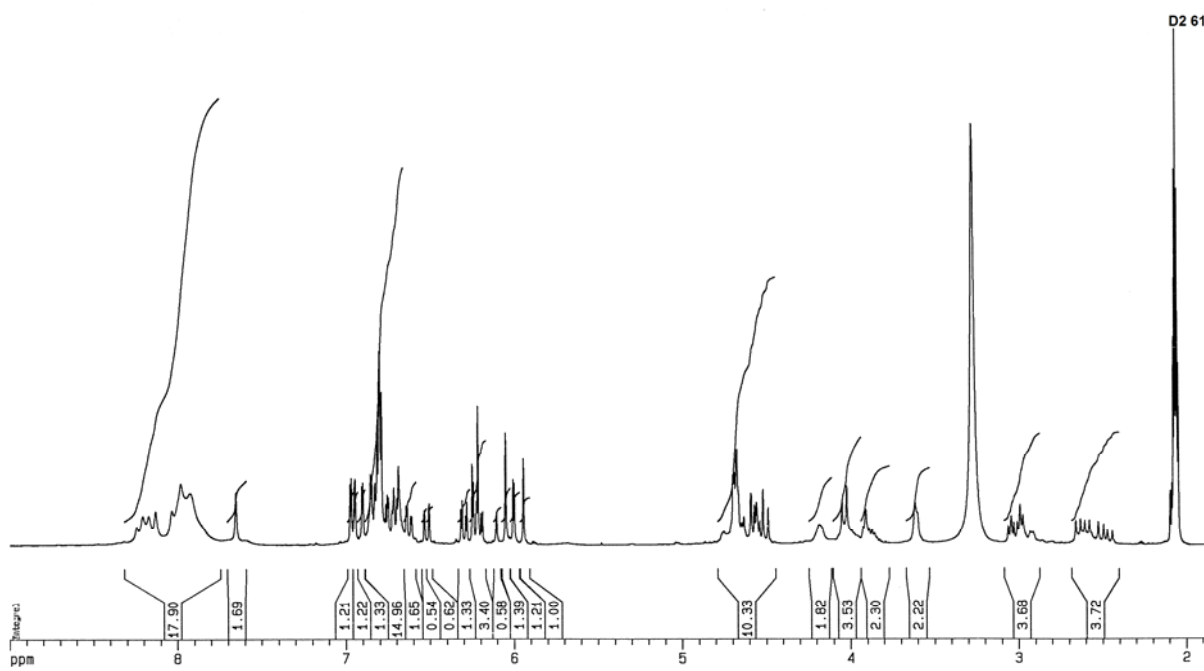


**FIGURE 7.3.1**
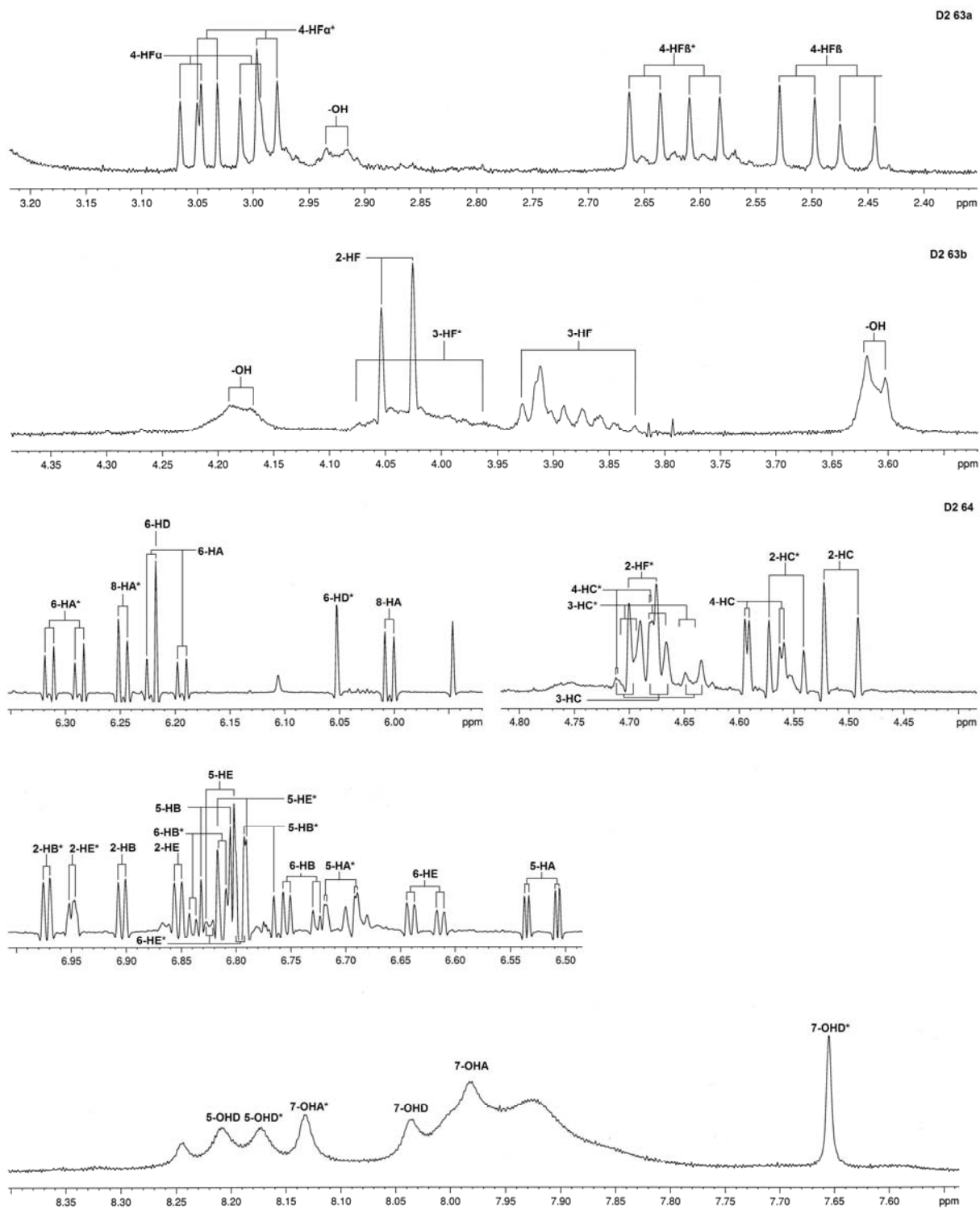
**FIGURE 7.3.2**

The COSY 45 experiment was used to assign the resonances of all the heterocyclic protons and the majority of the aromatic protons (Tables 7.3.1/7.3.2).

| "Compact" rotamer | C-ring | | | F-ring | | | |
|---|---|---|---|---|---|---|---|
| | 2 | 3 | 4 | 2 | 3 | 4α | 4β |
| chemical shift, δ | 4.51 | 4.67 | 4.58 | 4.04 | 3.83-3.93 | 3.03 | 2.49 |
| multiplicity | d | td | dd | d | m | dd | dd |
| coupling constant, Hz | 9.2 | 4.5<br>9.2 | 1.0<br>9.2 | 8.5 | broad | 5.8<br>-16.0 | 9.5<br>-15.8 |
| | | | | | | | |
| * Rotamer | C*-ring | | | F*-ring | | | |
| | 2 | 3 | 4 | 2 | 3 | 4α | 4β |
| chemical shift, δ | 4.56 | 4.67 | 4.70 | 4.69 | 3.95-4.08 | 3.01 | 2.66 |
| multiplicity | d | td | dd | d | m | dd | dd |
| coupling constant, Hz | 9.5 | 4.5<br>9.5 | 0.8<br>9.5 | 7.5 | broad | 5.5<br>-16.0 | 8.2<br>-16.0 |

**TABLE 7.3.1**

| "Compact" rotamer | A-ring | | | B-ring | | | E-ring | | | D-ring |
|---|---|---|---|---|---|---|---|---|---|---|
| | 8 | 5 | 6 | 2 | 5 | 6 | 2 | 5 | 6 | 8 |
| chemical shift, δ | 6.00 | 6.52 | 6.21 | 6.90 | 6.81 | 6.74 | 6.85 | 6.81 | 6.63 | 6.22 |
| multiplicity | d | dd | dd | dd | d | dd | d | d | dd | s |
| coupling constant, Hz | 2.5 | 1.2<br>8.2 | 2.5<br>8.2 | 2.0 | 8.0 | 2.0<br>8.0 | 2.0 | 8.2 | 2.0<br>8.2 | |
| | | | | | | | | | | |
| * Rotamer | A*-ring | | | B*-ring | | | E*-ring | | | D*-ring |
| | 8 | 5 | 6 | 2 | 5 | 6 | 2 | 5 | 6 | 8 |
| chemical shift, δ | 6.25 | 6.70 | 6.30 | 6.97 | 6.78 | 6.83 | 6.95 | 6.80 | 6.81 | 6.05 |
| multiplicity | d | dt | dd | dd | d | dd | d | d | dd | s |
| coupling constant, Hz | 2.5 | 0.8<br>8.0 | 2.5<br>8.0 | 1.9 | 8.0 | 1.9<br>8.0 | 2.0 | 8.0 | 2.0<br>8.0 | |

**TABLE 7.3.2**

Cross peaks between 4-H$_{F\alpha}$ and 4-H$_{F\beta}$ (Figure 7.3.3, D2 20) had half the responses missing. The lean of the cross peaks confirmed the magnitude and the negative sign of the $^2J_{4HF\alpha,4HF\beta}$ vicinal coupling constant.
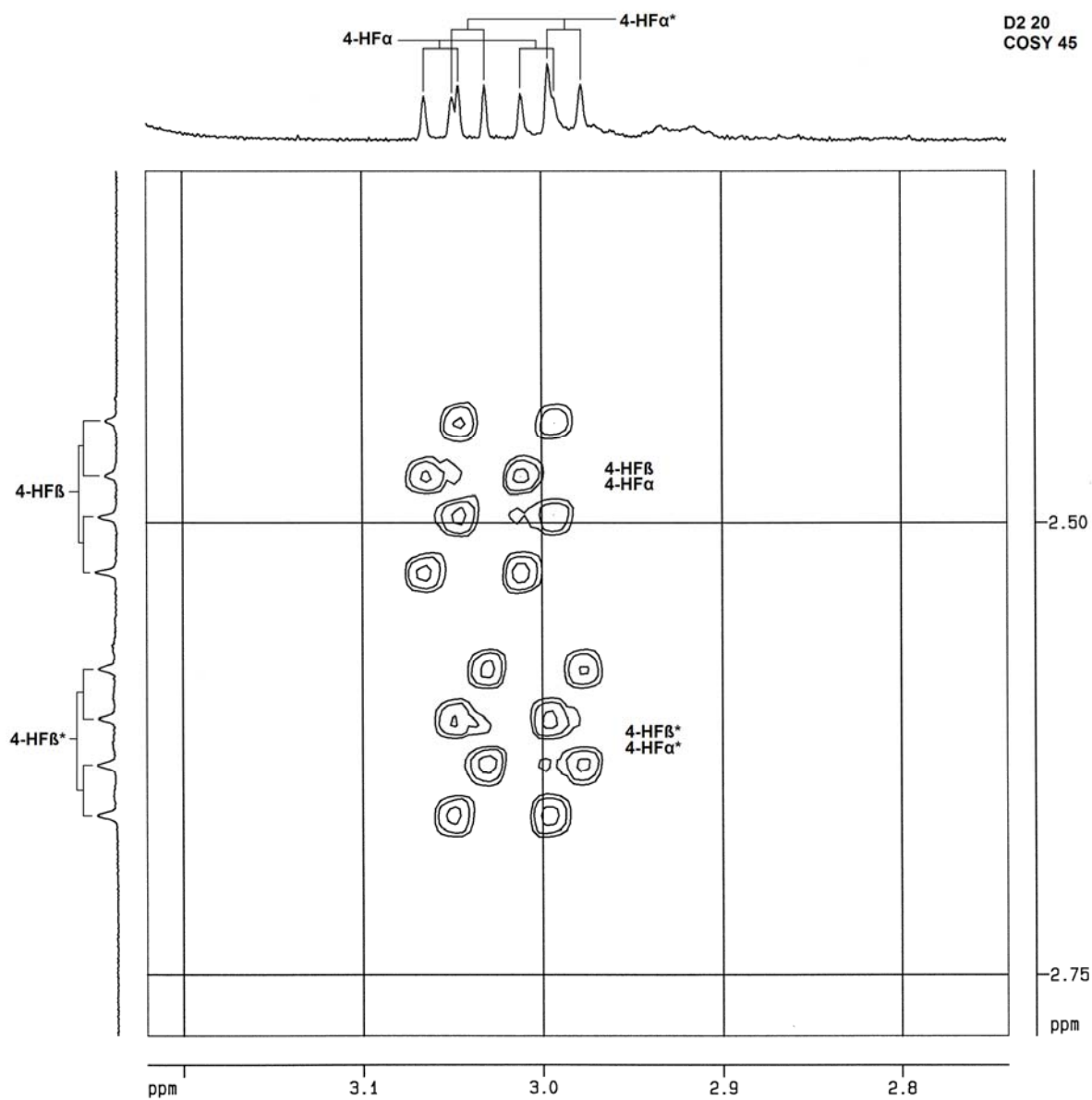


**FIGURE 7.3.3**

These assignments were used to assign the 3-H$_F$ resonances (Figure 7.3.4, D2 21). The 2-H$_F$* resonance was assigned by the appearance of cross peaks with the 4-H$_{F\beta}$* resonances. Half the responses are missing and the lean of the cross peaks confirms the magnitude and positive sign of the $^4J_{4HF,2HF}$ coupling constant.
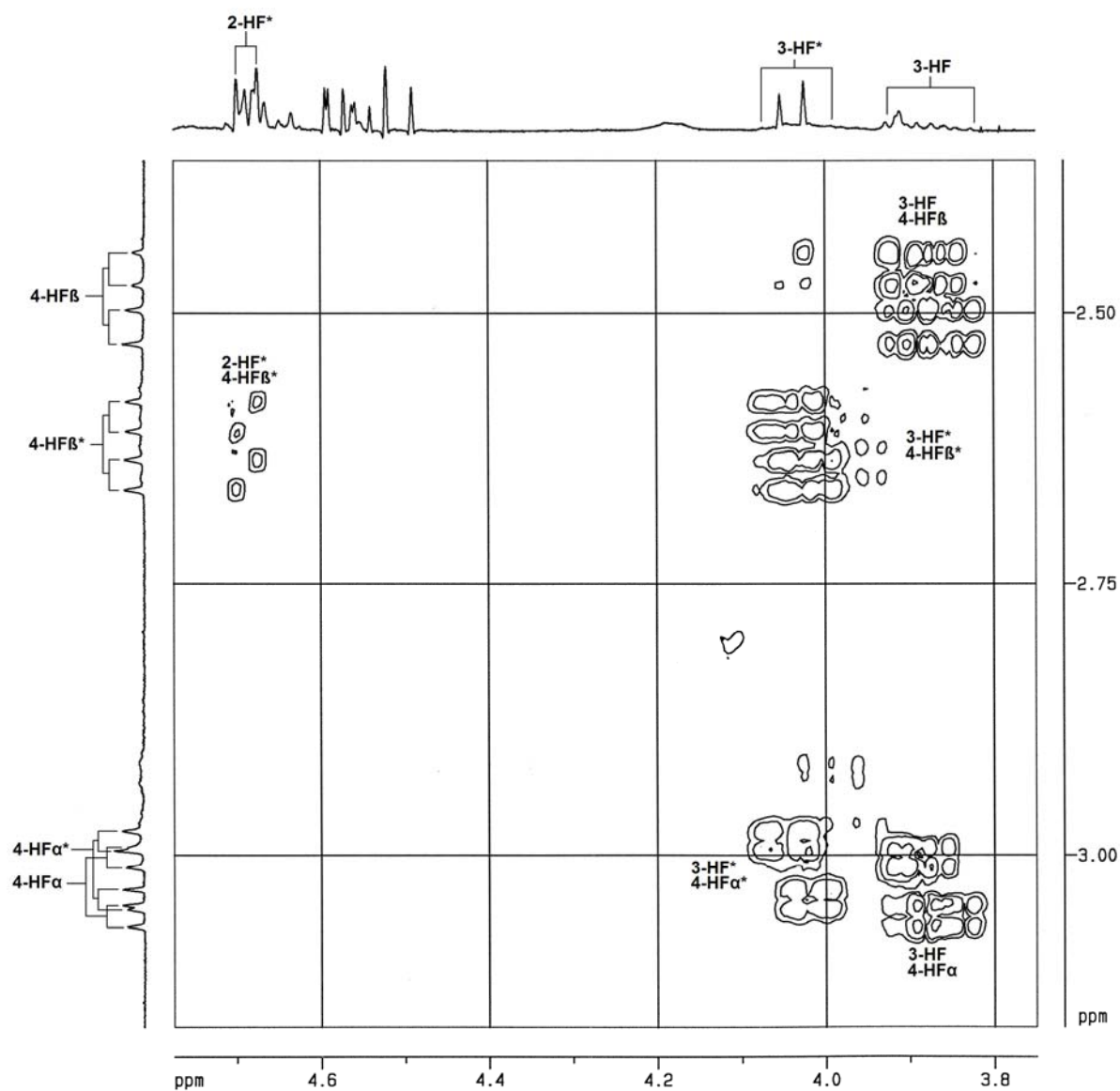


**FIGURE 7.3.4**

Both 6-H$_D$ resonances were assigned by the cross peaks with the respective 4-H$_F$ resonances (Figure 7.3.5, D2 31). Strong coupling between 4-H$_F$ and 6-H$_D$ implies that the 4-H$_F$→4C$_4$ bond is at an approximately 90$^o$ angle with respect to the plane of the D-ring. Because of the apparent similarity in intensity between the cross peaks of both sets of 4-H$_{F\alpha}$ and 4-H$_{F\beta}$ resonances with the respective 6-H$_D$ resonances, it can be interpreted that the F-ring of both conformers undergoes conformational exchange, with both the 4-H$_{F\alpha}$→4-C$_4$ and 4-H$_{F\beta}$→4-C$_4$ bonds forming approximately 90$^o$ angles with the 6-H$_D$→6-C$_D$ bonds and therefore also with respect to the planes of the D-rings, respectively.
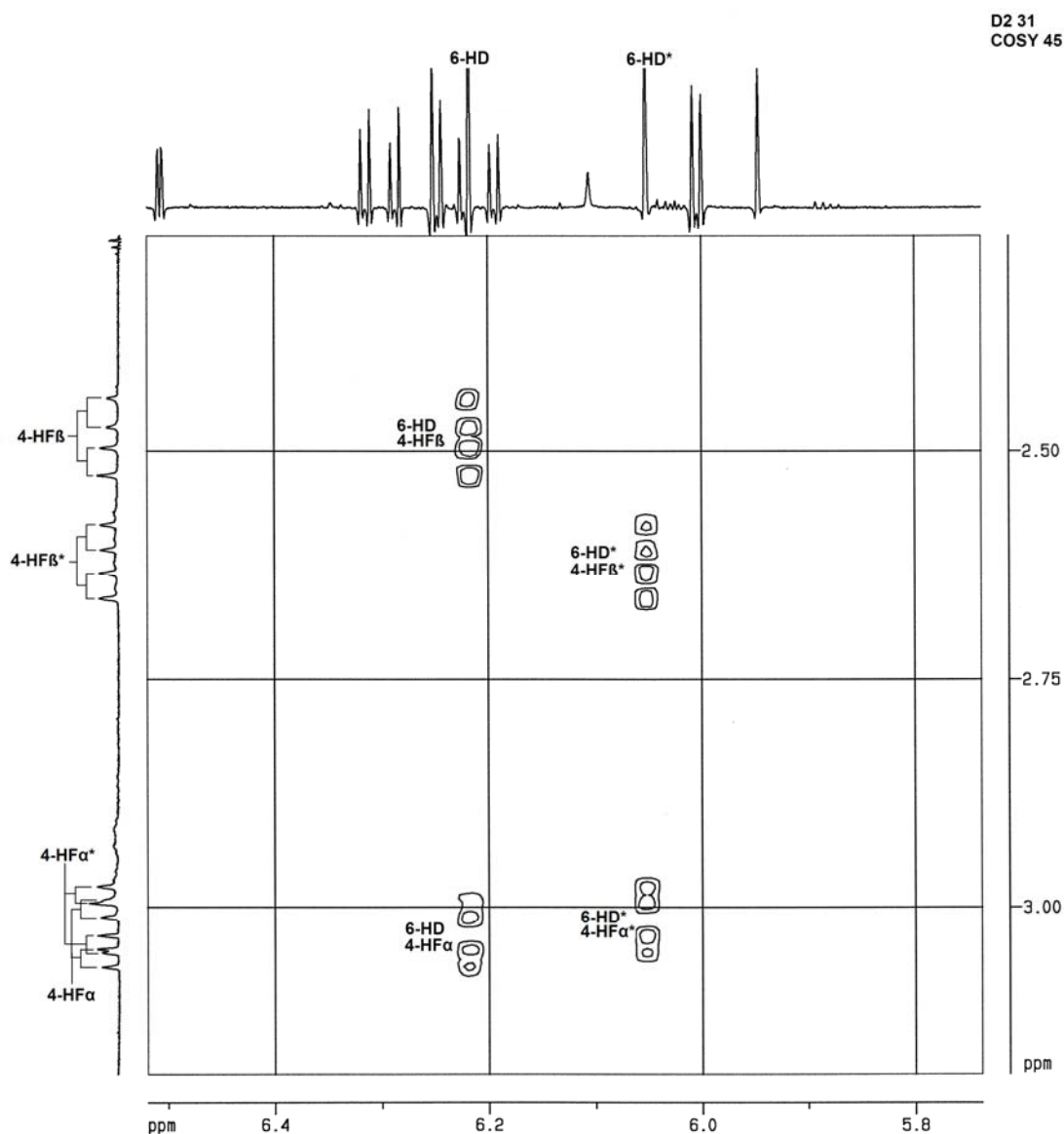


**FIGURE 7.3.5**

The 3-HF resonances were used to assign the 2-H$_F$ resonances (Figure 7.3.6, D2 22). This also confirmed the assignment of 2-H$_F$* (Figure 7.3.4, D2 21).
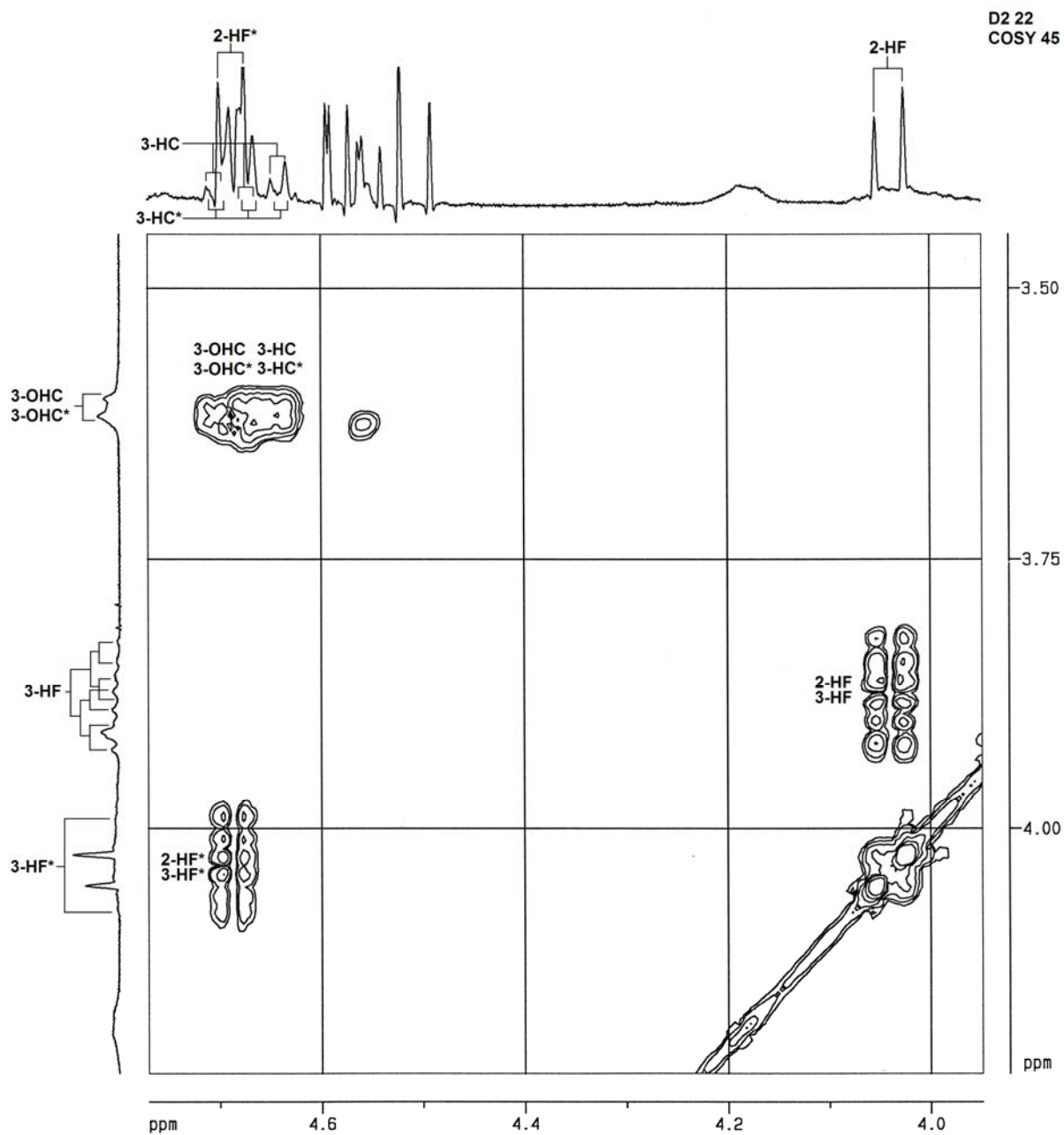


**FIGURE 7.3.6**

The 4-H$_C$ resonances were assigned by their cross peaks with the respective 6-H$_D$ resonances (Figure 7.3.7, D2 27). Strong coupling between 4-H$_C$ and 6-H$_D$ implies that the 4-H$_C$→4C$_C$ bonds are both at approximately 90$^o$ angles with the 6-H$_D$→6-C$_D$ bonds and therefore also with respect to the planes of the respective D-rings.
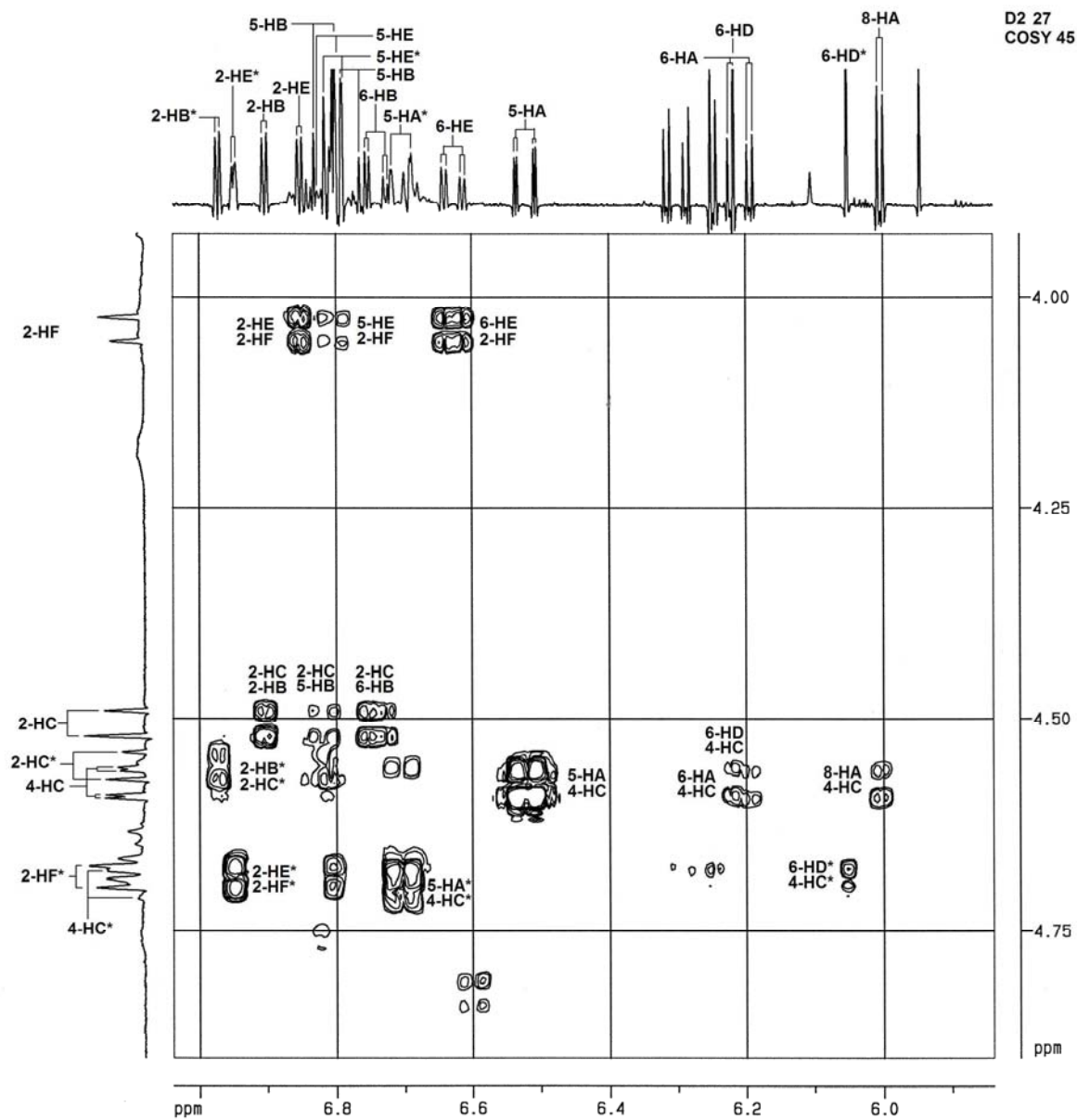


**FIGURE 7.3.7**

The resonances of both sets of C-ring protons are all in the 4.4 - 4.8 ppm region (Figure 7.3.8, D2 23) Unambiguous assignments of the 2-H$_C$* and 3-H$_C$* resonances were not possible due to their proximity to the diagonal, as well as overlap with the C-ring cross peaks. Both 3-H$_C$ resonances were confirmed by their cross peaks with the 3-OH$_C$ resonances (Figure 7.3.6, D2 22). The assignments of the 3-H$_C$ resonances are, however, not unambiguous as illustrated in the HMQC experiment (Figure 7.3.17, D2 60)
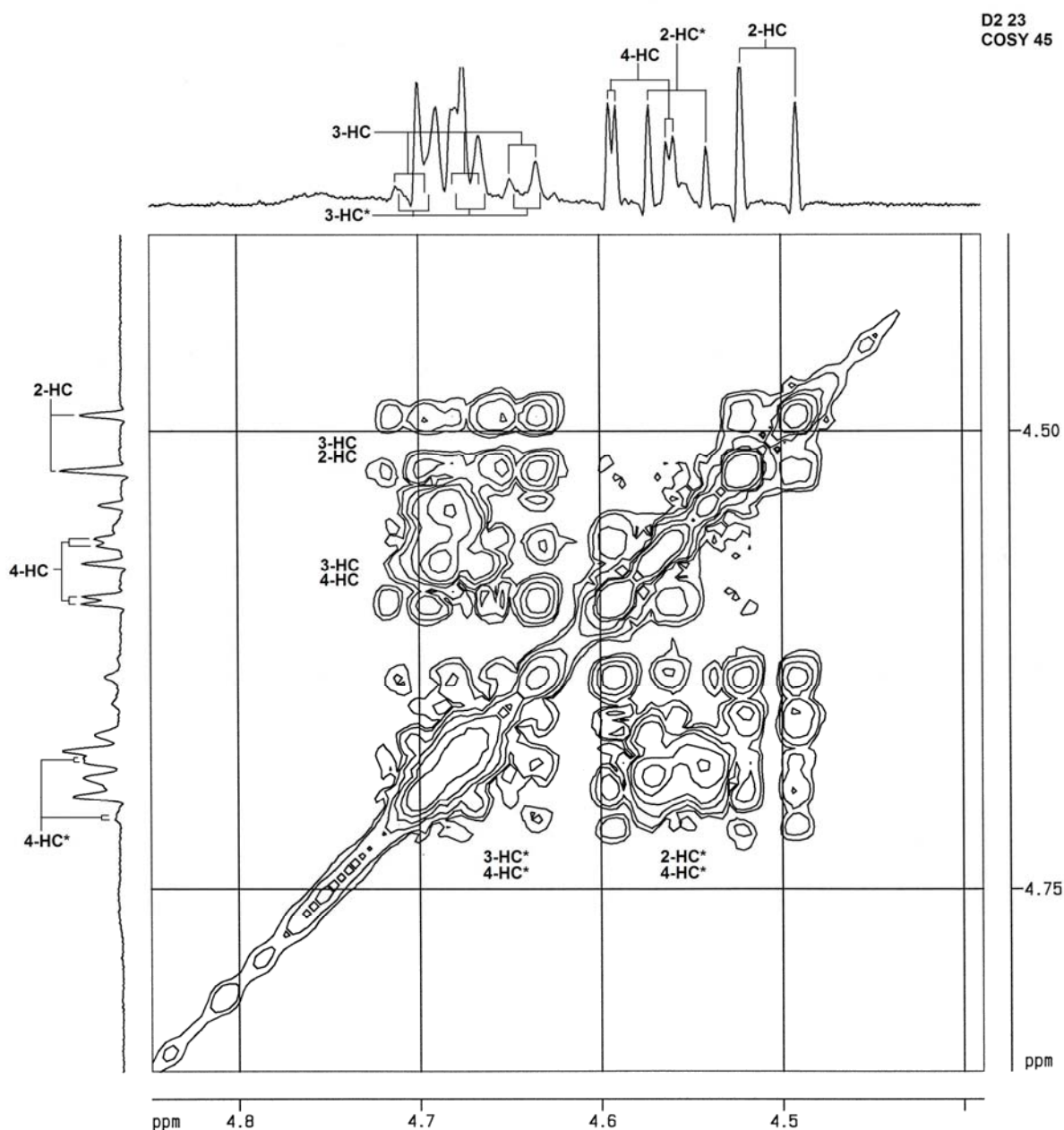


**FIGURE 7.3.8**

The resonances of the majority of aromatic protons were assigned from their cross peaks with heterocyclic protons (Figure 7.3.7, D2 27). These assignments were then used to assign the resonances of the rest of the aromatic protons (Figures 7.3.9/10, D2 33/24).
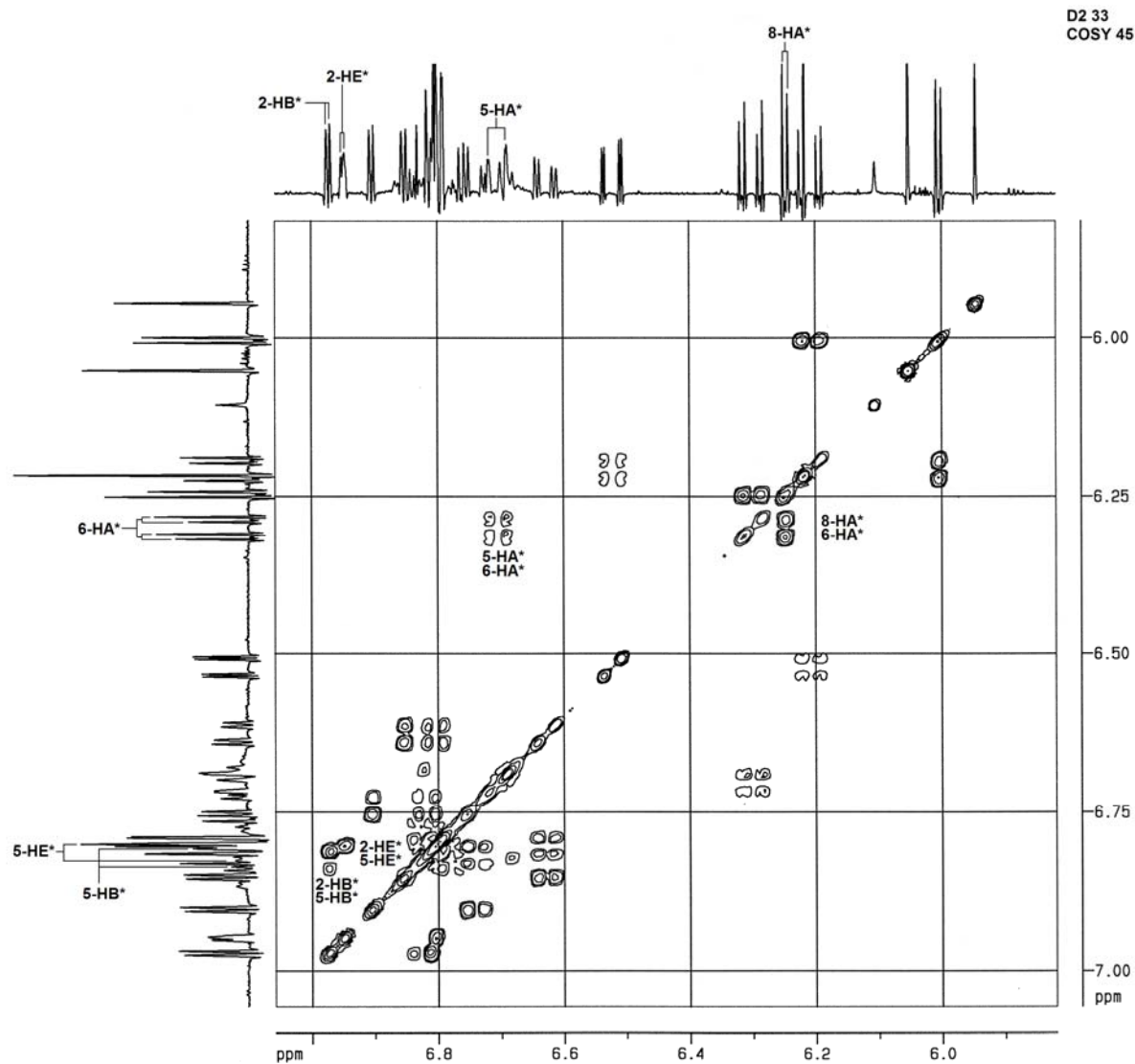


**FIGURE 7.3.9**

Unambiguous assignment of the 5-H$_E$* resonance was not possible due to its proximity to the 5-H$_E$ resonance and to the diagonal ((Figure 7.3.10, D2 24).

Due to the pronounced skewness of the 6-H$_E$* resonance, the responses of its cross peaks with other proton resonances do not have they same intensities, and are missing on the depth of the plots of the COSY 45 experiment (Figures 7.3.9/10, D2 33/24).



**FIGURE 7.3.10**

168
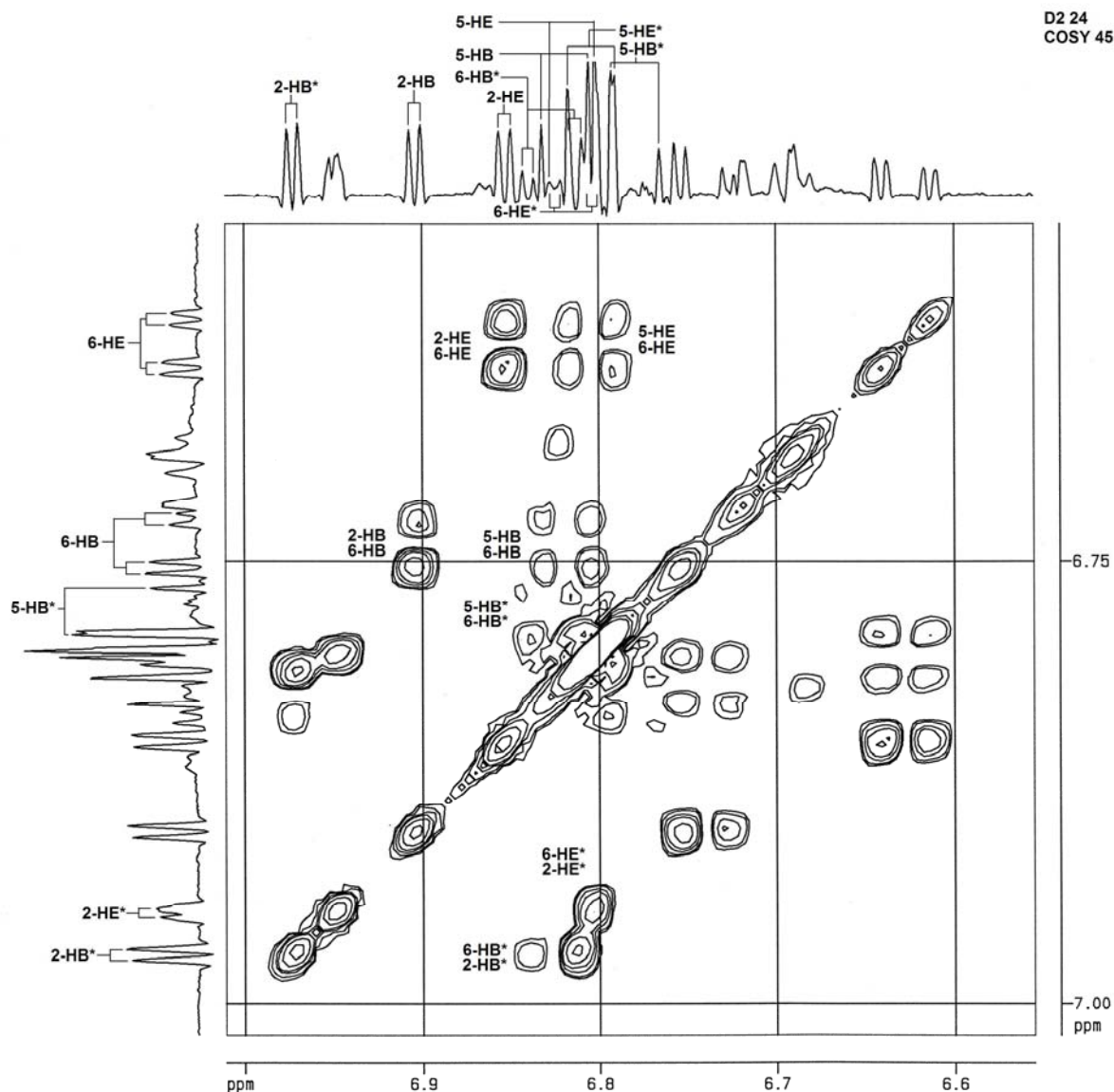
The NOESY PH experiment facilitated ambiguous assignments of the 7-OH$_D$ and 5-OH$_D$ resonances as a result of apparently equally strong cross peaks with the respective 6-H$_D$ resonances (Figure 7.3.11, D2 40).
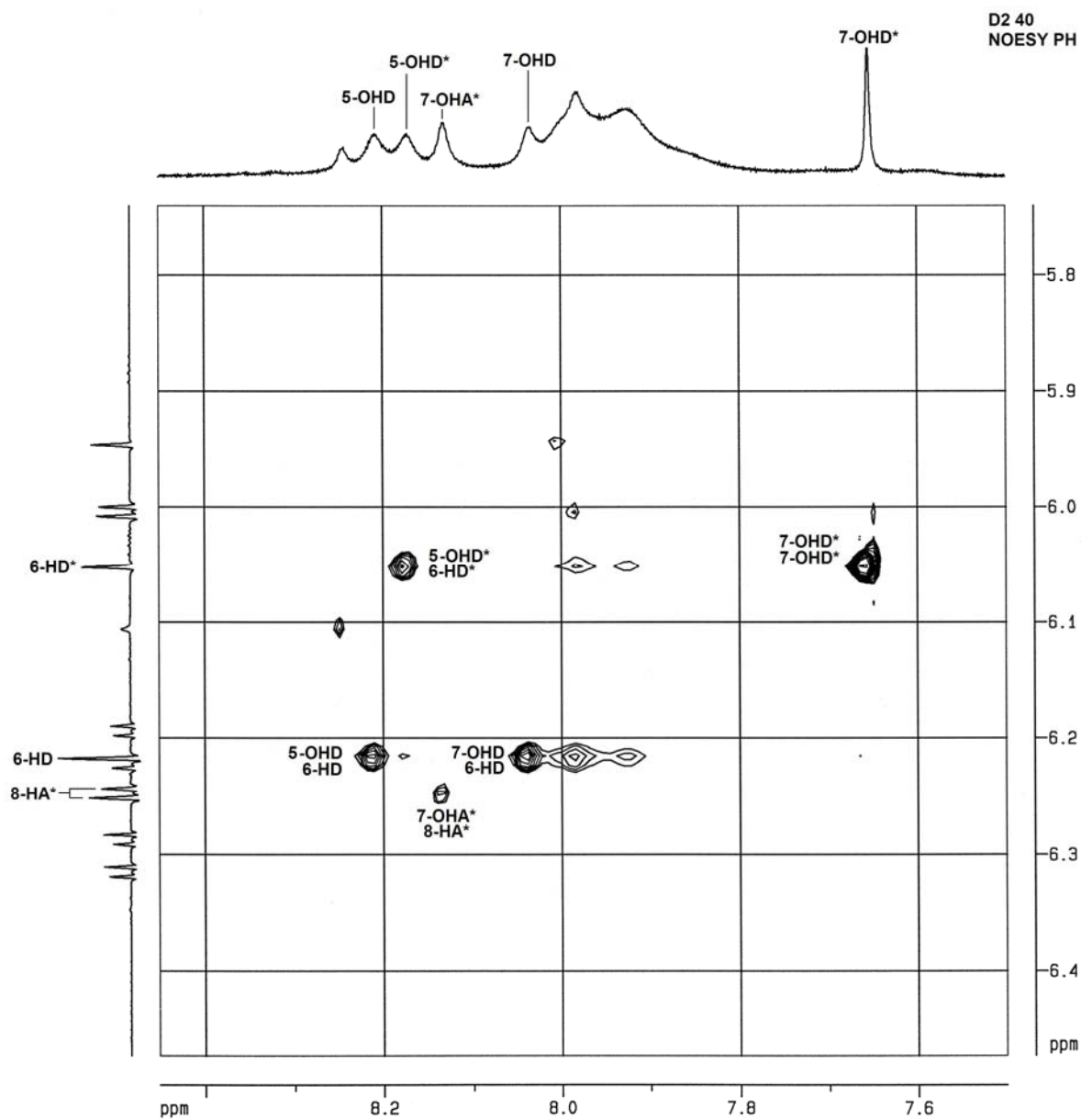


**FIGURE 7.3.11**

The COSY 45 experiment afforded unambiguous assignments due to stronger cross peaks between the 7-OH$_D$/6-H$_D$ resonances than between the 5-OH$_D$/6-H$_D$ resonances (Figure 7.3.12, D2 29).
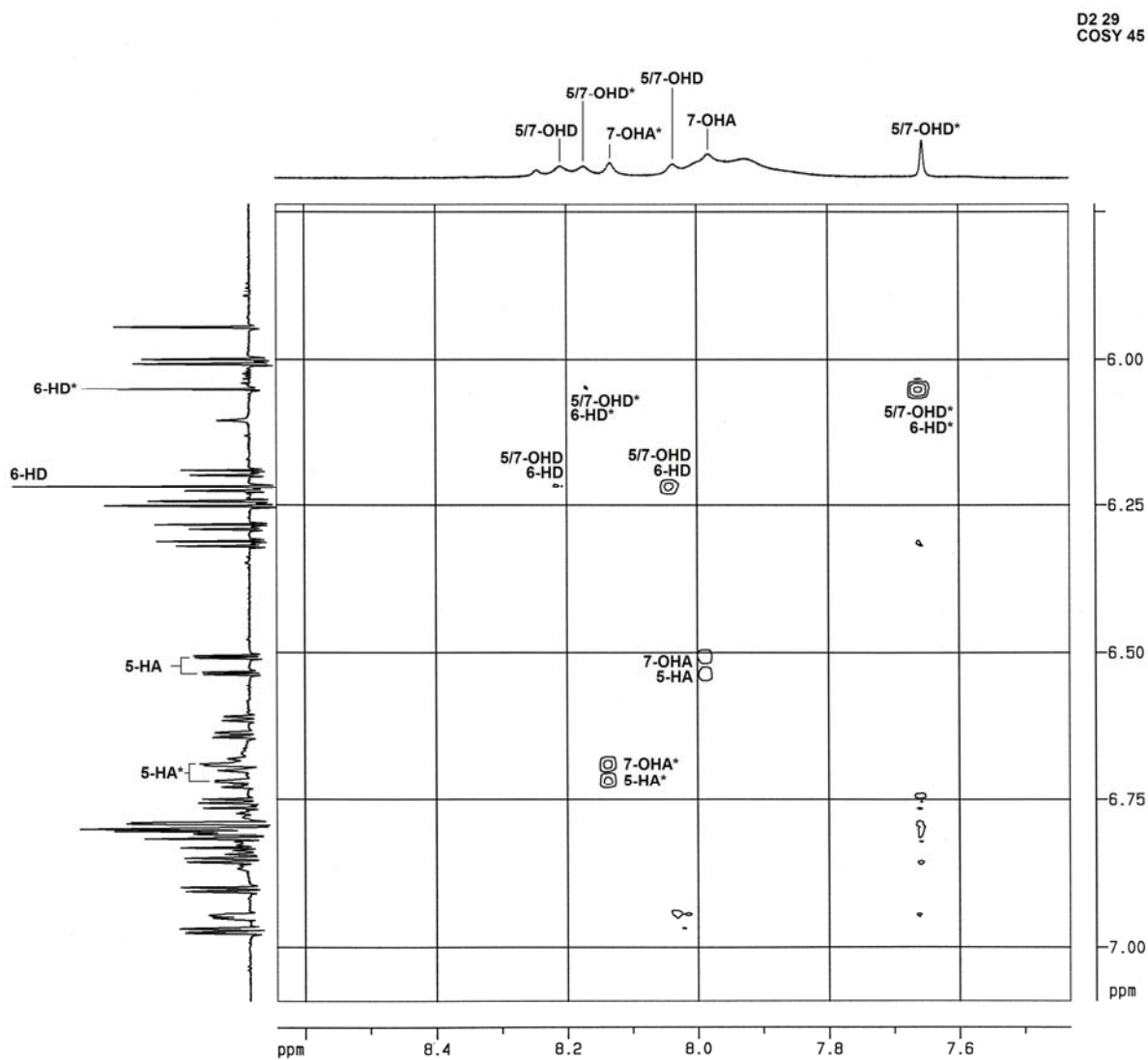


**FIGURE 7.3.12**

The extended *-rotamer was identified by cross peaks between the 3-H$_C^*$ and 7-OH$_D^*$ resonances. Cross peaks between the 4-H$_C$ and 7-OH$_D$ resonances identified the compact rotamer (Figure 7.3.13, D2 37). This assignment was further confirmed by the lower chemical shifts of the E- and B-ring resonances relative to those of the E*- and B*-rings.
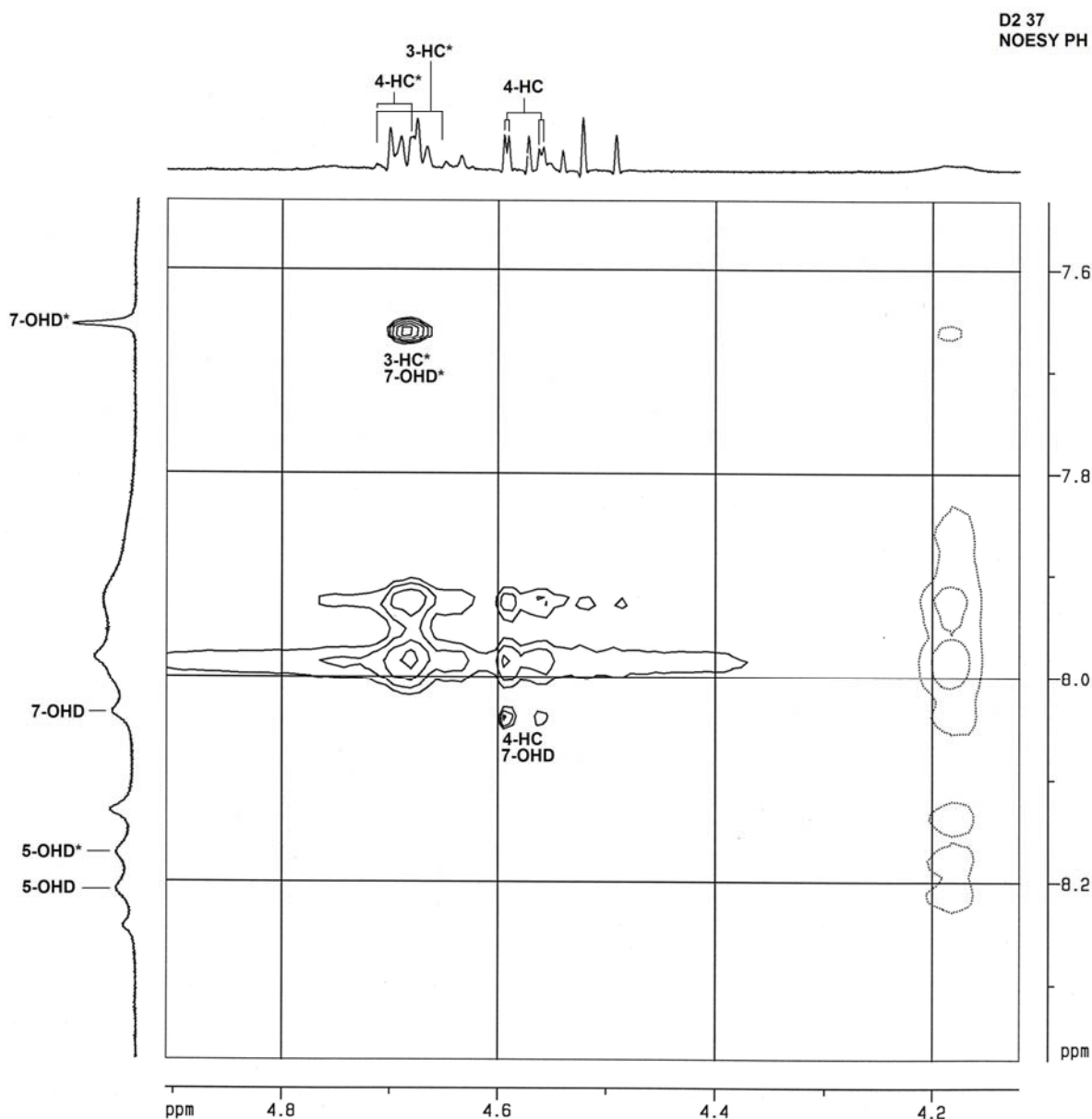


**FIGURE 7.3.13**

If Figure 7.3.13 is compared to the equivalent spectrum of fisetinidol (4α→8)-catechin (Figure

6.1.16, L3 39), a similar overlap of the 3-H$_C$* and 4-H$_C$* resonances is observed. The 3-H$_C$ resonances of fisetinidol (4α→8)-catechin, however does not overlap with the 3-H$_C$* and 4-H$_C$* resonances, rendering the assignment of the two rotamers easier in that case.

The cross peaks between the 4-H$_C$ and 7-OH$_D$ resonances of the compact rotamer on the NOESY PH spectrum are weaker than the cross peaks identifying the extended *-rotamer. The distance between 4-H$_C$ proton and 7-OH$_D$ is therefore larger than the distance between 3-H$_C$* and 7-OH$_D$*.

The magnitude of the coupling constants of both the C-rings indicates almost exclusive contributions of E-conformers (Table 7.3.3).

| COUPLING CONSTANT | ROTAMER | MAGNITUDE (Hz) |
|---|---|---|
| $^3J_{2-HC,3-HC}$ | compact | 9.0 |
| | extended (*) | 9.5 |
| $^3J_{3-HC,3-OHC}$ | both | 5.0 |
| $^3J_{3-HC,4-HC}$ | compact | 9.2 |
| | extended (*) | 9.0 |
| $^3J_{4-HC,5-HA}$ | compact | 1.0 |
| | extended (*) | 0.8 |

**TABLE 7.3.3**

The line shapes of the 3-H$_F$ resonance are broad and undefined, partially due to coupling with 3-OH$_F$ resonances, thus facilitating comparison with published line shapes.[97] The coupling constants were determined from the 2-H$_F$ and 4-H$_F$ resonances (Table 7.3.4).

| COUPLING CONSTANT | ROTAMER | MAGNITUDE (Hz) |
|---|---|---|
| $^3J_{2-HF,3-HF}$ | compact | 8.5 |
| | extended (*) | 7.5 |
| $^3J_{3-HF,4HF\beta}$ | compact | 9.5 |
| | extended (*) | 8.2 |
| $^3J_{3-HF,4HF\alpha}$ | compact | 5.8 |
| | extended (*) | 5.5 |
| $^3J_{3-HF\alpha,4HF\beta}$ | both | 16.0 |

**TABLE 7.3.4**

An HMQC experiment was done to assign some of the carbon resonances (Figures 7.3.15-

18, Appendix B). Both the HMQC and the $^{13}$C NMR spectra (Figure 7.3.14, D2 43) display very small chemical shift differences between the carbon resonances of the two rotamers. Thus, it was difficult to distinguish between the assignments of the two rotamers.
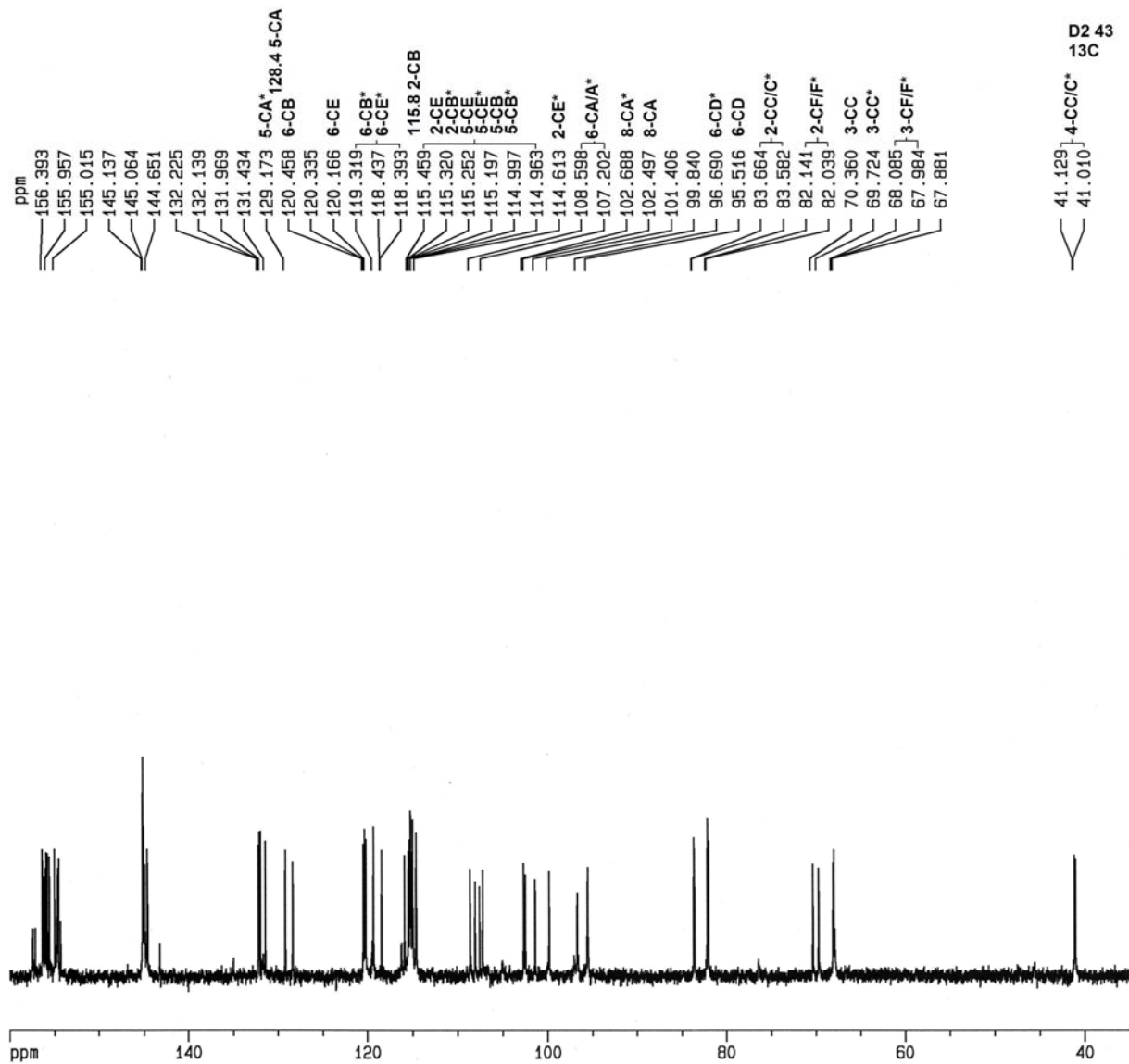


**FIGURE 7.3.14**

**FIGURE 7.3.15**

174
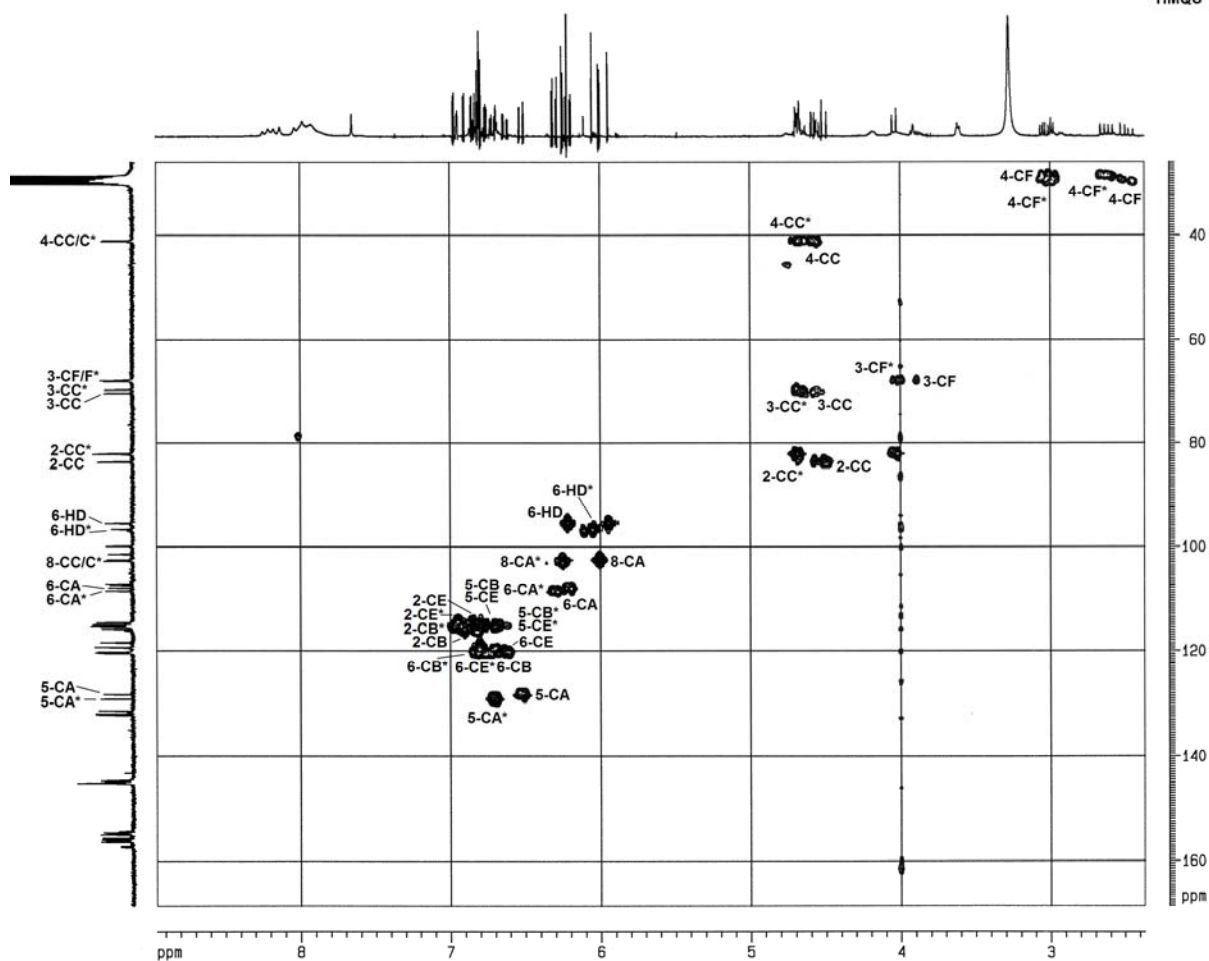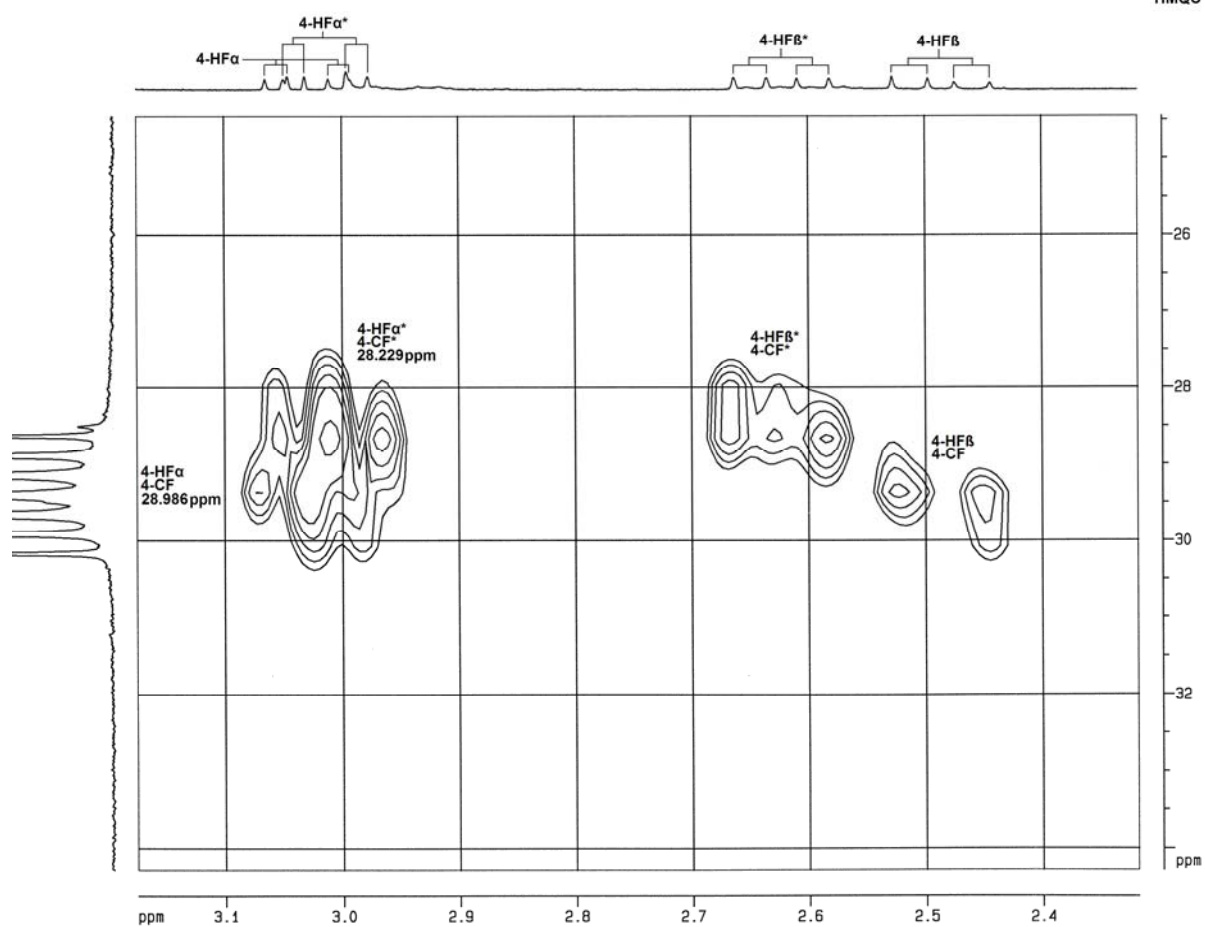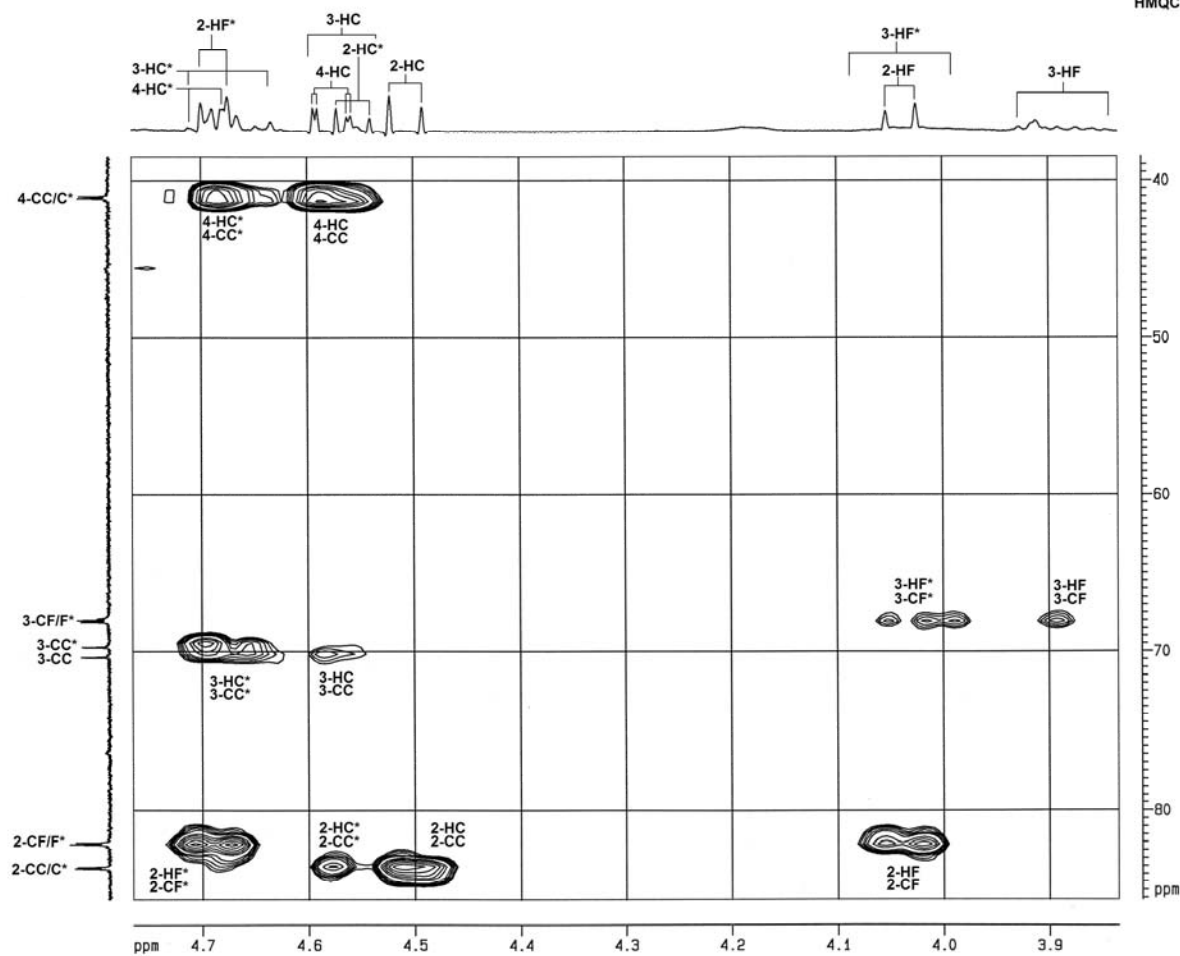
**FIGURE 7.3.16**

**FIGURE 7.3.17**
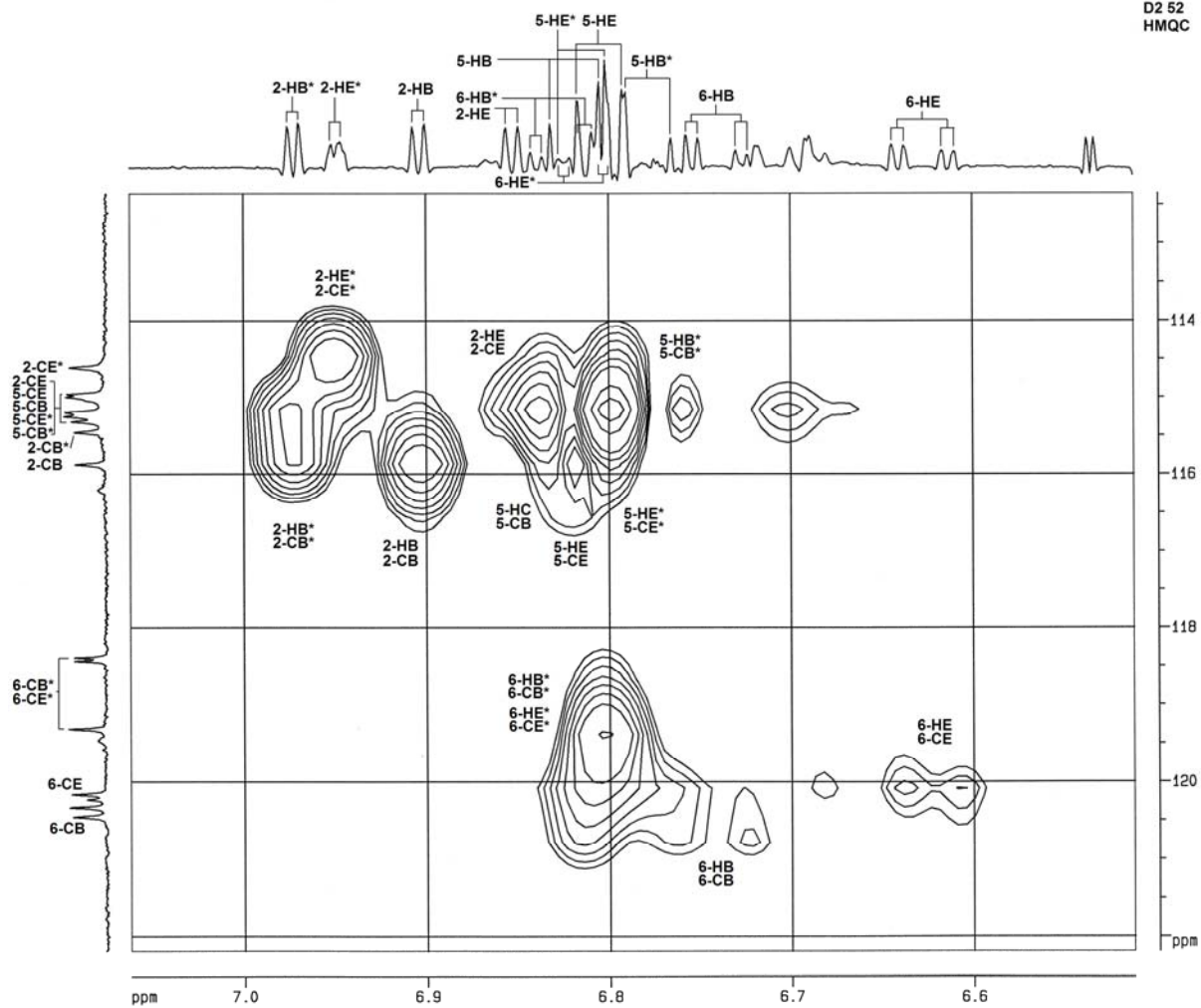
**FIGURE 7.3.18**

# CHAPTER 8

## The Circular Dichroism

## of Profisetinidin Dimers and Trimers in Methanol.

CD spectra were recorded in methanol. As the solvent was not extensively dried, it can be assumed that water was present in each sample, and that it would influence the conformations of the heterocyclic rings, especially the C-rings.

The C-rings of the dimers that display rotamers at ambient temperatures in acetone all have preferred E-conformations in the presence and/or absence of water according to the C-ring coupling constants observed in NMR experiments ($^3J_{2-HC,3-HC} \approx {}^3J_{3-HC,4-HC} \approx$ 9-10 Hz) (Appendix A).

There are two exceptions:

a) The fisetinidol-($4\alpha\rightarrow8$)-catechin dimer displays A-E interchange of the C-rings of both rotamers in the absence of water ($^3J_{2-HC,3-HC.}$ = 6.5 and $^3J_{3-HC,4-HC}$ 8.5)

b) The extended conformation of the fisetinidol-($4\alpha\rightarrow6$)-catechin dimer in the presence of water displays A-E conformational exchange of the C-ring ($^3J_{2-HC,3-HC.}$ = 6.2 and $^3J_{3-HC,4-HC}$ 6.2)

Compounds that don't display two distinct rotamers, have C-ring coupling constants in the order of $^3J_{2-HC,3-HC} \approx {}^3J_{3-HC,4-HC} \approx$ 2-3 Hz, which could be attributed to the predominant contribution of A conformers. $^3J_{2-HC,3-HC} \approx$ 2-3 Hz, but normally $^3J_{3-HC,4-HC}$ should be larger than 2-3 Hz, due to a larger 3-HC/4-HC dihedral angle. The only way in which the magnitude of both these coupling constants could have such small values is if all three hydrogen atoms were quasi-equatorial. This can be achieved if the C-ring assumes a boat or skewed boat conformation.

The F-rings all displayed E-A conformational exchange, with the E-conformer making a larger contribution according to the magnitude of the F-ring coupling constants. Line shape analysis (Figure 5.2.3), however, suggests skewed boat conformation.[97]

The trimers displayed C- and I-ring coupling constants that were of the same magnitude as those observed for each dimer having similar interflavanyl linkages as the trimer, e.g. the fisetinidol-(4α→8)-catechin-(6→4β)-fisetinidol trimer displayed the same C-ring coupling constants than the fisetinidol-(4α→8)-catechin dimer (similar to the C-ring of the trimer) and the fisetinidol-(4β→6)-catechin dimer (similar to the I-ring of the trimer).

The following factors should be taken into account when analyzing the CD spectra of dimers and trimers:

a)      The conformations of both the C- and F-rings in methanol might be different to those observed with NMR spectroscopy in acetone-$d_6$ as a result of differing degrees of intra- and inter-molecular hydrogen bonding.

b)      In comparison to the flavan-3-ols and 4-arylflavan-3-ols, there are a number of extra chromophores present that could influence the sign, amplitude and number of CE's of the dimers and trimers. A dimer has an extra flavan-3-ol unit, and a trimer has two separate C-4 substituents on two different flavan-3-ol units.

c)      Where a compound has 2 or more rotamers, each will also have a different CD-spectrum.

CD spectra were divided into 20 nm segments in order to better compare and identify Cotton effects. The spectra of dimers that exist as two separate rotamers (Table 8.1) as well as those that do not display rotamers on an NMR time-scale (Table 8.2), were compared with each other.

The CD curves of the free phenolic 4-arylflavan-3-ols are completely dominated by high amplitude CE's of the aryl chromophore at 220-240 nm. In contrast, all the dimers in this study have CD curves where two higher wavelength CE's at 269 - 278 nm and 290 – 300 nm have magnitudes that are larger than or equal to CE's at lower wavelengths.

The two fisetinidol-(4α→6 or 8)-catechin dimers that display rotamers at ambient termperatures have CD spectra with much less detail than the other compounds, possibly due to the opposing effects of the two rotamers on the circular dichroic effect.

| Fisetinidol-(4α→8)-catechin | | | | | *Ent*-fisetinidol (4β→8) catechin | | | | |
|---|---|---|---|---|---|---|---|---|---|
| **Conformation:** | **C-ring** | **E** | **F-ring** | **E-A** | **Conformation:** | **C-ring** | **E** | **F-ring** | **E-A** |
| **Configuration:** | **Upper Unit:** | | *2R,3S,4S* | | **Configuration:** | **Upper Unit** | | *2S,3R,4R* | |
| | **Lower Unit:** | | *2R,3S* | | | **Lower Unit** | | *2R,3S* | |

| Fisetinidol-(4α→6)-catechin | | | | | *Ent*-fisetinidol (4β→6) catechin | | | | |
|---|---|---|---|---|---|---|---|---|---|
| **Conformation:** | **C-ring** | **E** | **F-ring** | **E-A** | **Conformation:** | **C-ring** | **E** | **F-ring** | **E-A** |
| **Configuration:** | **Upper Unit:** | | *2R,3S,4S* | | **Configuration:** | **Upper Unit** | | *2S,3R,4R* | |
| | **Lower Unit:** | | *2R,3S* | | | **Lower Unit** | | *2R,3S* | |

TABLE 8.1

180

| Fisetinidol-(4β→8)-catechin | | | | | *Ent*-fisetinidol (4α→8) catechin | | | | |
|---|---|---|---|---|---|---|---|---|---|
| Conformation: | C-ring | A | F-ring | E-A | Conformation: | C-ring | A | F-ring | E-A |
| Configuration: | Upper Unit: | | *2R,3S,4R* | | Configuration: | Upper Unit | | *2S,3R,4S* | |
| | Lower Unit: | | *2R,3S* | | | Lower Unit | | *2R,3S* | |



| Fisetinidol-(4β→6)-catechin | | | | |
|---|---|---|---|---|
| Conformation: | C-ring | A | F-ring | E-A |
| Configuration: | Upper Unit: | | *2R,3S,4R* | |
| | Lower Unit: | | *2R,3S* | |
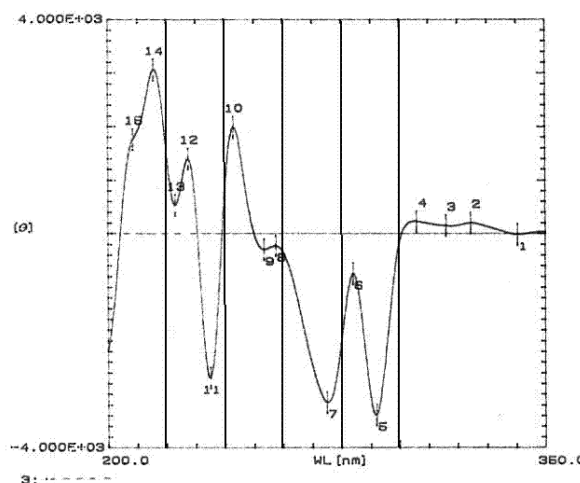
TABLE 8.2

As in the case of the 2,3-*trans*-flavan-3-ols and 2,3-*trans*-4-arylflavan-3-ols,[85,86] a negative CE at 292 – 304 nm confirmed the *2R*-configuration of the upper units of fisetinidol-(4α→8)-catechin, fisetinidol-(4ß→8)-catechin, fisetinidol-(4α→6)-catechin and fisetinidol-(4ß→6)-catechin. A positive CE at 289 – 302 nm confirmed the *2S*-configuration of the upper units of the *ent*-fisetinidol-(4α→8)-catechin, *ent*-fisetinidol-(4ß→8)-catechin and *ent*-fisetinidol-(4ß→6)-catechin (Table 8.2). The presence of a *2R*-configuration in the lower catechin unit of the *ent*-fisetinidol-catechin dimers did not seem to have any effect on the sign or the amplitude of the CE.

CE's at 230 - 240 nm completely dominated the CD spectra of the 4-arylflavan-3-ols.[85,86] Previous investigators ascribed a negative CE at that wavelength to be indicative of a 4α substituent and a positive CE of a 4β substituent. The CE's at 230-240 nm of the permethyl ether acetates of 4-arylflavan-3-ols as well as two of the free phenolic 4-arylflavan-3-ols were inconsistent with these observations and described as having abnormal CE's.[19,85,86]

The CE's of compounds with *2R,3S* configuration (Table 8.8) and those with *2S,3R* configuration of the upper units (Table 8.9) were compared with respect to the three major CE's observed at λ ≈ 240, 270 ,290 nm.

The signs of the CE's at λ ≈ 240 were not consistent with the orientations of the C-4 substituents of these compounds. The magnitudes of these CE's were also not as large as those observed for the free phenolic 4-arylflavan-3-ols.

The signs of the CE's at λ ≈ 290 nm were consistent with the configuration at C-2, namely negative for *2R* and positive for *2S.* The positive CE of the *2S* configuration of the ent-fisetinidol (upper) unit of the Quebracho dimers dominated any possible negative CE contribution by the *2R* configuration of the (lower) catechin unit.

The CE's at λ ≈ 270 nm were the only CE's that showed correlations between the configuration of the 4-C substituents namely a positive CE for a C-4α substituent and a negative CE for a C-4ß substituents.

A positive CE at λ ≈ 270 nm was indicative of a 4α substituent and a negative CE of 4β substituent for all the 4-arylflavan-3-ols[85,86] as well as all the dimers in this study. The 4α-arylflavan-4-ols had positive CE's at λ ≈ 270 nm with magnitudes ranging between 558 and 12050 θ. The 4ß arylflavan-3-ols had negative CE's at λ ≈ 270 nm with magnitudes ≈ 5000 θ. The large range in magnitude of the positive CE's at λ ≈ 270 nm displayed by the 4α-arylflavan-4-ols could be the reason that this correlation was not noticed in initial studies.

The occurrence of hydrogen bonding between $OH_D$ protons and either pyran ring oxygen atoms or other hydroxy groups, results in the appearance of sharp, pronounced peaks in the NMR spectrum due to very slow or no exchange of these hydrogen atoms. This is especially true of the resonances of the 7-$OH_D$* protons (extended conformers) that form hydrogen bonds with the pyran oxygen atoms of the C*-rings.

The signs of the CE's at λ ≈ 270 nm of the fisetinidol-(4→8)-catechin-(6→4)-fisetinidol trimers were compatible with the orientation of the fisetinidol-(4→8)-catechin bond. The two trimers with fisetinidol-(4α→8)-catechin (upper) units display positive CE's and the two trimers with fisetinidol-(4β→8)-catechin (upper) units display negative CE's. The CE of a catechin (6→4)-fisetinidol moiety was dominated by the CE of the fisetinidol-(4→8)-catechin unit in the same trimer. A slightly smaller CE was observed in the case of trimers with 4→8 bonds that have CE's with opposite signs to the CE's of the 6→4 bonds. In each case, the observed CE had the same sign as the CE of the 4→8 bond.
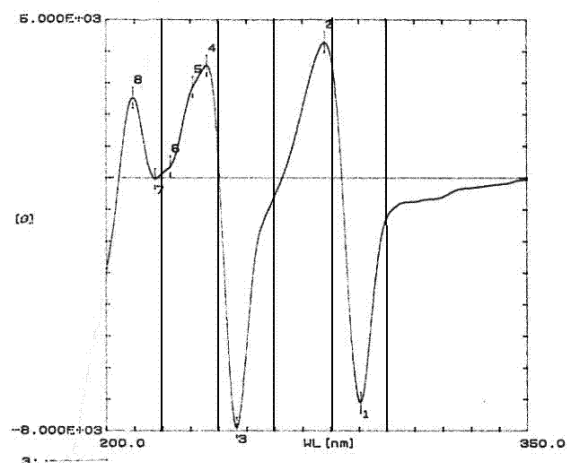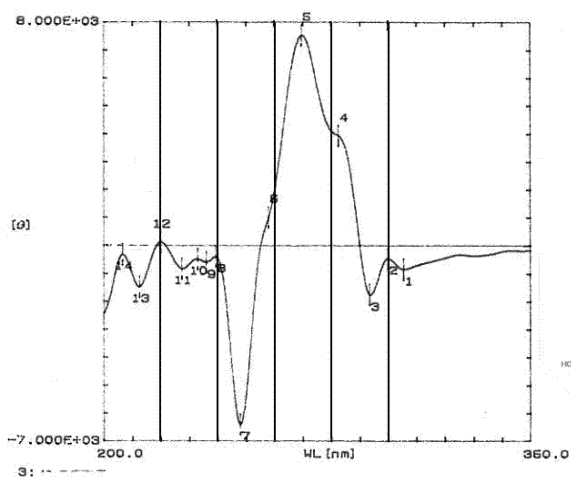


*Bis*-Fisetinidol-(4α→8),(4α→6)-catechin
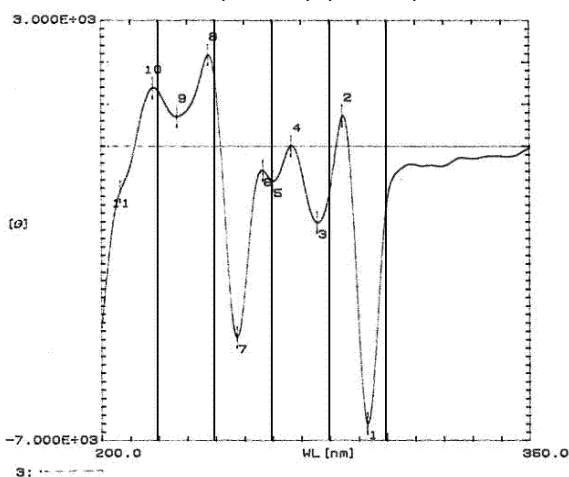


*Bis*-Fisetinidol-(4α→8),(4β→6)-catechin
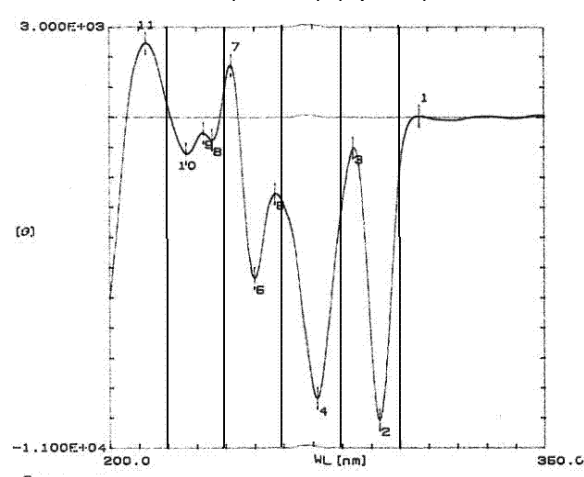


*Bis*-Fisetinidol-(4β→8),(4α→6)-catechin



*Bis*-Fisetinidol-(4β→8),(4β→6)-catechin

TABLE 8.3

A visual inspection of the CD spectrum of each trimer compared to the CD spectra of the two dimers having similar interflavanyl linkages as the trimer, confirmed that the CE's of the fisetinidol-(4→8)-catechin moiety dominate those of the fisetinidol-(4→6)-catechin units in the CD spectra of the trimers (Tables 8.4 – 7).

Fisetinidol-(4α→8)-catechin-(6→4α)-fisetinidol



Fisetinidol-(4α→8)-catechin



Fisetinidol-(4α→6)-catechin

TABLE 8.4

Fisetinidol-(4α→8)-catechin-(6→4β)-fisetinidol



Fisetinidol-(4α→8)-catechin



Fisetinidol-(4β→6)-catechin

TABLE 8.5

Fisetinidol-(4β→8)-catechin-(6→4α)-fisetinidol



Fisetinidol-(4β→8)-catechin



Fisetinidol-(4α→6)-catechin

TABLE 8.6

Fisetinidol-(4α→8)-catechin-(6→4β)-fisetinidol



Fisetinidol-(4β→8)-catechin



Fisetinidol-(4β→6)-catechin

TABLE 8.7

187

The quadrant rule was applied in an attempt to rationalise the signs of the CE's of all these compounds at $\lambda \approx 270$ nm in order to give an indication of the conformations of the heterocyclic rings and the interflavanyl bonds. Correlations between the results obtained from the CD experiments were then compared with the results of the NMR experiments (Table 8.10, Appendix A). Although there are some correlations, they are ambiguous due to the following factors:

a) In some cases the C-rings must assume almost impossible conformations with very high angle torsion in order to satisfy the application of the quadrant rule e.g. the compact rotamers of fisetinidol-(4α→8)-catechin and *ent*-fisetinidol-(4ß→8)-catechin.

b) It has already been shown that the C-rings can assume different conformations, and that they can have large effects on the sign and amplitude of the resulting CE's. This implies that a CD spectrum could be the summation of a number of different CE's from the different conformations.

c) The large number of positive and negative inflections as well as CD couplets observed in the CD spectra of all the compounds cannot be rationalised by the empirical aromatic quadrant rule.

d) The lack of definition or appearance of a similar number of CE's when comparing the dimers that display rotamers at ambient temperatures (Table 8.1).

e) The trimers (Table 8.3) each have two fisetinidol moieties with transition moment vectors that can interact in a number of ways with the transition moment vector of the D-ring of the catechin unit.

Theoretical calculations of biflavonoids[106] indicate that the compact and extended conformers indeed display very different CD spectra. When considered in conjunction with the conformational mobility of the C-ring in e.g. fisetinidol-(4α→8)-catechin and fisetinidol-(4α→6)-catechin, it is abundantly evident that the chiroptical characteristics of this class of compounds are too complex to be interpreted in terms of a simple empirical rule. We are in the process of setting up the appropriate infrastructure to theoretically calculate the electronic CD spectra of both the extreme conformers as far as rotation about the interflavanyl bond is concerned, and also take into account the conformational itinerary of the C-ring of biflavanoid-type profisetinidins. Once we begin to understand the chiroptical intricacies at the dimeric level, we may also venture into comprehension of CD characteristics at the trimeric level.

---

106 **Personal Communication Dr D Ferreira**

| Compound | Configuration | Config. | CD | NMR | λ nm | ME (θ) | λ nm | ME (θ) | λ nm | ME (θ) | λ nm | ME (θ) | λ nm | ME (θ) |
|---|---|---|---|---|---|---|---|---|---|---|---|---|---|---|
| | | | | | | | | | | | | | | 2R |
| Fisetinidol-(4α→2)-phloroglucinol | 2,3-trans-3,4-trans | 2,4-cis | | | 237 | -22980 | | | 272 | 8556 | | | 283 | -4491 |
| Fisetinidol-(4α→2)-resorcinol | 2,3-trans-3,4-trans | 2,4-cis | | | 237 | -11390 | | | 276 | 3787 | | | 290 | -2032 |
| Fisetinidol-(4α→8)-catechin | 2,3-trans-3,4-trans 2,3-trans | 2,4-cis | SB* | E E/A | 233 | 2900 | 250 | -810 | 270 | 3748 | | | 304 | -82 |
| Fisetinidol-(4α→6)-catechin | 2,3-trans-3,4-trans 2,3-trans | 2,4-cis | SB | E | 236 | 710 | 249 | -465 | 272 | 4957 | | | 293 | -1146 |
| | | | | | | | | | | | | | | |
| Fisetinidol-(4β→2)-phloroglucinol | 2,3-trans-3,4-cis | 2,4-trans | | | 237 | 12950 | | | 272 | -5981 | | | 290 | -7242 |
| Fisetinidol-(4β→2)-resorcinol | 2,3-trans-3,4-cis | 2,4-trans | | | 238 | 22400 | | | 274 | -4707 | | | 294 | -1499 |
| Fisetinidol-(4β→8)-catechin | 2,3-trans-3,4-cis 2,3-trans | 2,4-trans | SB | A | 236 | 1768 | 248 | -3144 | 271 | -11710 | 282 | 19.3 | 292 | -10990 |
| Fisetinidol-(4β→6)-catechin | 2,3-trans-3,4-ci 2,3-trans s | 2,4-trans | SB | A | 236 243 | -2691 1992 | 253 | -293 | 275 | -3148 | 284 | -743 | 292 | -3384 |
| | | | | | | | | | | | | | | |
| Fisetinidol-(4α→8)-catechin-(6→4α)-fisetinidol | 2,3-trans-3,4-trans 2,3-trans 2,3-trans-3,4-trans | 2,4-cis 2,4-cis | SB | E E | 240 236 | -389p -590v | 248 | -6395 | 270 | 7541 | 283 | 3945 | 294 | -1752 |
| Fisetinidol-(4α→8)-catechin-(6→4β)-catechin | 2,3-trans-3,4-trans 2,3-trans 2,3-trans-3,4-cis | 2,4-cis 2,4-trans | SB | E A | 236 | 3552 | 247 | -7887 | 278 | 42870 | | | 291 | -7093 |
| Fisetinidol-(4β→8)(4α→6)-catechin | 2,3-trans-3,4-cis 2,3-trans 2,3-trans-3,4-trans | 2,4-trans 2,4-cis | SB | A E | 238 | 2179 | 247 | -4545 | 275 | -1816 | 284 | 725 | 293 | -6585 |
| Fisetinidol-(4β→8)(4β→6)-catechin | 2,3-trans-3,4-cis 2,3-trans 2,3-trans-3,4-cis | 2,4-trans 2,4-trans | SB | A A | 236 | -757 | 242 | 1731 | 272 | -9382 | 284 | -1022 p | 293 | -10060 |

TABLE 8.8 (* SB = skewed boat)

| Compound | Configuration | Config | | λ nm | ME (θ) | λ nm | ME (θ) | λ nm | ME (θ) | λ nm | ME (θ) | λ nm | ME (θ) |
|---|---|---|---|---|---|---|---|---|---|---|---|---|---|---|
| | | | | | | | | | | | | | 2S |
| Ent-fisetinidol-(4α→8)-catechin | 2,3-trans-3,4-cis 2,3-trans | 2,4-trans | SB | 230 | 4301 | 242 | 907 | 272 | 4686 | 282 | -47.6 | 293 | 5379 |
| Ent-fisetinidol-(4β→8)-catechin | 2,3-trans-3,4-trans 2,3-trans | 2,4-cis | SB | 234 | 2901 | 248 256 | -436p -1048p | 271 | -7759 | | | 290 | 2288 |
| Ent-fisetinidol-(4β→6)-catechin | 2,3-trans-3,4-trans 2,3-trans | 2,4-cis | SB | 231 | 999 | 248 | 3298 | 270 | -5055 | 284 | 3307 | 289 293 302 | 2480 2948 2216 |

TABLE 8.9

| COMPOUND | ROTAMER | SIGN OF CE AT $\lambda \approx 270$ nm | QUADRANT RULE | CONFORMATION OF C-RING | CORRELATION WITH NMR DATA |
|---|---|---|---|---|---|
| **Fisetinidol-(4α→8)-catechin** | compact | positive | ⊕ ⊖ / ⊖ ⊕ | skewed boat<br>O-1 & C-4 above A-ring<br>C-ring protons quasi-axial | B and E rings parallel<br>Possible H-bonding between 3-OH$_C$ and 1-O$_F$<br>Plane of D-ring perpendicular to 4-H$_C$→4-C$_C$ bond.<br>Plane of B-ring parallel to 2-H$_C$→2-C$_C$ bond.<br>Plane of F-ring parallel to 2-H$_F$→2-C$_F$ bond.<br>OR<br>B and E rings parallel<br>E-ring underneath A-ring<br>Plane of D-ring parallel to 4-H$_C$→4-C$_C$ bond.<br>Plane of B-ring perpendicular to 2-H$_C$→2-C$_C$ bond.<br>Plane of F-ring perpendicular to 2-H$_F$→2-C$_F$ bond.<br>Possible H-binding between 3-OH$_C$ and 1-O$_F$ |
| | extended (*) | | ⊕ ⊖ / ⊖ ⊕ | skewed boat<br>O-1 & C-4 below A-ring<br>C-ring protons quasi-axial | Possible H-bonding between 3-OH$_C$* and 1-O$_F$*<br>Possible H-bonding between 7-OH$_D$* and 1-O$_C$* |
| **Fisetinidol-(4α→6)-catechin** | compact | positive | ⊕ ⊖ / ⊖ ⊕ | skewed boat<br>O-1 & C-4 below A-ring<br>C-ring protons quasi-axial | Possible H-bonding between 5-OH$_D$ and 1-O$_C$<br>Possible H-bonding between 7-OH$_D$ and 3-OH$_C$<br>Plane of D-ring ±45 º to 4-H$_C$→4-C$_C$ bond. |
| | extended (*) | | ⊕ ⊖ / ⊖ ⊕ | skewed boat<br>O-1 & C-4 below A-ring<br>C-ring protons quasi-axial | Possible H-bonding between 7-OH$_D$* and 1-O$_C$*<br>Possible H-bonding between 5- OH$_D$*and 3-OH$_C$*<br>Plane of D*-ring ±45 º to 4-H$_C$*→4-C$_C$* bond. |

| Compound | | Sign | Diagram | Conformation | Notes |
|---|---|---|---|---|---|
| **Fisetinidol-(4β→8)-catechin** | | negative | $\oplus$ ⟋ $\ominus$ / $\ominus$ — $\oplus$ | skewed boat<br>O-1 & C-4 above A-ring<br>C-ring protons quasi-equatorial | Possible H-bonding between 7-OH$_D$ and 1-O$_C$<br>Possible H-bonding between 1-O$_F$ and 3-OH$_C$ |
| **Fisetinidol-(4β→6)-catechin** | | negative | $\oplus$ ⟋ $\ominus$ / $\ominus$ — $\oplus$ | skewed boat<br>O-1 & C-4 above A-ring<br>C-ring protons quasi-equatorial | Possible H-bonding between 7-OH$_D$ and 1-O$_C$<br>Possible H-bonding between 5-OH$_D$ and 3-OH$_C$ |
| ***Ent*-fisetinidol-(4α→8)-catechin** | | positive | $\oplus$ — $\ominus$ / $\ominus$ ⟍ $\oplus$ | boat / skewed boat<br>O-1 & C-4 below A-ring<br>C-ring protons quasi-equatorial | Possible H-bonding between 7-OH$_D$ and 1-O$_C$<br>Possible H-bonding between 7-OH$_D$ and 1-O$_C$ if F-ring is in skewed boat conformation with O$_F$ -1 & C-4 above D-ring<br>Plane of B-ring perpendicular to 2-H$_C$→2-C$_C$ bond |
| ***Ent*-fisetinidol-(4β→8)-catechin** | compact | negative | $\oplus$ — $\ominus$ / $\ominus$ — $\oplus$ | boat / skewed boat<br>O-1 & C-4 below A-ring | B and E rings parallel<br>Possible H-bonding between 1-O$_F$ and 3-OH$_C$ |
| | extended (*) | | $\oplus$ ⟋ $\ominus$ / $\ominus$ — $\oplus$ | skewed boat<br>O-1 & C-4 above A-ring | Possible H-bonding between 7-OH$_D$*and 1-O$_C$*<br>Plane of D-ring parallel to 4-H$_C$*→4-C$_C$* bond. |
| ***Ent*-fisetinidol-(4β→6)-catechin** | compact | negative | $\oplus$ ⟋ $\ominus$ / $\ominus$ — $\oplus$ | | Possible H-bonding between 7-OH$_D$ and 1-O$_C$<br>Plane of D-ring parallel to 4-H$_C$→4-C$_C$ bond. |
| | extended (*) | | $\oplus$ ⟋ $\ominus$ / $\ominus$ — $\oplus$ | | Possible H-bonding between 5-OH$_D$*and 1-O$_C$*<br>Plane of D-ring parallel to 4-H$_C$→4-C$_C$ bond. |

TABLE 8.10

# EXPERIMENTAL

## CHAPTER 9

### Standard Experimental Methods

**9.1    CHROMATOGRAPHIC TECHNIQUES**

**9.1.1    Thin layer chromatography (TLC)**

Qualitative TLC was performed on pre-coated Merck plastic sheets (silica gel $PF_{254}$, 0.25mm) Preparative thin layer chromatography was performed on glass plates (20 x 20 cm), covered with Kieselgel $PF_{254}$ (1.0 mm, 100 g Kieselgel stirred in 230 ml distilled water per five plates). The plates were air-dried and used without prior activation.

Micro separations (1-4 mg per plate) were done on Merck precoated PLC plates: Silica gel 60 $PF_{254}$ 0.25 mm. After development the plates were dried in a fast air current, the different bands distinguished under a UV light (254 nm) and scraped off. Compounds were recovered from the adsorbent with acetone.

**9.1.2    Column chromatography (CC)**

Separations on Sephadex LH-20 were done on various column sizes and at differing flow rates (these will be specified in each instance) in ethanol and ethanol/water mixtures.

9.1.3   Formaldehyde-sulphuric acid spraying agent

TLC plates were sprayed lightly with a 2% (v/v) solution of formaldehyde (40%) in concentrated sulphuric acid and subsequently heated with a hot air current for optimum colour development.

### 9.1.4    Solvent abbreviations

The following abbreviations were used in the descriptions when the solvent systems used during the development of TLC plates are described:

|   |   |
|---|---|
| A | acetone |
| B | benzene |
| H | hexane |

## 9.2    CHEMICAL METHODS

### 9.2.1    Methylation with diazomethane

Methylations were performed with an excess of diazomethane, prepared by the reaction of potassium hydroxide ( 5g in a 95 % (v/v) ethanol solution) with *N*-methyl-*N*-nitroso-*p*-toluene sulphonamide (15 g) in ether and distilled directly into the previously prepared reaction mixture (250 mg dry phenolic material dissolved in methanol (50 ml) and cooled to $-10\ ^{o}C$). After the starting material had completely reacted according to TLC observations (usually after about 48 hours) at $-14\ ^{o}C$, the excess diazomethane and solvent were evaporated at room temperature

### 9.2.2    Acetylation

Dry phenolic material was dissolved in the minimum volume pyridine and twice the amount (per volume) of acetic anhydride was added. After about 8 to 16 hours at ambient temperature the reactions were terminated by adding ice. The excess pyridine was removed by washing with distilled water.

## 9.3 SPECTROSCOPIC METHODS

### 9.3.1 Nuclear Magnetic Resonance Spectroscopy

$^1$H NMR spectra were recorded on a Bruker AM-300 spectrometer at 300 MHz and $^{13}$C NMR spectra at 75 MHz

The solvents used were deuteriochloroform (CDCl$_3$) and deuterioacetone ((CD$_3$)$_2$CO).

Deuterioacetone was extensively dried by leaving it overnight on 3Å molecular sieves and distilling it either onto 3Å molecular sieves for storage, into a flask directly before use. $^1$H NMR spectra of the solvent after extensive drying and distillation indicated several peaks that were also observed on some of the $^1$H NMR spectra in this study (Appendix D).

If aromatic hydroxy peaks were still observed to be broad, a trace of cadmium nitrate monohydrate was added to the solution in the NMR tube in order to sharpen the peaks.

Chemical shifts were expressed in terms of part per million (ppm) on the δ scale and coupling constants were measured in Hz.

Abbreviations were used as follows:

| | |
|---|---|
| s | singlet |
| d | doublet |
| dd | doublet of doublets |
| dt | doublet of triplets |
| t | triplet |
| m | multiplet |
| b | broadened |

$^1$H NMR spectra were recorded at 293 K (20$^o$C), unless otherwise stated.

### 9.3.2 Circular Dichroism (CD)

CD spectra were recorded on a Jasco J-710 spectropolarimeter with methanol as solvent. The formula used to calculate the molecular ellipticity [Θ] was:

## 9.4 FREEZE DRYING

Phenolic material in aqueous solution was frozen by rotating the flask in an alcohol bath at $-20^{o}$C. The frozen sample was subsequently freeze-dried using a Virtis Freezemobile 12SL (40 millitorr).

# CHAPTER 10

## THE SYNTHESIS OF DIMERS AND TRIMERS FROM *Acacia mearnsii* AND DIMERS FROM *Schinopsis balansae*.

**10.1  THE SYNTHESIS OF FISETINIDOL-(4α→8)-CATECHIN, FISETINIDOL-(4ß→8)-CATECHIN, FISETINIDOL-(4ß→6)-CATECHIN AND FISETINIDOL-(4α→6)-CATECHIN.**

(+)-Catechin was dissolved in 100 ml ethanol. 700 ml 0.1 M HCl was added to the (+)-catechin solution while stirring vigorously. A solution of (+)-mollisacacidin dissolved in 25 ml ethanol was added drop wise to the catechin solution at room temperature over a period of 60 minutes. $N_2$ was bubbled through the solution until completion after 20h.

The reaction mixture was extracted with four aliquots of ethyl acetate. The extracts were combined and the solvent was evaporated under vacuum at $40^{\circ}C$ until 300 ml of the solution remained in the flask. 500ml of distilled water was then added to the ethyl acetate solution, and the rest of the ethyl acetate was completely removed under vacuum at $40^{\circ}C$. The remaining aqueous solution, with a pH = 2 (determined with Acilit pH 0-6 sticks from Merck), was freeze-dried.

The above procedure was repeated. The freeze-dried material from both reactions was combined and separated into two fractions that were

separated on two Sephadex LH-20 columns:

| REAGENT | REACTION A | | REACTION B | |
|---|---|---|---|---|
| | Mass (g) | mmol | Mass (g) | mmol |
| (+)-mollisacacidin | 2.0171 | 6.95 | 2.0317 | 7.00 |
| (+)-catechin | 12.0215 | 41.41 | 12.0145 | 41.4 |

| Column size | 45mm x 1150mm |
|---|---|
| Solvent | Ethanol |
| Mass applied | 18 g |
| Collection Time | 16 min |
| Fraction Volume | 20 ml |

| | SEPARATION 1 | | | SEPARATION 2 | | |
|---|---|---|---|---|---|---|
| FRAC-TION | TUBE NO | MASS (g) | CONTENTS | TUBE NO | MASS (g) | CONTENTS |
| 1 | 258–249 | - | catechin | 179-247 | - | catechin |
| 2 | 350-370 | - | empty | 248-309 | - | empty |
| 3 | 371-464 | 1.5493 | fisetinidol-(4α→8)-catechin | 310-410 | 1.4093 | fisetinidol-(4α→8)-catechin |
| 4 | 465-513 | 0 | unknown | 411-504 | 0.0359 | unknown |
| 5 | 514-581 | 1.3987 | fisetinidol-(4β→8)-catechin | 505-542 | 0.5134 | fisetinidol-(4β→8)-catechin + trimeric material |
| 6 | 582-617 | 0.7783 | fisetinidol-(4β→8)-catechin fisetinidol-(4β→6)-catechin | 543-597 | 01.5656 | fisetinidol-(4β→8)-catechin |
| 7 | 618-661 | 0 | fisetinidol-(4β→8)-catechin fisetinidol-(4β→6)-catechin | 598-629 | 0.5826 | fisetinidol-(4β→8)-catechin fisetinidol-(4β→6)-catechin |
| 8 | 662-730 | 0.2762 | fisetinidol-(4β→6)-catechin | 630-659 | 0.2117 | fisetinidol-(4β→8)-catechin fisetinidol-(4β→6)-catechin |
| 9 | 731-769 | 0.0863 | unknown | 660-754 | 0.3937 | fisetinidol-(4β→6)-catechin |
| 10 | 770-849 | 0.2582 | fisetinidol-(4β→6)-catechin + unknown | 755-868 | 0.2230 | unknown |
| 11 | 850-877 | 0.1758 | trimeric material | 869-986 | 0.5348 | fisetinidol-(4α→6)-catechin + unknown |
| 12 | 878-891 | 0.0487 | fisetinidol-(4α→6)-catechin | 987-1040 | 0.3453 | fisetinidol-(4α→6)-catechin |
| 13 | 892-971 | 0.3649 | fisetinidol-(4α→6)-catechin | | | |
| TOTAL: (exc. catechin) | | 4.9364 | | | 5.8153 | |

The structures were confirmed by spectroscopic comparison either with authentic samples[213], or their methylether acetates.[6] Methylether acetates were formed firstly by methylation of a 50 mg sample with diazomethane and subsequent acetylation of the reaction mixture with pyridine and acetic anhydride.

---

[213] Made available by courtesy of Dr P Steynberg

## 10.2 THE SYNTHESIS OF *ENT*-FISETINIDOL-(4α→8)-CATECHIN, *ENT*-FISETINIDOL-(4β→8)-CATECHIN AND *ENT*-FISETINIDOL-(4β→6)-CATECHIN.

(+)-Catechin (12 g, 41.3mmol) was dissolved in 100 ml ethanol and 700 ml 0.1 M HCl was added while stirring vigorously. (-)-Leucofisetinidin (*ent*-mollisacacidin) (2 g, 6.89mmol) was dissolved in 25 ml ethanol and added drop wise to the catechin solution at room temperature over a period of 60 minutes. $N_2$ was bubbled through the solution until completion after 20h.

The reaction mixture was extracted with ethyl acetate (3 x 200ml). The extracts were combined and the solvent was evaporated under vacuum at $40^{\circ}C$ until there was 300 ml of solution left over. 500ml of distilled water was added to the ethyl acetate solution, and the rest of the ethyl acetate was completely removed under vacuum at $40^{\circ}C$. The remaining aqueous solution, with a pH = 2 (determined with Acilit pH 0-6 sticks from Merck) was freeze-dried.

The freeze-dried material from both reactions was combined and separated on a Sephadex LH-20 column:

| Column size | 45mm x 1150mm | |
|---|---|---|
| Solvent | Ethanol | |
| Dead Volume | 3,5 *l* | |
| Fractions | Collection Time | Fraction Volume |
| 1 - 180 | 32 min | 20 ml |
| 181 - 650 | 64 min | 20 ml |

| FRACTION | TUBE NO | MASS (mg) | CONTENTS |
|---|---|---|---|
| 1 | 30 - 80 | | Catechin |
| 2 | 81 – 95 | 389 | catechin<br>*ent*-fisetinidol-(4α→8)-catechin |
| 3 | 96 – 129 | 597 | catechin<br>*ent*-fisetinidol-(4α→8)-catechin |
| 4 | 130 – 162 | 478 | *ent*-fisetinidol-(4α→8)-catechin |
| 5 | 163 – 171 | 37 | unknown material |
| 6 | 172 – 206 | 689 | *ent*-fisetinidol-(4β→8)-catechin |
| 7 | 207 – 230 | 487 | *ent*-fisetinidol-(4β→8)-catechin |
| 8 | 231 – 290 | 823 | *ent*-fisetinidol-(4β→8)-catechin<br>trimeric material |
| 9 | 291 – 335 | 149 | trimeric material |
| 10 | 336 – 345 | 29 | trimeric material<br>*ent*-fisetinidol-(4α→6)-catechin |
| 11 | 346 – 360 | 49 | trimeric material<br>*ent*-fisetinidol-(4α→6)-catechin |
| 12 | 361 – 378 | 73 | trimeric material<br>*ent*-fisetinidol-(4α→6)-catechin |
| 13 | 379 – 450 | 248 | *ent*-fisetinidol-(4α→6)-catechin |
| 14 | 451 – 480 | 45 | *ent*-fisetinidol-(4α→6)-catechin<br>unknown material |
| 15 | 481 – 518 | 76 | unknown material |
| 16 | 519 – 576 | 211 | *ent*-fisetinidol-(4β→6)-catechin |
| 17 | 577 – 650 | 153 | *ent*-fisetinidol-(4β→6)-catechin<br>trimeric material |

The structures were confirmed by spectroscopic comparison either with authentic samples[213], or their methylether acetates.[6] Methylether acetates were formed firstly by methylation of a 50 mg sample with diazomethane and subsequent acetylation of the reaction mixture with pyridine and acetic anhydride. Purification by preparative thin layer chromatography yielded the following results:

| DIMER | SOLVENT SYSTEM | NO OF TIMES DEVELOPED | R_F VALUE |
|---|---|---|---|
| *ent*-fisetinidol-(4α→8)-catechin | HBA 5:4:1 | 1 | 0.21 |
| *ent*-fisetinidol-(4ß→8)-catechin | HBA 5:4:1 | 2 | 0.20 |
| *ent*-fisetinidol-(4α→6)-catechin | HBA 5:4:1 | 3 | 0.12 |
| *ent*-fisetinidol-(4ß→6)-catechin | HBA 5:4:1 | 2 | 0.47 |

The $^1$H NMR spectra of both the methylether acetate and the free phenolic form of what was considered to be *ent*-fisetinidol-(4α→6)-catechin did not confirm its structure and was therefore omitted from this study.

## 10.3 THE SYNTHESIS OF FISETINIDOL-(4β→8)-CATECHIN-(6→4α)-FISETINIDOL AND FISETINIDOL-(4β→8)-CATECHIN-(6→4β)-FISETINIDOL.

Fisetinidol-(4β→8)-catechin, 2 g (3.56 mmol, 1.25 equivalents), was dissolved in 600 ml 0.1MHCl. (+)-Mollisacacidin, 0.8267g (2.85 mmol, 1.00 equivalents), was added to this solution. The solution was divided into four equal parts and each part was transferred to a 250 flask. The solutions were flushed with nitrogen and agitated ultrasonically under $N_2$ at a temperature of 30 – 36 $^{\circ}$C for 3 hours.[214] Upon completion, ice was added to the mixtures to quench the reaction. Each mixture was extracted with ethyl acetate (3 x 200ml). The extracts were combined and the solvent evaporated under vacuum at 40$^{\circ}$C until 300 ml of the solution remained in the flask. 500ml of distilled water was added and the remaining ethyl acetate completely removed under vacuum at 40$^{\circ}$C. The remaining aqueous solution was freeze-dried and separated by column chromatography on Sephadex LH-20:

| Column size | 45 mm x 620 mm |
|---|---|
| Solvent | Ethanol : $H_2O$; 1 : 1 |
| Dead Volume | 300 ml |
| Collection Time | 32 min |
| Fraction Volume | 20 ml |

| Fractions | Compound | Mass | % yield |
|---|---|---|---|
| 412 - 440 | fisetinidol-(4β→8)-catechin-(6→4α)-fisetinidol | 434.4 mg 0.52 mmol | 18.2 |
| 471 - 520 | fisetinidol-(4β→8)-catechin-(6→4β)-fisetinidol | 365.4 mg 0.438 mmol | 19.3 |

---

214    E Malan and A Sireeparsad, *Phytochemistry*, 1995, **38(1)**, 237.

## 10.4 THE SYNTHESIS OF FISETINIDOL-(4α→8)-CATECHIN-(6→4α)-FISETINIDOL AND FISETINIDOL-(4α→8)-CATECHIN-(6→4β)-FISETINIDOL.

Fisetinidol-(4α→8)-catechin, 2 g (3.56 mmol, 1.25equivalents), was dissolved in 600 ml 0.1M HCl. (+)-Mollisacacidin, 0.8267 g (2.85 mmol, 1.00 equivalents), was added to this solution. The solution was divided into four equal parts and each part was transferred to a 250 ml flask. The solutions were flushed with nitrogen and agitated ultrasonically under $N_2$ at a temperature of 30 – 36 $^oC$ for 3 hours.[214] Upon completion, ice was added to the mixtures to quench the reaction. Each mixture was extracted with ethyl acetate (3 x 200ml). The extracts were combined and the solvent evaporated under vacuum at $40^oC$ until 300 ml of the solution remained in the flask. 500ml of distilled water was added and the remaining ethyl acetate completely removed under vacuum at $40^oC$. The remaining aqueous solution was freeze-dried and separated by column chromatography on Sephadex LH-20:

| Column size | 45 mm x 620 mm |
| --- | --- |
| Solvent | Ethanol : $H_2O$; 1 : 1 |
| Dead Volume | 550 ml |
| Collection Time | 32 min |
| Fraction Volume | 20 ml |

| Fractions | Compound | Mass | % yield |
| --- | --- | --- | --- |
| 271 - 305 | fisetinidol-(4α→8)-catechin-(6→4α)-fisetinidol | 363.3 mg 0.44 mmol | 15.4 |
| 351 - 430 | fisetinidol-(4α→8)-catechin-(6→4β)-fisetinidol | 309.4 mg 0.37 mmol | 16.4 |

The structures of the compounds prepared in 10.3 and 10.4 were confirmed by spectroscopic comparison of their methylether acetates.[215] Methylether acetates were formed firstly by methylation of a 50 mg sample with diazomethane and subsequent acetylation of the reaction mixture with pyridine and acetic anhydride, followed by preparative thin layer chromatography.

---

[215] S Bonnet, Ph D Thesis, UOVS, 1993.

# APPENDIX A

## SUMMARY OF HETEROCYCLIC RING COUPLING CONSTANTS.

### FISETINIDOL-(4α→8)-CATECHIN (dry sample at 293 K)

| C-RING | | | F-RING | | |
|---|---|---|---|---|---|
| Coupling constant | Rotamer | Magnitude (Hz) | Coupling constant | Rotamer | Magnitude (Hz) |
| $^3J_{2-HC,3-HC}$ | compact | 6.5 | $^3J_{2-HF,3-HF}$ | compact | 7.5 |
| | extended (*) | 8.5 | | extended (*) | 7.5 |
| $^3J_{3-HC,3-OHC}$ | both | 4.5 | $^3J_{3-HF,4HFβ}$ | compact | 8.0 |
| $^3J_{3-HC,4-HC}$ | compact | 8.5 | | extended (*) | 8.0 |
| | extended (*) | 7.5 | $^3J_{3-HF,4HFα}$ | compact | 5.0 |
| $^3J_{4-HC,5-HA}$ | compact | broad triplet | | extended (*) | 5.0 |
| | extended (*) | broad | $^3J_{3-HFα,4HFβ}$ | both | 16.0 |
| Conformation | compact | E-A | Conformation | compact | E-A |
| | extended | E-A | | extended | E-A |

### FISETINIDOL-(4α→8)-CATECHIN (wet sample at 293 K)

| C-RING | | | F-RING | | |
|---|---|---|---|---|---|
| Coupling constant | Rotamer | Magnitude (Hz) | Coupling constant | Rotamer | Magnitude (Hz) |
| $^3J_{2-HC,3-HC}$ | compact | 9.5 | $^3J_{2-HF,3-HF}$ | compact | 7.5 |
| | extended (*) | 9.0 | | extended (*) | 7.5 |
| $^3J_{3-HC,3-OHC}$ | both | | $^3J_{3-HF,4HFβ}$ | compact | 8.5 |
| $^3J_{3-HC,4-HC}$ | compact | 9.0 | | extended (*) | 8.0 |
| | extended (*) | 9.0 | $^3J_{3-HF,4HFα}$ | compact | 5.5 |
| $^3J_{4-HC,5-HA}$ | compact | 1.0 | | extended (*) | 5.5 |
| | extended (*) | 1.0 | $^3J_{3-HFα,4HFβ}$ | both | 16.0 |
| Conformation | compact | E | Conformation | compact | E-A |
| | extended | E | | extended | E-A |

### *ENT*-FISETINIDOL-(4β→8)-CATECHIN (dry sample at 293 K)

| C-RING | | | F-RING | | |
|---|---|---|---|---|---|
| Coupling constant | Rotamer | Magnitude (Hz) | Coupling constant | Rotamer | Magnitude (Hz) |
| $^3J_{2-HC,3-HC}$ | compact | 9.0 | $^3J_{2-HF,3-HF}$ | compact | 8.5 |
| | extended (*) | 9.5 | | extended (*) | 7.5 |
| $^3J_{3-HC,3-OHC}$ | both | 5.0 | $^3J_{3-HF,4HFβ}$ | compact | 9.5 |
| $^3J_{3-HC,4-HC}$ | compact | 9.2 | | extended (*) | 8.2 |
| | extended (*) | 9.0 | $^3J_{3-HF,4HFα}$ | compact | 5.8 |
| $^3J_{4-HC,5-HA}$ | compact | 1.0 | | extended (*) | 5.5 |
| | extended (*) | 0.8 | $^3J_{3-HFα,4HFβ}$ | both | 16.0 |
| Conformation | compact | E | Conformation | compact | E-A |
| | extended | E | | extended | E-A |

**FISETINIDOL-(4α→6)-CATECHIN (wet and (dry) samples at 293 K)**

| C-RING | | | F-RING | | |
|---|---|---|---|---|---|
| Coupling constant | Rotamer | Magnitude (Hz) | Coupling constant | Rotamer | Magnitude (Hz) |
| $^3J_{2\text{-}HC,3\text{-}HC}$ | compact | 9.5 | $^3J_{2\text{-}HF,3\text{-}HF}$ | compact | 8.0 |
| | extended (*) | 6.2 (6.0) | | extended (*) | 8.0 |
| $^3J_{3\text{-}HC,3\text{-}OHC}$ | both of dry sample | 4.5 | $^3J_{3\text{-}HF,4HF\beta}$ | compact | 8.5 |
| $^3J_{3\text{-}HC,4\text{-}HC}$ | compact | 9.5 | | extended (*) | 8.5 |
| | extended (*) | 6.2 (6.0) | $^3J_{3\text{-}HF,4HF\alpha}$ | compact | 5.5 |
| $^3J_{4\text{-}HC,5\text{-}HA}$ | compact | 1.2 | | extended (*) | 5.5 |
| | extended (*) | broad | $^3J_{3\text{-}HF\alpha,4HF\beta}$ | both | 15.5 |
| **Conformation** | compact | **E** | **Conformation** | compact | **E-A** |
| | extended | **E-A** | | extended | **E-A** |

**ENT-FISETINIDOL-(4β→6)-CATECHIN (dry sample at 293 K)**

| C-RING | | | F-RING | | |
|---|---|---|---|---|---|
| Coupling constant | Rotamer | Magnitude (Hz) | Coupling constant | Rotamer | Magnitude (Hz) |
| $^3J_{2\text{-}HC,3\text{-}HC}$ | compact | 9.5 | $^3J_{2\text{-}HF,3\text{-}HF}$ | compact | 7.5 |
| | extended (*) | 10.0 | | extended (*) | 7.2 |
| $^3J_{3\text{-}HC,3\text{-}OHC}$ | both | 5.0 | $^3J_{3\text{-}HF,4HF\beta}$ | compact | 8.8 |
| $^3J_{3\text{-}HC,4\text{-}HC}$ | compact | 9.5 | | extended (*) | 8.5 |
| | extended (*) | ± 9.0 | $^3J_{3\text{-}HF,4HF\alpha}$ | compact | 5.8 |
| $^3J_{4\text{-}HC,5\text{-}HA}$ | compact | 1.2 | | extended (*) | 5.2 |
| | extended (*) | 1.2 | $^3J_{3\text{-}HF\alpha,4HF\beta}$ | both | 16.0 |
| **Conformation** | compact | **E** | **Conformation** | compact | **E-A** |
| | extended | **E** | | extended | **E-A** |

**FISETINIDOL-(4β→8)-CATECHIN (wet sample at 353 K)**

| C-RING | | F-RING | |
|---|---|---|---|
| Coupling constant | Magnitude (Hz) | Coupling constant | Magnitude (Hz) |
| $^3J_{2\text{-}HC,3\text{-}HC}$ | 2.0 | $^3J_{2\text{-}HF,3\text{-}HF}$ | 7.5 |
| $^3J_{3\text{-}HC,3\text{-}OHC}$ | V ery broad | $^3J_{3\text{-}HF,4HF\beta}$ | 7.5 |
| $^3J_{3\text{-}HC,4\text{-}HC}$ | 3.0 | $^3J_{3\text{-}HF,4HF\alpha}$ | 5.5 |
| $^3J_{4\text{-}HC,5\text{-}HA}$ | 1.0 | $^3J_{3\text{-}HF\alpha,4HF\beta}$ | 16 |
| **Conformation** | **A** | **Conformation** | **E-A** |

## ENT-FISETINIDOL-(4α→8)-CATECHIN (dry sample at 343 K)

| C-RING | | F-RING | |
|---|---|---|---|
| **Coupling constant** | **Magnitude (Hz)** | **Coupling constant** | **Magnitude (Hz)** |
| $^3J_{2\text{-}HC,3\text{-}HC}$ | 3.0 | $^3J_{2\text{-}HF,3\text{-}HF}$ | 7.5 |
| $^3J_{3\text{-}HC,3\text{-}OHC}$ | very broad | $^3J_{3\text{-}HF,4HF\beta}$ | 8.5 |
| $^3J_{3\text{-}HC,4\text{-}HC}$ | 3.0 | $^3J_{3\text{-}HF,4HF\alpha}$ | 5.5 |
| $^3J_{4\text{-}HC,5\text{-}HA}$ | 1.2 | $^3J_{3\text{-}HF\alpha,4HF\beta}$ | 16.2 |
| **Conformation** | **A** | **Conformation** | **E-A** |


## FISETINIDOL-(4β→6)-CATECHIN (dry sample)

| C-RING | | F-RING | |
|---|---|---|---|
| **Coupling constant** | **Magnitude (Hz)** | **Coupling constant** | **Magnitude (Hz)** |
| $^3J_{2\text{-}HC,3\text{-}HC}$ | 2.5 / 0.8 | $^3J_{2\text{-}HF,3\text{-}HF}$ | 5.5? (broad) |
| $^3J_{3\text{-}HC,3\text{-}OHC}$ | 2.5 (broad) | $^3J_{3\text{-}HF,4HF\beta}$ | 8.5 (broad) |
| $^3J_{3\text{-}HC,4\text{-}HC}$ | broad | $^3J_{3\text{-}HF,4HF\alpha}$ | 5.0 |
| $^3J_{4\text{-}HC,5\text{-}HA}$ | 1.2 | $^3J_{3\text{-}HF\alpha,4HF\beta}$ | 16.0 |
| **Conformation** | **A** | **Conformation** | **E-A** |

# APPENDIX B

## SUMMARY OF $^{13}$C NMR DATA

| | 2,3-*trans*-3,4-*trans* configuration | | | | 2,3-*trans*-3,4-*cis* configuration | | |
|---|---|---|---|---|---|---|---|
| | Fisetidinol-(4α→8)-catechin | Fisetidinol-(4α→6)-catechin | *Ent*-fisetidinol-(4ß→8)-catechin | *Ent*-fisetidinol-(4ß→6)-catechin | Fisetinidol-(4ß→8)-catechin | Fisetinidol-(4ß→6)-catechin | *Ent*-fisetinidol-(4α→8)-catechin |
| 4-CF | 28.44 | | 28.99 | 28.13 | 27.64 | 29.04 | 28.32 |
| 4-CF* | 27.62 | | 28.23 | 28.90[a] | | | |
| 4-CC | 41.25 | 41.02 | 41.01 | 41.02 | 31.18 | 31.19 | 31.45 |
| 4-CC* | 40.95 | 41.72 | 41.13 | 41.73 | | | |
| 3-CF | 67.93 | 67.85 | 67.98 | 67.86 | 67.42 | 68.10 | 68.16 |
| 3-CF* | 68.17[a] | 68.04[a] | 68.09[a] | 67.94[a] | | | |
| 3-CC | 69.99 | 70.67 | 70.36 | 70.61 | 71.98 | 72.52 | 72.10 |
| 3-CC* | 70.09[a] | 70.67 | 69.72 | 70.79[a] | | | |
| 2-CF | 81.46 | 82.09 | 82.04 | 82.15 | 81.78 | 82.26 | 82.13 |
| 2-CF* | 82.24 | 82.09 | 82.14[a] | 82.15 | | | |
| 2-CC | 83.60 | 83.72 | 83.70 | 83.70 | 81.04 | 81.27 | 80.84 |
| 2-CC* | 83.51[a] | 83.78[a] | 83.77[a] | 83.77[a] | | | |
| | | | | | | | |
| 6/8-CD | 95.55 | 95.58 | 95.52 | 95.67 | 97.44 | 94.50 | 97.63 |
| 6/8-CD* | 96.59 | 96.61 | 96.69 | 96.59 | | | |
| 8-CA | 102.62 | 102.84 | 102.50 | 103.09 | 102.66 | 102.55 | 102.66 |
| 8-CA* | 102.99 | 103.01[a] | 102.69 | 102.84 | | | |
| 6-CA | 108.34 | 108.62 | 107.20 | 108.72 | 108.15 | 108.13 | 108.17 |
| 6-CA* | 105.513 | 109.03[a] | 108.60[a] | 108.64 | | | |
| 2-CB | 114.76 to 115.76 | 115.21 | 115.8 | 114.93 to 115.49 | 112.84 | 112.58 | 112.70 |
| 2-CB* | 114.76 to 115.76 | 115.44[a] | 114.96[e] | 114.93 to 115.49 | | | |
| 2-CE | 114.76 to 115.76 | 114.88 | 115.00[e] | 114.93 to 115.49 | 114.20 | 114.86 | 114.72 |
| 2-CE* | 114.76 to 115.76 | 115.10[a] | 114.61 | 114.93 to 115.49 | | | |
| 5-CB | 114.76 to 115.76 | 115 to 117 | 115.20[e] | 120.36 | 115.39[d] | 116.83 | 115.82[c] |
| 5-CB* | 114.76 to 115.76 | 115 to 117 | 115.25[e] | 119.74[b] | | | |
| 5-CE | 114.76 to 115.76 | 115 to 117 | 115.32[e] | 120.36 | 115.62[d] | | 115.22 |
| 5-CE* | 114.76 to 115.76 | 115 to 117 | 115.46[e] | 119.79[b] | | | |
| 6-CE | 118.35 | 119.71 | 120.17 | 114.93 to 115.49 | 116.81[d] | 119.71 | 118.37 |
| 6-CE* | 119.50 | 119.71 | 118.40[f] | 114.93 to 115.49 | | | |
| 6-CB | 120.12 | 120.37 | 120.46 | 114.93 to 115.49 | 118.80[d] | 115.19 | 116.69[c] |
| 6-CB* | 120.40[a] | 120.37 | 118.44[f] | 114.93 to 115.49 | | | |
| 5-CA | 129.07 | 129.28 | 128.40 | 129.31 | 129.40 | 129.28 | 129.57 |
| 5-CA* | 129.31 | 129.09 | 129.17 | 129.06 | | | |

a   Chemical shifts in merged cells are interchangeable

b,c,d,e   Chemical shifts are interchangeable

f   Chemical shifts are interchangeable and could also be 119.32 ppm

Note:

The chemical shift difference of ± 10 ppm between 4-CC of the *2,3-trans-3,4-trans* and *2,3-trans-3,4-cis* configurations.

# APPENDIX C

## CD SPECTRA
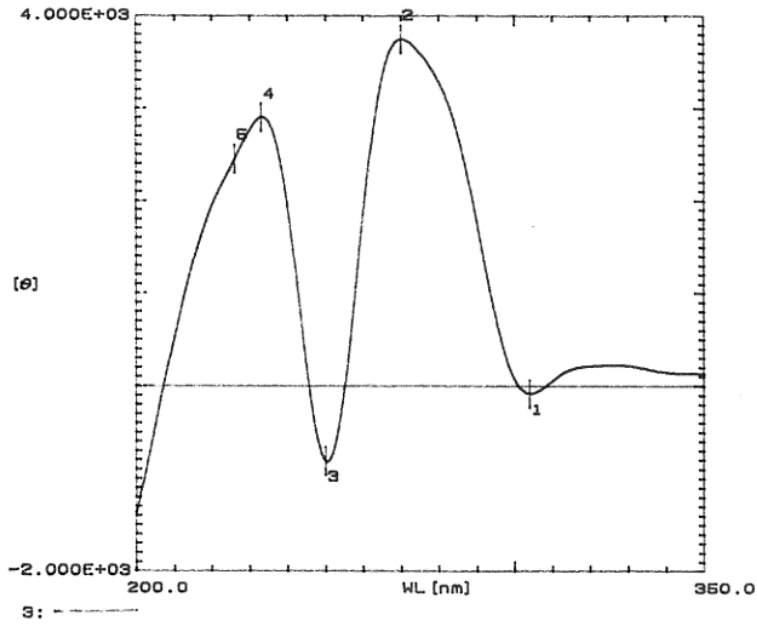


| No. | Wavelength | Value |
|-----|-----------|-------------|
| 1 | 304.00 nm | -8.212E+01 |
| 2 | 270.00 nm | 3.748E+03 |
| 3 | 250.00 nm | -8.101E+02 |
| 4 | 233.00 nm | 2.900E+03 |
| 5 | 226.00 nm | 2.453E+03 |
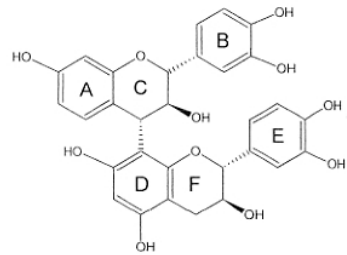
**FISETINIDOL-(4α→8)-CATECHIN**
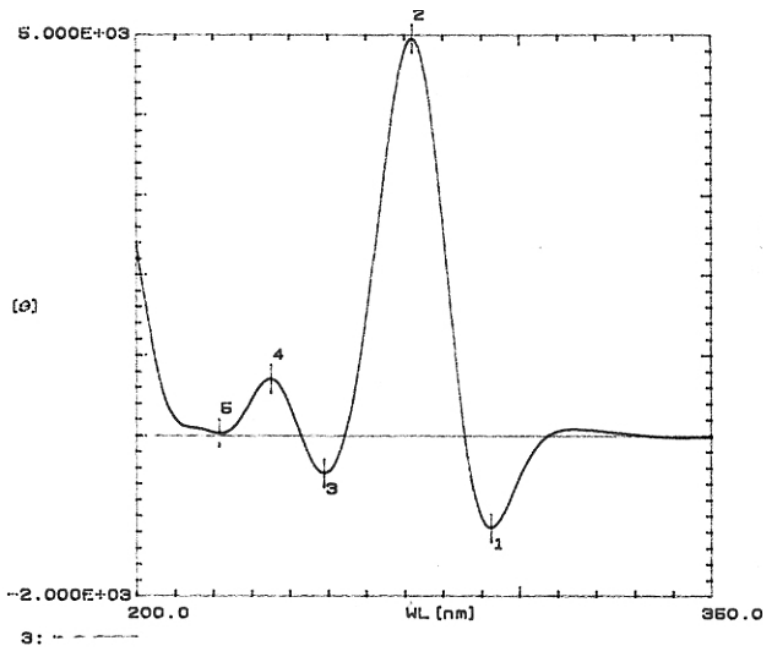


| No. | Wavelength | Value |
|-----|-----------|-------------|
| 1 | 292.50 nm | -1.146E+03 |
| 2 | 272.00 nm | 4.967E+03 |
| 3 | 249.00 nm | -4.654E+02 |
| 4 | 235.00 nm | 7.096E+02 |
| 5 | 221.50 nm | 3.441E+01 |
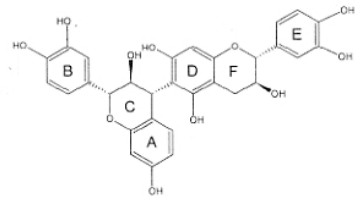
**FISETINIDOL-(4α→6)-CATECHIN**
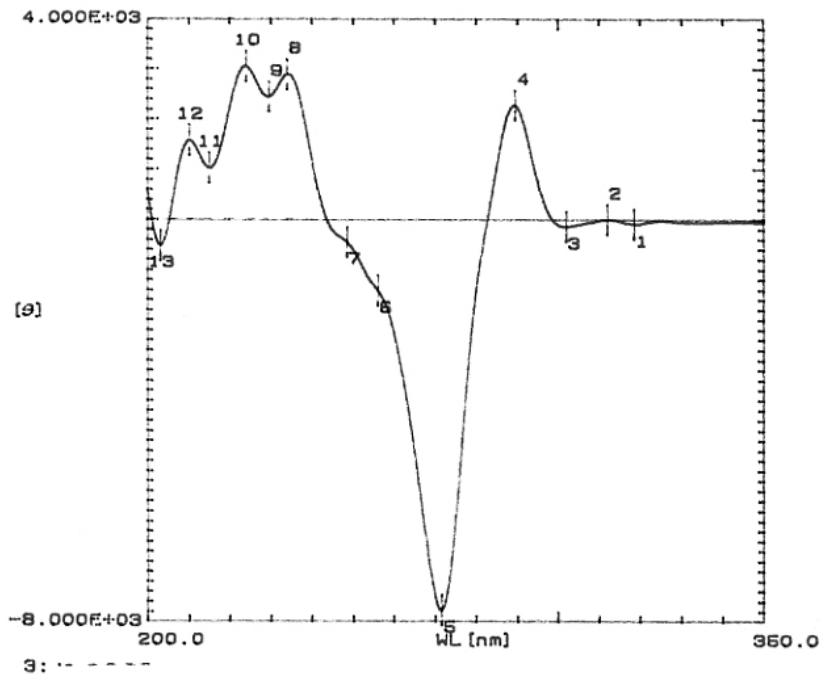
| No. | Wavelength | Value |
|---|---|---|
| 1 | 318.50 nm | −8.551E+01 |
| 2 | 312.00 nm | 6.262E+00 |
| 3 | 302.00 nm | −1.334E+02 |
| 4 | 289.50 nm | 2.288E+03 |
| 5 | 271.50 nm | −7.759E+03 |
| 6 | 256.00 nm | −1.408E+03 |
| 7 | 248.50 nm | −4.361E+02 |
| 8 | 234.00 nm | 2.901E+03 |
| 9 | 229.50 nm | 2.460E+03 |
| 10 | 224.00 nm | 3.061E+03 |
| 11 | 216.00 nm | 1.031E+03 |
| 12 | 210.00 nm | 1.586E+03 |
| 13 | 203.00 nm | −6.185E+02 |
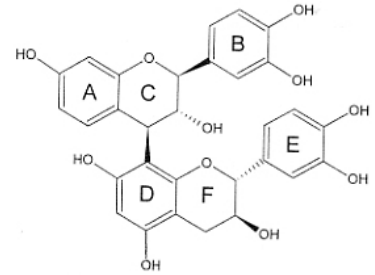
**ENT-FISETINIDOL-(4ß→8)-CATECHIN**
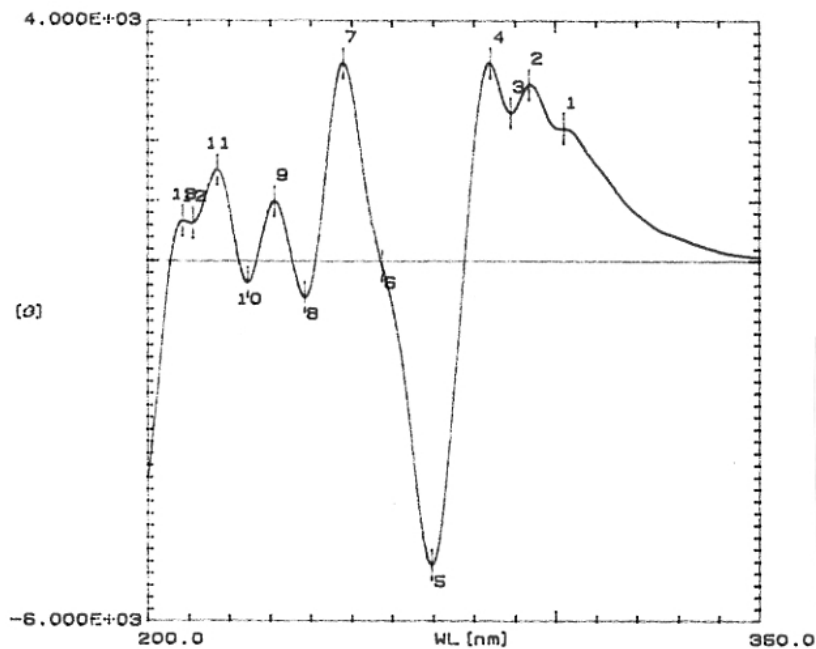


| No. | Wavelength | Value |
|---|---|---|
| 1 | 302.00 nm | 2.216E+03 |
| 2 | 293.50 nm | 2.948E+03 |
| 3 | 289.00 nm | 2.480E+03 |
| 4 | 284.00 nm | 3.307E+03 |
| 5 | 269.50 nm | −5.055E+03 |
| 6 | 267.50 nm | −7.264E+01 |
| 7 | 248.00 nm | 3.298E+03 |
| 8 | 238.50 nm | −5.937E+02 |
| 9 | 231.00 nm | 9.994E+02 |
| 10 | 224.50 nm | −3.600E+02 |
| 11 | 217.00 nm | 1.626E+03 |
| 12 | 211.00 nm | 6.373E+02 |
| 13 | 208.50 nm | 6.711E+02 |

**ENT-FISETINIDOL-(4ß→6)-CATECHIN**

C-2
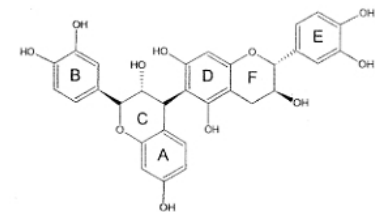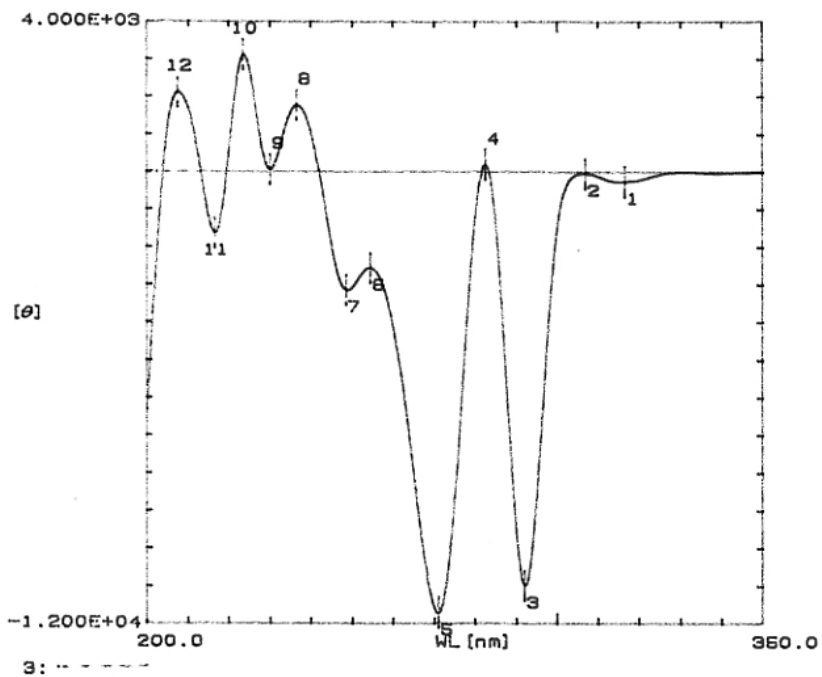
| No. | Wavelength | Value |
|-----|-----------|-------|
| 1 | 316.50 nm | −2.680E+02 |
| 2 | 307.00 nm | −4.543E+01 |
| 3 | 292.00 nm | −1.099E+04 |
| 4 | 282.50 nm | 1.938E+02 |
| 5 | 271.00 nm | −1.171E+04 |
| 6 | 264.50 nm | −2.564E+03 |
| 7 | 248.50 nm | −3.144E+03 |
| 8 | 236.50 nm | 1.768E+03 |
| 9 | 230.00 nm | 5.683E+01 |
| 10 | 223.50 nm | 3.120E+03 |
| 11 | 216.50 nm | −1.635E+03 |
| 12 | 207.50 nm | 2.113E+03 |
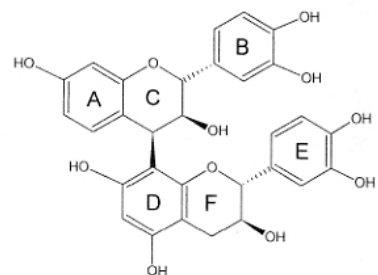
**FISETINIDOL-(4ß→8)-CATECHIN**
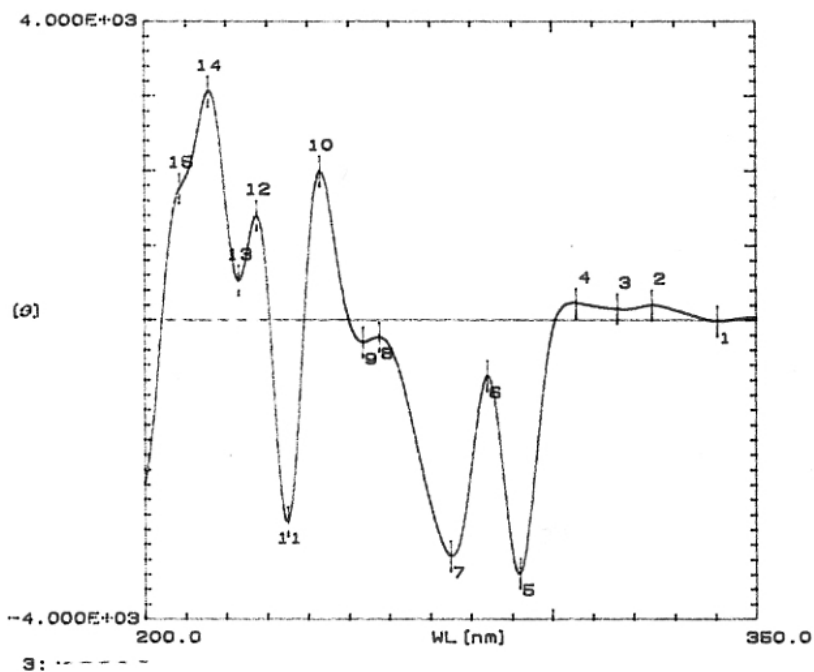


| No. | Wavelength | Value |
|-----|-----------|-------|
| 1 | 340.50 nm | −1.271E+01 |
| 2 | 324.50 nm | 2.042E+02 |
| 3 | 316.00 nm | 1.522E+02 |
| 4 | 306.00 nm | 2.301E+02 |
| 5 | 292.00 nm | −3.384E+03 |
| 6 | 284.00 nm | −7.427E+02 |
| 7 | 275.00 nm | −3.148E+03 |
| 8 | 257.50 nm | −2.234E+02 |
| 9 | 253.50 nm | −2.927E+02 |
| 10 | 243.00 nm | 1.992E+03 |
| 11 | 235.00 nm | −2.691E+03 |
| 12 | 227.50 nm | 1.401E+03 |
| 13 | 223.00 nm | 5.306E+02 |
| 14 | 215.50 nm | 3.061E+03 |
| 15 | 208.50 nm | 1.762E+03 |
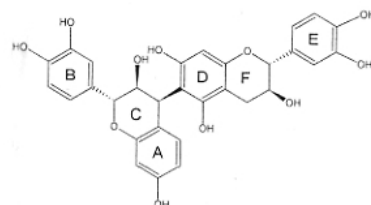
**FISETINIDOL-(4ß→6)-CATECHIN**
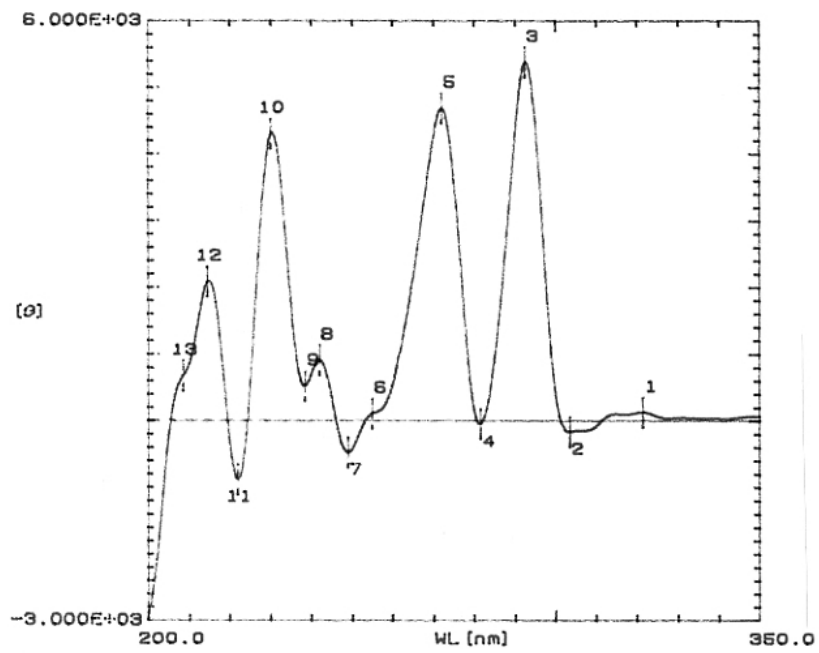
| No. | Wavelength | Value |
|---|---|---|
| 1 | 321.50 nm | 1.328E+02 |
| 2 | 303.50 nm | -1.634E+02 |
| 3 | 292.50 nm | 5.379E+03 |
| 4 | 281.50 nm | -4.761E+01 |
| 5 | 272.00 nm | 4.686E+03 |
| 6 | 255.00 nm | 1.083E+02 |
| 7 | 249.00 nm | -4.734E+02 |
| 8 | 242.00 nm | 9.074E+02 |
| 9 | 238.50 nm | 5.233E+02 |
| 10 | 230.00 nm | 4.301E+03 |
| 11 | 222.00 nm | -8.798E+02 |
| 12 | 214.50 nm | 2.084E+03 |
| 13 | 208.50 nm | 6.720E+02 |
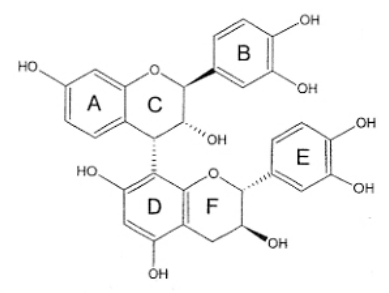
**ENT-FISETINIDOL-(4α→8)-CATECHIN**
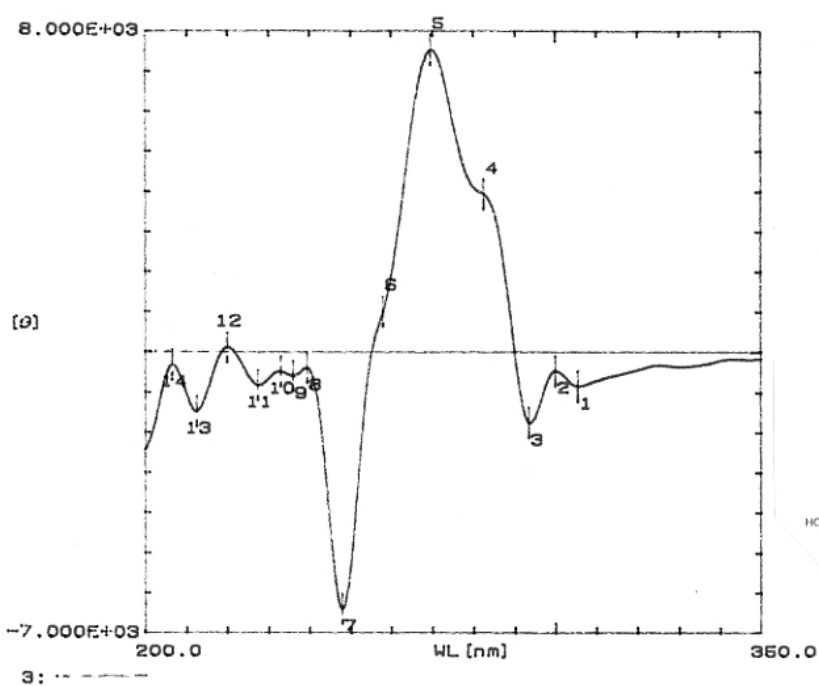


| No. | Wavelength | Value |
|---|---|---|
| 1 | 305.50 nm | -8.470E+02 |
| 2 | 300.00 nm | -4.667E+02 |
| 3 | 293.50 nm | -1.752E+03 |
| 4 | 282.50 nm | 3.945E+03 |
| 5 | 269.50 nm | 7.541E+03 |
| 6 | 258.00 nm | 1.021E+03 |
| 7 | 248.00 nm | -6.395E+03 |
| 8 | 239.50 nm | -3.890E+02 |
| 9 | 236.00 nm | -5.900E+02 |
| 10 | 233.00 nm | -4.743E+02 |
| 11 | 227.50 nm | -8.175E+02 |
| 12 | 220.00 nm | 1.209E+02 |
| 13 | 212.50 nm | -1.471E+03 |
| 14 | 206.50 nm | -3.140E+02 |
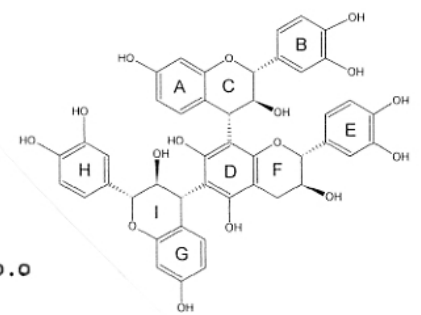
**FISETINIDOL-(4α→8)-CATECHIN-(6→4α)-FISETINIDOL**
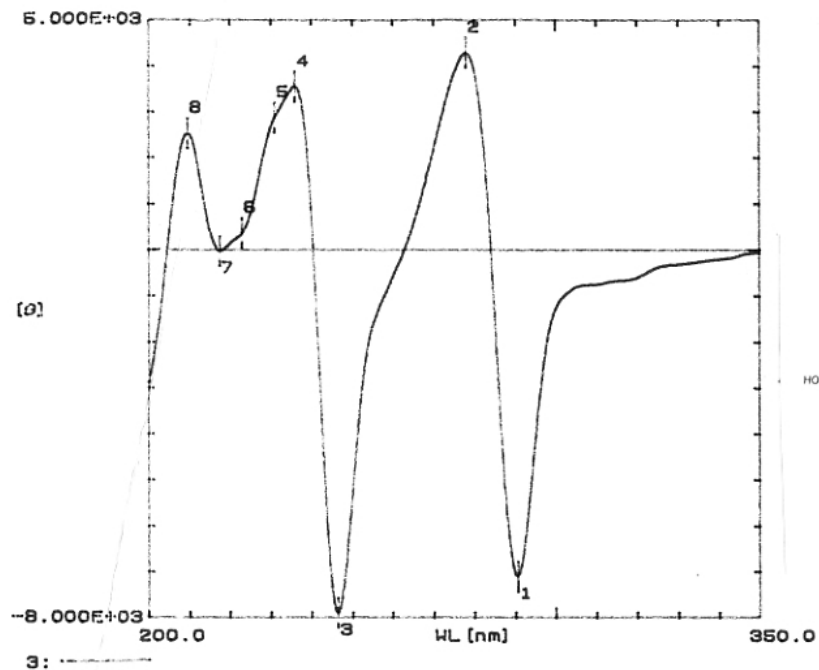
| No. | Wavelength | Value |
|-----|-----------|-------|
| 1 | 290.50 nm | -7.093E+03 |
| 2 | 278.00 nm | 4.287E+03 |
| 3 | 246.50 nm | -7.887E+03 |
| 4 | 236.00 nm | 3.552E+03 |
| 5 | 231.00 nm | 2.875E+03 |
| 6 | 223.00 nm | 3.630E+02 |
| 7 | 217.50 nm | -2.180E+01 |
| 8 | 209.50 nm | 2.537E+03 |
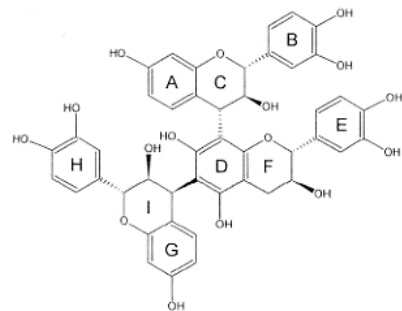
**FISETINIDOL-(4α→8)-CATECHIN-(6→4ß)-FISETINIDOL**
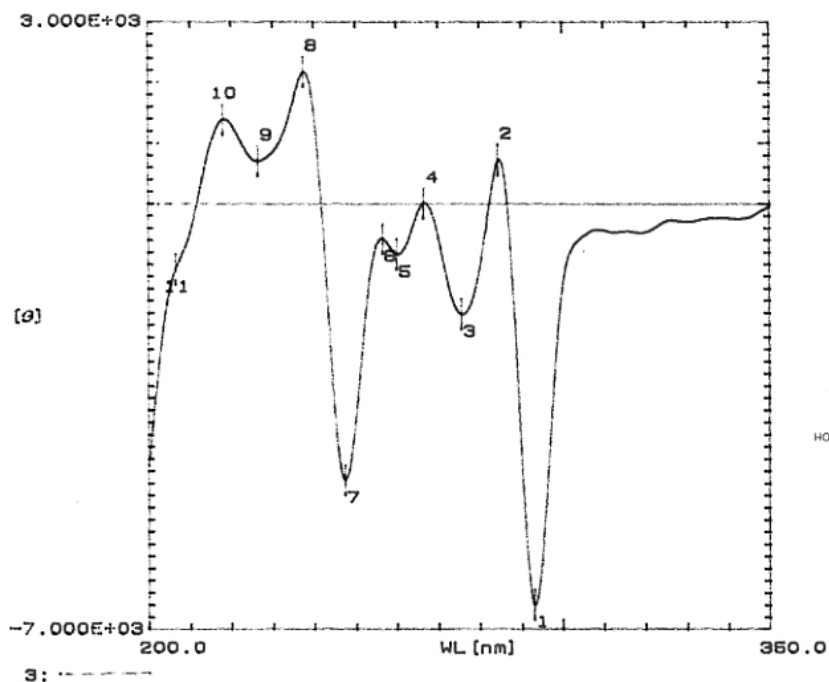


| No. | Wavelength | Value |
|-----|-----------|-------|
| 1 | 293.00 nm | -6.585E+03 |
| 2 | 284.50 nm | 7.262E+02 |
| 3 | 275.50 nm | -1.816E+03 |
| 4 | 266.50 nm | 1.017E+01 |
| 5 | 260.00 nm | -8.323E+02 |
| 6 | 255.50 nm | -5.746E+02 |
| 7 | 247.50 nm | -4.545E+03 |
| 8 | 237.50 nm | 2.179E+03 |
| 9 | 226.50 nm | 7.067E+02 |
| 10 | 218.00 nm | 1.392E+03 |
| 11 | 206.50 nm | -1.082E+03 |

**FISETINIDOL-(4ß→8)-CATECHIN-(6→4α)-FISETINIDOL**

C-5
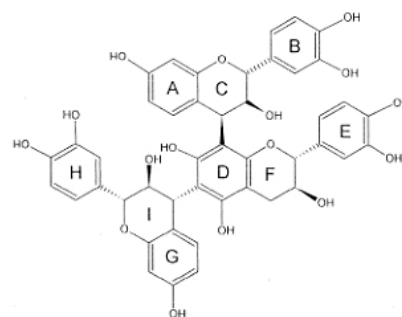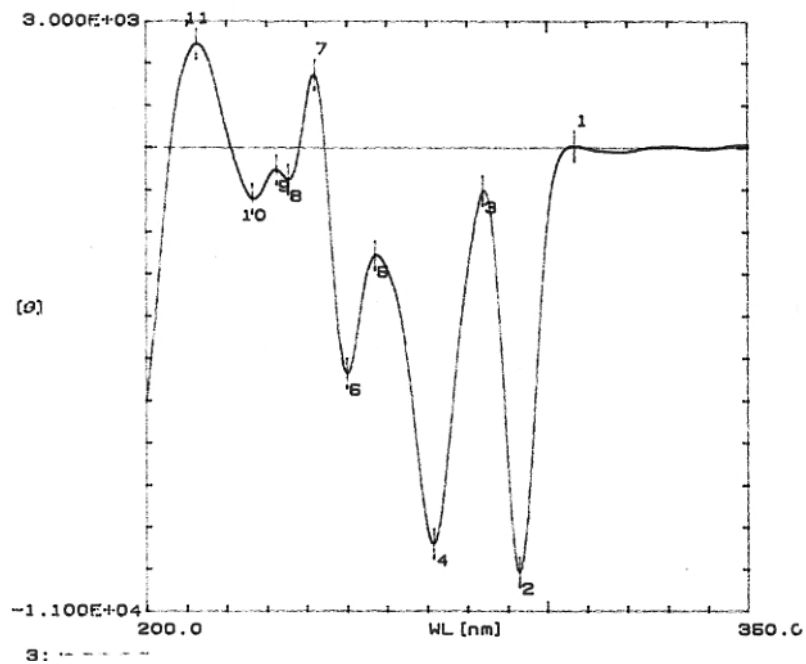
| No. | Wavelength | Value |
|---|---|---|
| 1 | 307.00 nm | 4.015E+01 |
| 2 | 293.00 nm | −1.006E+04 |
| 3 | 284.00 nm | −1.022E+03 |
| 4 | 271.50 nm | −9.382E+03 |
| 5 | 257.00 nm | −2.554E+03 |
| 6 | 250.00 nm | −5.348E+03 |
| 7 | 242.00 nm | 1.731E+03 |
| 8 | 235.50 nm | −7.565E+02 |
| 9 | 232.50 nm | −5.229E+02 |
| 10 | 226.50 nm | −1.211E+03 |
| 11 | 212.50 nm | 2.462E+03 |
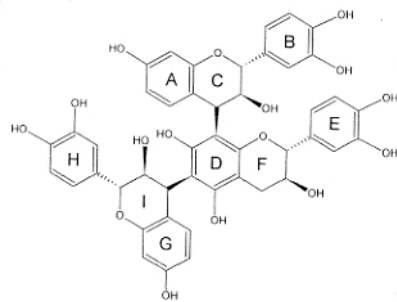
**FISETINIDOL-(4ß→8)-CATECHIN-(6→4ß)-FISETINIDOL**

# APPENDIX D

## ACETONE d$_6$ SPECTRA

ACETONE-d6
DIRECTLY FROM
MERCK AMPOULE
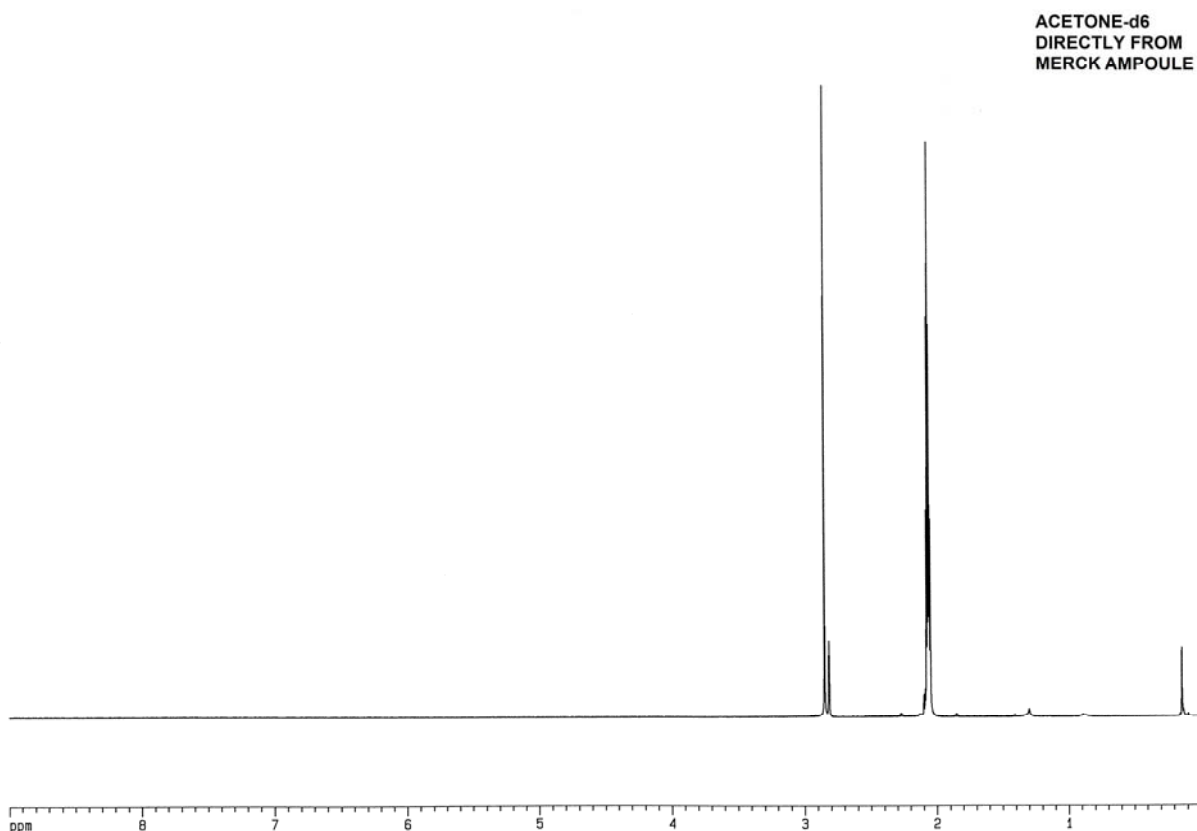


**Notes:**

Extensive drying of acetone-d$_6$ over molecular sieves with subsequent distillation did remove water to a certain extent, but it also added other impurities that could affect the appearance of a spectrum and possibly interact with the compounds being studied. (See spectra below)

The dryness of the compound is therefore of paramount importance. Better quality spectra would probably be achieved if compounds are freeze dried immediately prior to spectroscopic investigations and dissolved in solvents straight from ampoules instead of vials without any drying.

ACETONE-d6
AFTER DRYING
AND
DISTILLATION

ACETONE-d6
AFTER DRYING
AND DISTILLATION

D-2
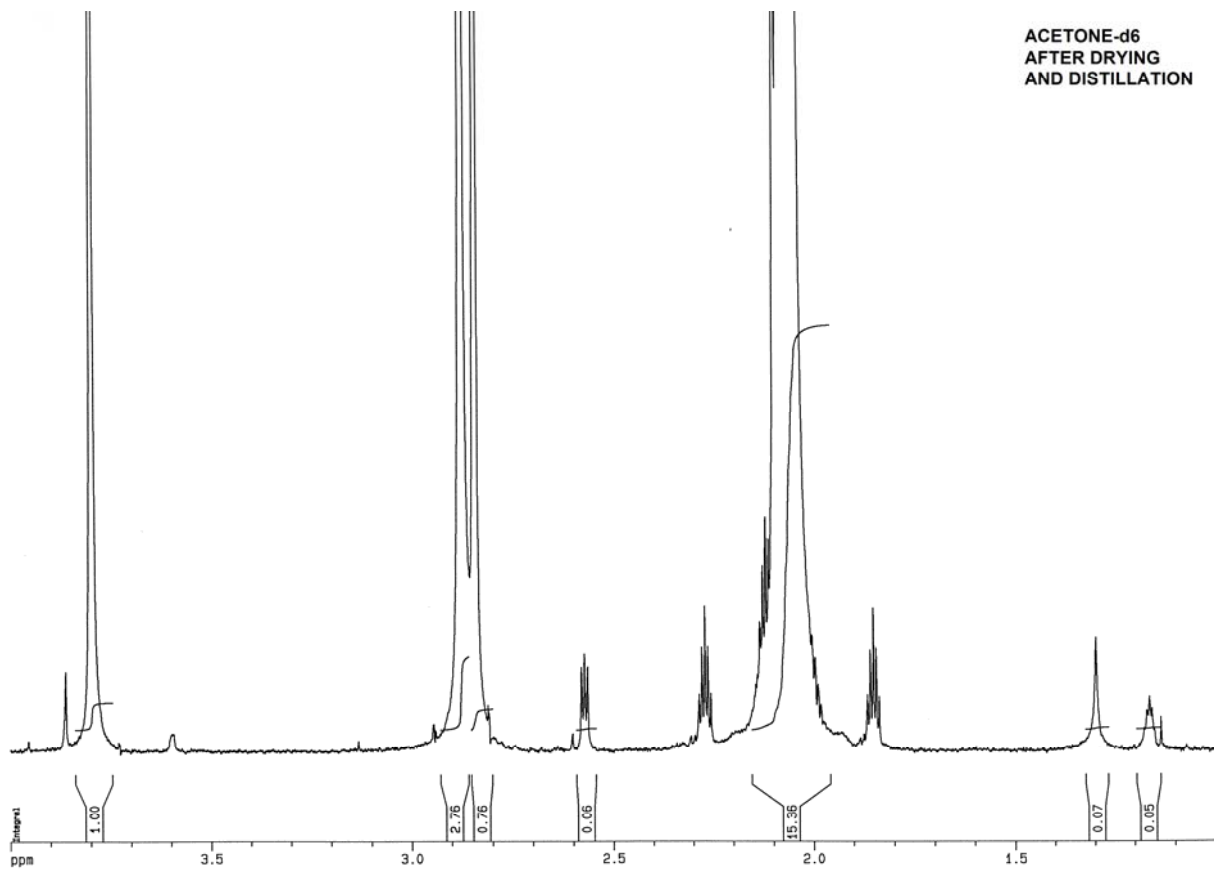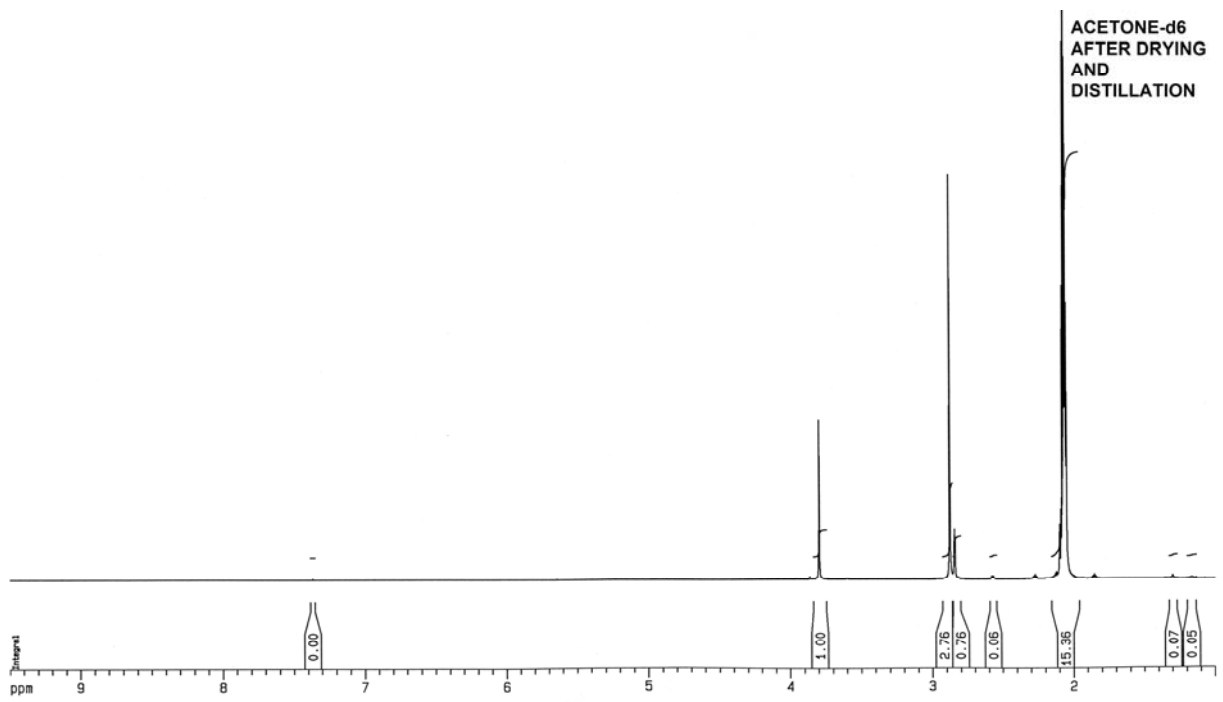
ACETONE-d6 FROM MERCK
AMPOULE AFTER 41 HOURS
ON MOLECULAR SIEVES
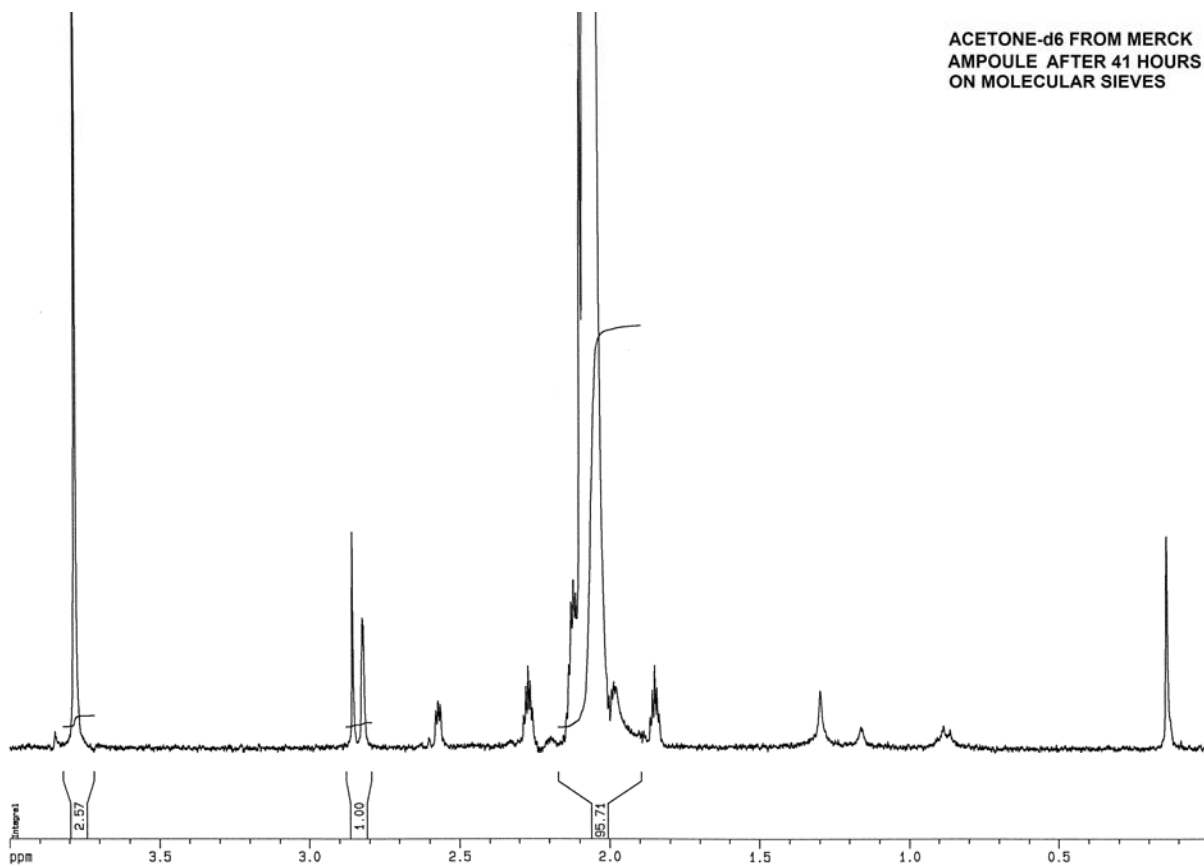


ACETONE-d6 FROM
MERCK AMPULE
AFTER 24 HOURS ON
MOLECULAR SIEVES

D-3

ACETONE-d6 FROM
ANOTHER MERCK AMPULE
AFTER 24 HOURS ON
MOLECULAR SIEVES
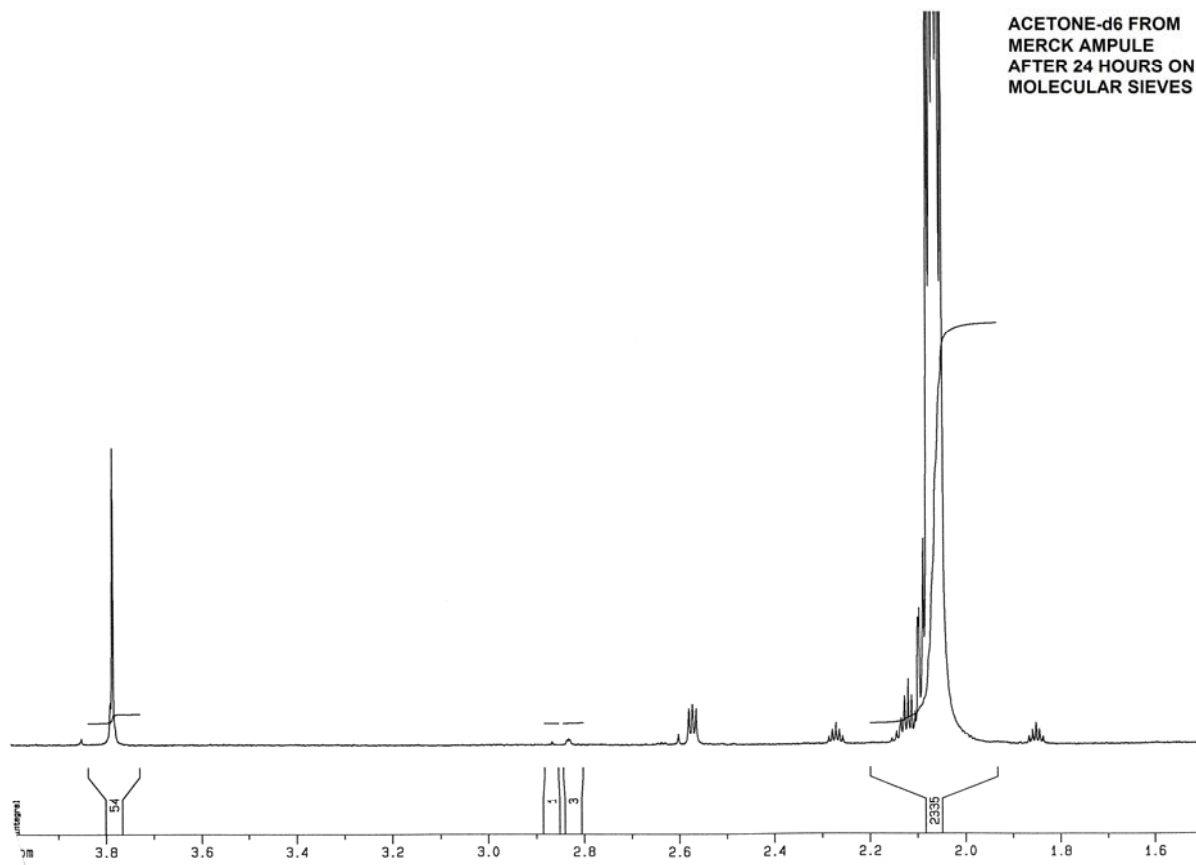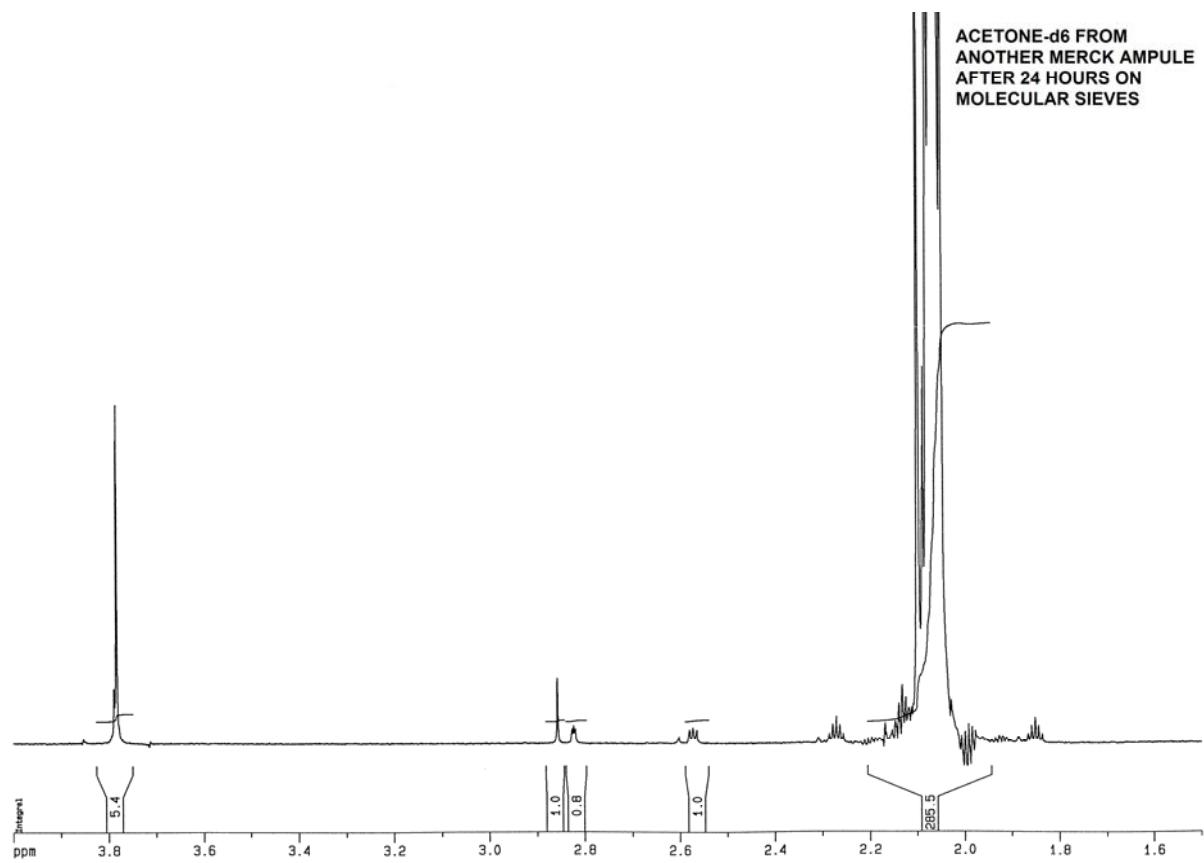
# SUMMARY

The profisetinidins are an important class of condensed tannins, or proanthocyanidins. Historically, studies towards the structure and conformation of proanthocyanidins were done on their peracetate and permethyl acetate derivatives.

A current upsurge in industrial and biological applications of proanthocyanidins has prompted the present efforts at detailed analysis of the conformational behaviour of the naturally occurring free phenolic oligomeric profisetinidins. Studies towards the structure and conformational analysis of a small number of free phenolic dimeric procyanidins that are 4→8 coupled and only one free phenolic dimeric profisetinidin, fisetinidol-(4α→8)-catechin, have hitherto been reported.

This study centres on the use of $^{1}$H, $^{13}$C, gradient COSY, COSY 45, COSY 90W, NOESY PH and HMQC NMR experiments in different solvents and at different temperatures to assign the hydrogen and some carbon resonances of the free phenolic profisetinidins that are found in commercially important southern hemisphere trees, namely Black Wattle (*Acacia mearnsii)* and Quebracho *(Schinopsis balansae*). These results, together with data obtained from CD spectra in methanol, were then used to study the conformations of these compounds.

Dimers with 2,3-*trans*-3,4-*trans* (2,4-*cis*) configuration, namely fisetinidol-(4α→8)-catechin, fisetinidol-(4α→6)-catechin, *ent*-fisetinidol-(4β→8)-catechin and *ent*-fisetinidol-(4β→6)-catechin all displayed sets of duplicate resonances on $^{1}$H NMR spectra, indicating the presence of rotamers on an NMR time-scale at ambient temperatures. The proton resonances of the rotamers of the 4→6 linked dimers displayed insignificant chemical shift differences due to the similar magnetic environments and linear shape of both rotamers.

The proton resonances of the rotamers of the 4→8 linked dimers displayed significant chemical shift differences due to the presence of compact and extended rotamers resulting in large changes in magnetic environment due to anisotropic effects.

The type of solvent, temperature as well as the relative presence of water or cadmium nitrate had a strong influence on the relative concentrations of the rotamers, the conformations of the heterocyclic C- and F-rings as well as the visibility of hydroxy groups. The F-rings all

displayed A/E- conformational exchange with line shapes indicating possible skewed boat conformations in some instances. The C-ring conformations ranged from rings with A/E conformational exchange to preferred E-conformers.

The dimers with 2,3-*trans*-3,4-*cis* (2,4-*trans*) configuration, namely fisetinidol-(4β→8)-catechin, fisetinidol-(4β→6)-catechin and *ent*-fisetinidol-(4α→8)-catechin displayed only one set of resonances on $^{1}$H NMR spectra at ambient temperatures. The presence of intramolecular hydrogen bonding and limited conformational exchange was confirmed by the following observations:

a) Selective broadening of proton resonances in both the heterocyclic and aromatic regions of 1D NMR spectra.
b) Sharpening of resonances in 1D spectra at elevated temperatures.
c) The presence of abundant coupling between heterocyclic and aromatic ring protons as observed on 2D spectra.
d) Coupling between 2-$H_C$ and 4-$H_C$ on 2D NMR spectra.

The C-rings had preferred A-conformations, with the F-rings displaying A/E conformational exchange with line shapes indicating possible skewed boat conformations in some instances.

2D NMR experiments afforded estimations, in some cases, of the angles between the plane of the B-ring and the 2-$C_C$→2-$H_C$ bond, the plane of the D-ring and the 4-$C_F$→4-$H_F$ bond as well as the plane of the D-ring and the 4-$C_C$→4-$H_C$.

The resonances of 4-$C_C$ of the 2,3-*trans-3,4-trans* dimers displayed significant chemical shift differences (± 41 ppm) compared to 4-$C_C$ of the 2,3-*trans-3,4-cis* dimers (± 31 ppm).This could serve as a possible indicator of the relative configurations of the C-rings of 2,3-*trans* profisetinidins dimers.

CD studies of al seven abovementioned dimers, as well as four trimers from *Acacia mearnsii* displayed complex curves with a number of strong Cotton effects. Although some trends were observed, it was abundantly evident that the chiroptical characteristics of this class of compounds are too complex to be interpreted in terms of the empirical quadrant rule.

# OPSOMMING

Die profisetinidiene vorm 'n belangrike klas van gekondenseerde tanniene, oftewel proantosianidiene. Die oorgrote meerderheid studies om die struktuur en konformasie van hierdie verbindings te bepaal, is op hulle perasetaat en metieleterasetaat derivate gedoen.

Die toename in industriële en biologiese toepassings van proantosianidiene het gelei tot die huidige studies om 'n gedetailleerde analise van die konformasionele gedrag van vry fenoliese oligomeriese profisetinidiene te doen. Slegs etlike vry fenoliese dimeriese prosianidiene wat 4→8 gekoppel is en slegs een vry fenoliese dimeriese profisetinidien, naamlik fisetinidol-(4α→8)-katesjien, is tot op hede bestudeer.

Hierdie studie behels die gebruik van $^1$H, $^{13}$C, gradient COSY, COSY 45, COSY 90W, NOESY PH en HMQC KMR eksperimente in verskillende oplosmiddels en by verskillende temperature om die waterstof en sommige van die koolstof resonanse van die dimeriese profisetinidiene gevind in die kommersiëel belangrike Swart Wattel (*Acacia mearnsii)* en Quebracho *(Schinopsis balansae*). Beide hierdie bome kom in die suidelike halfrond voor. Hierdie resultate, tesame met die data wat verkry is van SD spektra in metanol, is gebruik om die konformasies van hierdie verbindings te bestudeer.

Dimere met 2,3-*trans*-3,4-*trans*- (2,4-*cis*-) konfigurasie, naamlik fisetinidol-(4α→8)-katesjien, fisetinidol-(4α→6)-katesjien, *ent*-fisetinidol-(4β→8)-katesjien en *ent*-fisetinidol-(4β→6)-katesjien vertoon almal stelle gedupliseerde resonanse in $^1$H KMR spektra, wat op die teenwoordigheid van twee rotamere op 'n KMR tydskaal by kamertemperatuur dui. Die proton resonanse van die dimere wat 4→6 gekoppel is, het geen betekenisvolle chemiese verskuiwings getoon nie. Dit kan toegeskryf word aan die soortgelyke magnetiese omgewings van die rotamere, asook hulle liniêre oriëntasie.

Die proton resonanse van die dimere wat 4→8 gekoppel is, het betekenisvolle chemiese verskuiwings getoon wat toegeskryf kan word aan die teenwoordigheid van kompakte en verlengde rotamere, met beduidende verskille in magnetiese omgewings as gevolg van anisotropiese effekte. Die tipe oplosmiddel, temperatuur, asook die teenwoordigheid van water en kadmium nitraat, het 'n sterk invloed op die relatiewe konsentrasies van die rotamere, die konformasies van die heterosikliese C- en F-ringe asook die sigbaarheid van hidroksie groepe gehad. Die konformasies van die F-ringe het almal op A/E-konformasionele

uitruiling gedui, met lynvorm analise wat ook moontlike skewe boot konformasies aandui. Die konformasies van die C-ringe het gestrek van A/E konformasionele uitruiling tot voorkeur E-konformere.

Dimere met 2,3-*trans*-3,4-*cis*- (2,4-*trans*-) konfigurasie, naamlik *ent*-fisetinidol-(4α→8)-katesjien, fisetinidol-(4β→6)-katesjien en fisetinidol-(4β→8)-katesjien het slegs een stel resonanse op $^{1}$H KMR spektra getoon by kamertemperatuur. Dit kan verklaar word aan die hand van waterstofbindings wat konformasionele uitruiling beperk, en is bevestig deur die volgende waarnemings:

a) Selektiewe verbreding van sommige proton resonanse in beide die heterosikliese en aromatiese areas van $^{1}$H KMR spektra.

b) Resonansverskerping by verhoogde temperature.

c) Die oorvloedige teenwoordigheid van koppeling tussen heterosikliese en aromatise protone soos waargeneem op 2D spectra.

d) Koppeling tussen 2-$H_C$ en 4-$H_C$ op 2D spektra.

Die C-ringe het almal voorkeur A-konformasies getoon en die F-ringe A/E konformasie uitruiling met lynvorm analise wat ook moontlike skewe boot konformasies in sommige gevalle aandui.

Beraamde skattings kon in sommige gevalle van die hoeke tussen die vlak van die B-ring en die 2-$C_C$→2-$H_C$ binding, die vlak van die D-ring en die 4-$C_F$→4-$H_F$ binding asook die vlak van die D-ring en die 4-$C_C$→4-$H_C$ binding vanaf 2D KMR eksperimente gedoen word.

Die resonanse van 4-$C_C$ van die 2,3-*trans-3,4-trans* dimere het beduidende chemiese verskuiwingsverskille getoon (±41 ppm) in vergelyking met 4-$C_C$ van die 2,3-*trans-3,4-cis* dimere (± 31 ppm). Dit kan as 'n moontlike indikator van die relatiewe konfigurasies van die C-ringe van 2,3-*trans* profisetinidien dimere dien.

CD studies van al sewe bogenoemde dimere, asook vier trimere vanuit *Acacia mearnsii* het komplekse kurwes tot gevolg gehad wat elk 'n aantal hoë amplitude Cotton effekte vertoon het. Alhoewel sommige algemene neigings waargeneem is, is dit baie duidelik dat die chiroptiese eienskappe van hierdie klas verbindings nie in terme van die empiriese kwadrantreël geïnterpreteer kan word nie.

# KEY WORDS

Free Phenolic Profisetinidins

Dimeric Profisetinidins

Trimeric Profisetinidins

Flavan-3-ols

Conformational Analysis

Nuclear Magnetic Resonance

Circular Dichroism

Acacia mearnsii

Schinopsis balansae